Horbachevskyi National Medical University, Ternopil', Ukraine
Ukrainian Scientific Research Institute of Medicine of Transport, Odesa, Ukraine
Bohomolets' Institute of Physiology of NAS, Kyïv, Ukraine
Nicolaus Copernicus University, Torun, Poland

Editors
Mykhaylo M. Korda
Anatoliy I. Gozhenko
Igor L. Popovych
Ivan M. Klishch

NEUROTROPIC, HORMONAL AND IMMUNOTROPIC ACTIVITY OF URIC ACID

MONOGRAPH

TERNOPIL'
Ukrmedknyha
2024

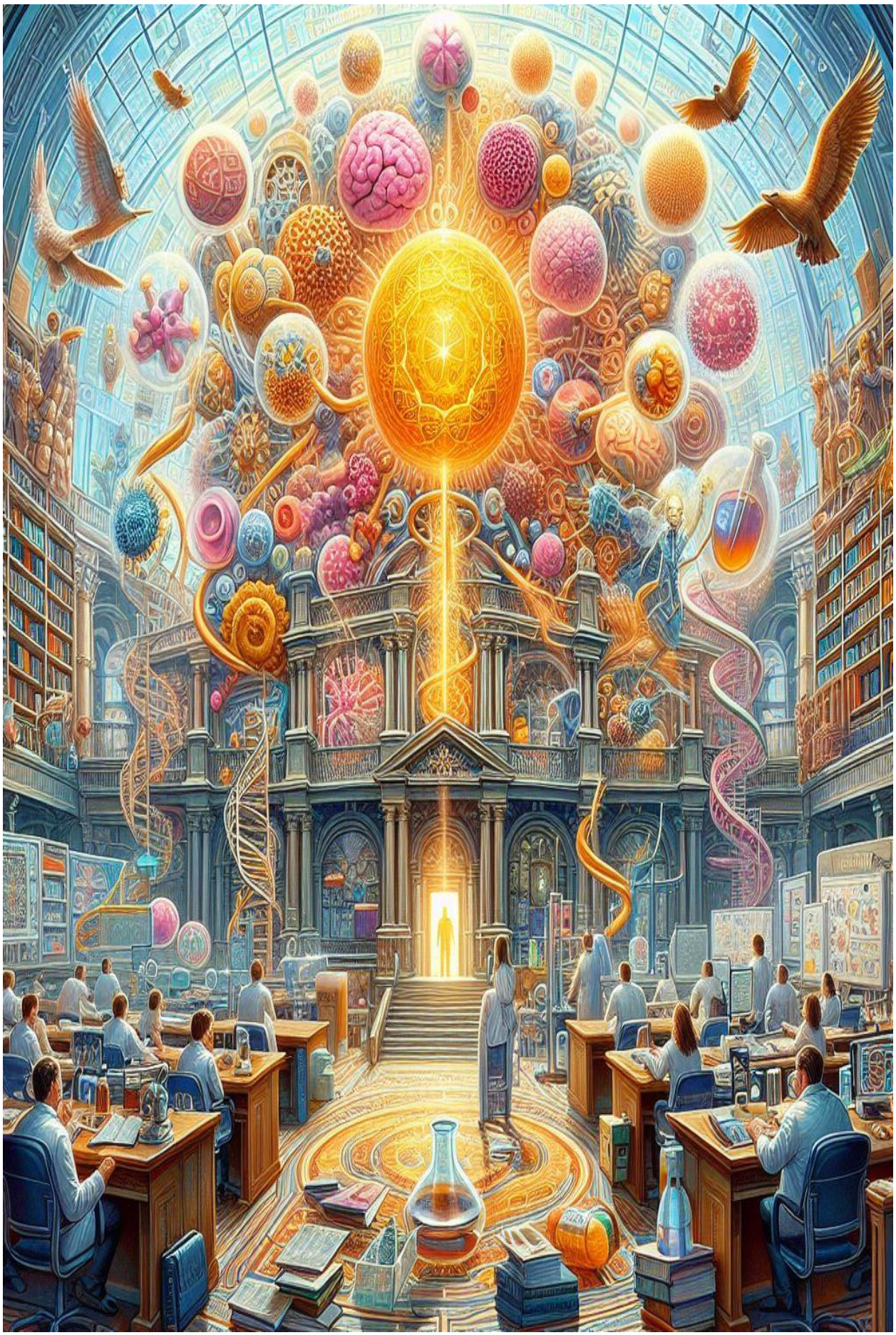

Horbachevskyi National Medical University, Ternopil', Ukraine
Ukrainian Scientific Research Institute of Medicine of Transport, Odesa, Ukraine
Bohomolets' Institute of Physiology of NAS, Kyïv, Ukraine
Nicolaus Copernicus University, Torun, Poland

Editors

Mykhaylo M. Korda
Anatoliy I. Gozhenko
Igor L. Popovych
Ivan M. Klishch

NEUROTROPIC, HORMONAL AND IMMUNOTROPIC ACTIVITY OF URIC ACID

MONOGRAPH

TERNOPIL'
Ukrmedknyha
2024

Recommended for publication by the Academic Council State Institution
"Horbachevskyi National Medical University"
(Protocol No. 3 of March 27, 2024)

Reviewers:
Roman Ivanovych Yanchiy, Doctor of Biological Sciences, Professor, laureate of the O.O. Bogomolets Prize, Head of the Immunophysiology Department at the O.O. Bogomolets Institute of Physiology of the National Academy of Sciences of Ukraine.
Ruslan Serhiyovych Vastiyanov, Doctor of Medical Sciences, Professor, Honored Scientist and Technologist of Ukraine, Head of the Department of General and Clinical Physiology named after V.V. Pidvysotsky of Odesa National Medical University.

DEDICATED TO IVAN YAKOVYCH HORBACHEVSKYI

Korda MM, Gozhenko AI, Popovych IL, Klishch IM, Bombushkar IS, Korda IV, Badiuk NS, Zukow WA, Smagliy VS. Neurotropic, hormonal and immunotropic activity of uric acid. Monograph. Ternopil': Ukrmedknyha; 2024: 206 p. ISBN 978-966-673-487-0 DOI https://doi.org/10.5281/zenodo.10990426

This monograph presents the results of priority experimental and clinical-physiological research on the relationship between uricemia and uricosuria with parameters of urea, creatinine, electrolyte exchange, as well as the nervous, endocrine and immune systems. In line with the concepts of the neuroendocrine-immune complex and the functional-metabolic continuum, using discriminant and canonical correlation analysis methods, it is demonstrated that the uric acid molecule exhibits significant physiological activity and can be considered the fourth endogenous signaling molecule alongside NO, CO, and H_2S.

For biochemists, pathophysiologists, neurologist, endocrinologists, and immunologists.

ISBN 978-966-673-487-0
DOI https://doi.org/10.5281/zenodo.10990426

Table of Contents

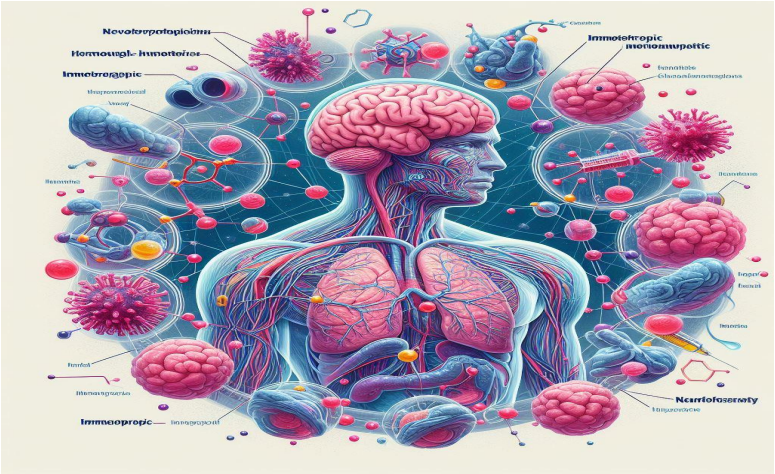

Annotation

In an experiment on healthy rats, a wide range of parameters of uric acid exchange was revealed, and it was shown for the first time that 34 **immune** parameters out of 41 registered were significantly correlated with them. Uricosuria (to a greater extent) and uricemia (to a lesser extent), taken together, determine the state of immunity by 71%. Uric acid stimulates the phagocytosis of Staph. aureus by neutrophils (but not monocytes) of the blood, increases the relative content of lymphocytes in general and B-lymphocytes in particular in the blood, T-lymphocytes and macrophages in the thymus and fibroblasts in the spleen, and also increases the entropy of the blood immunocytogram. On the other hand, uric acid reduces the entropy of the blood leukocytogram, the total content of leukocytes in the blood and the relative content of monocytes and rod-shaped neutrophils in the leukocytogram, natural killers in the immunocytogram, as well as the entropy of the thymocytogram and the content of epitheliocytes and reticulocytes in it.

It was shown that among the **neuro-endocrine** factors of adaptation, uricosuria and uricemia are negatively correlated with HRV-markers of sympathetic tone and circulating catecholamines, the plasma level of corticosterone and the thickness of the fascicular zone of the adrenal cortex, as well as the plasma level of triiodothyronine and the Ca-P marker calcitonin activity, on the other hand, and positively correlated with HRV-marker of vagal tone and urinary excretion of 17-ketosteroids. The rate of determination of neuro-endocrine adaptation factors by uric acid is 62%. The cumulative determining influence of parameters of uric acid exchange (due to the significant advantage of uricosuria over uricemia) on the constellation of **metabolic** parameters is 56%. Diuresis and excretion of phosphates and potassium are subject to the maximum positive determination by uric acid, excretion of calcium, creatinine and urea are determined to a lesser extent, levels of creatinine, urea and potassium in plasma are even less determined, and magnesiumuria is subject to the minimum determination.

In human of both sexes, patients with chronic pyelonephritis in the phase of remission, four variants of uric acid exchange were found too. In 34%, moderate hypouricosuria is combined with lower borderline uricemia. In 24%, moderately increased uricosuria is associated with normal uricemia. In 17%, moderately increased uricosuria is combined with pronounced hypouricemia. Finally, in 25% of patients, subliminal uricemia is accompanied by marked hyperuricosuria.

Among all the registered parameters, 28 were selected as identifying four variants of uric acid metabolism. In addition to uricosuria and uricemia by definition, the discriminant model included 10 **neuroendocrine** parameters (6 EEG, vagal tone, indices of sympatho-vagal balance of Kerdö and Baevsky, calcitonin), 5 parameters of **immunity** (activity and completion of phagocytosis by neutrophils of gram-positive bacteria, the level of total lymphocytes and IgG in the blood and IgA in saliva), two **informational** parameters (Popovych's strain index of the leukocytogram and the Entropy of the immunocytogram), 6 parameters of **metabolism** (serum magnesium, potassium, phosphates and creatinine, creatinineuria, body mass index), as well as markers of chronic pyelonephritis (**bacteriuria**) and microbiota (***Bifidobacteria***).

According to the results of the canonical correlation analysis, it was established that balneotherapy-induced changes in uricemia downregulate changes in PSD of beta-rhythm in 5 loci and alpha-rhythm in the T5 locus, as well as calcitonin and T-helpers. On the other hand, changes in PSD of delta-rhythm in the T5 locus, the alpha-rhythm in the P4 and P3 loci, serum levels of calcium, magnesium, chloride and sodium, as well as monocytes and CIC are subject to upregulation. The changes in uricosuria downregulate changes in PSD of the alpha-rhythm index and serum levels of testosterone and catecholamines, but upregulate changes in HRV-markers of vagal tone, serum PTH and blood T-helper lymphocytes levels as well as diuresis and excretion of urea, magnesium, phosphates, calcium and potassium. In general, the rate of uric acid determination of the dynamics of the listed parameters of the body is 96%.

Sexual dimorphism in relationships between serum uric acid and some psycho-neuro-endocrine parameters was found in another cohort of subjects.

The obtained results develop and complement the concept that endogenous uric acid has physiological activity, which is manifested in the modulation of the parameters of the neuroendocrine-immune complex and metabolism.

The materials from the monograph have been reflected in the following publications:

1. Popovych IL, Gozhenko AI, Bombushkar IS, Korda MM, Zukow W. Sexual dimorphism in relationships between of uricemia and some psycho-neuro-endocrine parameters. Journal of Education, Health and Sport. 2015; 5(5): 556-581.
2. Gozhenko AI, Smagliy VS, Korda IV, Zukow W, Popovych IL. Cluster analysis of uric acid exchange parameters in female rats. Journal of Education, Health and Sport. 2019; 9(11): 277-286.
3. Gozhenko AI, Smagliy VS, Korda IV, Badiuk NS, Zukow W, Popovych IL. Features of immune status in different states of uric acid metabolism in female rats. Journal of Education, Health and Sport. 2019; 9(12): 167-180.
4. Gozhenko AI, Smagliy VS, Korda IV, Badiuk NS, Zukow W, Popovych IL. Functional relationships between parameters of uric acid exchange and immunity in female rats. Actual problems of transport medicine. 2019; 4(58): 123–131.
5. Smagliy VS, Gozhenko AI, Korda IV, Badiuk NS, Zukow W, Kovbasnyuk MM, Popovych IL. Variants of uric acid metabolism and their immune and microbiota accompaniments in patients with neuroendocrine-immune complex dysfunction. Actual problems of transport medicine. 2020; 1(59): 114–125.
6. Gozhenko AI, Smagliy VS, Korda IV, Badiuk NS, Zukow W, Kovbasnyuk MM, Popovych IL. Relationships between parameters of uric acid exchange and immunity as well as microbiota in patients with neuroendocrine-immune complex dysfunction. Journal of Education, Health and Sport. 2020; 10(1): 165-175.
7. Gozhenko AI, Smagliy VS, Korda IV, Badiuk NS, Zukow W, Kovbasnyuk MM, Popovych IL. Relationships between changes in uric acid parameters metabolism and parameters of immunity and microbiota in patients with neuroendocrine-immune complex dysfunction. Journal of Education, Health and Sport. 2020; 10(2): 212-222.
8. Popovych IL, Bombushkar IS, Badiuk NS, Korda IV, Zukow W, Gozhenko AI. Features of the state of neuro-endocrine factors of adaptation under different options of uric acid metabolism in healthy female rats. Journal of Education, Health and Sport. 2020; 10(3): 352-362.
9. Bombushkar IS, Gozhenko AI, Korda IV, Badiuk NS, Zukow W, Popovych IL. Features of the exchange of electrolytes and nitrogenous metabolites under different options of uric acid exchange in healthy female rats. Journal of Education, Health and Sport. 2020; 10(4): 405-415.
10. Bombushkar IS. Features of the state of the neuroendocrine-immune complex and electrolyte-nitrogenous exchange under different variations of uric acid metabolism in female rats. Journal of Education, Health and Sport. 2020; 10(5): 410-421.
11. Kozyavkina NV, Popovych IL, Popovych DV, Zukow W, Bombushkar IS. Sexual dimorphism in some psycho-neuro-endocrine parameters at human. Journal of Education, Health and Sport. 2021; 11(5): 370-391.
12. Bombushkar IS, Gozhenko AI, Badiuk NS, Smagliy VS, Korda MM, Popovych IL, Blavatska OM. Relationships between uric acid exchange parameters and neuroendocrine adaptation factors [in Ukrainian]. Bulletin of Maritime Medicine. 2022; 2(95): 59-74.
13. Bombushkar IS, Korda MM, Żukow X, Popovych IL. Sexual dimorphism in relationships between of plasma uric acid and some psycho-neuro-endocrine parameters. Journal of Education, Health and Sport. 2022; 12(12): 357-372.
14. Bombushkar IS. Metabolic accompaniments of variants of uric acid exchange. Journal of Education, Health and Sport. 2022; 12(12): 372-390.
15. Gozhenko AI, Korda MM, Smagliy VS, Badiuk NS, Zukow W, Klishch MI, Korda IV, Bombushkar IS, Popovych IL. Uric Acid, Metabolism, Neuro-Endocrine-Immine Complex [in Ukrainian]. Odesa. Feniks; 2023: 229.
16. Bombushkar IS, Popovych IL, Zukow W. Relationships between the parameters of uric acid exchange and electroencephalograms in humans. Journal of Education, Health and Sport. 2023; 13(3): 458-485.
17. Popovych IL, Bombushkar IS, Żukow X, Kovalchuk HY. Uric acid, neuroendocrine-immune complex and metabolism: relationships. Journal of Education, Health and Sport. 2023; 36(1): 135-159.

IVAN YAKOVYCH HORBACHEVSKY - A PIONEER IN THE SYNTHESIS OF URIC ACID IN VITRO

Academician Ivan Gorbachevsky left behind a considerable legacy in the world of science, consisting of numerous scientific works that have retained their value, continue to inspire, and awe biochemists. His passion for knowledge and the pursuit of truth were evident even during his school years when he attended Ternopil Gymnasium. His involvement in the secret student group "Hromada" (Community) played a role in this. Members of the group read the works of Taras Shevchenko, Panteleimon Kulish, and Ivan Kotliarevsky, with the goal of awakening national consciousness and exploring the historical past of their people. However, he embarked on his scientific path for the first time while already a student and working as a demonstrator in the Department of Medical Chemistry under Professor Ludwig.

As a 22-year-old student in 1875, he conducted his first independent scientific work, dedicated to the vestibular nerve, and published it in the proceedings of the Vienna Academy of Sciences. This achievement earned him recognition from the university administration and admission to the German scientific society.

Three years later, in the same proceedings of the Vienna Academy of Sciences, his new scientific work appeared, titled "On the Decomposition Products Formed Under the Action of Hydrochloric Acid on Albuminoids." Then, in 1882, another publication followed titled "On the Digestion of Elastin," which he conducted under the influence of the enzyme pepsin. Having obtained amino acids as the final products from albuminoids and elastin, the young assistant Ivan Gorbachevsky came to the entirely logical conclusion that these were the building blocks from which proteins were constructed. Thus, Ivan Gorbachevsky's early scientific works were dedicated to the physiology of digestion. This research direction was quite common among scientists at that time, and it was passed on to the young assistant by Professor Ludwig.

However, by then, Ivan Gorbachevsky was already captivated by the idea of synthesizing organic compounds, especially those found in the human body, the functions of which were unknown. Such substances were considered to be exclusively characteristic of living organisms, and it was believed that they could not be synthesized outside the body.

Gorbachevsky's attention was drawn to a substance discovered in urine in 1776 by the Swedish researcher K. Scheele, which he named uric acid. A bit later, this acid was also found in urinary stones associated with gout attacks.

Many renowned scientists sought to artificially synthesize uric acid. Eminent biochemists like Liebig, Wöhler, Fischer, A. Rosen, and Nensky dedicated themselves to this goal but without success. Nensky even claimed to have synthesized uric acid first. However, fate had a different plan. Gorbachevsky was familiar with the work of the German scientist D. Stecker, who had established that upon heating uric acid with hydrogen iodide, it decomposed into carbon dioxide, ammonia, and the amino acid glycine.

Logical reasoning led him to assume that the ammonia and carbon dioxide obtained by Stecker from the heating of uric acid were the end products of uric acid decomposition, which, obviously, had formed from uric acid itself. This is why the young scientist, Ivan Gorbachevsky, at the Institute of Medical Chemistry at the University of Vienna, used the products of uric acid breakdown, glycine, and urea, for the synthesis of uric acid. Taking a mixture of these two substances in a 1:10 ratio, he heated it to a temperature of 230°C, cooled the melt, and then dissolved it in diluted potassium lye. Subsequently, using a magnesium mixture and a solution of [Ag(NH3)2]OH, silver urate was precipitated. Uric acid was obtained from the alkaline solution upon acidification with hydrochloric acid. Thus, for the first time in the history of world science, in 1882, uric (ureatic) acid was synthesized. This discovery brought great fame and honor to Austrian science, especially the University of Vienna.

The significant attention devoted to the synthesis of uric acid by scientists can be explained not only by the fact that it was first synthesized by a young, relatively unknown worker at the University of Vienna, but also by the fact that many famous scientists around the world had worked

unsuccessfully on this issue. Furthermore, during this period, there was a dominant vitalistic approach in biology and medicine, according to which substances characteristic of living organisms could not be artificially obtained outside of them.

Ivan Gorbachevsky's work on the synthesis of uric acid contributed to the advancement of science and our understanding of the biological role and origin of uric acid in the body. This laid the foundation for his future theory on uric acid formation in the human body and other mammals.

After 1882, the entire scientific community began to take notice of Ivan Gorbachevsky. Some were enthusiastic and joyful about his discovery, while others were surprised and skeptical. Skeptics couldn't believe that a young 28-year-old Slavic scientist had achieved what many renowned German and French chemists had failed to do. Not only did this young scientist manage to synthesize a substance that others couldn't using his original method, but he also defended his priority in scientific discussions with opponents. Based on scientific facts and the results of his own research, Ivan Gorbachevsky convincingly proved the correctness of his findings, and most of his opponents agreed with him and became his friends.

Ivan Gorbachevsky's discovery of uric acid synthesis led to his appointment as an associate professor of medical chemistry at Charles University in Prague in 1983, and within a few months, he became a full professor. Here, he developed the foundations and organized the field of medical chemistry, which the university had lacked before his arrival. At the beginning of his professorial career in Prague, he taught not only chemistry but also pharmacology, physiology, and lectured on dietetics and toxicology.

However, the main focus of his scientific work at that time was the study of nitrogen compound metabolism and the synthesis of organic compounds in general.

In 1885, Ivan Gorbachevsky achieved the synthesis of methyluric acid by heating uric acid with methylglyoxal or isopropyl ether of allophanic acid. Then, in 1887, he proposed another method, which involved melting uric acid with chloroacetic acid or trichloroacetic acid or the amide of the latter. All these synthesis methods, pioneered by our compatriot, became classic and engraved Ivan Gorbachevsky's name in golden letters in the annals of world science.

In 1885, Ivan Gorbachevsky also successfully synthesized another crucial nitrogen-containing compound for the body - creatine. He proposed a volumetric method for determining nitrogen in various body fluids, which found application both in experiments and in clinical practice.

In the following years, Professor Gorbachevsky directed his research towards understanding the mechanisms of uric acid formation in mammals' bodies. In 1889, while studying this question, he discovered the enzyme xanthine oxidase, which plays a role in the oxidation of the purine compound xanthine into uric acid. By 1890, Gorbachevsky published a paper in a German chemistry journal on the origin of uric acid in mammals' bodies.

The following year, he became the first among biochemists to establish a connection between the transformation of xanthine bases, produced during nucleic acid breakdown, and the biosynthesis of uric acid. Through experiments with mammalian leukocytes, our scientist demonstrated that uric acid is formed from nuclear components of cells. His systematic studies on uric acid synthesis, the establishment of its chemical structure, and experiments on mammals' transformations of purine bases allowed him to propose the world's first theory of uric acid formation in the body. This groundbreaking theory was presented in 1891 in Wiesbaden when Ivan Gorbachevsky delivered his report on "The Theory of Uric Acid Formation." This theory, based on all his previous research, logically reflected the concept of nucleic acid transformations.

The theory of uric acid formation in the body has not lost its significance to this day. Contemporary views on uric acid biosynthesis have only been slightly supplemented with new data regarding the influence of various exogenous and endogenous factors on uric acid biosynthesis and its content in body tissues. The direction initiated by Gorbachevsky continues to flourish in many scientific schools worldwide, especially in the study of nucleic acid metabolism disorders.

It can be confidently stated, echoing the French scientist Coste (1953), that the works of Academician Ivan Horbachevsky on the artificial synthesis of uric acid and the investigation of its biosynthesis in the organism remain unrivaled and significant to this day.

Between 1891 and 1893, Ivan Horbachevsky published works that demonstrated that the formation of uric acid and its content in the organism significantly depend on a person's clinical condition, nutritional factors, the type of food products consumed, and more.

It's worth noting that while developing the theory of uric acid formation, Professor Horbachevsky simultaneously developed a methodology for isolating nucleic acids from organ tissues. His work on this topic was published in 1898 in a paper titled "A General Method for Extracting Nucleic Acid from Organs" ("Likarskiy zbirnyk NTSh," 1898, Vol. 1, pp. 1-4). Modern methods for extracting nucleic acids are essentially slight modifications of the approach proposed by our compatriot.

Ivan Horbachevsky, who consistently worked in the field of natural sciences, also took an interest in the life of his fellow countrymen, particularly the economic condition of peasants. He collected materials on topics related to the physiology, hygiene, and nutrition of the population. This represented a new scientific direction in the field of medical and biological research. The results of his research in this area were published in an article titled "Contributions to the Knowledge of the Rural Population of Galician Podillya," which was published in "Likarskiy zbirnik NTSh" in 1899, Vol. 2, Issue 2, page 1.

Professor Ivan Horbachevsky's recognized authority in the scientific world is evident from his election as Vice President of the International Medical Congress, held in Paris from August 2 to 9, 1900, where he also served as the President of the Chemical Section. During the congress, Ivan Horbachevsky led the Ukrainian delegation.

In the same year, he presided over the Biological Section at the 3rd Congress of Czech Naturalists and Physicians in Prague. At this event, he presented a paper titled "On the Formation of Fat in the Animal Organism." Additionally, another one of his methodologies for detecting blood pigment for forensic medical purposes was published in the congress proceedings.

Much of Ivan Horbachevsky's time was occupied by his work on the Regional Sanitary Council, aimed at improving the environment and reducing the negative health impact of industrial waste on people's health. As the outbreak of World War I approached, his scientific work did not slow down despite his extensive commitments to teaching and public affairs.

During this period, he conducted interesting and original research on the issue of pellagra. In 1911, he published a series of works on this topic, including "Experimental Approaches to the Etiology of Pellagra." Based on observations of the diets of pellagra patients, he concluded that the cause of this disease was the inadequacy of nutrition, primarily from plant-based foods, particularly corn products, which seemed to lack certain vitamins, similar to the known vitamins A, B, C, and D. Horbachevsky's hypothesis was later confirmed with the discovery of vitamin "PP" as the anti-pellagra factor.

The following year marked the publication of another work in the journal of Czech physicians titled "On Poisoning with Alcohol - Denatured Methyl Alcohol," in which he described the effects of alcohol on the organism. He also published a paper in the same journal in 1916 titled "On Lead Poisoning When Using Galvanized Iron Water Pipes," addressing toxicological issues.

Ivan Horbachevsky's research had a significant impact on the population of Prague. His work on sanitary standards for drinking water led to the construction of a water supply system from the clean Izera River instead of the polluted Vltava River. This led to a significant reduction in typhoid fever cases. However, later investigations revealed that the use of galvanized water pipes did not pose such a significant risk of poisoning, and Horbachevsky conducted further research and recommendations to minimize or eliminate the illness.

Professor Ivan Horbachevsky's research and contributions reflected his keen awareness of the social needs of the population, particularly issues related to malnutrition and food quality. His research papers, such as "Experimental Studies on the Nutritional Value of Lichens" (1917),

exemplify this commitment. Unfortunately, this research direction did not receive further development due to his appointment as Minister of Health, which demanded a great deal of his daily work. Nevertheless, his scientific approach to finding new methods and sources of nutritious human food, initiated by Prof. Horbachevsky, continues to be relevant today, as a significant portion of the global population still lacks adequate nutrition, especially in terms of protein-rich food. Ivan Horbachevsky's genius was directed towards addressing this problem as early as 1917.

With the dissolution of the Austro-Hungarian Empire, Horbachevsky became an active participant in the formation of the Western Ukrainian People's Republic (ZUNR). He developed a healthcare program for the ZUNR, organized the opening of the Ukrainian Free University in Vienna and Prague, and served as its rector in 1923-1924 and 1931-1935. In 1924, he published the first Ukrainian university textbook on "Organic Chemistry" in Prague and worked extensively on Ukrainian scientific chemical terminology.

As a renowned scientist, Ivan Horbachevsky was elected as an academician of the All-Ukrainian Academy of Sciences (VUAN) in 1925. In Prague, he founded and chaired the administration of the "Museum of the Liberation Struggle of Ukraine" society. He prepared numerous medical professionals and scientists for service in Ukraine. He also organized and chaired the First and Second Ukrainian Congresses in Prague in 1926 and 1932.

With the declaration of independence of the Carpatho-Ukrainian State in 1939, Horbachevsky organized a committee for the defense of Carpathian Ukraine in Czechoslovakia.

For many years, Horbachevsky was a professor of organic chemistry at the Ukrainian Free University in Prague and served as its rector for several years. His scientific legacy comprises more than 50 publications in German, Czech, and Ukrainian languages.

Professor Ivan Horbachevsky made a significant contribution to the development of Ukrainian scientific chemical terminology, which was of great importance for Ukrainian science and culture. He dedicated much time and effort to establishing and popularizing Ukrainian terminology in the field of chemistry.

In the first Ukrainian textbook on organic chemistry published in 1924, Ivan Horbachevsky expanded and explained his approach to introducing Ukrainian chemical terminology. He aimed to make it accessible and understandable for students and scientists by combining Ukrainian and international terms.

Notably, in 1927-1928, Ivan Horbachevsky chaired the Chemical Commission for Nomenclature at the Ukrainian Economic Academy in Poděbrady. This commission developed the principles of Ukrainian chemical terminology, which were published in the "Protocol" dated January 4, 1928. Prominent chemistry professors were among its members.

His final work on the subject, "The Current State of Ukrainian Nomenclature of Inorganic Chemistry," like his previous efforts, was used and implemented by scientists in Ukraine. In preparing textbooks in the Ukrainian language, he extensively studied folk chemical terminology and compared it with international and other Slavic chemical nomenclatures.

In 1903, Professor Ivan Horbachevsky published an article titled „Remarks on Chemical Terminology” in the collection of the Shevchenko Scientific Society (NTSh). This article marked the beginning of Ukrainian chemical nomenclature, which was essential for him in writing chemistry textbooks.

According to Professor Ivan Horbachevsky, the nomenclature he proposed for the main types of chemical compounds, based on a combination of Ukrainian folk terminology and international systems, is exceptionally straightforward, logical, and poses no difficulties in its understanding and adoption. He was deeply convinced that over time, in line with the progress of science and language, chemical nomenclature would continue to evolve and adapt.

Professor Ivan Horbachevsky's proposed nomenclature for organic (1924-1926) and inorganic (1939-1941) compounds formed the basis for the classification and nomenclature of chemical substances, which were developed and implemented in Ukraine before the Second World War.

Throughout his long life, Ivan Horbachevsky initiated and advanced numerous new scientific disciplines. His genius spanned fields such as inorganic, organic, and biological chemistry, hygiene, forensic medicine, and toxicology. In the field of biochemistry, he made significant contributions by researching protein structure and digestion, vitamins, purine metabolism, the structure and isolation of nucleic acids, dietary hygiene, and the search for new nutritious food products.

Equally important for the advancement of science was his establishment of a scientific school that continued his work. Among his most prominent students in Czechoslovakia were academician, professor, and medical doctor Emanuel Formanek (1869-1922), who essentially succeeded Ivan Horbachevsky as the head of the chemistry department at Charles University in 1918. Other notable students included Professor Karel Cherni (1871-1921), Professor Doctor Antonin Gamzik, Professor Doctor Richter, Professor Doctor Karel Kacel, Professor Doctor Jan Shula, Doctor Kukula, Professor Doctor Mlodajowski, Professor Nadislav Gashkoveci, Professor Doctor Sillaba, Professor Doctor Emil Schwagr, and others.

The name of Ivan Horbachevsky is indeed well-known in the scientific world and is engraved with golden letters in the annals of global science. The portrait of Rector Ivan Horbachevsky, along with portraits of other rectors, adorns the walls of the central hall of the main building of Charles University, where solemn meetings of the university's academic council take place. A bust of Academician, Professor, and Doctor Ivan Horbachevsky, created by the renowned Ukrainian sculptor M. Brynsky, stands among the busts of academicians in the Czech Academy of Sciences building in Prague. Ivan Horbachevsky's name has been resurrected from Soviet oblivion and is held in great esteem in his homeland. Ivan Horbachevsky continues to work for Ukraine and its independence to this day.

INTRODUCTION

Uric acid has traditionally been viewed as the end product of DNA/RNA degradation in humans and primates, devoid of any beneficial physiological activity. Furthermore, uric acid has long been recognized as a causative factor in gout and kidney stone disease. From a modern medical perspective, elevated uric acid levels are undesirable. Medical literature indicates a connection between elevated uric acid levels and an increased risk of cardiovascular diseases. Hypertension is also positively associated with high serum uric acid levels [Kanbay M et al, 2016]. Serum uric acid is a strong and independent risk factor for the development of diabetes in middle-aged and older individuals [Lv Q et al, 2013; Sluijs I et al, 2015; Johnson RJ et al, 2015]. Uric acid is considered a danger signal responsible for exacerbating osteoarthritis through inflammasome activation [Schett G et al, 2016]. At the same time, antioxidant properties of uric acid have been noted, which counteract neurodegeneration in Parkinson's disease and demyelination in multiple sclerosis [Morelli M et al, 2010; Wang L et al, 2016]. Uric acid may play a fundamental role in tissue healing by initiating an inflammatory process necessary for tissue regeneration, neutralizing oxygen free radicals, and mobilizing endothelial precursor cells [Nery RA et al, 2015]. Sofaer JA and Emery AF [1981], as well as Efroimson V.P. [1987], considered hyperuricemia as one of the factors contributing to increased intellectual activity (even genius), based on the abnormally high frequency of gout and kidney stone disease among outstanding individuals.

At the core of the physiological activity of uric acid lies its molecular similarity (2,6,8-trioxypurine) to the molecules of methylxanthines: caffeine (2,6-dioxo-1,3,7-trimethylxanthine), theobromine (2,6-dioxo-3,7-dimethylxanthine), and theophylline (2,6-dioxo-1,3-dimethylxanthine or 1,3-dimethylxanthine), which, in turn, are structural homologs of the physiologically active endogenous adenosine [(2R,3R,4R,5R)-2-(6-aminopurin-yl)-5-(hydroxymethyl)oxolan-3,4-diol], acting as non-selective antagonists of its receptors, primarily A2A and A1 [Cinel I, Gur S, 2000; Monahan TS et al, 2000; Arlova L et al, 2004; Pousti A et al, 2004; Morelli M et al, 2010; Navalta JW et al, 2016]. Ivasyvka SV, Popovych IL, Aksentiychuk BI, and Flyunt IS hypothesized that alongside exogenous methylxanthines, which enter the body through coffee, tea, cocoa, chocolate, medications, and so on, uric acid is an endogenous non-selective antagonist of adenosine receptors, based on a known analogy with endorphins, strophanthin, and cannabinoids. To test this hypothesis, they conducted a large-scale clinical-physiological study, the results of which are summarized in a monograph [2004]. Observing 66 women and 298 men receiving treatment at the Truskavets resort, the authors found a wide range of physiological activity of endogenous uric acid. Specifically, uricemia correlated with parameters of protein-nitrogen metabolism (levels of albumins and alpha1, alpha2, beta, and gamma globulin fractions in the blood, as well as urea), electrolyte metabolism (plasma and erythrocyte sodium and potassium levels, plasma calcium, magnesium, chloride, and phosphates, Na,K-ATPase activity, Ca-ATPase and Mg-ATPase activity of erythrocyte membranes), lipid metabolism, and lipid peroxidation, as well as glucose tolerance tests. In another group of patients, the authors found a link between uricemia levels and immune parameters ($CD4^+$, $CD8^+$, $CD19^+$ lymphocyte levels, Igg M, G, and A, as well as CIC in the blood, phagocytic function of neutrophils and monocytes). The third set of tests included hemostasis parameters, the fourth - parameters of the autonomic nervous system, hemodynamics, and bicycle ergometry. Changes in uricemia levels under the influence of balneotherapy were accompanied by changes in the mentioned parameters. Importantly, not only the magnitude of correlation coefficients but even their signs were determined by the phase of chronic calculous pyelonephritis and/or the type of general adaptation reaction.

The cited research has some limitations. Firstly, the authors only recorded the uric acid levels in the plasma in the morning, which reflects only the situational (phase) state of its metabolism, whereas a more informative and integrated parameter is its excretion with daily urine. Secondly, the immunotropic activity of uric acid was assessed only based on the

parameters of the blood immunogram, so the question of its influence on the parameters of thymocyte and splenocyte gram remains open and can only be resolved through animal experiments. Thirdly, the vegetotropic activity of uric acid was assessed only by the HRV parameters of Bayevsky RM, whereas temporal and spectral parameters of HRV are considered more informative. Fourthly, the battery of tests did not include hormones, at least immunotropic ones, which is important in the context of the concept of the neuro-endocrine-immune complex [Popovych IL, 2009], research in the field of which has been recognized by experts as the main trend of the last decade in Ukrainian balneology [Portnychenko AG, 2015]. Therefore, the study of the physiological activity of uric acid remains relevant.

Our goal was to assess the physiological activity of uric acid based on its associations with the parameters of the neuro-endocrine-immune complex and metabolism under the conditions of an experiment on healthy rats and clinical-physiological observation of patients with chronic pyelonephritis in remission. To achieve this goal, it was necessary to identify quantitative and qualitative variants-clusters of uric acid metabolism in healthy rats and clarify which parameters of the neuro-endocrine-immune complex and metabolism distinguish these clusters from each other. Analyze canonical correlation relationships between uricemia and uricosuria on one hand and parameters of the neuro-endocrine-immune complex and metabolism on the other. In the clinical-physiological observation of patients with chronic pyelonephritis in remission, identify quantitative and qualitative variants-clusters of uric acid metabolism and the characteristic parameters of the central and autonomous nervous, endocrine and immune systems, metabolism, and the microbiota of feces and urine associated with them. Analyze canonical correlation relationships between uric acid metabolism parameters, on the one hand, and parameters of the central and autonomous nervous, endocrine and immune systems, metabolism, and microbiota of feces and urine, on the other hand. Finally, analyze canonical correlation relationships between individual changes in uricemia and uricosuria under the influence of balneotherapy, on one hand, and parameters of the neuro-endocrine-immune complex, metabolism, and microbiota, on the other hand.

CHAPTER 1
PHYSIOLOGICAL AND PATHOGENIC ACTIVITY OF URIC ACID (LITERATURE REVIEW)

Uric acid is a small organic heterocyclic compound found in both lower and higher organisms. It is primarily synthesized in the liver, intestines, and other tissues such as muscles, kidneys, and vascular endothelium, as the end product of the exogenous pool of purines (adenine and guanine) derived from RNA and DNA. Additionally, living and dying cells break down their nucleic acids, converting adenine and guanine into uric acid. Deamination and dephosphorylation transform adenine and guanine into inosine and guanosine, respectively. The enzyme purine nucleoside phosphorylase converts inosine and guanosine into purine bases, hypoxanthine, and guanine, respectively, with guanine further deaminated by guanase into xanthine. Xanthine is then oxidized to uric acid by xanthine oxidase [Chaundary K et al, 2013; Maiuolo J et al, 2016].

Liu D et al [2019] demonstrated that in all organs examined in their study, the expression level of xanthine dehydrogenase highly correlated with the level of uric acid, as well as adenosine deaminase, an enzyme indirectly associated with uric acid synthesis. These findings led the authors to suggest that uric acid was locally synthesized from degraded nucleosides. As for urate oxidase, it was highly expressed mainly in the liver. The results indicate that uric acid was nearly the end product of purines in extrahepatic organs of rats and could be transported to the liver for further degradation.

In most species, uric acid can be further processed into highly soluble allantoin, even into ammonia [Smyth CJ et al, 1998]. Gout, as a condition, arose in humans and other primates after an evolutionary loss of urate oxidase, a catabolic enzyme of uric acid (mostly confined to the liver), which converts uric acid into allantoic acid.

Humans, along with several other primates, cannot oxidize uric acid into the more soluble compound allantoin due to the absence of the enzyme urate oxidase (uricase). Urate oxidase can metabolize uric acid into highly soluble 5-hydroxyisourate, which is further broken down into allantoic acid and ammonia, both of which are easily excreted by the kidneys. However, several primates, including humans, have lost the functional activity of urate oxidase because the uricase mRNA in humans contains two premature stop codons, rendering it a pseudogene [Chang BS, 2014; Kratzer JT et al, 2014]. Mammals that possess functional urate oxidase typically have serum uric acid levels of 10–20 μg/mL. In contrast, the uric acid level in humans and human-like primates is 3–10 times higher due to parallel nonsense mutations that led to pseudogenization of the urate oxidase gene during the early Miocene era [Chang BS, 2014; Kratzer JT et al, 2014].

Typically, the majority (2/3) of daily uric acid excretion occurs through the kidneys, with the remainder excreted through feces and sweat. Serum uric acid is freely filtered in the renal glomeruli, and approximately 90% of the filtered uric acid is reabsorbed, similar to amino acids and glucose, to a lesser extent sodium [Ames BN et al, 1981; Enomoto A et al, 2002; Maiuolo J et al, 2016]. These continuous efforts to block the elimination of metabolic "waste" suggest the fallacy of such an interpretation of uric acid and support the notion that it plays a significant physiological role. Let's delve further into this aspect.

Physiological Functions of Uric Acid

Endothelial Function. Unlike studies confirming the ability of uric acid to impair the integrity of vascular endothelial cells [Oberbach A et al, 2014], it has been shown that an extremely low level of uric acid in serum, caused by a loss-of-function mutation in the SLC22A12 gene encoding the URAT1 transporter in vascular endothelial cells and proximal renal tubules, leads to endothelial dysfunction in vivo [Sugihara S et al, 2015]. These findings challenge the notion that uric acid causes cardiovascular and renal diseases by disrupting the integrity and function of the endothelium [Sugihara S et al, 2015; Iso T et al, 2015; Nery RA et al, 2015]. Indeed, uric acid may play a fundamental role in tissue healing by initiating an

inflammatory process necessary for tissue repair, scavenging oxygen free radicals, and mobilizing endothelial precursor cells [Nery RA et al, 2015].

Uric acid serves as a potent mediator of type 2 immune responses. Elevated uric acid levels have been detected in the peritoneal cavity of mice after injection of the widely used clinical adjuvant alum (aluminum hydroxide) [Kool M et al, 2008; 2008a; 2011]. Experiments involving intraperitoneal injections of harmless ovalbumin protein or ovalbumin with alum to mice, in combination with 0 or 50 units of uricase, demonstrated that uric acid is necessary and sufficient for inducing antibody immune responses against ovalbumin [Kool M et al, 2011].

It has been established that the adjuvanticity of Th2, provided by alum, is mediated through cell damage leading to the induction of uric acid, which acts as a danger signal promoting the generation of inflammatory dendritic cells derived from monocytes [Kool M et al, 2008; 2008a; 2011]. These findings document the key role of uric acid in inducing protective antibody responses to various human vaccines that include alum as an adjuvant.

The release of uric acid has also been demonstrated in the airways of asthma patients and mice exposed to allergens and found to be necessary for enhancing Th2 cell immunity, eosinophilic airway inflammation, and bronchial hyperreactivity to inhaled innocuous proteins and house dust mite allergens. Additionally, the administration of sodium urate (MSU) crystals along with the inhalation of harmless proteins induced vigorous type 2 immunity. The adjuvanticity of uric acid was mediated through the activation of spleen tyrosine kinase (Syk) and phosphoinositide 3 (PI3) kinase. Thus, uric acid was identified as a crucial initiator and amplifier of allergic inflammation in vivo [Kool M et al, 2011].

Allergens, which often contain proteases, particularly cysteine proteases, as well as cysteine peptidases like papain and bromelain, are capable of stimulating barrier epithelial cells to produce type 2 cytokines such as thymic stromal lymphopoietin (TSLP), interleukin (IL)-25, and IL-33, which are responsible for skewing the immune environment toward a type 2 axis and hypersensitive inflammation. It has been shown that allergens and cysteine peptidases, like papain, induce stress and damage to tissue cells, especially barrier epithelial cells, leading to the release of uric acid. Uric acid activates epithelial cells to release TSLP and IL-33, but not IL-25, and has been identified as a key factor regulating the development of type 2 immune responses to cysteine protease allergens [Hara K et al, 2014].

Epithelial cells in the human and mouse respiratory tracts constitutively secrete uric acid. The exposure of mice to environmental particulate matter and house dust containing cysteine peptidases led to increased production and secretion of uric acid by mucosal epithelial cells and resulted in allergic sensitization. This sensitization was shown to be inhibited by uricase [Gold MJ et al, 2016]. Indeed, uric acid is now recognized as an alarm factor, similar to ATP, high mobility group box 1 (HMGB1) protein, interleukin-33 (IL-33), and a prominent and potent mediator of type 2 immune responses involving epithelial cells, innate lymphoid cells, eosinophils, basophils, and mast cells [Anthony RM et al, 2007; Kool M et al, 2008; 2008a; 2011; Willart MA et al, 2013; Lambrecht BN et al, 2014; Hara K et al, 2014; Gold MJ et al, 2016].

Resistance to parasites. The protective immune response against many helminth parasites relies on type 2 immune responses [Anthony RM et al, 2007]. According to El Ridi R and Tallima H [2017], there is no information available regarding the contribution of uric acid to the development of protective type 2 immune responses against nematodes. As for schistosomiasis, cysteine peptidases such as papain, Schistosoma mansoni B1 cathepsin (SmCB1), Schistosoma mansoni L3 cathepsin (SmCL3), and Fasciola hepatica L1 cathepsin (FhCL1) did not induce allergic reactions in mice or hamsters. Instead, they showed a 50-65% reduction in S. mansoni and Schistosoma haematobium infections by generating polarized (papain, SmCL3, FhCL) or predominant (SmCB1) type 2 responses involving the release of TSLP, IL-4, IL-5, IL-13, and the generation of IgG1 antibodies [El Ridi R et Tallima H, 2013; El Ridi R et al, 2014; 2014a; Tallima H et al, 2015; Abdel Aziz N et al, 2016].

Subcutaneously injected papain or helminth cysteine peptidase interacts with epithelial cells, leading to the release of TSLP, the main cytokine in innate and adaptive type 2 immune

responses [El Ridi R et Tallima H, 2013; Lambrecht BN et al, 2014; Hammad H et al, 2015; Abdel Aziz N et al, 2016].

The generated type 2 cytokines recruit and activate innate type 2 lymphoid cells, eosinophils, basophils, and mast cells, as well as support the production of IgG1 antibodies against cysteine peptidase, thus directing the immune system, at the time of infection, toward a type 2 immune response. Eosinophils, basophils, and mast cells, with their cytotoxic proteins, proteases, peroxidases, and extracellular traps, join forces to harm migrating schistosome larvae and notably damage the endothelial cells of blood capillaries. Endothelial cell trauma in blood sinusoids, when worms start to grow, feed on blood, excrete and secrete cysteine peptidases, triggers the release of uric acid. Elevated uric acid levels in the lungs and liver of immunized and non-immunized animals infected with schistosomes are in full accordance with the fact that uric acid is constitutively present in normal cells, particularly liver cells, intestinal cells, and vascular endothelial cells, and its concentration increases when cells are damaged, releasing uric acid from dying cells [Ames BN et al, 1981; Shi Y et al, 2003; Kool M et al, 2008; 2008a; 2011; Kono H et al, 2010; Ghaemi-Oskoue F et Shi Y, 2011; Willart MA et al, 2013; Hara K et al, 2014; Lambrecht BN et al, 2014; Hammad H et al, 2015; Gold MJ et al, 2016].

In the liver sinusoids, when the worms begin to grow, ingest blood, excrete, and secrete cysteine peptidases, type 2 immune effectors and cytokines damage hepatocytes, triggering uric acid release. Uric acid has been linked to non-alcoholic fatty liver disease (NAFLD), and it has been demonstrated to play a causative role in liver fat accumulation by stimulating increased synthesis and release of fatty acids, especially arachidonic acid, from lipid depots and cell membranes [Araya J et al, 2004; Szabo G et al, 2012; Wrang W et al, 2013; Choi YJ et al, 2014; Ma DW et al, 2016; Spahis S et al, 2015; Zhang X et al, 2015].

Thanks to its potent antioxidant properties, uric acid hinders the activity of lipoxygenases and serves as a substrate for the enzyme cyclooxygenase. Thus, it allows arachidonic acid to gain access to parasites and mediate their demise, as arachidonic acid has been found to be an effective schistosomicide both in vitro and in vivo in mice, hamsters, and children infected with S. mansoni [El Ridi R et al, 2010; 2012; 2016; Selim S et al, 2014; Barakat R et al, 2015].

El Ridi R and Tallima H [2017] formulated the concept of the anti-schistosomal protective axis—cysteine peptidase-induced type 2 response/uric acid/arachidonic acid, in which arachidonic acid is considered not only a safe and effective drug but, more importantly, a natural schistosomicide [Amaral KB et al, 2016]. Since mice and hamsters have functional uricase and typically have serum uric acid levels of 10–20 μg/mL, unlike humans where serum uric acid levels are significantly higher [Chang BS, 2014; Kratzer JT et al, 2014], it is expected that a cysteine peptidase-based vaccine will achieve significantly higher levels of protection in children than in mice and hamsters [Tallima H et al, 2017].

Antioxidant. Uric acid serves as a powerful antioxidant in the human body. In fact, over half of the plasma's antioxidant capacity in humans is derived from uric acid [Ames BN et al, 1981; Becker BF, 1993]. Uric acid is a potent scavenger of reactive oxygen species (ROS) and peroxynitrite and functions as an antioxidant [Ames BN et al, 1981; Becker BF, 1993; Glantzounis GK et al, 2005; Sautin YY et al, 2008]. It is found in high concentrations in the cytosol of normal human and mammalian cells, particularly in the liver [Shi Y et al, 2003], endothelial cells of blood vessels, and nasal secretions in humans, where it serves as an antioxidant [Peden DB et al, 1990; 1993].

Protection against Neurological and Autoimmune Diseases. Neurons are predominantly distributed in the brain. According to current understanding, the brain of rats constitutes about 0.4% of body mass but consumes 10-20% of cardiac output. Because the brain requires a significant amount of oxygen to support its complex function, genes directly involved in ATP synthesis should be expressed at high levels. It's not surprising that the gene expression levels were generally higher than in other organs. Theoretically, during biological oxidation, a substantial amount of oxygen radicals will also be generated, which can then potentially damage neurons.

Uric acid is a potent scavenger of peroxynitrite and an antioxidant. One clinical observation supporting its antioxidant action is the almost complete absence of multiple sclerosis in gout patients [Hooper DC et al, 1998]. Conversely, there is a strong association between low levels of uric acid in blood serum and an increased risk of developing multiple sclerosis [Hooper DC et al, 1998; Drulovic J et al, 2001; Sotgiu S et al, 2002; Rentzos M et al, 2006]. Both in humans and in a mouse model of multiple sclerosis (experimental autoimmune encephalomyelitis), a high level of uric acid in the blood serum can halt the progression of the disease. It is also suggested that moderate levels of uric acid may provide protection during ischemic stroke [Seet RCS et al, 2010]. Peroxynitrites and reactive oxygen species are believed to be responsible for myelin degradation in multiple sclerosis and can be inhibited by high levels of uric acid. Based on this knowledge, some reports have even concluded that uric acid plays a role in neuroprotection [Hosomi A et al, 2012]. A meta-analysis of published data convincingly showed that patients with multiple sclerosis have lower levels of uric acid in their blood serum compared to healthy controls, identifying low uric acid levels as a potential biomarker for multiple sclerosis [Wang L et al, 2016].

Low levels of uric acid in blood plasma have also been associated with neurological disorders [Alvarez-Lario B et al, 2011; Fang P et al, 2013; Wang L et al, 2016], Parkinson's disease [Annanmaki T et al, 2007; De Vera M et al, 2008; Schlesinger I et al, 2008; Andreadou E et al, 2009; Pan M et al, 2013], and Alzheimer's disease [Maesaka JK et al, 1993; Lu N et al, 2016]. Additionally, conditions like Pemphigus vulgaris, an autoimmune disorder characterized by the formation of skin and mucous membrane blisters [Yousefi M et al, 2011], and flat lichen, an autoimmune inflammatory disease of mucous and skin tissue, have also been linked to low levels of uric acid in saliva [Bakhtiari S et al, 2017].

The theory, first proposed in the 1950s, suggests that uric acid is a structural homolog of caffeine (which, in turn, is a structural homolog of adenosine) and that high levels of uric acid contributed to alertness in primates and the development of human intelligence [Sofaer JA et Emery AF, 1981]. However, uricase deficiency, a factor that promotes increased uric acid, was considered a significant step in the evolution and development of the human brain [Johnson RJ et al, 2005; Alvarez-Lario B et al, 2010]. Nevertheless, uricase deficiency is a common phenomenon in lower animals such as birds and reptiles [Keebaugh AC, Thomas JW, 2010].

On the other hand, the heart, which is the second organ with high energy consumption, also had low uric acid levels. Similarly, the duodenum had the highest uric acid levels among organs, but there were no reports indicating that the intestinal tract was an organ with high energy consumption. Therefore, a study by Liu D et al [2019] concluded that uric acid likely does not play a significant role in protecting neurons by scavenging oxygen radicals, at least in a physiological state, although it is a genuine restorative substance.

Blood Pressure Support. One alternative theory suggests that uric acid retention may compensate for hyponatremic conditions to maintain relatively high blood pressure, and this may have been advantageous in past epochs when dietary salt availability was limited [Watanabe S et al, 2002].

However, epidemiological data indicate a strong correlation between hyperuricemia and hypertension [Mortada I, 2017]. Nevertheless, the relationship between uric acid and blood pressure is considered associative rather than causative. Both conditions are age-dependent, and there have been rare specific experimental evidence confirming the hypothesis that hyperuricemia can lead to hypertension and vice versa. Additionally, there have been almost no indications of uric acid-lowering drugs being associated with blood pressure reduction [Cammalleri L, Malaguarnera M, 2007]. According to the analysis, uric acid likely does not play a significant role in supporting blood pressure.

Pathogenic Potential of Uric Acid.

Uric acid as an indicator of cell death. Uric acid is a purine metabolite, and purines in the body primarily come from endogenously degraded nucleosides and partially from the diet. Nucleosides can originate from used DNA or RNA. Cells in an energetic state of metabolism

require a lot of mRNA for protein synthesis, and the used mRNA will degrade. Then, some of them will be recycled to synthesize new mRNA, and some will be converted to uric acid. However, when a cell dies, the entire nucleus, where a lot of DNA is located, along with the RNA in the cytoplasm, can degrade, and many of the nucleic acids will be converted to uric acid, rather than being recycled. Since the nucleus contains even more nucleotides than the cytoplasm, dead cells will lead to increased uric acid production.

Unlike the release of nucleosides from the nucleus, the release of nucleosides from the cytoplasm doesn't signify anything. In other words, there was no significant correlation between uric acid and energy metabolism. RCD (regulated cell death) is the primary physiological pathway of cell death, and Casp3 (caspase-3) is the major executor of RCD pathways [Galluzzi L et al, 2018]. Since uric acid in the organ strongly correlated with gene expression levels, the results of Liu D et al [2019] confirmed that uric acid is primarily a result of cell death. However, in a physiological state, dead cells are often replaced by regenerated cells, a process associated with the activation of Ki67, an important nuclear protein [Zhou Y, Hu W et al, 2017; Gerring Z et al, 2015]. Since cell proliferation in the heart and liver was a major process in neonatal rats, cell death in these two neonatal organs was unlikely to occur. However, the gastrointestinal tract in both neonatal and normal rats may be associated with many deaths and cell regeneration to transform itself.

Pathogenic Potential of Uric Acid in Cancer. In clinical settings, progressive cancer often accompanies the death of tumor cells, such as breast cancer. Degraded nucleosides in dead tumor cells transform into uric acid and lead to increased uricemia. Interestingly, there was no significant correlation between Ki67 (a marker of cell proliferation) and uricemia in breast cancer patients, only a very slight trend. This phenomenon was different from what was observed in normal rats. The reason might be associated with cell death, which leads to cell regeneration in normal rats, while proliferation of tumor cells leads to cell necrosis in cancer patients. When breast cancer is treated with chemotherapy, many tumor cells are killed. Nucleosides in the cells are converted into uric acid, leading to increased uricemia. Indeed, elevated uricemia, including hyperuricemia and even gout, has been widely considered an important marker of tumor lysis syndrome [Cammalleri L, Malaguarnera M, 2007; Koratala A, 2017].

Liu D et al [2019] investigated the biological function of uric acid. The authors conducted a correlation analysis between uric acid in the organs of rats and gene expression (measured by FPKM values). During diagnosis, they analyzed the uric acid levels in the serum of breast cancer patients or patients with benign breast tumors, as well as in breast cancer patients immediately after chemotherapy. There were 1,937 mRNAs whose expression levels significantly correlated with uric acid levels, and most of them were related to purine or nucleoside metabolism, cellular metabolism, cell cycles, and cell death pathways. Further analysis showed that uricemia strongly correlated with cell death, not cell viability. Uricemia in breast cancer patients was higher than in patients with benign breast tumors, and uricemia increased after chemotherapy. All results suggest that uric acid is primarily synthesized from local nucleosides derived from dead cells and can be an important biomarker for cell death, rather than an antioxidant for neuroprotection.

Cardiovascular Diseases and Uric Acid. Hyperuricemia has been shown to be associated with the development of hypertension and cardiovascular diseases through the induction of growth factors, hormones, cytokines, and autacoids [Sanchez-Lozada LG et al, 2006; Mazzali M et al, 2010; Kanbay M et al, 2016]. Experimental studies have demonstrated that uric acid can penetrate into the smooth muscle cells of blood vessels through the organic anion transport system, leading to the activation of multiple signal transduction pathways, culminating in increased expression of inflammatory mediators. The consequences include elevated blood pressure, hypertrophy of vascular smooth muscle cells, and hypertension [Mazzali M et al, 2010; Kanbay M et al, 2013]. Additionally, soluble uric acid induces dysfunction of vascular endothelial cells, including changes in cell proliferation and the induction of cell aging and apoptosis by activating the renin-angiotensin system (the hormonal system that regulates sodium

concentration in the blood plasma and blood pressure) and initiating the production of reactive oxygen and nitrogen species, as well as endoplasmic reticulum stress [Yu MA et al, 2010; Park JH et al, 2013; Li P et al, 2016].

Metabolic Syndrome and Uric Acid. Metabolic syndrome is the term used to describe a cluster of risk factors that pose a threat to heart disease and other health issues, including diabetes and stroke. Cardiovascular diseases, type 2 diabetes, and non-alcoholic fatty liver disease (NAFLD) are manifestations of metabolic syndrome [Hjortnaes J et al, 2007; Sanchez-Lozada LG et al, 2006; Choi HK et Curhan G, 2007; Choi HK et Ford ES, 2007; Jalal DI, 2016; Kanbay M et al, 2016].

Uric acid has been implicated in the development and progression of metabolic syndrome. Elevated uric acid levels are associated with an increased risk of developing metabolic syndrome, and it has been suggested that uric acid may contribute to the development of insulin resistance and other metabolic abnormalities that characterize the syndrome [Kanbay M et al, 2016].

Additionally, uric acid is linked to the development of non-alcoholic fatty liver disease (NAFLD), which is one of the components of metabolic syndrome. Elevated uric acid levels have been associated with the severity of NAFLD, and it is believed that uric acid may play a role in the pathogenesis of this condition [Jalal DI, 2016].

So, uric acid appears to be involved in the complex interplay of factors contributing to metabolic syndrome and its associated health risks.

Insulin Resistance and Type 2 Diabetes. An elevated level of serum uric acid is also considered one of the best independent predictors of diabetes and typically precedes the development of both insulin resistance and type 2 diabetes. This is because it has been found that a quarter of diabetes cases can be attributed to high levels of serum uric acid, and an elevated uric acid level in the bloodstream is closely associated with insulin resistance and type 2 diabetes [Dehghan A et al, 2008]. In response to conflicting findings [Sluijs I et al, 2015], a meta-analysis of prospective cohort studies [Lv Q et al, 2013] and a critical review [Johnson RJ et al, 2015] have confirmed that serum uric acid is a strong and independent risk factor for diabetes development in middle-aged and older individuals.

The increase in consumption of fructose-containing beverages, food, and table sugar (sucrose = glucose + fructose) over the past centuries has led to increased weight gain, accumulation of visceral and liver fat, insulin resistance, and diabetes. This dietary pattern has also resulted in increased uric acid production, which contributes to the development of metabolic syndrome, including diabetes.

In the liver, the enzyme ketohexokinase phosphorylates fructose, leading to a decrease in intracellular phosphates and ATP. The reduction in intracellular phosphates activates AMP deaminase, which catabolizes AMP to inosine monophosphate and, ultimately, to uric acid through the hypoxanthine-xanthine pathway [Schwarzmeier JD et al, 1974; Johnson RJ et al, 2013]. Subsequently, the increased amount of intracellular uric acid is released into the bloodstream, inducing inflammation in endothelial cells, muscle fibers of renal vessels, and Langerhans islets in the pancreas [Johnson RJ et al, 2013]. Additionally, elevated serum uric acid levels significantly correlated with the severity of albuminuria and diabetic retinopathy in patients with type 2 diabetes [Liang CC et al, 2016].

Non-alcoholic fatty liver disease (NAFLD). The high levels of serum uric acid in numerous clinical and experimental studies [Araya J et al, 2004; Szabo G et Csak T, 2012; Wang W et al, 2013; Choi YJ et al, 2014; Zhang X et al, 2015]. The role of serum uric acid in the development of NAFLD has recently been elucidated through the indirect generation of uric acid, leading to the increased expression of thioredoxin (TXN)-interacting protein (TXNIP) and ROS-dependent dissociation of TXN from TXNIP. This interaction then activates NLRP3, initiating an inflammatory process in both parenchymal and non-parenchymal liver cells and resulting in the release of IL-1β and IL-18. The inflammatory signal of the ROS-TXNIP pathway induces the dysregulation of genes related to lipid metabolism and the accumulation of lipids due to the excessive expression of lipogenic enzymes such as acetyl-coenzyme A (CoA) carboxylase 1,

fatty acid synthase, and stearoyl-CoA desaturase 1 [Szabo G et Csak T, 2012; Wang W et al, 2013; Zhang X et al, 2015].

Another mechanism of fat accumulation in the liver mediated by uric acid involves uric acid inducing oxidative stress in the endoplasmic reticulum of hepatocytes, leading to the breakdown into an active form and translocation of the Sterol Regulatory Element-Binding Protein (SREBP), which regulates the expression and activity of lipogenic enzymes [Choi YJ et al, 2014]. Analysis of the fatty acid composition of liver phospholipids in NAFLD patients revealed a significant increase in arachidonic acid content and the ratio of polyunsaturated fatty acids n-6/n-3 compared to control values [Araya J et al, 2004]. It has been shown that the plasma fatty acid profile of individuals with NAFLD is associated with an increase in omega-6 polyunsaturated fatty acids, especially arachidonic acid, compared to healthy controls [Spahis S et al, 2015; Ma DW et al, 2016].

Disorders of kidney function. It has been shown that the regulation of uric acid transport in the renal tubules depends on several proteins belonging to the organic anion transporter (OAT) family. The product of the SLC22A12 gene, urate transporter 1 (URAT1), is highly, if not exclusively, expressed in the kidneys on the apical membrane of proximal tubules and was the first identified reabsorptive transporter for urates. OAT4, similar to URAT1 in location and function, is also involved in the reabsorption of uric acid. OAT1 and OAT3, encoded by the SLC22A6 and SLC22A8 genes, respectively, are located on the basolateral membrane of proximal tubules in the kidneys and form the renal tubular secretory pathway primarily involved in the luminal excretion of uric acid [Maiuolo J et al, 2016; Bruno CM et al, 2016]. Additionally, the glucose transporter GLUT9 has been demonstrated to play an instrumental role in the reabsorption and exit of uric acid from the interstitium, as mutations in its encoding gene SLC2A9 are associated with abnormalities in uric acid utilization [Doering A et al, 2008; Bruno CM et al, 2016].

Increased uric acid production, impaired renal excretion, or a combination of both can lead to hyperuricemia [Maiuolo J et al, 2016; Bobulescu IA et al, 2012]. Hyperuricemia increases the risk of acute kidney injury [Xu X et al, 2017], impairs the contractile activity of intraglomerular mesangial cells [Convento MS et al, 2011], and causes damage to mesangial and proximal tubular epithelial cells, possibly through TLR-dependent regulation of NLRP3 and IL-1β [Xiao J et al, 2015; 2015a]. Additionally, hyperuricemia is an independent risk factor for chronic kidney disease in type 2 diabetes due to endothelial cell damage and the release of the alarmin HMGB1, which stimulates TLRs to induce proinflammatory and chemotactic cytokines, smooth muscle cell proliferation, and NLRP3 inflammasome activation [Kim SM et al, 2015].

Furthermore, uric acid can accumulate in the kidneys, leading to the formation and deposition of stones. Kidney stones and urinary tract infections are the most common urinary tract problems. Uric acid stones account for 10% of all kidney stones and are the second most common cause of urolithiasis after calcium oxalate and phosphate stones. The primary risk factor for uric acid crystallization and stone formation is a low urinary pH (below 5.5) due to impaired uric acid excretion in the urine. The main causes of low urinary pH, in addition to high uric acid excretion, include chronic diarrhea, severe dehydration, and diabetic ketoacidosis [Jalal DI, 2016].

Gout. Gout is a condition that arises due to the deposition of monosodium urate (MSU) crystals in the joints and periarticular tissues, not soluble uric acid. These crystals do not always cause inflammation in the joints. Initially, they must be coated with serum proteins before interacting directly with the cell membrane of joint cells or through receptors. Subsequently, they stimulate the cytosolic molecular platform involved in innate immunity, including cysteine protease and caspase 1-activating NOD-like receptor P3 (NLRP3) inflammasome, which is responsible for the proteolytic cleavage of pro-interleukin-1β (IL-1β) and the maturation and release of active IL-1 in the joint [Martinon F et al., 2006].

Neutrophils are recruited and activated in response to the release of IL-1, producing reactive oxygen species (ROS), proteolytic enzymes, extracellular traps, and pro-inflammatory

chemokines and cytokines, which, in turn, recruit and activate macrophages. The formation of neutrophil extracellular traps (NETs) is governed by IL-1β and has been shown to contain the alarmin HMGB1, which sustains the pro-inflammatory potential of NETs. Accordingly, the pathogenesis of acute gout results from the cross-talk between MSU crystal-induced NLRP3 inflammasome activation, IL-1 release, and neutrophil accumulation [Martinon F et al., 2006; Mitroulis I et al., 2011; 2013; Busso N et Ea HK, 2012; Amaral FA et al., 2012].

The steps of alarm. Monosodium urate (MSU) crystals have been identified as an endogenous danger signal that forms after the release of uric acid from dying cells. Damaged cells rapidly break down their RNA and DNA, releasing pyrimidines that are catabolized to beta-alanine and beta-aminoisobutyrate, and purines that are catabolized to uric acid, leading to its accumulation.

The cytosol contains approximately 4 mg/ml of uric acid with a significant increase after the degradation of nucleic acids from damaged cells [Shi Y et al., 2003; Martinon F, 2010; 2010a]. Uric acid is soluble in biological fluids up to 70 mg/l (417 μM/l), and it is completely soluble in human blood, which has a constitutive concentration of 40–60 mg/l (238-357 μM/l). In humans, about 70% of uric acid disposal occurs through the kidneys, and in 5–25% of individuals, impaired renal excretion leads to hyperuricemia (>120 mg/l or 714 μM/l). An increase in uric acid concentration above its solubility level leads to its precipitation as monosodium urate (MSU) crystals, especially in joint spaces, causing severe inflammatory episodes in some people, while most individuals with hyperuricemia remain asymptomatic and do not develop gout symptoms [Martinon F, 2010; Ghaemi-Oskouie F et Shi Y, 2011]. It is likely that the development of gout requires hyperuricemia to be associated with defects in genes regulating urate transport and homeostasis, such as the urate-anion exchanger, urate transporter 1 (URAT1), and glucose transporter GLUT9 [Doering A et al., 2008; Dalbeth N et Merriman T, 2009; Martinon F, 2010].

Deposited urate crystals primarily accumulate in joint connective tissues, tendons, kidneys, and occasionally in heart valves and the pericardium, readily interacting with serum proteins [Spilberg I, 1975]. It has been shown that a group of mouse IgM antibodies facilitates uric acid crystallization in vitro and binds to monosodium urate (MSU) crystals [Kanevets U et al., 2009; Martinon F, 2010].

Deposited monosodium urate (MSU) crystals in joint spaces interact with resident macrophages and infiltrating neutrophils, monocytes, as well as non-hematopoietic synovial and endothelial cells. All these cells can phagocytose or endocytose crystals, leading to their activation and release of hydrolytic enzymes, reactive oxygen species, numerous danger-associated molecular patterns (DAMPs), which can be sensed by cell surface receptors and intracellular receptors of the innate immune system [Busso N et So A, 2010; 2012].

Sodium urate crystals adopt a needle-like structure and are expected to damage the cell's plasma membrane of surrounding cells. This cellular injury is sensed by extracellular receptors from the Toll-like receptor (TLR) family, specifically TLR-2 or TLR-4 [Busso N et So A, 2010; 2012; Joosten LA et al., 2010; 2011]. The response involves the generation of pro-IL-1β and TNF. Additionally, crystals are taken up by resident phagocytes, leading to an increase in intracellular sodium content, changes in cell osmolarity, water influx, and subsequently, a decrease in intracellular potassium concentration. It is evident that this danger signal can activate a member of the nucleotide-binding and oligomerization domain (NOD)-like receptor (NLR) subfamily, which includes NLRP1, NLRP3, and NLRC4.

The NLRP3 receptor essentially consists of a central NOD domain, a leucine-rich repeat (LRR) sensor domain at the carboxyl end, and a pyrin effector domain (PYD) at the amino end. Stimulation of the sensor domain leads to molecule oligomerization and the recruitment of an adaptor protein called ASC (apoptosis-associated speck-like protein containing a caspase recruitment domain). The PYD domain of NLRP3 interacts with the PYD domain of ASC, which additionally contains an activation and recruitment domain for caspases [Tschopp J et Schroder K, 2010] (Figure 1.1).

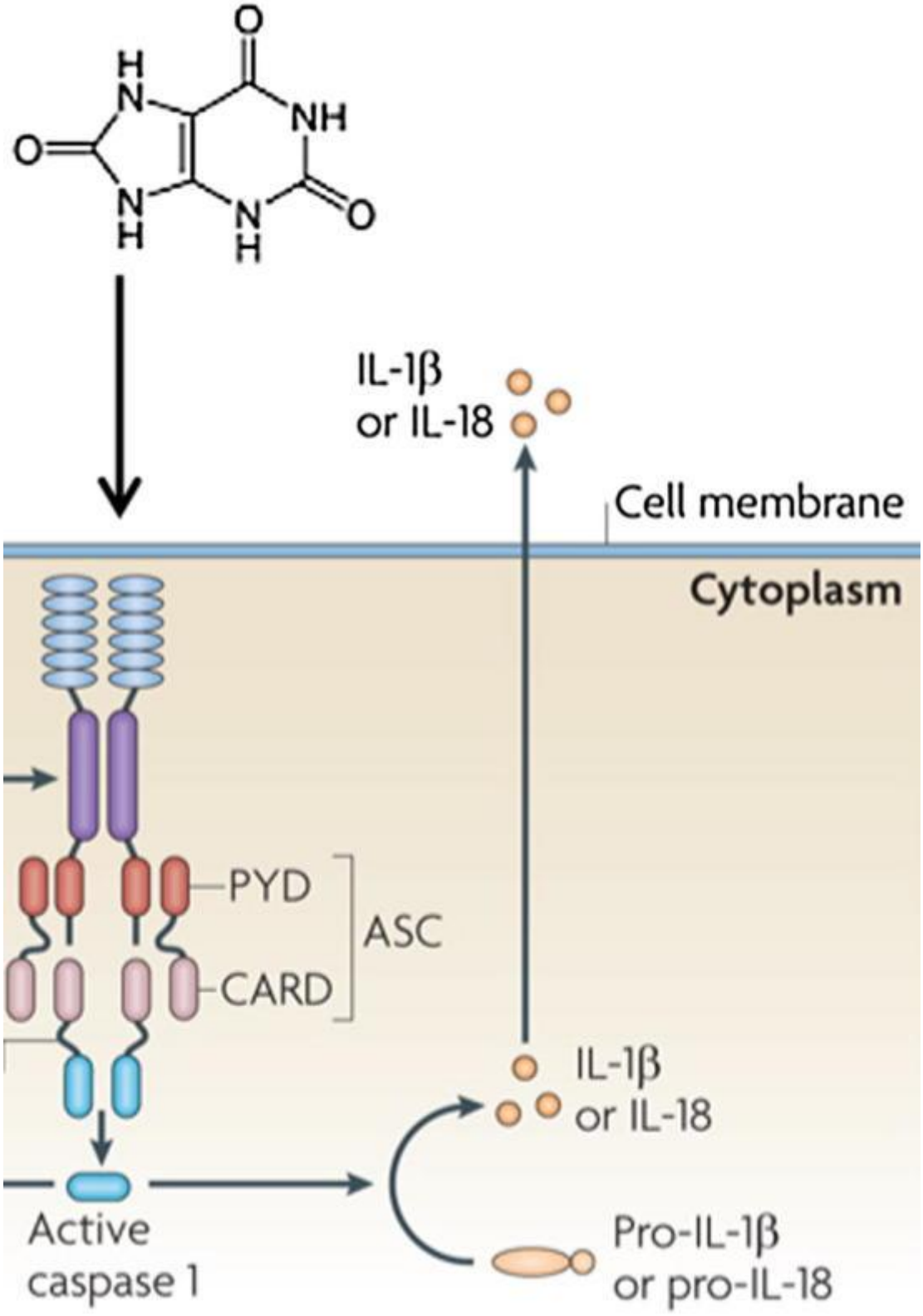

Figure 1.1. The Key Alarm Step [Tschopp J and Schroder K, 2010].

Uric acid, C5H4N4O3, 7,9-dihydro-1H-purine-2,6,8(3H)-trione, with a molecular mass of 168 Da, is a product of the metabolic breakdown of purine nucleotides (adenine and guanine). Sodium urate (MSU) crystals in the joints stimulate the inflammasome, NLRP3. The leucine-rich repeat (LRR) domain at the carboxyl end of NLRP3 acts as a sensor for pathogen-associated (PAMP) or danger-associated (DAMP) molecular structures that arise due to MSU.

Ligand binding leads to receptor oligomerization and enables the amino-terminal pyrin domain (PYD) to interact with the adapter ASC, which recruits pro-caspase-1 through its CARD domain and subsequently activates it. The active cysteine protease processes pro-IL-1β, which is then ready to be released from the cell as the biologically active proinflammatory agent, IL-1β (17 kDa).

The CARD domain of ASC can recruit and activate caspase-1, which cleaves the inactive 31 kDa precursor of IL-1β (pro-IL-1β) into the mature, biologically active 17 kDa IL-1β and additionally induces a lytic form of cell death known as pyroptosis [Martinon F et al, 2006; Franchi L et al, 2009; Schroder K et al, 2010; Tschopp J et Schroder K, 2010; Schorn C et al, 2011; Broz P et Dixit VM, 2016].

However, in vitro and in vivo studies have not fully reproduced NLRP3- and caspase-1-dependent IL-1β release caused by sodium urate crystals in several instances [Joosten LA et al, 2010; 2011]. Furthermore, the presence of free fatty acids was required for crystals to induce gouty-like reactions in mice via TLR-2 interaction, ASC activation, and caspase-1 activation but not NLRP3 and IL-1β release [Joosten LA et al, 2010].

The controversy regarding the mechanism of urate-induced inflammation in gout is not entirely resolved, but all researchers agree on the association of sodium urate with the release of IL-1β, recruitment and activation of neutrophils, and their roles in inflammation [Desaulniers P et al, 2006]. The functions of IL-1β are diverse and include inducing fever (an endogenous pyrogen) by resetting the hypothalamic thermostat in the brain, promoting collagenase expression and muscle and cartilage breakdown (catabolin), causing inflammation, and recruiting and activating neutrophils [Martinon F et al, 2006; Desaulniers P et al, 2006; Martinon F, 2010; 2010a; Popa-Nita O et Naccache PH, 2010; Mitroulis I et al, 2011; Ghaemi-Oskoue F et Shi Y, 2011; 2013; Amaral FA et al, 2012; Busso N et Ea HK, 2012].

Uric acid is also considered a danger signal responsible for exacerbating osteoarthritis through inflammasome activation, as a direct correlation has consistently been observed between the severity of knee osteoarthritis and synovial, but not serum, uric acid levels, IL-1β, and IL-18 [Denoble AE et al, 2011; Schett G et al, 2016].

The precipitation of sodium urate and crystallization is likely. A crucial step in the development of gout, as the pro-inflammatory effect of uric acid depends on its conversion into sodium urate crystals. However, the biology of crystal formation is not yet fully understood. Typically, a serum uric acid level above 405 μM/L (6.8 mg/dL) is considered hyperuricemia. Still, it is challenging to replicate crystallization at this concentration in standard in vitro buffers [Kanevets U et al, 2009]. Additionally, gout has a rapid onset, while the crystallization process in vitro occurs relatively slowly. These observations suggest that there may be mechanisms that promote crystal formation in vivo. It is noted that uric acid levels inside cells can be very high [Shi Y et al, 2003]. However, reports of intracellular urate crystal formation are not available. One possible determinant could be the availability of sodium, which is much higher in the bloodstream than in the cytosol. Hyperuricemia is associated with excessive consumption of certain dietary items, particularly red meat and alcohol. Furthermore, widespread cell death often leads to persistent urate precipitation. Therefore, cancer treatment (e.g., chemotherapy and radiation therapy) is a situation where uric acid activity levels need to be actively controlled to prevent gout attacks [Steele TH, 1999]. Nevertheless, a high level of uric acid in the bloodstream does not necessarily lead to gout, as only about 10% of hyperuricemic individuals experience gout episodes [Vitart V et al, 2008]. However, gout can occasionally occur in individuals with normal uric acid levels [Schlesinger N et al, 2009]. It is evident that additional factors must be involved in urate precipitation. Crystals rarely appear in central organs or deep cavities but are usually found in extremities, primarily due to the lower temperature in the distal parts of the joints. Over the past few decades, mathematical models have been proposed to outline the rate of crystallization regarding environmental factors such as temperature, pH, salt, vibration, and even the materials of the container in which experiments are conducted [Kippen I et al, 1974; Tak HK et al, 1980; Fiddis RW et al, 1983; Iwata H et al, 1989].

One of the recent advances in understanding sodium urate precipitation involves the potential role of antibodies. The participation of natural antibodies in this process was first reported by Kam M et al [1992; 1994]. They described an unexpected phenomenon at the time: serum from gout patients could precipitate uric acid solutions, while control serum could not. To further investigate this, they immunized rabbits with sodium urate. The resulting immune serum precipitated soluble uric acid into crystals but did not induce crystallization of other salt solutions. Conversely, serum from rabbits immunized with crystals composed of two different control salts could precipitate those specific crystals. Cross-precipitation was not observed. The active factor was traced to serum IgG. This led them to speculate that serum antibodies could specifically recognize crystalline surfaces and may serve to stabilize initial crystalline nuclei, thus limiting the rate of crystallization. In other words, these antibodies seemed to push the solubility/crystallization equilibrium to the latter.

Kanevets U et al [2009] found that mice also had antibodies that precipitated uric acid. These antibodies turned out to be natural without any immune induction. Unlike the data from previous authors, in this study, almost all urate-binding antibodies were IgM, existing in both sodium urate crystal-immunized mice and non-immunized mice. Purified IgM antibodies facilitated the precipitation of sodium urate from uric acid solution in a buffered phosphate salt solution. Injection of these antibodies into recipient mice reduced their serum uric acid solubility, indicating the formation of sodium urate crystals in the host. Most importantly, B cell-deficient mice (i.e., mice unable to produce antibodies against sodium urate) could not perceive uric acid as a danger signal (i.e., they did not exhibit crystal-dependent immune responses). However, when the same mice were administered purified antibodies, they were able to detect the presence of uric acid in an immunization mode and elicit CD8 T-cell responses against the co-administered antigen. Overall, according to Ghaemi-Oskouie F et Shi Y [2011], antibodies against sodium urate crystals, among other factors, likely play a significant role in the phase transition and, consequently, the biological functions of these crystals.

Inflammatory pathways. Sodium urate crystals can be recognized by innate phagocytes, including dendritic cells (DCs), macrophages, and neutrophils. It has been shown that antigen-presenting cells (APCs) can sense uric acid as one of the pro-inflammatory endogenous signals released by damaged cells or tissues. These molecular structures associated with damage can trigger a systemic inflammatory response similar to molecular patterns associated with pathogens [Shi Y et al., 2003]. There is a long list of inflammatory pathways involved in the response to sodium urate crystals. Nevertheless, research in this field has primarily focused on two main areas.

One direction is rooted in classical immunology, concentrating on processes such as opsonization of antibodies and complement fixation. The other, more contemporary, direction of research focuses on the role of recognizing the immune pattern structure of the crystal. This includes responses from Toll-like receptors (TLRs) and leucine-rich repeat motifs (LRRs), which are nucleotide-binding sensor domains in NLRPs, including those that activate inflammasomes (multiprotein complexes that serve as platforms for IL-1 activation). One of the earliest hypotheses, which suggested that crystal recognition primarily occurs through membrane binding of lipids, has been revisited and studied again.

Inflammatory Phagocytosis. Early studies showed that MSU crystals isolated from sites of gouty inflammation are coated with immunoglobulins, primarily IgG [Nasage M et al., 1989; Ortiz-Bravo E et al., 1993; Landis RC et Haskard DO, 2001]. The configuration of these antibodies on the crystal surface has been described both in humans (IgG) and in mice (IgM). The Fab portions of the antibodies are used for binding to the crystal, while the Fc portion is oriented aside [Kozin F et McCarty DJ, 1980]. Sodium urate crystals engulfed by macrophages are often also coated with antibodies, indicating the role of Fc receptor-mediated phagocytosis. In phagocytes, urate covered with IgG promotes the production of superoxide anion [Nasage M et al., 1989]. There is evidence that phagocytic responses to crystals may also depend on FcRs but not on Fc or IgG. It has been shown [Barabe F et al., 1998; Desaulniers P et al., 2001] that

the CD16 receptor (FcγRIII) on neutrophils can directly bind to the crystal surface, inducing intracellular tyrosine phosphorylation dependent on CD11b. The same recognition mechanism may work for structurally different crystals, such as calcium pyrophosphate dihydrate, through a similar mechanism. These observations, according to Ghaemi-Oskouie F and Shi Y [2011], bring the phagocytic receptor (CD16) into a disorder that is often associated with severe inflammation. How CD16 can recognize at least two different crystals without the help of antibody coatings on their surfaces still needs to be determined.

Complement System. Both the classical and alternative pathways of complement activation are involved in mediating urate crystal-induced inflammation. Initially, peptides on the surface of crystals incubated with blood serum were analyzed using electrophoresis, and C1q, C1r, and C1s, with C1q being the most prominent, were detected [Terkeltaub R et al., 1983]. Since control (non-sodium urate) crystals did not show a similar enrichment, these data suggest that the surface of sodium urate crystals can convert C1 and adsorb the resulting fragments, leading to classical pathway activation. While these processes likely depend on the presence of Fc antibodies to convert C1q, it was actually questioned whether antibody coating on the crystal is necessary for classical pathway activation, as these crystals can initiate C3 activation in the absence of immunoglobulins [Naft GB et Byers PH, 1973]. Regarding the alternative pathway, it was established that the crystal surface does not induce the conversion of factor B or C3 individually. However, in the presence of all members of this pathway, both of these factors can be cleaved without the involvement of the classical pathway (i.e., in serum deficient in C2) [Fields TR et al., 1983]. In this cascade, C5 fragments are generated (including C5a, a potent chemotaxis mediator). However, it is unknown how the crystalline surface can trigger complement fixation. As for the consequences of complement activation in response to sodium urate crystal, the formation of membrane attack complexes is important. In mice with C6 deficiency (required for membrane attack complex), both gouty inflammation and associated IL-8 production are significantly reduced [Tramontini N et al., 2004].

TL Receptors. TLRs are critical sensors of microbial presence both inside and outside cells. However, there is speculation that they may also recognize substances from endogenous sources. For instance, heat shock proteins and high mobility group box protein 1 (HMGB1) have been shown to trigger inflammatory responses through TLR4. It has been reported that sodium urate can interact with two TLRs, TLR2 and TLR4, along with the associated receptor CD14. Using antibody blocking and transfection methods, it was established that sodium urate interacts with TLR2 on chondrocytes to induce nitric oxide production [Liu-Bryan R, Pritzker K, 2005]. Similarly, it was found that macrophages rely on TLR2/TLR4 for sodium urate recognition, leading to IL-1β production [Liu-Bryan R, Scott P, 2005]. The same research group suggested that CD14 may also bind to sodium urate crystals [Scott P et al, 2006]. This binding led to the production of CXCL1 and the release of IL-1β. It is unclear whether all three structures need to interact with sodium urate simultaneously or whether each of them is used by specific cell types under different circumstances. Furthermore, not all studies supported this model. For example, Chen CJ et al [2006], using TLR knockouts and gene transfectants, failed to document the necessity of these receptors in a peritoneal gout model.

Inflammasomes and Interleukin-1β. It has been shown [Martinon F et al, 2006] that the production of IL-1β in response to stimulation with sodium urate (MSU) is lost in macrophages deficient in NLRP3 (formerly NALP3, also known as cryopyrin). NLRP3 regulates the cleavage of pro-IL-1β into its secreted/active form by caspase-1. It was found that NLRP3, associated with the apoptosis-associated speck-like protein (ASC), and caspase-1 form a unique inflammasome (referred to as the NLRP3 inflammasome) responsible for controlled MSU-induced IL-1β production, as well as IL-18. Hoffman HM et al [2010] showed that the deletion of the leucine-rich repeat (LRR) domain (previously characterized as a sensor domain for inflammasome activation) at the C-terminus of NLRP3 resulted in decreased IL-1β production in macrophages stimulated with MSU. These studies confirm the role of NLRP3 in controlled MSU-induced IL-1β release and suggest that LRR serves as a sensor for MSU. It has also been

shown that NLRP3 is necessary for uric acid's ability to act as an adjuvant in antibody induction [Eisenbarth SC et al, 2008], and the presence of uric acid in vaccine preparations induces uric acid production, which subsequently triggers APC activation [Kool M et al, 2008]. This chain of events suggests a role for NLRP3 in adjuvanticity, as NLRP3 is necessary for MSU-mediated IL-1β production. However, the role of inflammasomes in vaccination remains a subject of debate, as several other research groups that also applied uric acid as an adjuvant did not observe antibody production loss in mice with NLRP3 deficiency [Eisenbarth SC et al, 2008; Kool M et al, 2008a].

One puzzling aspect of the MSU/inflammasome model is how MSU crystals, which appear to be mostly extracellular, can gain access to the intracellular inflammasome. Hornung V et al [2008] reported that phagolysosomes formed in macrophages upon the ingestion of sodium urate (as well as uric acid) were unstable, which could allow for the intracellular release of phagocytosed crystals. The discharge of these solid materials into the cytosol was accompanied by the release of cathepsin B, which itself can lead to NLRP3 activation through an as-yet-undetermined mechanism [Hornung V et al, 2008]. It is important to recognize that such a scenario implies the release of phagolysosomal contents, which has long been considered a signal for cell death [De Duve C et Wattiaux R, 1966]. While this mode of activation may participate in acute inflammation, it may be less applicable to the generation of an immune response, as antigen-presenting cells containing ruptured phagolysosomes would need to survive long enough to migrate to draining lymph nodes and exert a delayed adjuvant effect.

The binding of lipids. In the context of MSU crystal-cell interactions has been revisited by Ghaemi-Oskouie F et Shi Y [2011], updating some details regarding signaling mechanisms. Back in 1976, Mandel NS [1976] proposed that the surfaces of sodium urate crystals could directly interact with the plasma membrane through crystal-lipid interactions. He suggested that the surface roughness, and therefore the extent of electrostatic interactions, was responsible for cellular responses. While this concept was supported in several studies, it was largely overshadowed as subsequent researchers turned to protein-based receptors as the primary mediators of cellular responses. Ghaemi-Oskouie F et Shi Y [2011], on the other hand, became interested in crystal-lipid interactions based on their inability - despite significant efforts - to identify a protein receptor specific for sodium urate on dendritic cells. While such receptors may exist (and candidates like TLR2/4, CD14, and CD16 have been identified) on macrophages and neutrophils, they do not appear to function on dendritic cells. In contrast, the authors found that depleting cholesterol from the plasma membrane completely blocked the dendritic cell response to sodium urate.

Using atomic force microscopy and synthetic chemistry, Ghaemi-Oskouie F et Shi Y [2011] outlined the following sequence of events on a dendritic cell: 1) Sodium urate crystals form a spatially tight intermolecular interaction (possibly hydrogen bonding) with cholesterol on the cell surface within the first 30 seconds after contact with the dendritic cell, leading to lipid sorting due to membrane fluidity; 2) Lipid sorting aggregates immune receptor tyrosine-based activation motif (ITAM)-containing receptors, which are predominantly segregated into cholesterol/sphingolipid-rich lipid raft regions; 3) In the dendritic cell, Syk kinase is recruited to this accumulation and subsequently activates phosphatidylinositol 3-kinase (PI3K); and 4) This PI3K-mediated activation initiates actin/microfilament-associated activity, allowing further accumulation of signaling molecules on the plasma membrane for autoamplification.

The proposed model by Ghaemi-Oskouie F et Shi Y [2011] indeed provides an explanation for how solid particles, even without a specific protein receptor, can trigger strong activation of dendritic cells in a manner independent of opsonization and antibody binding. They suggest that this specific mechanism works in parallel with traditional protein/receptor-based recognition. However, their theory makes two straightforward and testable predictions: 1) Disrupting membrane lipids should inhibit crystal-mediated activation; reducing cholesterol levels, both through synthesis and in the plasma membrane, should reduce crystal-mediated

sodium urate inflammation in vivo; and 2) Syk/PI3K deficiency should abolish cellular responses mediated by sodium urate crystals.

The proposed pathways of sodium urate crystal activation by Ghaemi-Oskouie F et Shi Y [2011] are illustrated in Figure 1.2

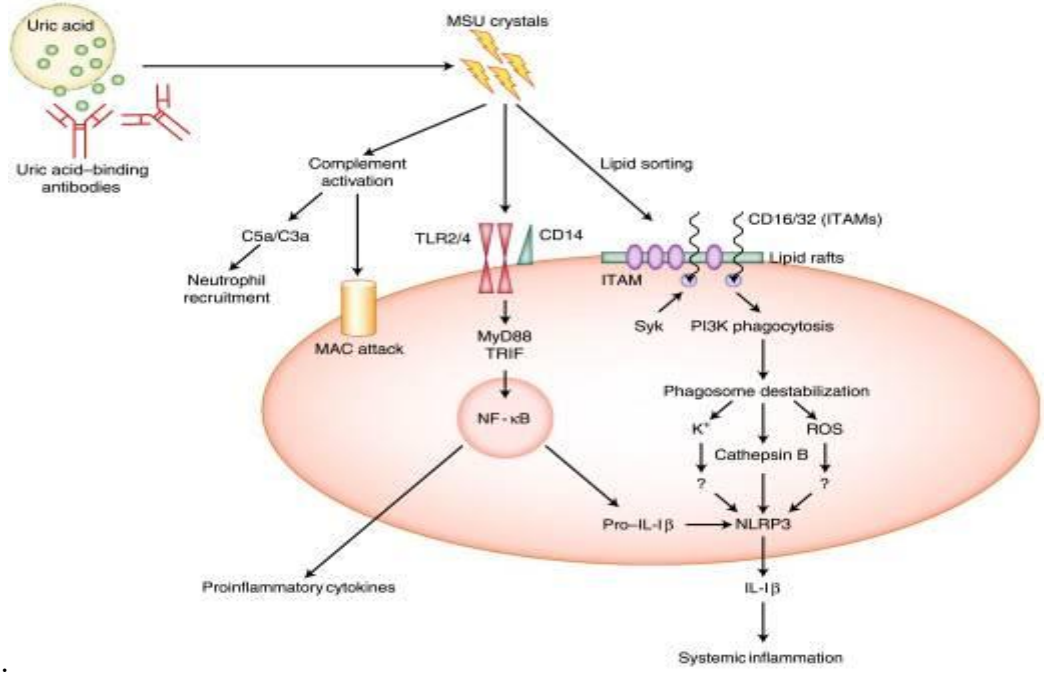

Figure 1.2. Pathways of cellular activation by sodium urate crystals [Ghaemi-Oskouie F et Shi Y, 2011]

Uric acid released from damaged cells forms sodium urate crystals upon binding with specific antibodies. These crystals activate components of the complement system through both classical and alternative pathways, generating C3a and C5a, as well as membrane-attacking complexes (MAC). By engaging the plasma membrane, the crystal interacts with protein receptors TLR2/4 and CD14, likely initiating the MyD88/TRIF pathway, leading to NF-κB activation. This cascade can regulate the activation of antigen-presenting cells (APC) and the production of other proinflammatory cytokines, besides IL-1β and IL-18. Sodium urate crystals can also bind to cholesterol, inducing lipid sorting, which recruits Syk via lipid raft-enriched receptors containing immunoreceptor tyrosine activation motifs (ITAM), such as CD16 and CD32. Subsequently, Syk initiates opsonin-independent phagocytosis through phosphatidylinositol 3-kinase (PI3K). The interaction of sodium urate crystals with CD16 may be independent of lipid sorting. Phagocytosed crystals cause damage to the phagolysosome membrane, resulting in the release of reactive oxygen species, potassium, and cathepsin B from vesicles. The latter triggers NLRP3 inflammasome activation through an as-yet-unknown pathway. This pathway regulates IL-1β production and may be responsible for systemic inflammation. Question marks indicate speculative links.

Hyperuricemia and Inflammation. Uric acid is primarily excreted in the urine and then reabsorbed in the epithelial cells of the proximal convoluted tubule by urate transporters, such as urate transporter 1 (URAT1), a transmembrane protein that is highly expressed in endothelial cells, adipocytes, and chondrocytes of cartilage [Price KL et al, 2006; Sautin YY et al, 2007; Sugihara S et al, 2015; Zhang B et al, 2019].

The normal level of uric acid in the blood is 2.4–6.0 mg/dL (143-357 μM/L) for women and 3.4–7.0 mg/dL (202-417 μM/L) for men [Bardin T et Richette P, 2014; Chen-Xu M et al, 2019]. Hyperuricemia is a pathological condition characterized by uric acid levels in the blood exceeding the upper limits, which is significantly associated with metabolic syndrome and increased cardiovascular risk [Lyngdoh T et al, 2011; Liu Z et al, 2015; Yu TY et al, 2016]. In this regard, a study conducted in 22,983 Chinese adults demonstrated that individuals with hyperuricemia have a higher prevalence of cardiovascular risk factors such as dyslipidemia, hypertension, and type 2 diabetes compared to individuals with normal uric acid levels [Wu J et

al, 2017]. The concentration of uric acid is directly related to the number of cardiovascular risk factors; in other words, cardiovascular risk increases when uric acid levels rise.

The association between hyperuricemia and cardiovascular diseases is accompanied by low-grade inflammation, characterized by enhanced proinflammatory activation of macrophages [Kushiyama A et al, 2012; Wu J et al, 2017]. Consequently, the influence of allopurinol (an inhibitor of uric acid production) on ApoE-/- mice reduces not only the size of atherosclerotic plaques but also the infiltration of macrophages and their expression of TNF-α and IL-1β, typical proinflammatory cytokines [Kushiyama A et al, 2012]. This pioneering work first proposed a link between uric acid and macrophages in the context of cardiovascular diseases.

Macrophages are innate immune cells that differentiate from monocytes and play a prominent role in phagocytosis, inflammation, and wound healing [Wynn TA et al, 2013]. Macrophages exhibit remarkable plasticity, with the ability to organize both proinflammatory reactions and anti-inflammatory actions depending on the extracellular environment [Murray PJ, 2017]. In the presence of prototype molecules such as lipopolysaccharide (LPS) and/or interferon-gamma (IFN-γ), human macrophages display proinflammatory functions, producing TNF-α, IL-1β, CD11c, and TLR4 receptor [Martinez FO et al, 2006; Li G et al, 2017]. Conversely, the influence of dexamethasone or cytokines such as IL-4 and IL-13 on macrophages leads them to adopt an anti-inflammatory profile characterized by the production of IL-10 and CD206 [Martinez FO et al, 2006]. Furthermore, the influence of pro- or anti-inflammatory stimuli on macrophages also affects their expression of molecules involved in leukocyte trafficking, such as CX3C chemokine receptor 1 (CX3CR1) and CC chemokine receptor type 2 (CCR2) [Amsellem V et al, 2017; Deci MB et al, 2018]. Importantly, inflammation activation enhances the ability of macrophages to engulf bacteria compared to macrophages with an anti-inflammatory function [Zhang M et al, 2016; Lam RS et al, 2016].

Association of hyperuricemia with the risk of developing metabolic abnormalities and cardiovascular diseases is linked to heightened proinflammatory activity of macrophages [Lu W et al, 2015; Haryono A et al, 2018]. However, it remains unknown whether hyperuricemia simply coincides with changes in macrophage activity or if uric acid is capable of directly inducing proinflammatory activation of human macrophages. While previous data suggest that a high level of uric acid is associated with increased proinflammatory activity in human macrophages, there is still no convincing data on this.

For this reason, Martínez-Reyes CP et al [2020] investigated the impact of increasing uric acid concentrations on the proinflammatory or anti-inflammatory ability of primary human macrophages in vitro and then examined the potential molecular mechanism involved. Primary human monocytes were differentiated into macrophages for subsequent exposure to 0, 0.23, 0.45, or 0.9 mM/L uric acid for 12 hours in the presence or absence of 1 mM/L probenecid. Flow cytometry was used to measure the production of inflammatory markers and phagocytic activity, which was determined as the percentage of macrophages containing GFP-labeled Escherichia coli. qPCR was used to measure the expression of urate transporter 1 (URAT1) by macrophages.

The authors found that uric acid dose-dependently stimulates the production of TNF-α but not IL-1β by human macrophages, which were previously differentiated from monocytes, as confirmed by cell size and CD14 expression. TNF-α and IL-1β are known to be proinflammatory cytokines that play a key role in fever, cachexia, tumorogenesis inhibition related to pyroptosis, cell death, and immune cell recruitment [McGeough MD et al, 2017; Patel HJ et Patel BN, 2017; Kaplanov I et al, 2019]. However, TNF-α, but not IL-1β, is consistently associated with elevated levels of uric acid in serum in several pathological scenarios. For example, the level of uric acid in serum increases as TNF-α-producing monocytes also increase in women with preeclampsia [Peracoli MT et al, 2011]. Similarly, it has been shown that uric acid stimulates the expression of TNF-α in the vascular smooth muscle cells of Sprague-Dawley rats [Tang L et al, 2017]. On the other hand, plasma IL-1β showed a very weak association with an increase in serum uric acid levels in 1684 women and men, while TNF-α levels in serum increased in the same proportion as uric acid in plasma [Lyngdoh T et al, 2011].

Along with the previous information, the results of Martínez-Reyes CP et al [2020] provide significant experimental evidence that uric acid may contribute to an inflammatory state, primarily by stimulating the production of TNF-α in human macrophages. It is well-known that the synthesis of TNF-α depends on the TLR4-dependent signaling pathway, while the production of IL-1β depends on the activity of the NLRP3 inflammasome (NOD-LRR- and pyrin domain-containing protein 3) [He Y et al, 2013; Lin X et al, 2015; Grebe A et al, 2018]. For this reason, Martínez-Reyes CP et al [2020] decided to assess TLR4 in the same differentiated in vitro macrophages. TLR4 is a transmembrane protein capable of recognizing various molecular structures associated with damage (DAMPs) and molecular structures associated with pathogens (PAMPs), including free fatty acids and LPS [Park BS et Lee JO, 2013; Rocha DM et al, 2015]. After activation, TLR4 can induce NF-kB activation, leading to the production of TNF-α [Harada et al, 2003]. The authors demonstrated that TLR4 is produced in human macrophages in response to uric acid in the same way as TNF-α. It has been shown that the risk of gout is directly associated with the rs2149356 polymorphism, which is associated with high levels of TLR4 production [Rasheed H et al, 2016]. Similarly, it has been demonstrated that uric acid promotes the expression of TLR4 mRNA in adipocytes of rats in vitro [Zhang J et al, 2019]. Therefore, Martínez-Reyes CP et al [2020] suggest that uric acid may be capable of inducing the production of TNF-α through the activation of TLR4, a phenomenon that imparts pro-inflammatory characteristics to human macrophages. However, they also caution that the idea that uric acid can activate TLR4 should be approached with caution, as they only assessed TLR4 at the protein level without evaluating its ability as a cellular signal transducer.

Furthermore, the study aimed to confirm the evident pro-inflammatory capacity of macrophages by analyzing CD11c and CD206. CD11c is a β-2 integrin that is highly expressed in monocytes and macrophages with pronounced pro-inflammatory functions, whereas CD206, also known as the mannose receptor, is a C-type lectin predominantly expressed in mouse and human macrophages, exhibiting anti-inflammatory actions [Arnold IC et al, 2016; Torres-Castro I et al, 2016; Nawaz A et al, 2017]. The authors found that uric acid can increase the production of CD11c while simultaneously decreasing the number of macrophages expressing CD206. In this regard, it has previously been reported that blocking uric acid synthesis with uricase reduces the number of CD11c+ monocytes in mice [Kool M et al, 2008], indicating a connection between uric acid production and CD11c. In parallel, it has been shown that macrophages from the synovial fluid of gout patients tend to have reduced expression of CD206 compared to macrophages from patients with rheumatoid arthritis [Jeong JH et al, 2019]. Overall, this information is consistent with the idea that macrophages adopt pro-inflammatory functions while losing their anti-inflammatory capacity in the presence of elevated uric acid levels.

The idea that uric acid can act as a direct pro-inflammatory stimulus for human macrophages is further supported by two additional facts presented by Martínez-Reyes CP et al [2020]: the expression pattern of CX3CR1 and CCR2 and the phagocytic activity of macrophages. CX3CR1 and CCR2 are involved in mediating the recruitment of monocytes to sites of inflammation, where these cells differentiate into macrophages and orchestrate inflammatory reactions or tissue repair [Bjorkander S et al, 2013; Lee M et al, 2018]. Interestingly, numerous studies consistently report the downregulation of CX3CR1 and CCR2 in the presence of prototypical inflammatory stimuli like LPS. Pioneering work, for example, reported a significant decrease in CX3CR1 expression in circulating monocytes from both septic patients and those incubated with LPS [Pachot A et al, 2008]. Similarly, the impact of LPS in vitro and in vivo on peripheral blood cells in mice can reduce CCR2 expression with direct consequences for macrophage migratory capacity [Zhou Y, Yang Y et al, 1999; Heesen M et al, 2006]. Therefore, the expression of CX3CR1 and CCR2 seems to behave similarly in macrophages exposed to both LPS and uric acid, providing substantial experimental evidence regarding the potential inflammatory role of this metabolite in macrophages.

Additionally, it is well-known that macrophages with pro-inflammatory functions exhibit a greater ability to phagocytose bacteria compared to anti-inflammatory macrophages [Zhang M et

al, 2016; Lam RS et al, 2016]. Martínez-Reyes CP et al [2020] also demonstrated that the impact of increasing concentrations of uric acid on macrophages gradually improved their phagocytic activity, once again confirming the notion that uric acid acts as a direct pro-inflammatory stimulus for these immune cells.

In addition to investigating the apparent pro-inflammatory effect of uric acid on macrophages, Martínez-Reyes CP et al [2020] explored its potential molecular mechanism. The production of TNF-α, TLR4, and CD11c in response to uric acid exhibited a typical dose-response relationship, with a maximum effect and plateau observed, indicative of saturation and cancellation of the observed effect [Salahudeen MS et Nishtala PS, 2017]. The dose-response relationship is explained by the interaction between the ligand and its receptor [Auerbach A, 2016; Salahudeen MS et Nishtala PS, 2017], suggesting the possible involvement of a molecule capable of transporting uric acid inside the macrophage, as is the case with URAT1.

Martínez-Reyes CP et al. [2020] have made significant contributions to our understanding of the potential pro-inflammatory effects of uric acid on human macrophages. They observed that human macrophages express URAT1, a transmembrane protein previously reported primarily in endothelial cells, adipocytes, and chondrocytes of cartilage [Zhang B et al, 2019]. Notably, the expression of URAT1 in macrophages decreased with increasing concentrations of uric acid. This observation may partially explain why the expression of TNF-α, TLR4, and CD11c reached saturation points, subsequently leading to a decrease in their protein levels. Given that uric acid can increase the transcriptional activity of NF-kB in the pancreatic β-cell line Min6 [Jia L et al, 2013], Martínez-Reyes CP et al [2020] hypothesize that the production of TNF-α in macrophages may depend on the interaction between uric acid, URAT1, and possibly NF-kB.

It is known that probenecid acts as a competitive inhibitor of URAT1, thus preventing the reabsorption and transport of uric acid by proximal tubule cells in the kidney [Tan PK et al, 2016]. Blocking URAT1 was found to abolish the production of TNF-α and the phagocytic activity previously observed with uric acid, indicating that the pro-inflammatory effect of uric acid is entirely dependent on its uptake into macrophages. In this regard, it was previously proposed that the entry of sodium urate into THP-1 cells could induce IkB phosphorylation via Src family tyrosine kinases, leading to NF-kB activation and, ultimately, the production of pro-inflammatory cytokines [Liu-Bryan R et Liote F, 2005].

Martínez-Reyes CP et al [2020] concluded that uric acid acts as a pro-inflammatory stimulus for cultured in vitro primary human macrophages by increasing the production of TNF-α, TLR4, and CD11c, enhancing macrophage phagocytic activity, and reducing the expression of CD206, CX3CR1, and CCR2. The possible mechanism through which uric acid exerts its pro-inflammatory action on human macrophages involves URAT1 in a dose-dependent manner. URAT1, in turn, may amplify NF-kB activation and lead to the production of pro-inflammatory cytokines through pathways yet to be fully elucidated. The functional demonstration of probenecid application further supports the idea that the influx of uric acid into macrophages has anti-inflammatory effects, partially dependent on URAT1. These results provide substantial experimental evidence supporting the notion that elevated uric acid levels may directly contribute to a systemic inflammatory state mediated by macrophages, which, in turn, is associated with an increased cardiovascular risk in patients with chronic diseases. Further research is needed to fully explore the idea that uric acid may act as a metabolic ligand with pro-inflammatory effects on human macrophages.

Conclusion:

The molecule uric acid exhibits significant physiological activity, both detrimental and beneficial to the body, making research in this area highly relevant.

CHAPTER 2

EXPERIMENT ON RATS

Conformity to ethical standards. Experiments on animals have been carried out in accordance with the provisions of the Helsinki Declaration of 1975, revised and supplemented in 2002 by the Directives of the National Committees for Ethics in Scientific Research. The modern rules for the maintenance and use of laboratory animals complying with the principles of the European Convention for the Protection of Vertebrate Animals used for scientific experiments and needs are observed (Strasbourg, 1985).

Experimental designe. The experiment was performed on 60 healthy female Wistar rats weighing 220-300 g, divided into 6 groups. 10 animals of the first group remained intact, consuming tap water from drinkers ad libitum. The rats of the other groups were injected once through a tube in a dose of 1.5 ml/100 g for 6 days with tap water, healing Naftussya and Sofia waters of the Truskavetsian deposit, as well as native Hertz water and its artificial salt analogue, respectively. The chemical composition of the used waters, according to the data of the Truskavetsian hydro-geological operational station, is given in Table 2.1.

Table 2.1. Chemical composition of used mineral waters

	Daily Water	Sofiya Water	Hertsa Water	Hertsa Salt analogue	Naftussya Water
Electrolytes, mM/L					
Na^+	0,5	156	196,7	196,7	0,6
Cl^-	3,4	142	205	205	1,0
HCO_3^-	2,9	7,5	5,6	5,6	8,2
Ca^{2+}	3,4	5,3	3,40	3,40	2,9
Mg^{2+}	0,5	4,3	3,44	3,44	2,3
K^+	0,4	0,3	0,4	0,4	0,3
SO_4^{2-}	1,2	13,1	0,1	0,1	1,0
Trace elementes, mg/L					
H_2SiO_3	5	4,43	9,88	0	9,5
H_3BO_3	0,25	8,39	42,76	0	0,200
Br^-	8,3	6,7	21,17	0	0,034
J^-	0,025	1,29	6,62	0	0,004
F^-	0,95	0,52	0,57	0	0,160
Organic substances, mg/L					
Corg	5,0	5,5	34	0	12,8
Norg	0,02	0,8	0,14	0	0,33

The day after the completion of the drinking course, at first, animals were placed in individual chambers with perforated bottom for collecting daily urine.

Then they assessed the state of autonomous regulation. For this purpose, under an easy ether anesthesia, for 15-20 sec ECG was recorded in the lead II, inserting needle electrodes under the skin of the legs. A series of approximately 120 cycles, the duration of which was determined by the caliper with an accuracy 0,1 mm (2 msec), divided into 6-msec intervals, followed by the calculation of the parameters of the HRV: Mode (Mo), Amplitude of the mode (AMo) and Variation scope (MxDMn) as markers of the humoral channel of regulation (first of all, circulating catecholamines), sympathetic and vagal tones respectively [Baevskiy RM et al, 1984].

The experiment was completed by decapitation of rats in order to collect as much blood as possible.

The plasma levels of the hormones of adaptation were determined: corticosterone, triiodothyronine and testosterone (by the ELISA); as well as electrolytes: calcium (by reaction with arsenase III), magnesium (by reaction with colgamite), phosphates (phosphate-molybdate method), chloride (mercury-rhodanidine method), sodium and potassium (both in plasma and in

erythrocytes) by flamming photometry; nitric metabolites: creatinine (by Jaffe's color reaction by Popper's method), urea (urease method by reaction with phenolhypochlorite), uric acid (uricase method), medium molecular polypeptides (by spectrophotometric method), bilirubin (by diazoreaction using the Jedrashik-Kleghorn-Grof method); lipid peroxidation products: diene conjugates (spectrophotometry of the heptane phase of the lipids extract [Gavrilov VB, Mishkorudnaya MI, 1983]) and malonic dyaldehide (in the test with thiobarbituric acid [Andreyeva LI et al, 1988]), antioxidant enzymes: superoxide dismutase erythrocytes (according to the degree of inhibition of reduction of nitroblue tetrazolium in the presence of N-methylphenazonium metasulphate and NADH [Makarenko YeV, 1988]) and catalase plasma (at the rate of decomposition of hydrogen peroxide [Korolyuk MA et al, 1988]), as well as amylase (Karavay's amyloclastic method with starch substrate) and glucose (glucose-oxidase method).

Most of the listed parameters of metabolism were also determined in daily urine. By the size of the diuresis and the level of creatinine in plasma and urine, glomerular filtration and tubular reabsorption were calculated. In addition, the osmolarity of the urine was measured by the cryostatic method as well as level of 17-ketosteroids by reaction with meta-dinitrobenzene.

The analyzes were carried out according to the instructions described in the manual [Goryachkovskiy AM, 1998]. The analyzers "Tecan" (Oesterreich), "Pointe-180" ("Scientific", USA) and "Reflotron" (Boehringer Mannheim, BRD) were used with appropriate sets and a flamming spectrophotometer "СФ-47".

According to the parameters of electrolyte exchange, hormonal activity was evaluated: Parathytoid by coefficients $(Cap/Pp)^{0,5}$ and $(Cap•Pu/Pp•Cau)^{0,25}$, calcitonin by coefficients $(1/Cap•Pp)^{0,5}$ and $(Cau•Pu/Cap•Pp)^{0,25}$ as well as mineralocorticoid by coefficients $(Nap/Kp)^{0,5}$ and $(Nap•Ku/Kp•Nau)^{0,25}$, based on their classical effects and recommendations by IL Popovych [2000].

In a sample of the blood we analysed Leukocytogram (LCG), ie the relative content of lymphocytes (L), monocytes (M), eosinophils (Eo), basophils (Bas), rod-shaped (RN) and polymorphonuclear (PMN) neutrophils. Based on these data, the Entropy of the Leukocytogram (hLCG) was calculated according to the formula derived by Popovych IL [2007] on the basis of the classical Shannon's CE [1948] formula:

$$hLCG = - [L•\log_2 L+M•\log_2 M+Eo•\log_2 Eo+Bas•\log_2 Bas+RN•\log_2 RN+PMN•\log_{2PM} N]/\log_2 6.$$

The parameters of immunity were determined according to the tests of the 1st and 2nd levels of the WHO, as described in the manual [Perederiy VG et al, 1995]: the relative content of the population of T-lymphocytes in a test of spontaneous rosette formation with erythrocytes of sheep by Jondal M et al [1972], their theophylline-resistant (T-helper) and theophyllin-susceptible (T-cytolytic) subpopulations (by the test of sensitivity of rosette formation to theophylline by Limatibul S et al [1978]; the population of B-lymphocytes by the test of complementary rosette formation with erythrocytes of sheep by Bianco C [1970]. Natural killers were identified as large granules contain lymphocytes. The content of zero-lymphocytes (0L) was calculated by the balance method. For these components, the Entropy of the Immunocytogram (hICG) was calculated:

$$hICG = - [Th•\log_2 Th+Tc•\log_2 Tc+B•\log_2 B+NK•\log_2 NK+0L•\log_2 0L]/\log_2 5.$$

The blast transformation reaction of T-lymphocytes to phytohemagglutinin was performed separately [Perederiy VG et al, 1995].

About the state of the phagocytic function of neutrophils (microphages) and monocytes (macrophages) were judged by the phagocyte index, the microbial count and the killing index for Staphylococcus aureus (ATCC N25423 F49) [Douglas SD, Quie PG, 1981; Bilas VR, Popovych IL, 2009].

After decapitation, the spleen, thymus and adrenal glands were removed from the animals. Immune organs weighed and made smears-imprints for counting splenocytogram and thymocytogram [Belousova OI, Fedotova MI, 1968; Bilas VR, Popovych IL, 2009]. For them CE Shannon's entropy was calculated too.

In the adrenal glands after weighing, the thickness of glomerular, fascicular, reticular and medullar zones was measured under a microscope.

Digital material is statistically processed on a computer using the software package “Microsoft Excell” and "Statistica 6.4 Statsoft Inc" (Tulsa, OK, USA).

2.1. VARIANTS OF URIC ACID EXCHANGE

The primary analysis revealed a wide range of uric acid metabolism, which are characterized by its level in the blood and excretion with urine. As we can see, the correlation between uricemia and uricosuria is statistically significant, but only mediocre in force (Fig. 2.1). This indicates the need to register both uric acid parameters for adequate assessment of the state of its exchange.

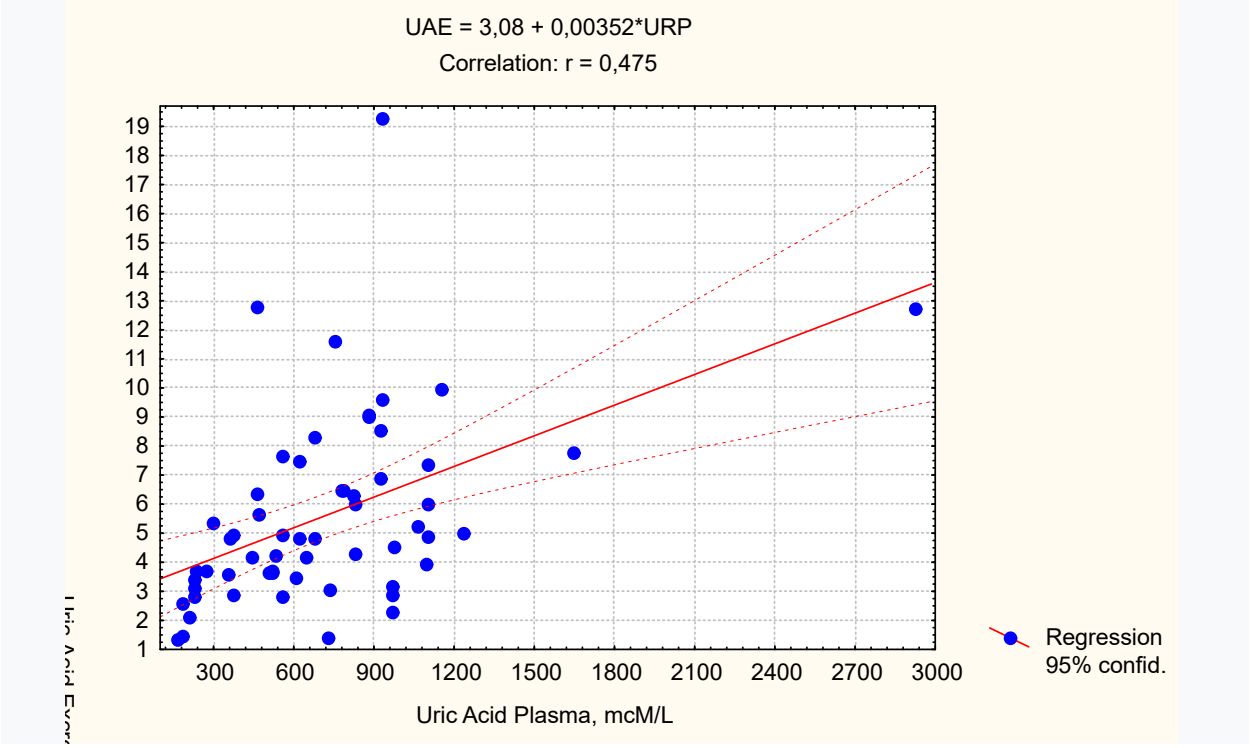

Fig. 2.1. Scatterplot of correlation between Uricemia (X-line) and Uricosuria (Y-line)

To create homogeneous groups, we used cluster analysis. While the routine methodical approach only allows one to alternately analyze one or another feature of the statistical sample, the use of cluster analysis makes it possible to take into account all features simultaneously. Taking into account the entire set of features of individuals, taken in their relationship and the conditioning of some of them (derivatives) by others (main, determining) makes it possible to carry out a natural classification that reflects the nature of things, their essence. It is believed that knowing the essence of an object boils down to the identification of those qualitative properties that actually define this object and distinguish it from others [Aldenderfer MS, Blashfield RK, 1985; Mandel ID, 1988]. Clustering according to immunity parameters is implemented by the iterative k-means method. In this method, the object is assigned to the class to which the Euclidean distance is minimal. The main principle of the structural approach to distinguishing homogeneous groups is that objects of one class are close, and objects of different classes are distant. In other words, a cluster (image) is an accumulation of points in an n-dimensional geometric space in which the average distance between points is less than the average distance from these points to the rest.

Usually, the number of clusters is arbitrary. We stopped at four, because three clusters is trivial, and a larger number of clusters is difficult to perceive and compare, and besides, they

become less numerous in composition. Euclidean distance documents that the clusters are clearly distinguished by the totality of uricemia and uricosuria (Tables 2.2 and 2.3).

Table 2.2. Euclidean distances between clusters

Distances below the diagonal. Squared distances above the diagonal

Clusters	Sn+U-+	S+Un+	SnUn+	S-Un-
Sn+U-+	0	51559	48301	183667
S+Un+	227	0	199666	429845
SnUn+	220	447	0	43593
S-Un-	429	656	209	0

Table 2.3. Cluster members are distant from the center of the respective cluster

S-Un- Cluster contains 15 cases

	Case No.	Case No.	Case No.	Case No.	Case No.	Case No.	Case No.	Case No.	Case No.	Case No.	Case No.	Case No.	Case No.	Case No.	Case No.
	C_2	C_9	C_12	C_25	C_27	C_32	C_34	C_37	C_39	C_43	C_47	C_49	C_51	C_56	C_57
Distance	45,	66,	20,	82,	72,	26,	68,	19,	9,5	52,	36,	80,	20,	24,	52,

SnUn+ Cluster contains 17 cases

	Case No.	Case No.	Case No.	Case No.	Case No.	Case No.	Case No.	Case No.	Case No.	Case No.	Case No.	Case No.	Case No.	Case No.
	C_4	C_5	C_8	C_11	C_14	C_26	C_30	C_33	C_35	C_38	C_41	C_50	C_54	C_55
Distance	26,	87,	47,	65,	47,	63,	65,	1,6	,4	65,	87,	16,	38,	25,

Case No.	Case No.	Case No.
C_42	C_45	C_48
32,	80,	1,9

Sn+U-+ Cluster contains 19 cases

	Case No.	Case No.	Case No.	Case No.	Case No.	Case No.	Case No.	Case No.	Case No.	Case No.	Case No.	Case No.	Case No.	Case No.	Case No.	Case No.
	C_1	C_3	C_6	C_7	C_13	C_16	C_17	C_18	C_20	C_21	C_22	C_28	C_29	C_44	C_46	C_60
Distance	48,	30,	56,	98,	41,	47,	10,	10,	63,	41,	74,	24,	78,	73,	24,	74,

Case No.	Case No.	Case No.
C_53	C_58	C_59
29,	79,	94,

S+Un+ Cluster contains 9 cases

	Case No.	Case No.	Case No.	Case No.	Case No.	Case No.	Case No.	Case No.	**Case No.**
	C_10	C_15	C_19	C_24	C_31	C_36	C_40	C_52	C_23
Distance	63,	25,	62,	62,	325,	62,	86,	36,	330

According to the results of the variance analysis, the main cluster-forming parameter, judging by the η^2 criterion, was uricemia (Table 2.4).

Table 2.4. Analysis of variance

Parameters of Uric Acid Exchange	Between SS	Within SS	η^2	R	F	signif. p
Uricemia	10643659	560927	0,950	0,975	261	10^{-6}
Uricosuria	153	452	0,253	0,503	4,7	0,003

Note. The parameters of dispersion analysis are calculated according to the following formulas:

$\eta^2=Sb^2/(Sb^2+Sw^2)$,
$R=\eta$,
$F=[Sb^2(n-k)]/[Sw^2(k-1)]$, where
Sb^2 – between dispersion;
Sw^2 – within dispersion;
n – number of animals (60);
k – number of groups (4).

To qualitatively assess the state of uric acid exchange in different clusters, we calculated the average values of uricemia, uricosuria, and clearance, as well as their variability in intact rats. For uricemia, they are 662 μM/L (Cv=0,516), for uricosuria – 5,72 μM/100g BM•24 h (Cv=0,939), for clearance – 6,16 μM/min (Cv=0,595). Taking the range of -0.5σ ÷ 0.5σ as a narrowed norm, we will obtain a range of 490÷830 μM/L for uricemia, 3,0÷7,5 μM/100 g BM•24 h for uricosuria, 4,33÷7,99 μL/100 g BM•min for clearance (Table 2.5 and Fig. 2.2).

Table 2.5. Average values of parameters of uric acid metabolism in rats of different clusters

		Clusters of Uric Acid Exchange (n)			
Parameters of Uric Acid Exchange	Norm (10)	S-Un- (15)	SnUn+ (17)	Sn+U± (19)	S+Un+ (9)
Uric Acid Serum, μM/L	**662**	**259**	**554**	**865**	**1379**
Uric Acid Excretion, μM/100g BM•24h	**5,72**	**3,32**	**5,46**	**6,63**	**7,00**
Uric Acid Clearens, μL/100g BM•min	**6,16**	**8,95**	**7,02**	**5,33**	**3,63**

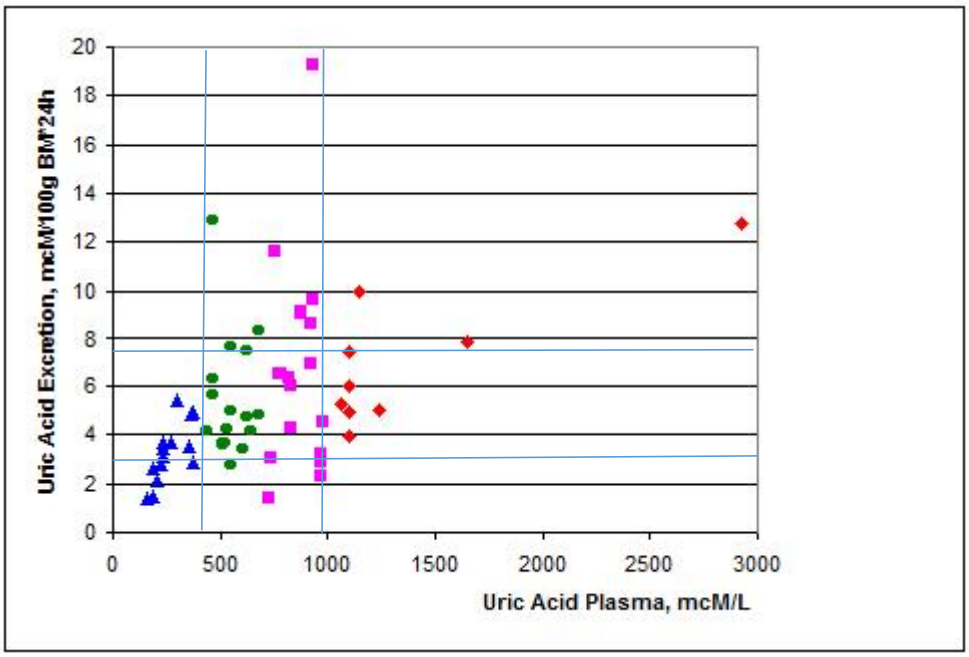

Fig. 2.2. Clusters of rats with different uric acid metabolism.
Vertical lines mark the limits of uricemia, horizontal lines limit the range of uricosuria (-0,5σ ÷ 0,5σ)

Based on the accepted criteria, 28,3% of animals were diagnosed with normouricemia in combination with normal or slightly increased excretion of uric acid (**SnUn+** cluster). In 25,0% of rats, hypouricemia is combined with normal or slightly reduced uricosuria (**S-Un-** cluster). In 31,7% of animals, the normal or slightly increased level of uric acid in the plasma is accompanied by a very pronounced dispersion of uricosuria (**Sn+Un±** cluster). In the remaining 15,0% of rats, pronounced hyperuricemia is combined with normal or slightly increased uricosuria (**S+Un+** cluster).

Since the variability of uricosuria is almost twice that of uricemia, we will apply the Z-values of these parameters calculated by the formula:

$$Z = (V/N-1)/Cv,$$

which are more informative from the point of view of physiology (Fig. 2.3).

It was established that hypouricemia (cluster centroid: -1.18±0.05) is associated with hypo- and normouricosuria (centroid: -0.45±0.06). This indicates increased urate clearance (+0.76±0.17) as a characteristic of a "urate-losing" kidney. Uricemia of the lower normal zone (centroid: -0.32±0.05) corresponds to the zero zone of uricosuria (centroid: -0.05±0.11) and normal urate

clearance (+0.24±0.24). Moderate hyperuricemia (centroid: +0.59±0.06) is accompanied by a wide spectrum of uricosuria and normal urate clearance (-0.23±0.20). On the other hand, pronounced hyperuricemia (centroid: +2.10±0.59) is characterized by reduced urate clearance (-0.69±0.10) - a "urate-retaining" kidney.

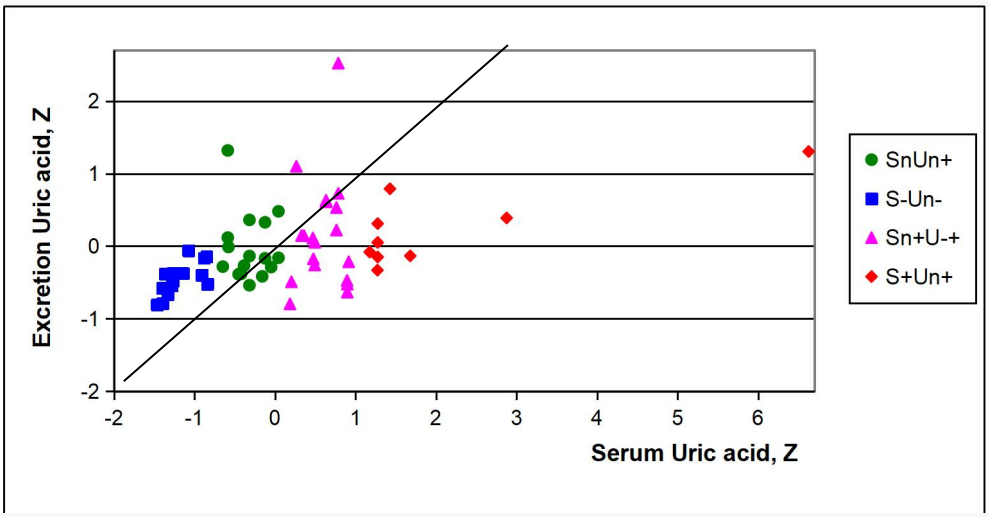

Fig. 2.3. Normalized levels (Z-units) of uricemia (line X) and uricosuria (line Y) in rats of different clusters

In order to find out the influence of the chemical composition of mineral water used by animals on the type of uric acid metabolism, an analysis of the relationship between quality indicators was carried out. A factor sign was a balneosis of a certain composition (or its absence), and the resulting sign was the type of uric acid metabolism, that is, a combination of uricemia and uricosuria (Table 2.6).

According to calculations based on formulas [Sepetliev D, 1968], the correlation between two series of qualitative parameters is very significant.

$\xi^2 = [(\Sigma n^2/Nx)/N] - 1 = 0,80$

$\varphi^2 = \xi^2 - (x-1)(y-1)/N = 0,80 - (6-1)(4-1)/60 = 0,55$

$R = \{\varphi^2/(1+\varphi^2)[xy/(x-1)(y-1)]^{0,5}\}^{0,5} = [0,55/1,55 \bullet (24/15)^{0,5}]^{0,5} = 0,670$

$\mu R = (1-R^2)/(N-2)^{0,5} = 0,072.$

Table 2.6. Correlation table for analyzing the relationship between balneofactors and clusters of uric acid exchange

Бальнеофактор		**Кластери обміну сечової кислоти**					
		S-Un- (15)	SnUn+ (17)	Sn+Un-+ (19)	S+Un+ (9)	Всього	$(\Sigma n^2/Nx)/N$
Відсутній (інтактні щурі)	n n^2/Nx	3 0,90	2 0,40	3 0,90	2 0,40	10 2,60	0,26
Водопровідна Вода	n n^2/Nx	2 0,40	4 1,60	3 0,90	1 0,10	10 3,00	0,30
Біоактивна вода Нафтуся	n n^2/Nx	3 0,90	4 1,60	3 0,90	0 0	10 3,40	0,34
Мінеральна вода Софія	n n^2/Nx	2 0,40	4 1,60	2 0,40	2 0,40	10 2,80	0,28
Мінеральна вода Герца	n n^2/Nx	3 0,90	1 0,10	3 0,90	3 0,90	10 2,80	0,28
Сольовий аналог води Герца	n n^2/Nx	2 0,40	2 0,40	5 2,50	1 0,10	10 3,40	0,34
Всього	Ny	15	17	19	9	60	1,80

However, visual analysis shows that both intact rats and those loaded with different mineral waters are more or less evenly distributed among the four clusters. Therefore, in order to dispel or confirm doubts, at the next stage we conducted an analysis of the canonical correlation

between the parameters of the chemical composition of tap and mineral waters, on the one hand, and the levels of uricemia and uricosuria - on the other hand.

According to calculations according to the formula:
$|r| = \{\exp[2t/(n - 1,5)^{0,5}] - 1\}/\{\exp[2t/(n - 1,5)^{0,5}] + 1\}$,
for a sample with n=60, the critical level of the modulus of the correlation coefficient |r| at $p<0,05$ ($t>2,00$) is 0,25, at $p<0,02$ ($t>2,39$) is 0,30, at $p<0,01$ ($t>2,66$) is 0,33, at $p<0,001$ ($t>3,46$) is 0,42.

No significant relationship was found (Table 2.7). However, the weak positive correlations of uricemia with the content of sodium and chloride ions, trace elements boron, iodine and bromine, as well as organic carbon in the consumed water are worthy of attention. Instead, uricosuria is weakly negatively correlated with the content of sulfate, calcium, and organic nitrogen in the water.

Table 2.7. Matrix of correlation coefficients between components of the chemical composition of used liquids and parameters of uric acid metabolism

	Correlations)	
	Uricemia	Uricosuria
Na	0,212	-0,030
Cl	0,220	-0,012
Ca	0,008	-0,193
SO4	-0,049	-0,215
H3BO3	0,225	0,030
Br	0,187	0,046
J	0,225	0,030
Corg	0,172	0,051
Norg	-0,049	-0,214

When conducting the canonical correlation analysis, the program included only 6 chemical parameters in the model, the combined influence of which determines the state of uric acid metabolism by only 8% (Table 2.8 and Fig. 2.4).

Table 2.8. Factor structure of chemical and urate canonical roots

Root	left set
Variable	R
Na	0,919
Cl	0,904
SO4	0,366
H3BO3	0,813
J	0,814
Norg	0,366

Root	right set
Variable	R
Uricosuria	-0,203
Uricemia	0,763

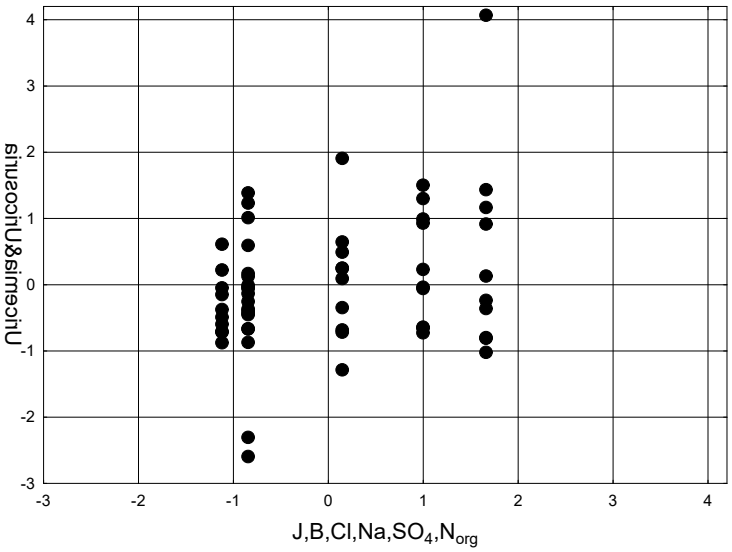

R=0,278; R^2=0,077; $\chi^2_{(12)}$=7,0; p=0,854; Λ Prime=0,879

Fig. 2.4. Canonical correlation between the chemical composition of used waters (X axis) and parameters of uric acid exchange (Y axis)

2.2. FEATURES OF THE STATE OF IMMUNITY UNDER DIFFERENT VARIANTS OF URIC ACID EXCHANGE

Since the analysis of variance showed that the η^2 criterion for uricemia was significantly greater than for uricosuria (0,95 vs 0,25), uricemia was chosen as the main parameter in evaluating the characteristics of immune status in different states of uric acid exchange. According to the screening results, three pairs of patterns of immune accompaniment of uricemia were formed.

The first pair of patterns reflects quasi-linear relationships, both the strengthening of immunity and its suppression (Fig. 2.5). In particular, hypouricemia is accompanied by a decrease in the level of T-lymphocytes in the thymus and their cytolytic subpopulation and the population of 0-lymphocytes in the blood, the entropy of the blood immunocytogram, the content of fibroblasts in the spleen and the intensity of phagocytosis of microbes by blood neutrophils (Table 2.9).

Two quasi-zero clusters of uricemia correspond to quasi-zero levels of this constellation of 6 immune parameters, while hyperuricemia causes them to increase. On this basis, the pattern is nominated as immunoenhansing.

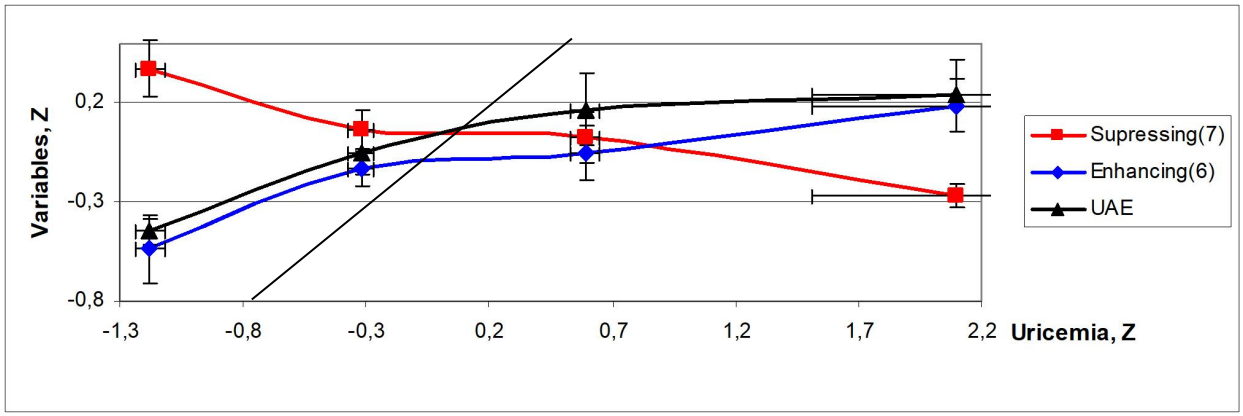

Fig. 2.5. The first pair of patterns of relationships between uricemia (X axis) and parameters of uricosuria and immunity (Y axis)

Instead, another immune constellation (thymus plasma cells, thymocyte entropy, spleen reticulocytes, rod neutrophils, natural killer cells and blood monocytes and their microbial count)

is suppressed in hyperuricemia, while in normuricemia it is within the normal range, and in the case of hypouricemia it is activated. This reflects the immunosuppressive effect of uric acid on the listed parameters. The second pair of patterns reflects the well-known U-shaped dependence (Fig. 2.6). In this case, immune extremes are observed in a cluster of moderately elevated uricemia. In particular, the upper limit level was found in relation to macrophages and Hassall's bodies of the thymus, macrophages and entropy of the splenocytogram, T-helpers and polymorphonuclear blood neutrophils. Instead, minimal levels are found for thymus epitheliocytes, spleen macrophages and lymphocytes, blood basophils and B-lymphocytes, as well as for the activity and completion of phagocytosis of microbes by blood neutrophils. Changes in the level of uricemia both on the right and on the left are accompanied by a decrease (U-minus-shaped pattern) or an increase (U-plus-shaped pattern) in the levels of immune parameters.

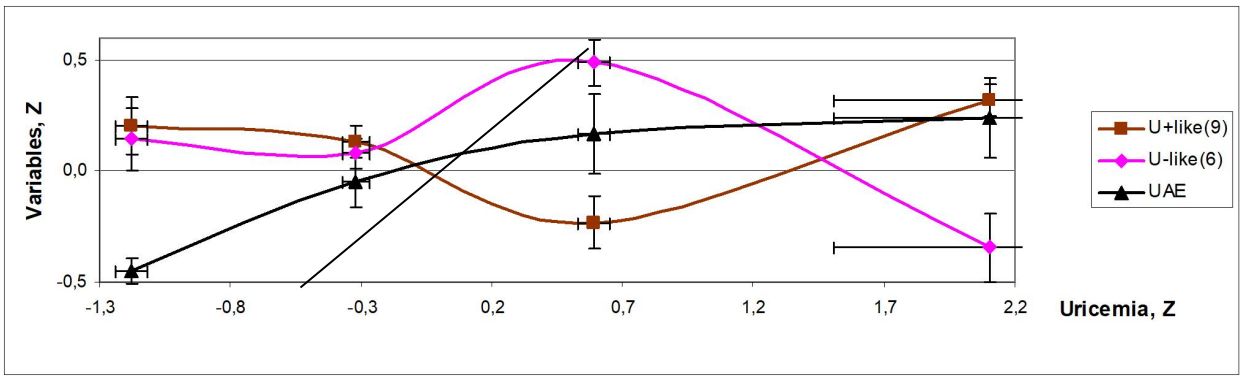

Fig. 2.6. The second pair of patterns of relationships between uricemia (X axis) and parameters of uricosuria and immunity (Y axis)

The third pair of patterns is characterized by localization of optimal quasi-zero points of immune parameters in a cluster of moderately reduced uricemia. Oppositely directed deviations in the level of uricemia are accompanied by an increase in the level of reticulocytes in the thymus, lymphoblasts in the spleen, plasma cells in the blood and entropy of the leukocytogram (U-activating pattern), on the one hand, and a decrease in the mass of the spleen and the content of plasma cells in the splenocytogram, as well as lymphoblasts in the thymus and leukocytes in the blood (U-suppressive pattern) - on the other hand (Fig. 2.7).

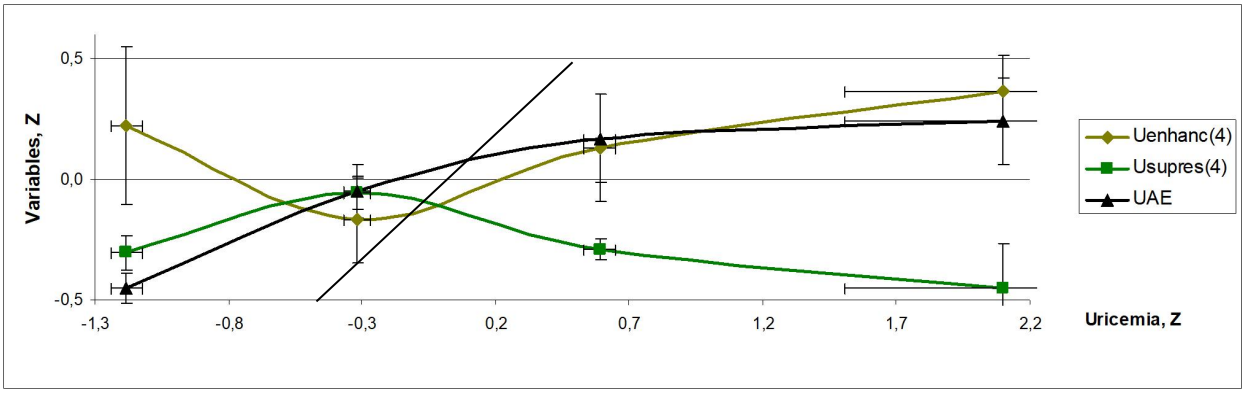

Fig. 2.7. The third pair of patterns of relationships between uricemia (X axis) and uricosuria and immunity (Y axis)

And only 7 of the 41 registered immune parameters (thymus weight, content of endothelial cells in the thymocytogram, eosinophils in the spleen, eosinophils and total lymphocytes in the blood, as well as the phagocytic index of monocytes and the reaction of blast transformation of T-lymphocytes to the mitogen FHA) remain stably normal at qualitatively different levels uricemia and uricosuria (reactive pattern) (Fig. 2.8).

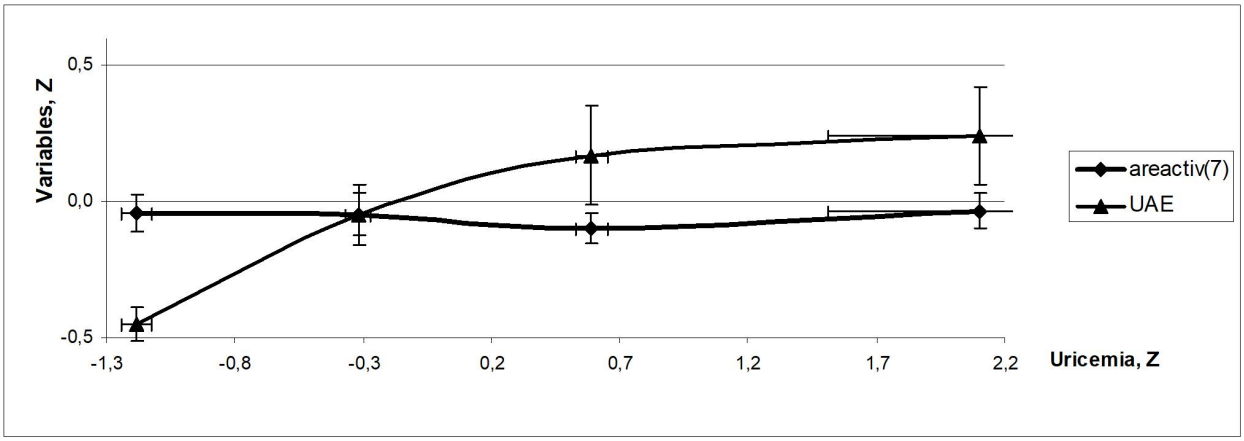

Fig. 2.8. Pattern of lack of response of immune parameters to the state of uric acid exchange

In order to identify exactly those immune parameters, the totality of which clusters of uric acid metabolism differ significantly from each other, a discriminant analysis was performed (method forward stepwise [Klecka WR, 1989]). The program selected only 15 indicators for inclusion in the model (3 related to the **thymus**, 4 to the **spleen**, 7 to the **blood**, as well as **uricemia**), while others, including **uricosuria**, were outside the discriminating model (Tables 2.9 and 2.10).

Table 2.9. Summary of the stepwise analysis of immune variables ranked by the Λ criterion

Variables currently in the model	F to enter	p-level	Λ	F-value	p-level
Uricemia, µM/L	46	10^{-6}	,290	45,6	10^{-6}
Macrophages Thymus, %	4,3	,008	,235	19,5	10^{-6}
0 Lymphocytes Blood, %	4,3	,008	,189	14,3	10^{-6}
Microphages Spleen, %	3,1	,036	,161	11,6	10^{-6}
T helper Lymphocytes, %	2,6	,061	,140	10,0	10^{-6}
Plasmocytes Thymus, %	2,5	,070	,122	8,9	10^{-6}
Entropy Splenocytogram	2,2	,101	,108	8,0	10^{-6}
Leukocytes Blood, G/L	2,1	,117	,096	7,4	10^{-6}
PMN Neutrophils, %	1,7	,185	,087	6,8	10^{-6}
Stab Neutrophils, %	1,4	,269	,080	6,3	10^{-6}
Spleen Mass Index, µg/g BM	1,3	,289	,074	5,9	10^{-6}
Macrophages Spleen, %	1,7	,179	,066	5,6	10^{-6}
B Lymphocytes, %	1,4	,256	,060	5,3	10^{-6}
T cytolytic Lymphocytes, %	1,6	,209	,054	5,1	10^{-6}
Lymphoblastes Thymus, %	1,3	,282	,050	4,9	10^{-6}

Table 2.10. Summary of the analysis of discriminant functions for immune variables ranked by structural coefficient

Step 15, N of vars in model: 15; Grouping: 4 grps; Wilks' Λ: 0,0498; approx. $F_{(45)}$=4,9; $p<10^{-6}$

	Clusters of Uric acid Exchange (n)				Parameters of Wilks' Statistics					
Variables currently in the model	S+Un+ (9)	Sn+U± (19)	SnUn+ (17)	S-Un- (15)	Wilks' Λ	Partial Λ	F-remove	p-level	Tolerancy	Norm (10)
Uricemia, µM/L	1379	865	554	259	,215	,232	46,4	10^{-6}	,648	662
0 Lymphocytes, %	23,1	22,8	21,8	15,5	,063	,789	3,74	,018	,626	22,2
T cytolytic Lymph, %	16,4	16,0	15,9	15,8	,055	,900	1,56	,214	,504	16,0
Plasmocytes Thym, %	1,67	1,83	1,88	2,40	,061	,820	3,08	,037	,681	1,80
Stab Neutrophils, %	3,11	3,16	3,25	3,40	,052	,958	,62	,606	,482	3,60
Macrophages Thy, %	2,11	3,56	2,88	3,07	,063	,788	3,76	,016	,599	2,70
T helper Lymphoc, %	28,4	32,0	31,3	30,5	,062	,800	3,51	,023	,653	31,5
Macrophags Spleen,%	7,89	9,11	8,18	7,87	,055	,904	1,48	,234	,667	7,90
Entropy Splenocytogr	0,741	0,761	0,751	0,752	,063	,790	3,72	,018	,646	0,753
PMN Neutrophils, %	26,4	29,3	25,8	27,8	,055	,912	1,35	,272	,498	26,0

Microphag Spleen, %	13,9	**11,8**	13,1	13,8	,054	,918	1,26	,302	,793	13,0
B Lymphocytes, %	16,3	**15,1**	16,4	16,3	,056	,882	1,88	,148	,475	16,0
Spleen MInd,µg/g BM	304	287	**321**	264	,059	,847	2,53	,070	,654	312
Lymphoblasts Thy, %	6,67	7,06	**7,41**	7,27	,054	,914	1,32	,282	,744	7,40
Leukocytes Blood,G/L	11,56	11,40	**11,98**	11,35	,059	,841	2,64	,062	,551	12,68
Variables currently not in the model	**S+Un+ (9)**	**Sn+U± (19)**	**SnUn+ (17)**	**S-Un- (15)**	Wil-ks' Λ	Parti-al Λ	F to enter	p-level	Tole-rancy	**Norm (10)**
Uricosuria, µM/100g•d	**7,00**	6,63	5,46	**3,31**	,048	,957	,61	,613	,738	5,72
Entropy Immunocyt	**0,888**	0,883	0,878	**0,874**	,048	,968	,45	,721	,716	0,874
Microb Count Neutro	**8,2**	8,0	7,8	**7,3**	,049	,992	,10	,957	,801	8,6
Lymphocyts Thym, %	**70,7**	69,2	69,5	**68,2**	,049	,993	,10	,962	,587	70,3
Fibroblasts Spleen, %	8,3	8,4	8,1	**7,2**	,049	,986	,19	,904	,707	8,2
Microb Count Monoc	**4,1**	4,7	4,6	**5,0**	,048	,964	,51	,676	,819	5,0
Reticulocyts Spleen,%	**14,20**	15,11	15,06	**15,13**	,049	,974	,36	,783	,648	14,30
Entropy Thymocytogr	**0,531**	0,556	0,551	**0,570**	,049	,986	,19	,902	,488	0,538
Monocytes Blood, %	**3,67**	4,11	5,12	**5,87**	,049	,981	,26	,854	,758	4,80
Bactericidity Mon, G/l	**0,51**	0,84	0,64	**1,14**	,049	,980	,25	,850	,750	0,72
Natur Killers Blood,%	**15,1**	15,6	15,7	**16,6**	,049	,985	,21	,888	,741	15,6
Hassal corp Thym, %	1,56	**2,06**	1,88	2,07	,048	,963	,52	,672	,710	1,70
Killing Ind Neutro,%	52,1	**51,3**	53,7	55,1	,048	,966	,48	,700	,802	50,7
Phagoc Ind Neutro, %	70,9	**68,8**	69,7	69,4	,048	,972	,39	,762	,829	69,5
Lymphocyts Spleen,%	49,0	**47,7**	48,2	48,3	,049	,989	,16	,924	,150	48,7
Epitheliocyt Thym, %	9,6	**8,9**	9,2	9,6	,049	,990	,14	,933	,517	8,8
Basophiles Blood, %	0,44	**0,26**	0,35	0,27	,046	,932	1,00	,403	,711	0,30
Plasmocytes Blood, %	0,83	0,80	**0,58**	0,96	,048	,957	,62	,608	,446	0,47
Entropy Leukocytogr	0,616	0,577	**0,558**	0,565	,048	,973	,38	,769	,782	0,596
Lymphoblas Spleen,%	4,00	4,16	**3,76**	4,27	,050	,999	,01	,998	,405	3,90
Reticulocyts Thym, %	5,11	4,83	**4,47**	4,80	,049	,977	,32	,814	,665	4,70
Plasmocyts Spleen, %	1,44	2,05	**2,18**	1,93	,049	,980	,28	,836	,457	2,50
Thymus Mass Index	0,028	0,026	0,030	0,032	,049	,978	,30	,824	,575	0,028
Endotheliocyts Thy,%	2,67	2,56	2,76	2,60	,047	,941	,86	,472	,499	2,60
RBTL on PhHA, %	76,8	75,9	78,3	78,4	,047	,942	,84	,478	,705	78,8
Eosinophils Spleen, %	1,22	1,63	1,41	1,53	,049	,980	,28	,839	,707	1,50
Eosinophiles Blood, %	3,89	3,79	3,47	3,67	,049	,986	,20	,897	,848	4,60
Phagoc Ind Monoc, %	3,00	2,95	2,74	2,83	,048	,973	,37	,772	,711	2,90
Lymphocyts Blood, %	62,4	59,3	62,1	59,0	,050	,998	,03	,992	,133	60,7

The identifying information contained in the 15 discriminant variables is condensed into three roots. The first root contains 75,5% of the discriminant power (r*=0,918; Wilks' Λ=0,050; $\chi^2_{(45)}$=148; $p<10^{-6}$), the second - 20,3% (r*=0,768; Wilks' Λ=0,316; $\chi^2_{(28)}$=57; $p<10^{-3}$), while the third root 4,2% only and is insignificant (r*=0,478; Wilks' Λ=0,772; $\chi^2_{(13)}$=13; p=0,467). Calculation of the values of the discriminant roots for each animal as the sum of the products of unstandardized (raw) coefficients on the individual values of the discriminant variables together with the constant (Table 2.11) enable the visualization of each rat in the information space of the roots.

Table 2.11. Standardized and raw coefficients and constants for discriminant immune variables

Coefficients	Standardized			Raw		
Variables	Root 1	Root 2	Root 3	Root 1	Root 2	Root 3
Uricemia, µM/L	-1,183	-,008	-,153	-,0049	-,00003	-,0006
Macrophages Thymus, %	,205	,732	,088	,194	,694	,084
0 Lymphocytes Blood, %	-,558	,238	,423	-,081	,035	,061
Microphages Spleen, %	,206	-,326	-,149	,108	-,171	-,078
T helper Lymphocytes, %	,181	,682	,140	,050	,189	,039
Plasmocytes Thymus, %	,475	-,312	-,278	,593	-,390	-,348
Entropy Splenocytogram	-,387	,571	-,164	-17,64	26,01	-7,489
Leukocytes Blood, G/L	-,460	,350	,405	-,098	,075	,087
PMN Neutrophils, %	,050	,520	-,252	,008	,081	-,039

Stab Neutrophils, %	,095	-,360	-,132	,082	-,309	-,114
Spleen Mass Index, µg/g BM	-,296	-,235	,747	-,0046	-,00363	,0116
Macrophages Spleen, %	,192	,403	-,269	,110	,231	-,154
B Lymphocytes, %	,047	-,631	,229	,015	-,200	,073
T cytolytic Lymphocytes, %	-,373	,347	-,213	-,117	,109	-,067
Lymphoblastes Thymus, %	,002	,303	,519	,0023	,308	,528
			Constants	16,39	-28,94	-,470
			Eigenvalues	5,350	1,440	,296
		Cumulative Proportions		,755	,958	1,000

As we can see, on the plane of the first two roots (Fig. 2.9), in which 95,8% of the information is condensed, the demarcation between the clusters is quite clear. Localization of the members of the **S-Un-** cluster in the right (positive) zone of the first root axis reflects (Table 2.12) a combination of hypouricemia with an increased content of plasma cells in the thymus and a reduced content of 0-lymphocytes in the blood with normal levels of T-cytolytic lymphocytes and rod-shaped neutrophils. The opposite left (negative) zone of the axis is occupied by members of the **S+Un+** cluster, which reflects a combination of hyperuricemia with a reduced content of plasma cells in the thymus and rod-shaped neutrophils in the blood and an increased content of Tc- and O-lymphocytes in it. The central (near-zero) zone of the axis is occupied by members of two other clusters, in which a normal level of uricemia is accompanied by normal levels of the mentioned immune parameters. It seems that uric acid upregulates the content of T-cytolytic and 0-lymphocytes in the blood, instead it downregulates the content of rod-shaped neutrophils and plasma cells in the thymus. Attention is drawn to the not entirely clear separation along the axis of the first root of the members of the **Sn+U±** and **SnUn+** (the distance between the centroids is 1,46). The latter is much larger along the axis of the second root (1,84), due to the top position of the **Sn+U±** cluster.

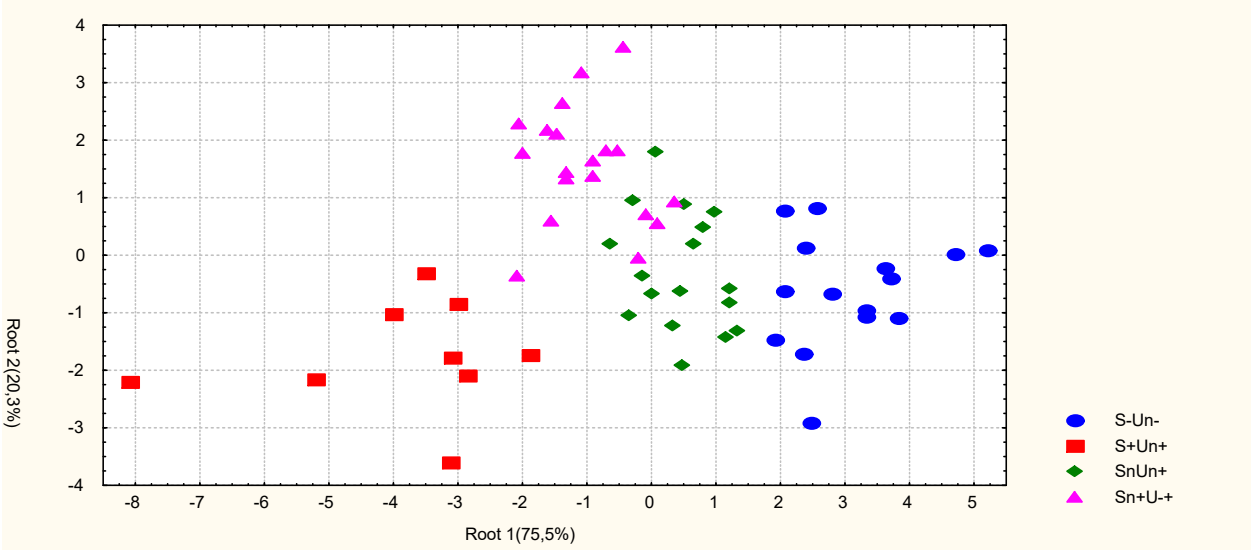

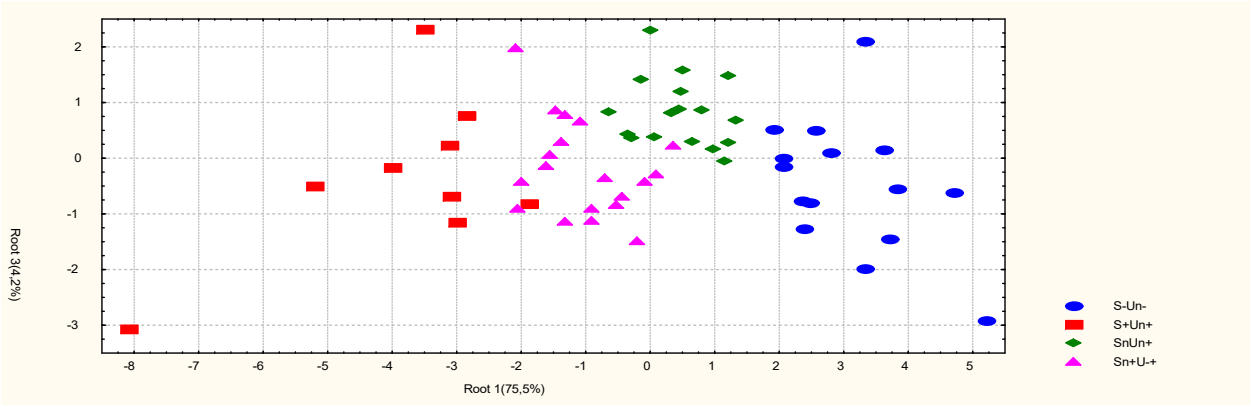

Fig. 2.9. Scattering of individual values of the first and second discriminant neuro-endocrine roots of rats of different clusters

Table 2.12. Correlations between immune variables and roots, centroids of clusters and Z-values of clusters

	Correlations Variables-Roots			S+Un+	Sn+U±	SnUn+	S-Un-
Root 1 (75,5%)	Root 1	Root 2	Root 3	**-3,86**	**-1,01**	**+0,45**	**+3,09**
Uricemia	**-,669**	-,053	-,402	**+2,10**	**+0,59**	**-0,32**	**-1,18**
Uricosuria	currently not in the model			**+0,24**	**+0,17**	**-0,05**	**-0,45**
0 Lymphocytes Blood	**-,172**	,114	,324	**+0,15**	**-0,10**	**-0,07**	**-1,08**
T cytolytic Lymphocytes	**-,026**	-,024	-,026	**+0,19**	**-0,02**	**-0,05**	**-0,08**
Plasmocytes Thymus	**,135**	-,041	-,215	**-0,17**	**+0,04**	**+0,10**	**+0,76**
Stab Neutrophils	**,038**	-,020	-,026	**-0,45**	**-0,41**	**-0,34**	**-0,19**
Bactericidity of Monocytes	currently not in the model			**-0,30**	**-0,12**	**+0,18**	**+0,61**
Root 2 (20,3%)				-1,75	**+1,56**	-0,28	-0,62
Macrophages Thymus	,072	**,347**	-,079	-0,44	**+0,64**	+0,16	+0,27
T helper Lymphocytes	,047	**,245**	,195	-0,99	**+0,14**	-0,07	-0,31
Macrophages Spleen	-,042	**,248**	-,015	-0,01	**+0,76**	+0,17	-0,02
Entropy Splenocytogram	,035	**,241**	-,040	-0,43	**+0,25**	-0,08	-0,03
PMN Neutrophils	,002	**,143**	-,280	+0,07	**+0,48**	-0,03	+0,27
Microphages Spleen	,051	**-,366**	-,076	+0,63	**-0,82**	+0,08	+0,56
B Lymphocytes Blood	,023	**-,147**	,107	+0,11	**-0,32**	+0,12	+0,09
Root 3(4,2%)				-0,34	-0,20	**+0,82**	-0,47
Spleen Mass Index	-,071	-,041	**,544**	-0,08	-0,25	**+0,09**	-0,48
Lymphoblastes Thymus	,088	,033	**,285**	-0,87	-0,41	**+0,01**	-0,16
Leukocytes Blood	-,002	-,012	**,102**	-0,19	-0,21	**-0,12**	-0,22

This position reflects increased levels of thymic and splenic macrophages and polymorphonuclear blood neutrophils in its members, as well as splenocytogram entropy combined with reduced levels of splenic macrophages and blood B-lymphocytes. However, in this cluster the level of T-helpers is normal, while in others it is reduced. It seems that the upper limit level of uricemia upregulates/downregulates the levels of 6 immune parameters, without affecting the level of T-helpers, and both its decrease and increase are accompanied by a decrease in the levels of these immune parameters to normal, and T-helpers - even lower (Table. 2.12).

Along the axis of the third root, members of the **SnUn+** cluster occupy the top position. This reflects their normal spleen mass, the level of lymphoblasts in the thymus and leukocytes in the blood, while the members of other clusters have these parameters reduced (Table 2.12). Therefore, the optimal for these immune parameters is the lower limit level of uricemia, then its deviation in any direction causes their decrease.

In general, in the information space of the three discriminant roots, all four clusters are clearly demarcated among themselves, that is, they differ from each other in terms of uricemia and the constellation of 14 parameters of immunity. This demarcation is documented by calculating the squared Mahalanobis distances between clusters (Table 2.13).

Table 2.13. Squares of Mahalanobis distances between clusters (above the diagonal) and F-criteria (df=15,4) and p-levels (below the diagonal)

Clusters	S-Un-	S+Un+	SnUn+	Sn+U-+
S-Un-	0	53	9	23
S+Un+	13,5 10^{-6}	0	24	20
SnUn+	3,5 10^{-3}	6,3 10^{-6}	0	7
Sn+U-+	9,1 10^{-6}	5,6 10^{-5}	3,0 0,003	0

The selected discriminant variables were used to identify the belonging of one or another rat to one or another cluster. This goal of discriminant analysis is realized with the help of classification functions (Table 2.14). These functions are special linear combinations that maximize the variance between groups and minimize the variance within groups. The coefficients of the classification functions are not standardized, so they are not interpreted. The object belongs to the group with the maximum value of the function, calculated by summing the products of the values of the variables and the coefficients of the classifying functions plus a constant.

Table 2.14. Coefficients and constants of classification functions for immune support of uric acid metabolism clusters

Clusters	S+Un+	Sn+U±	SnUn+	S-Un-
Variables	p=,150	p=,317	p=,283	p=,250
Uricemia, µM/L	,107	,093	,085	,073
Macrophages Thymus, %	19,85	22,70	21,80	21,97
0 Lymphocytes Blood, %	3,544	3,436	3,317	3,012
Microphages Spleen, %	3,524	3,254	3,647	4,092
T helper Lymphocytes, %	2,244	3,017	2,784	2,802
Plasmocytes Thymus, %	-20,67	-20,32	-19,09	-16,95
Entropy Splenocytogram	2603	2638	2557	2511
Leukocytes Blood, G/L	6,829	6,809	6,616	6,219
PMN Neutrophils, %	3,168	3,453	3,276	3,320
Stab Neutrophils, %	-8,333	-9,136	-8,566	-8,099
Spleen Mass Index, µg/g BM	,0817	,0582	,0700	,0442
Macrophages Spleen, %	-,430	,624	,206	,616
B Lymphocytes, %	-5,624	-6,232	-5,770	-5,756
T cytolytic Lymphocytes, %	11,09	11,11	10,67	10,41
Lymphoblastes Thymus, %	14,46	15,56	15,53	14,75
Constants	-1314	-1355	-1277	-1228

The application of classification functions enables the retrospective identification of two clusters without error, and the other two - with two errors (Table 2.15), i.e., the overall accuracy is 93,3%.

Table 2.15. Classification matrix for uric acid metabolism clusters
Rows: observed classifications; columns: predicted classifications

Clusters	Percent Correct	S+Un+ p=,150	Sn+U± p=,317	SnUn+ p=,283	S-Un- p=,250
S+Un+	100	9	0	0	0
Sn+U±	89,5	0	17	2	0
SnUn+	88,2	0	2	15	0
S-Un-	100	0	0	0	15
Total	93,3	9	19	17	15

In conclusion, we consider it expedient to make a kind of rebranding of patterns created only from discriminating immune variables (Fig. 2.10).

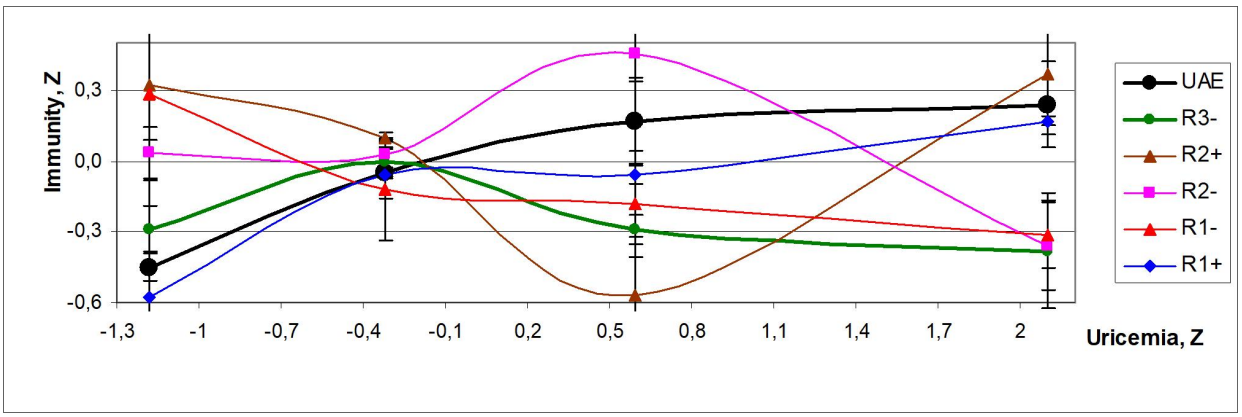

Fig. 2.10. Variants of relationships between uricemia (X-axis) and uricosuria and immune variables (Y-axis) condensed in discriminant roots (R)

As we can see, reducing the number of variables did not significantly affect the appearance of the patterns, but the U-activating pattern did not.

2.3. RELATIONSHIPS BETWEEN PARAMETERS OF URIC ACID EXCHANGE AND IMMUNITY

Previously, we obtained in female rats a wide range of uric acid metabolism parameters, divided into four clusters, quantitatively and qualitatively different from each other. Because uric acid has been identified as an endogenous adjuvant that drives immune responses in the absence of microbial stimulation [Ghaemi-Oskouie F and Shi Y, 2011], in this subdivision, functional relationships of uricemia and uricosuria with the parameters of immunity will be analyzed.

According to calculations by the formula:

$|r| = \{\exp[2t/(n - 1,5)^{0,5}] - 1\}/\{\exp[2t/(n - 1,5)^{0,5}] + 1\}$,

for a sample of n=60 critical value |r| at $p<0,05$ ($t>2,00$) is 0,25, at $p<0,02$ ($t>2,39$) is 0,30, at $p<0,01$ ($t>2,66$) is 0,33, at $p<0,001$ ($t>3,46$) is 0,42.

Screening of linear correlation coefficients between uricosuria and uricemia, on the one hand, and the recorded parameters of immunity, on the other hand, revealed the following. First of all, uricosuria is stronger than uricemia due to the parameters of immunity.

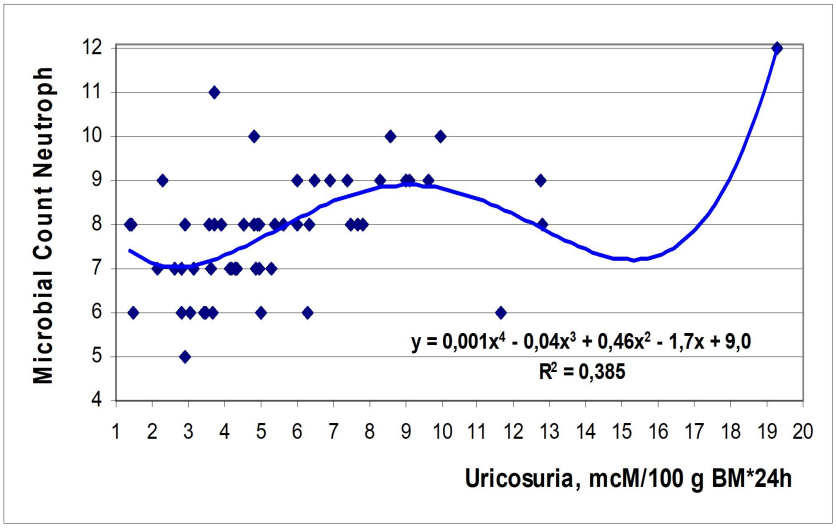

Fig. 2.11. Scatterplot of correlation between Uricosuria (X-line) and Microbial Count of blood Neutrophils (Y-line)

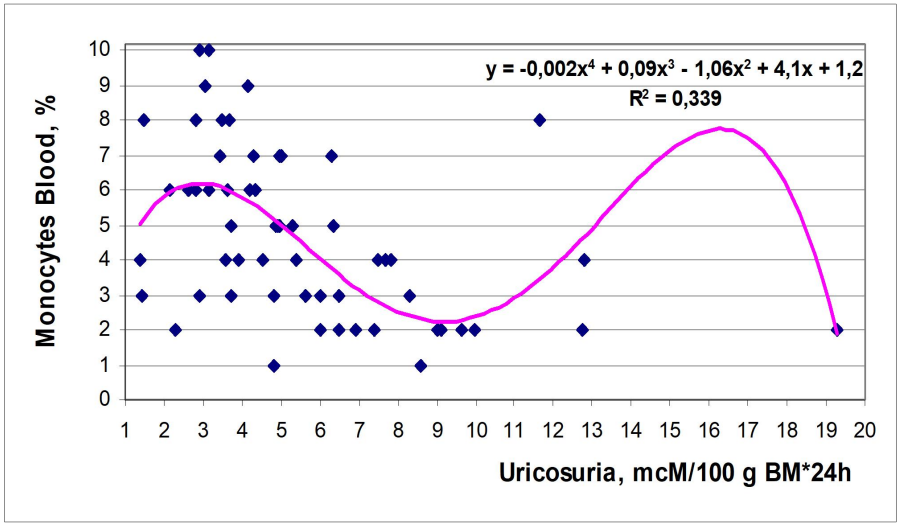

Fig. 2.12. Scatterplot of correlation between Uricosuria (X-line) and blood level of Monocytes (Y-line)

In particular, the maximum linear correlation coefficient was found between uricosuria and microbial count of blood neutrophils (r=0,53; R^2=0,281). More precisely, the dependence is approximated by the fourth-order curve (Fig. 2.11). Less commonly associated urocosuria with a relative content of monocytes in blood (r=-0,45; R^2=0,203). The relationship between them is clearly nonlinear (Fig. 2.12).

The effect of uricosuria on the relative blood content of natural killer cells is similar in strength (r=-0,41; R^2=0,168) (Fig. 2.13).

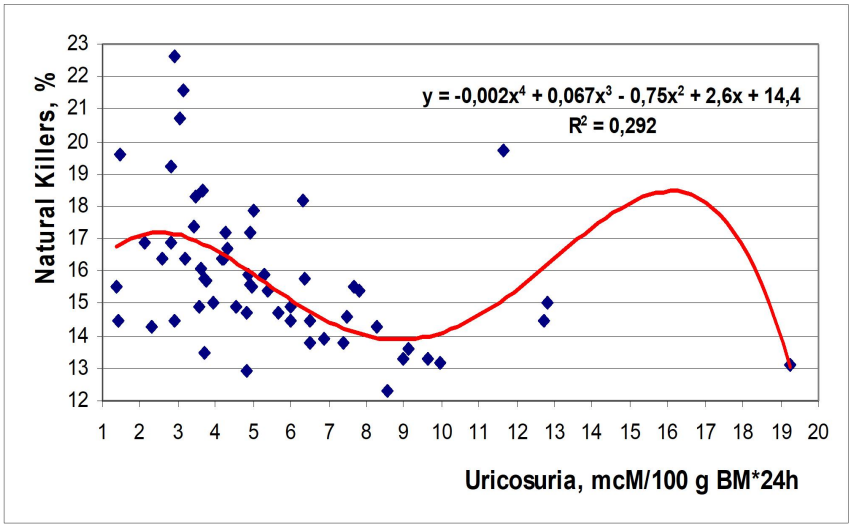

Fig. 2.13. Scatterplot of correlation between Uricosuria (X-line) and blood level of Natural Killer cells (Y-line)

In addition, a significant positive correlation of uricosuria with phagocytic index of blood neutrophils (r=0,31), T-lymphocytes content in the thymocytogram (r=0,30) and pan-lymphocytes in blood leukocytogram (r=0,29) and negative correlation with the content in the thymocytogram of epitheliocytes (r=-0,30) and reticulocytes (r=-0,27), as well as with the entropy of thymocytogram (r=-0,25).

However, when constructing a regression model with the stepwise exclusion, 6 of mentioned parameters were out of the model, instead it revealed some parameters of immunity with insignificant correlation coefficients (Table 2.16). This is probably due to the nonlinear nature of the relationships. Uricosuria was found to determine the immune status of female rats by 59% (Table 2.16 and Fig. 2.14).

Table 2.16. Regression Summary for Uricosuria
R=0,768; R^2=0,590; Adjusted R^2=0,481; $F_{(12)}$=5,4; $p<10^{-5}$

		Beta	St. Err. of Beta	B	St. Err. of B	$t_{(45)}$	p-level
Variables	r		Intercpt	-51,60	19,87	-2,60	,013
Microbial Count Neutrophils	**,53**	,501	,224	1,201	,537	2,24	,030
Lymphocytes Thymus, %	**,29**	,163	,122	,205	,154	1,33	,189
Fibroblastes Spleen, %	,20	,295	,103	,556	,193	2,88	,006
Macrophages Thymus, %	,18	,227	,109	,660	,317	2,08	,043
B Lymphocytes Blood, %	,17	,169	,102	,175	,105	1,66	,104
Entropy Immunocytogram	,12	,120	,106	39,50	34,83	1,13	,263
Monocytes Blood, %	**-,45**	-,468	,316	-,639	,432	-1,48	,146
Natural Killers Blood, %	**-,41**	,545	,321	,813	,478	1,70	,096
Eosinophiles Spleen, %	**-,35**	-,155	,113	-,611	,446	-1,37	,178
Stub Neutrophils Blood, %	-,23	-,173	,104	-,485	,293	-1,66	,105
Leukocytes Blood, 10^9/L	-,17	-,156	,106	-,110	,074	-1,48	,146
Basophiles Blood, %	-,14	-,152	,104	-,981	,669	-1,47	,150

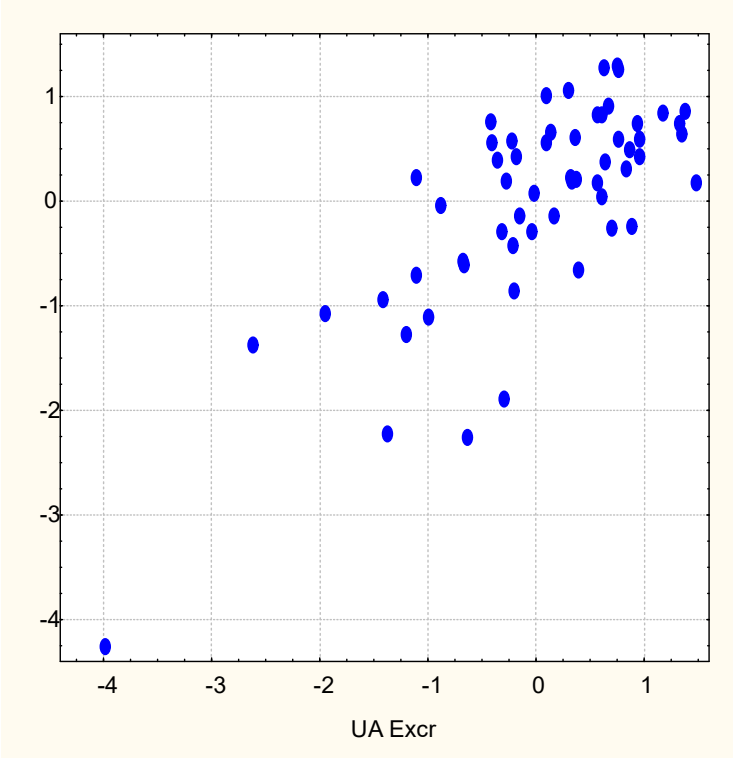

R=0,769; R^2=0,591; $\chi^2_{(13)}$=44; $p<10^{-4}$; Λ Prime=0,409
Fig. 2.14. Scatterplot of canonical correlation between Uricosuria (X-line) and the Immunity (Y-line) in female rats

Uricemia is much weaker than uricosuria, determines the immune status of female rats by only 40% (Table 2.17 and Fig. 2.15). Not included in the model association of uricemia with microbial count of blood neutrophils (r=0,25) and the content of Hassal's corpuscles in the thymocytogram (r=-0,28) also deserve attention.

Table 2.17. Regression Summary for Uricemia
R=0,630; R^2=0,396; Adjusted R^2=0,252; $F_{(11)}$=2,7; p=0,008

		Beta	St. Err. of Beta	B	St. Err. of B	$t_{(46)}$	p-level
Variables	r		Intercpt	-3873	10553	-,37	,715
Monocytes Blood, %	**-,35**	-1,022	,385	-188,5	70,9	-2,66	,011
Natural Killers Blood, %	-,23	,546	,397	109,9	79,9	1,38	,176
Reticulocytes Spleen, %	-,19	-,327	,152	-80,9	37,6	-2,16	,036
Entropy Thymocytogram	-,19	,692	,473	10652	7288	1,46	,151

Entropy Splenocytogram	-,15	-,462	,267	-10607	6136	-1,73	,091
Plasmocytes Spleen, %	-,11	-,180	,166	-60,9	56,0	-1,09	,282
Lymphocytes Thymus, %	,18	,933	,488	158,9	83,2	1,91	,062
Fibroblastes Spleen, %	,13	,180	,135	45,8	34,3	1,34	,188
Reticulocytes Thymus, %	,12	,331	,137	120,6	49,7	2,43	,019
Lymphocytes Spleen, %	,12	-,444	,279	-78,1	49,1	-1,59	,118
Phagocytic Index Neutroph, %	,09	-,177	,166	-20,5	19,3	-1,07	,292

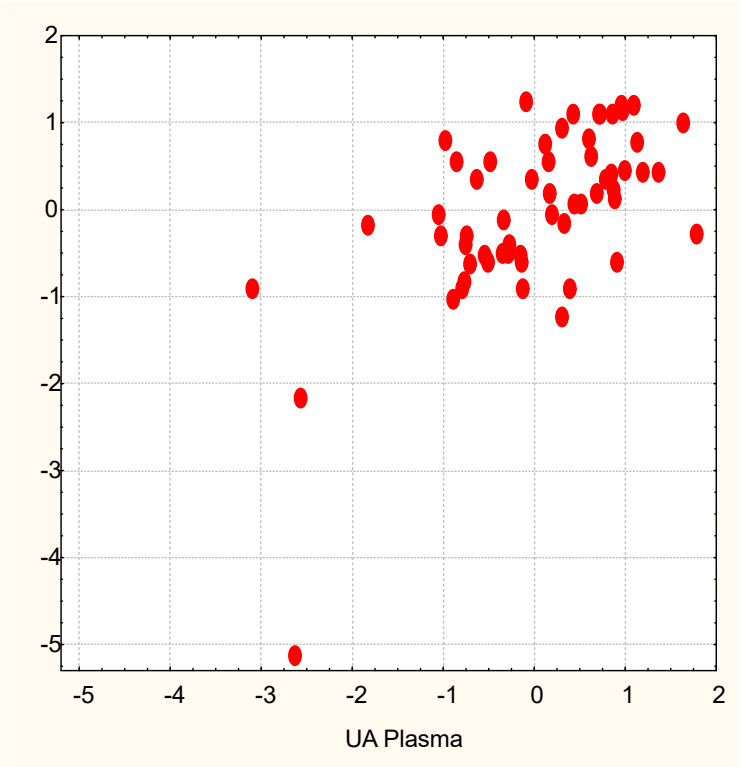

R=0,629; R^2=0,396; $\chi^2_{(11)}$=25,5; p=0,007; Λ Prime=0,604

Fig. 2.15. Scatterplot of canonical correlation between Uricemia (X-line) and the Immunity (Y-line) in female rats

This condition with determination seems quite logical, since uricemia, unlike uricosuria, reflects only the situational (biorhythmic) level of uric acid in the body.

At the final stage, an analysis of the canonical correlation between the two parameters of uric acid metabolism, on the one hand, and the parameters of immunity, on the other, conducted. It is found that the causal canonical root receives a factor load from uricosuria twice that from uricemia (Table 2.18). Interestingly, the factor loadings coincide quite well with the coefficients of variability of these parameters in intact animals (0,939 and 0,516, respectively).

Table 2.18. Factor loads on canonical roots of uric acid metabolism and immunity parameters as well as correlation coefficients between them

Right set	R		
Uricosuria	**-,996**		
Uricemia	**-,548**	UrU	UrS
Left set	R	r	r
Microbial Count Neutrophils	**-,638**	**,53**	**,25**
Phagocytic Index Neutroph, %	**-,360**	**,30**	,09
Lymphocytes Thymus, %	**-,357**	**,29**	,18
Pan-Lymphocytes Blood, %	**-,330**	**,30**	,07
Fibroblastes Spleen, %	**-,229**	,20	,13
Macrophages Thymus, %	-,208	,18	-,05
B Lymphocytes Blood, %	-,204	,17	-,04
Entropy Immunocytogram	-,168	,12	,20
Reticulocytes Spleen, %	-,006	,04	-,19

Monocytes Blood, %	**,538**	**-,45**	**-,35**
Natural Killers Blood, %	**,496**	**-,41**	-,23
Eosinophiles Spleen, %	**,393**	**-,35**	-,10
Epitheliocytes Thymus, %	**,350**	**-,29**	-,09
Entropy Thymocytogram	**,305**	**-,25**	-,19
Reticulocytes Thymus, %	**,289**	**-,26**	,12
Stub Neutrophils Blood, %	**,270**	-,23	-,14
Leukocytes Blood, 10^9/L	,219	-,17	-,07
Basophiles Blood, %	,166	-,14	-,01
Hassal's corpuscles Thymus, %	,145	-,09	**-,28**
Entropy Splenocytogram	,132	-,10	-,15
Lymphocytes Spleen, %	,024	-,02	,12
Plasmocytes Spleen, %	,022	-,01	-,11

Judging by the factor loadings on the immune canonical root, the most significant **enhancing** effect of endogenous uric acid is increase in the intensity and activity of the phagocytosis of microbes by neutrophils (but not monocytes) of blood. In addition, uric acid increases the relative content of lymphocytes in general and B-lymphocytes in particular in the blood and T-lymphocytes in the thymus. Less significant effect of uric acid on the increase in the content of fibroblasts in the spleen and macrophages in the thymus, as well as the increase in entropy of the immunocytogram of blood.

On the other hand, uric acid significantly **reduces** the total blood content of leukocytes and the proportion of monocytes and young forms of neutrophils in leukocytogram, as well as natural killer cells in immunocytogram. In addition, uric acid reduces the entropy of thymocytogram and the proportion of epitheliocytes and reticulocytes in it as well as of eosinophils in the splenocytogram.

Unfortunately, the bone marrow cytogram was not investigated in this study. But even without this, we get the impression that uric acid does not meet the classic characteristics of neither stressors nor antistressors.

Taken together, both parameters of uric acid metabolism determine the immunity status of healthy female rats by 71% (Fig. 2.16).

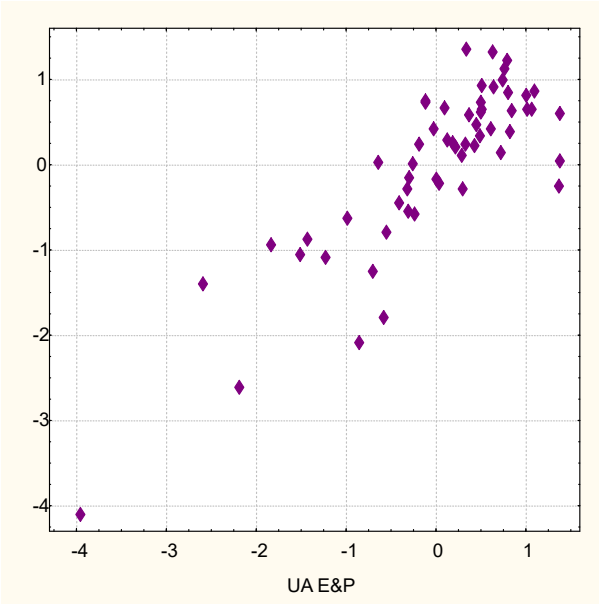

R=0,844; R^2=0,712; $\chi^2_{(46)}$=77; p=0,003; Λ Prime=0,175

Fig. 2.16. Scatterplot of canonical correlation between Uricosuria and Uricemia (X-line) and the Immunity (Y-line) in female rats

We consider it appropriate to cite the results of long-standing clinical observations regarding the effect of adaptation status on the strength and even the nature of correlating relationships of uricemia with parameters of immunity [Ivassivka SV et al, 2004]. It was found that in

individuals with **normal** adaptation status, classified as a harmonic general adaptation reaction, correlation with the activity and intensity of phagocytosis of Staph. aureus by neutrophils is positive (r=0,57 and 0,20, respectively), and with the monocyte site in the leukocytogram and the total leukocyte count is negative (r=-0,23 and -0,34, respectively), which is consistent with our data in **healthy** rats. In contrast, in individuals with premorbid (disharmonious) and pathologic general adaptation reactions the connections come to naught or reverse. The negative nature of correlation of uricemia with the level in the immunocytogram of natural killers found in healthy rats is confirmed in two groups of people with minimal suppression (r=-0,32 and -0,19); on the other hand, in cases of deeper suppression, the connection reverses (r=+0,15).

2.4. FEATURES OF THE STATE OF NEURO-ENDOCRINE FACTORS OF ADAPTATION UNDER DIFFERENT VARIANTS OF URIC ACID EXCHANGE

We previously identified 4 variants-clusters of uricemia and uricosuria in rats. Using the method of discriminant analysis, it was shown that the clusters differ from each other in the constellation of immunity parameters, which to one degree or another correlate with uricemia and uricosuria. Even earlier in our laboratory, the connection of uricemia with autonomous tone and general adaptive reactions in urological patients was revealed [Ivassivka SV et al, 2004]. Therefore, the aim of next study was to identify autonomic and endocrine adaptogenic factors, the combination of which differentiates previously formed quantitative and qualitative variants of uric acid metabolism in rats.

Applying the already described method of discriminant analysis, we found 11 variables that are recognizable in relation to the four clusters (Table 2.19).

Table 2.19. Summary of the stepwise analysis of neuro-endocrine variables ranked by the Λ criterion

Variable Enter	F to enter	p-value	Lambda	F-value	p-value
Uricemia	45,6	0,00000	0,290	45,6	0,000000
Parathyroid Activity	10,2	0,00002	0,187	24,1	0,000000
MxDMn as Vagotone	2,8	0,04599	0,161	16,3	0,000000
Corticosterone	2,1	0,11471	0,144	12,6	0,000000
Medullary Zone Adrenals	2,7	0,05243	0,124	10,8	0,000000
Calcitonin Activity	2,6	0,06466	0,108	9,6	0,000000
17-KS Urine	2,2	0,09718	0,095	8,7	0,000000
Ca/K Plasma	1,8	0,16403	0,086	7,9	0,000000
Fascicular Zone Adrenals	1,7	0,18613	0,078	7,3	0,000000
Reticular Zone Adrenals	1,2	0,30845	0,072	6,7	0,000000
Adrenals Mass Index	1,1	0,36145	0,067	6,2	0,000000

Among them, in addition to **uricemia** by definition, 6 indicators were found that reflect the state of glucocorticoid, androgenic and catechomaminincretory functions of the **adrenal glands**, as well as **HRV**-marker of vagal tone and electrolyte markers of **sympatho-vagal balance** as well as **calcitonin** and **parathyroid** activity. Instead, **uricosuria**, **HRV-**markers of sympathetic tone and circulating catecholamines, indicators of mineralocorticoid function of the adrenal glands, testosterone (the source of which in females is the reticular zone of their cortex), as well as triiodothyronine were outside the discriminating model (Table 2.20).

The identifying information contained in the 11 discriminant variables is condensed into three roots. The first root contains 66,4% of the discriminant power (r*=0,879; Wilks' Λ=0,067; $\chi^2_{(33)}$=139; p<10^{-6}), second - 21,6% (r*=0,724; Wilks' Λ=0,296; $\chi^2_{(20)}$=63; p<10^{-5}), and third - 12,0% (r*=0,615; Wilks' Λ=0,621; $\chi^2_{(9)}$=25; p=0,004).

Table 2.20. Summary of the analysis of discriminant functions for neuro-endocrine variables ranked by structural coefficient

Step 11, N of vars in model: 11; Grouping: 4 grps; Wilks' Λ: 0,0674; approx. $F_{(33)}$=6,2; $p<10^{-6}$

	Clusters of Uric acid Exchange (n)				Parameters of Wilks' Statistics					
Variables currently in the model	S- Un- (15)	Sn Un+ (17)	Sn+ U± (19)	S+ Un+ (9)	Wil-ks' Λ	Parti-al Λ	F-re-move	p-level	Tole-rancy	Norm (10)
Uricemia, µM/L	259	554	865	1379	0,171	0,395	23,5	10^{-6}	0,915	662
MxDMn HRV as Vagal Tone, msec	26	45	39	101	0,095	0,713	6,16	0,001	0,555	53
(Cau•Pu/Pp•Cap)^{0,25} as Calcitonin Activity	1,90	1,57	1,53	1,49	0,082	0,826	3,23	0,031	0,528	1,67
(Cap•Pu/Pp•Cau)^{0,25} as Parathyrin Activity	2,15	1,55	1,71	1,93	0,085	0,790	4,07	0,012	0,677	2,08
(Cap/Kp)^{0,5} as Sympat/Vagal balance	0,92	0,79	0,85	0,91	0,077	0,876	2,18	0,103	0,460	0,89
Fascicular Zone of Adrenals, µM	444	409	374	413	0,075	0,903	1,64	0,193	0,761	402
Corticosterone, nM/L	437	532	422	321	0,082	0,827	3,22	0,031	0,649	482
Medullary Zone of Adrenals, µM	80	78	98	84	0,079	0,851	2,69	0,057	0,703	94
17-Ketosteroides Ex-cretion, nM/100g•24h	55	69	83	62	0,076	0,890	1,89	0,145	0,871	61
Adrenals Mass Index, mg/100g Body Mass	27,7	25,9	27,7	25,7	0,072	0,933	1,09	0,361	0,901	25,2
Reticular Zone of Adrenal Cortex, µM	43,2	47,1	40,5	40,8	0,073	0,927	1,20	0,321	0,867	42,7
Variables currently not in the model	S- Un- (15)	Sn Un+ (17)	Sn+ U± (19)	S+ Un+ (9)	Wil-ks' Λ	Parti-al Λ	F to enter	p-level	Tole-rancy	Norm (10)
Uricosuria, µM/100 g•24h	3,31	5,46	6,63	7,00	0,067	0,997	0,05	0,986	0,398	5,72
AMo HRV as Sympathetic tone, %	70	57	66	42	0,066	0,978	0,34	0,799	0,417	56
Moda HRV as Humo-ral Channel, msec	110	118	111	134	0,067	0,997	0,05	0,984	0,230	124
Testosterone, nM/L	4,19	4,84	5,40	3,65	0,064	0,942	0,93	0,434	0,764	3,93
(Nap•Ku/Kp•Nau)^{0,25} as Mineralocort Activ	3,12	3,09	2,83	3,03	0,064	0,944	0,88	0,457	0,437	2,73
Glomerular Zone of Adrenals, µM	194	187	179	197	0,067	0,986	0,21	0,889	0,757	191
Triiodothyronine, nM/L	2,40	2,28	2,14	2,18	0,067	0,997	0,05	0,986	0,508	2,14

Having applied the previous algorithm, we calculate the values of the discriminant roots for each animal according to the raw coefficients and constants given in Table 2.21 with the subsequent visualization of each rat in the information space of the roots.

Table 2.21. Standardized and raw coefficients and constants for discriminant neuro-endocrine variables

Variable	Standardized Coefficients		
	Root 1	Root 2	Root 3
Uricemia	0,884	0,319	-0,113
Parathyroid Activity	-0,327	0,614	0,277
MxDMn as Vagotone	0,393	-0,100	1,017
Corticosterone	0,135	-0,487	0,583
Medullary Zone Adrenals	-0,068	-0,058	-0,738
Calcitonin Activity	-0,442	0,582	-0,047
17-KS Urine	0,163	-0,273	-0,418
Ca/K Plasma	-0,287	0,465	-0,497
Fascicular Zone Adrenals	0,157	0,043	0,532
Reticular Zone Adrenals	-0,133	-0,365	0,012
Adrenals Mass Index	-0,133	0,250	-0,269

Variable	Raw Coefficients		
	Root 1	Root 2	Root 3
Uricemia	0,0037	0,0013	-0,0005
Parathyroid Activity	-0,9733	1,8291	0,8254
MxDMn as Vagotone	0,0099	-0,0025	0,0257
Corticosterone	0,0008	-0,0029	0,0035
Medullary Zone Adrenals	-0,0020	-0,0017	-0,0219
Calcitonin Activity	-1,2204	1,6064	-0,1286
17-KS Urine	0,0041	-0,0068	-0,0104
Ca/K Plasma	-1,7617	2,8499	-3,0468
Fascicular Zone Adrenals	0,0020	0,0005	0,0068
Reticular Zone Adrenals	-0,0130	-0,0356	0,0012
Adrenals Mass Index	-0,0307	0,0578	-0,0622
Constant	2,319	-7,507	0,377

On the plane of the first two roots (Fig. 2.17), in which 88% of the information is condensed, only two clusters are clearly demarcated. The localization of members of the **S-Un-** cluster in the left (negative) zone of the first root axis reflects (Table 2.22) a combination of hypouricemia with reduced vagal tone and increased calcitonin activity. Despite not being formally included in the discriminant model (due to duplication/excess of information), hypouricosuria, increased sympathetic tone and circulating catecholamines level (a marker of which is 1/Mode HRV) deserve attention as characteristic signs. The opposite right (positive) zone of the axis is occupied by members of the **S+Un+** cluster, which reflects the combination of hyperuricemia with slightly increased uricosuria and significantly increased vagal tone and reduced calcitonin activity, and thus reduced sympathetic tone and the level of catecholamines in the blood. The members of the remaining two clusters occupy an intermediate position along the axis of the first root and are partially mixed.

Additional delimitation of these clusters occurs along the axis of the second root. As can be seen, members of the **SnUn+** cluster occupy the lower zone of the axis (centroid: -1,41), which reflects their reduced parathyroid activity and serum Ca/K ratio in combination with a completely normal thickness of the fascicular zone of the adrenal cortex and a slightly increased level of corticosterone, while in members of the **Sn+U±** cluster (centroid: -0,08), the first two parameters are reduced to a lesser extent, the fascicular zone is slightly thickened, and the corticosterone level is slightly reduced.

Along the axis of the third root, members of the **Sn+U±** cluster occupy the lower zone (centroid: -1,06), which reflects the **maximum** for the sample mass index of the adrenal glands, the thickness of their medullary zone, and the excretion of 17-ketosteroids in combination with the **minimum** for sampling the thickness of the reticular zone of the adrenal glands. It should be noted that the maximum serum level of testosterone (secreted by the adrenal glands) in

combination with the minimum for sampling the thickness of the glomerular zone of the adrenal glands and mineralocorticoid activity, as well as serum triiodothyronine, are also not included in the model.

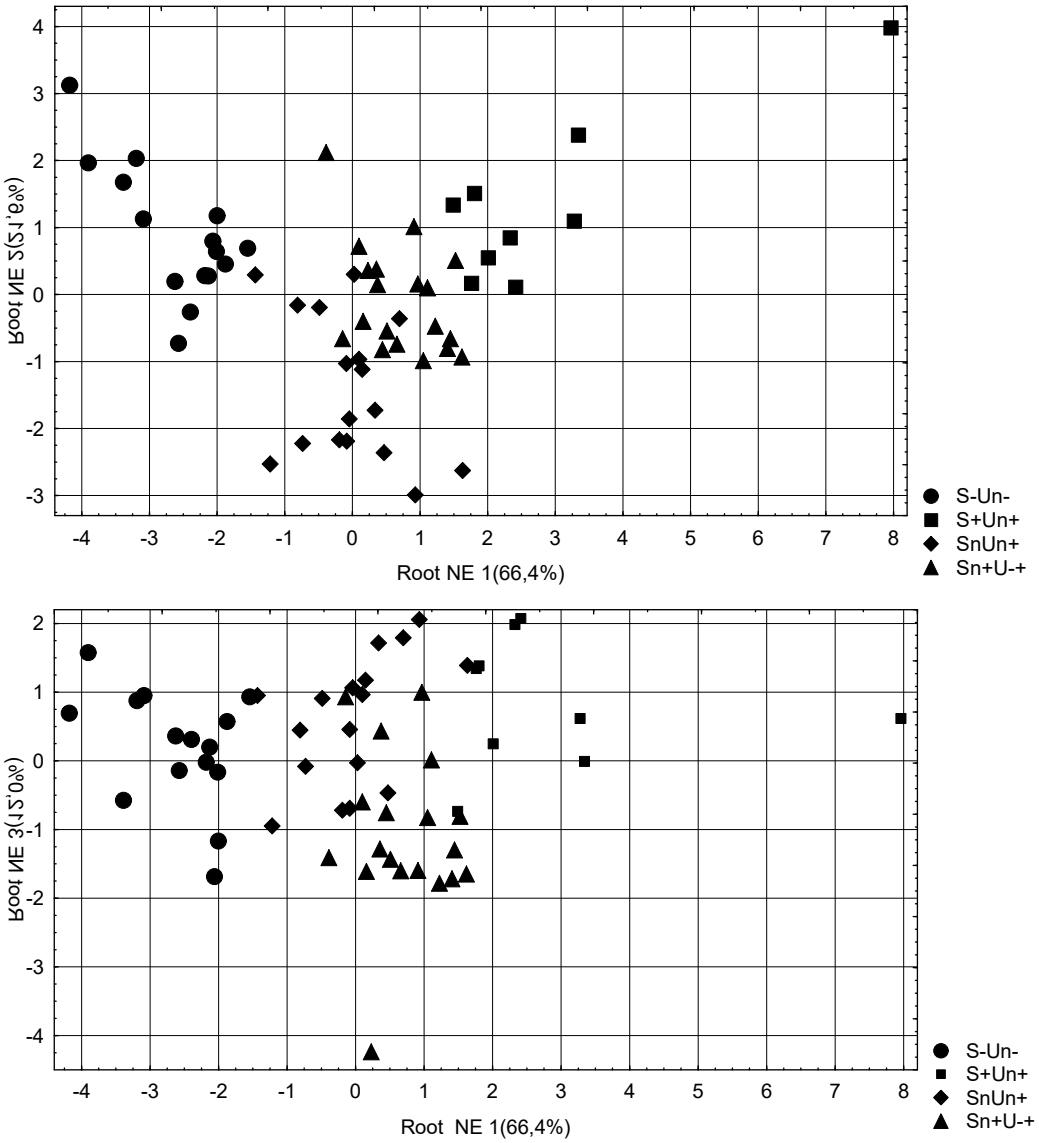

Fig. 2.17. Scattering of individual values of the discriminant neuro-endocrine roots of rats of different clusters

Table 2.22. Correlations between neuro-endocrine variables and roots, centroids of clusters and Z-values of clusters

	Correlations Variables-Roots			S-Un-	SnUn+	Sn+U-+	S+Un+
Root 1(66,4%)	Root 1	Root 2	Root 3	**-2,61**	-0,05	+0,71	**+2,93**
Uricemia	**,823**	,366	-,0109	**-1,18**	-0,32	+0,59	**+2,10**
Uricosuria	currently not in the model			**-0,45**	-0,05	+0,17	**+0,24**
MxDMn as Vagal tone	**,284**	,175	,374	**-0,63**	-0,18	-0,34	**+1,18**
Calcitonin Activity	**-,231**	,160	,097	**+0,62**	-0,25	-0,37	**-0,47**
AMo as Sympathetic tone	currently not in the model			**+0,84**	+0,05	+0,60	**-0,77**
1/Mode as Catecholamines	currently not in the model			**+0,92**	+0,42	+0,89	**-0,71**
Root 2(21,6%)	Root 1	Root 2	Root 3	+0,90	**-1,41**	-0,08	+1,33
Parathyroid Activity	-,175	**,597**	,102	+0,13	**-1,08**	-0,75	-0,31
(Ca/K)^{0,5} Plasma	-,040	**,315**	,033	+0,17	**-0,58**	-0,27	+0,11
Fascicular Zone Adrenals	-,119	**,120**	**,312**	+0,49	**+0,08**	+0,49	+0,13
Corticosterone	-,105	**-,356**	,068	-0,36	**+0,40**	-0,47	-1,28
Root 3(12,0%)	Root 1	Root 2	Root 3	+0,18	+0,59	**-1,06**	+1,83

Medullary Zone Adrenals	,052	,028	**-,295**	-0,43	-0,50	**+0,14**	-0,30
17-Ketosteroides Excretion	,073	-,116	**-,272**	-0,11	+0,14	**+0,40**	+0,02
Adrenals Mass Index	-,063	,072	**-,223**	+0,49	+0,13	**+0,49**	+0,10
Testosterone	currently not in the model			+0,25	+0,85	**+1,38**	-0,26
Reticular Zone Adrenals	-,051	-,185	**,213**	+0,06	+0,58	**-0,29**	-0,25
Glomerular Zone Adrenals	currently not in the model			+0,07	-0,08	**-0,27**	+0,15
Mineralocorticoid Activity	currently not in the model			+0,50	+0,46	**+0,12**	+0,39
Triiodothyronine	currently not in the model			+0,46	+0,24	**0,00**	+0,07

In general, in the information space of the three discriminant roots, all four clusters are clearly demarcated among themselves, that is, they differ significantly from each other in terms of uricemia and the constellation of 10 neuro-endocrine parameters. This demarcation is documented by calculating the squared Mahalanobis distances between clusters (Table 2.23).

Table 2.23. Squares of Mahalanobis distances between clusters (above the diagonal) and F-criteria (df=11,5) and p-levels (below the diagonal)

Clusters	S-Un-	S+Un+	SnUn+	Sn+U-+
S-Un-	0	31	12	14
S+Un+	13,2 10^{-6}	0	16	11
SnUn+	7,2 10^{-6}	7,2 10^{-6}	0	5
Sn+U-+	8,5 10^{-6}	4,8 10^{-5}	3,4 0,002	0

The selected neuro-endocrine variables were used to identify the belonging of one or another rat to one or another cluster with the help of classification functions (Table 2.24).

Table 2.24. Coefficients and constants of classification functions for neuro-endocrine support of uric acid metabolism clusters

Variable	S-Un- p=,250	S+Un+ p=,150	SnUn+ p=,283	Sn+U-+ p=,317
Uricemia	0,003	0,024	0,009	0,015
Parathyroid activity	11,00	6,932	4,621	4,947
Vagal tone	-0,062	0,009	-0,020	-0,059
Corticosterone	-0,001	0,005	0,010	0,001
Medullary Zone Adrenals	0,108	0,081	0,097	0,130
Calcitonine activity	33,39	27,24	26,51	27,92
17-Ketosteroides urine	0,004	0,017	0,026	0,038
Ca/K ratio plasma	72,05	61,53	59,73	67,21
Fascicular Zone Adrenals	0,053	0,069	0,060	0,051
Reticular Zone Adrenals	0,277	0,191	0,326	0,267
Adrenals Mass Index	1,970	1,784	1,733	1,889
Constant	-127,2	-119,6	-101,0	-109,4

The overall classification accuracy is 90,0% (Table 2.25).

Table 2.25. Classification matrix for uric acid metabolism clusters
Rows: observed classifications; columns: predicted classifications

Clusters	Percent Correct	S+Un+ p=,150	Sn+U-+ p=,317	SnUn+ p=,283	S-Un- p=,250
S+Un+	88,9	**8**	**1**	0	0
Sn+U-+	89,5	0	**17**	**2**	0
SnUn+	82,4	0	**2**	**14**	**1**
S-Un-	100	0	0	0	**15**
Total	90,0	8	20	16	16

Now let's analyze the connections between parameters of uric acid metabolism, on the one hand, and neuro-endocrine adaptation factors, on the other. The matrix illustrates (Table 2.26) that uricosuria has wider and closer connections than uricemia. In particular, uricosuria correlates significantly ($_{0,05}|r|\geq 0,25$) positively with the excretion of 17-ketosteroids and vagal tone, but negatively with the level of triiodothyronine, and the thickness of the fascicular zone of the adrenal cortex. The regression model also included 1/Mode HRV as measure of the level of circulating catecholamines (Table 27).

Table 2.26. Matrix of correlations between parameters of uric acid metabolism and neuro-endocrine factors of adaptation

Variable	Uricemia	Uricosuria
Uricemia	1,00	0,48
Uricosuria	0,48	1,00
Calcitonin activity	-0,30	-0,09
Vagal tone	0,42	0,21
Sympathetic tone	-0,29	-0,10
1/Mode	-0,28	-0,19
Corticosterone	-0,21	-0,02
Testosterone	-0,05	-0,20
Glomerular ZAC	-0,02	-0,19
Fascicular ZAC	-0,23	-0,45
Triiodothyronine	-0,23	-0,47
17-Ketosteroides	0,09	0,56

Table 2.27. Regressive model for neuro-endocrine adaptation factors and uricosuria

N=60	R=0,780; R^2=0,609; Adjusted R^2=0,573 F(5,5)=16,8; p<10^-5					
	Beta	St. Err. of Beta	B	St. Err. of B	t(54)	p-value
		Intercpt	14,3	3,2	4,54	0,00003
MxDMn	0,339	0,161	0,0239	0,0114	2,10	0,04056
1/Mode	0,225	0,161	0,0356	0,0255	1,40	0,16775
Fasc ZAC	-0,208	0,111	-0,0083	0,0044	-1,88	0,06615
T3	-0,318	0,112	-2,5152	0,8886	-2,83	0,00651
17-KS	0,595	0,087	0,0471	0,0069	6,85	0,00000

This constellation of neuro-endocrine adaptation factors is determined by uricosuria by 61%.

In the regression model for uricemia, after stepwise exclusion, only three variables remained, determined by uricemia by only 29% (Table 2.28). However, the sympathetic tone, circulating catecholamines, the fascicular zone and the corticosterone secreted by it are worth attention, which are negatively determined by uricemia.

Table 2.28. Regressive model for neuro-endocrine adaptation factors and uricemia

N=60	R=0,535; R^2=0,287; Adjusted R^2=0,248; F(3,6)=7,5; p=0,0003					
	Beta	St. Err. of Beta	B	St. Err. of B	t(56)	p-value
		Intercpt	1584,77	407,70	3,89	0,0003
Calcitonin activity	-0,310	0,115	-346,72	129,23	-2,68	0,0096
Vagal tone	0,356	0,117	3,41	1,12	3,04	0,0035
Triiodothyronine	-0,197	0,119	-212,54	127,80	-1,66	0,1019

Canonical correlation analysis shows that the combined determining influence of both parameters of uric acid metabolism exceeds the influence of uricosuria alone by only 1,4% (Fig. 2.18).

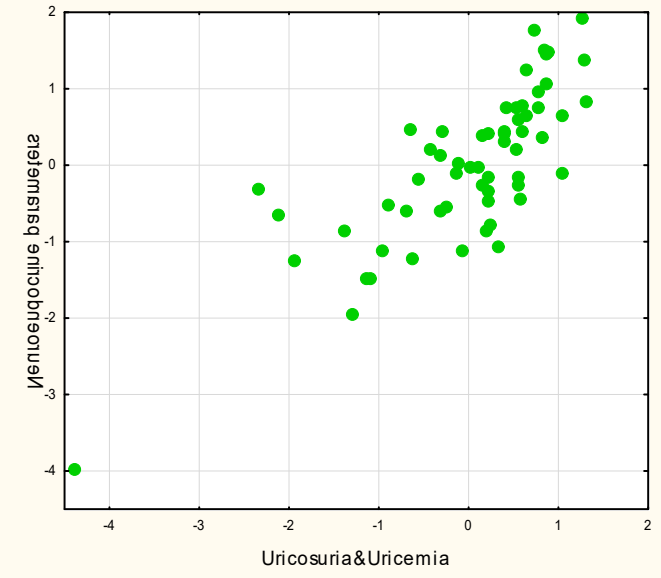

$R=0,789$; $R^2=0,623$; $\chi^2_{(12)}=69$; $p<10^{-6}$; Λ Prime$=0,284$

Fig. 2.18. Scatterplot of the canonical correlation between uricosuria and uricemia (X axis) and neuro-endocrine adaptation factors (Y axis) of female rats

Judging by the factor loadings (Table 2.29), the excretion of 17-ketosteroids was subject to maximum upregulation by uric acid, to a lesser extent to vagal tone, instead, triiodothyronine and the fascicular zone of the adrenal cortex were subject to downregulation, as well as, to a lesser extent, catecholamines and calcitonin.

Table 2.29. Factor structure of canonical roots of uric acid and neuro-endocrine adaptation factors

Root	left set
Variable	R
Uricosuria	-1,000
Uricemia	-0,450

Root	right set
Variable	R
Calcitonin activity	0,106
Vagal tone	-0,252
Catecholamines	0,227
Fascicular ZAC	0,576
Triiodothyronine	0,594
17-Ketosteroides	-0,721

2.5. FEATURES OF THE EXCHANGE OF ELECTROLYTES AND NITROGENOUS METABOLITES UNDER DIFFERENT VARIANTS OF URIC ACID EXCHANGE

We previously identified 4 variants-clusters of uricemia and uricosuria in rats. Using the method of discriminant analysis, it was shown that the clusters differ from each other in the constellation of immune, autonomic and endocrine parameters, which to one degree or another correlate with uricemia and uricosuria. Even earlier in our laboratory, the connection of uricemia with parameters of electrolytes and nitrogenous exchange in urological patients was revealed [Ivassivka SV et al, 2004]. Therefore, the aim of next study was to identify the electrolytes and

nitrogenous metabolites, the combination of which differentiates previously formed quantitative and qualitative variants of uric acid metabolism in rats.

The discriminant analysis procedure included in the model, in addition to uricemia, 10 variables characteristic of four clusters (Tables 2.30 and 2.31). They represent the concentration of glucose, urea, phosphates, magnesium and potassium in plasma, and the latter in erythrocytes, as well as the excretion of creatinine, urea, phosphates and calcium with urine. Other registered parameters of metabolism, primarily uricosuria and urine osmolality, as well as excretion of sodium, chloride, magnesium and phosphates as well as plasma levels of creatinine, calcium, chloride and sodium, and the latter in erythrocytes, were outside the discriminant model.

Table 2.30. Summary of the stepwise analysis of metabolic variables ranked by the Λ criterion

Variable Enter	F to entrer	p-value	Lambda	F-value	p-value
Uricemia	45,6	0,000000	0,290	45,6	0,000000
Magnesium Plasma	9,9	0,000026	0,189	23,9	0,000000
Phosphates Plasma	5,6	0,002132	0,144	17,8	0,000000
Phosphates Excretion	5,1	0,003749	0,112	15,1	0,000000
Potassium Plasma	4,3	0,008442	0,090	13,4	0,000000
Urea Plasma	3,5	0,021897	0,074	12,1	0,000000
Potassium Erythrocytes	2.7	0.055483	0.064	11.0	0.000000
Creatinine Excretion	1,7	0,173862	0,058	9,9	0,000000
Glucose Plasma	1,2	0,330486	0,054	9,0	0,000000
Urea Excretion	1,1	0,349804	0,050	8,2	0,000000
Calcium Excretion	1,2	0,308472	0,047	7,6	0,000000

Table 2.31. Summary of the analysis of discriminant functions for metabolic variables ranked by structural coefficient

Step 11, N of vars in model: 11; Grouping: 4 grps; Wilks' Λ: 0,0466; approx. $F_{(33)}$=7,6; $p<10^{-6}$

	Clusters of Uric acid Exchange (n)				**Parameters of Wilks' Statistics**					
Variables currently in the model	**S+ Un+ (9)**	**Sn+ U± (19)**	**Sn Un+ (17)**	**S- Un- (15)**	Wilks' Λ	Partial Λ	F-remove	p-level	Tolerancy	**Norm (10)**
Uricemia, µM/L	**1379**	865	554	259	0,154	0,302	35,4	10^{-6}	0,840	662
Creatinine Excretion µM/100 g•24h	**11,9**	12,6	12,6	8,6	0,052	0,903	1,65	0,190	0,460	8,7
Potassium Erythrocytes, mM/L	**89,6**	87,3	86,2	85,0	0,055	0,847	2,77	0,052	0,771	87,0
Glucose Plasma, mM/L	**5,63**	5,27	5,29	5,28	0,050	0,926	1,22	0,314	0,889	4,95
Urea Plasma, mM/L	**5,29**	8,76	9,29	9,39	0,056	0,824	3,27	0,029	0,656	7,42
Magnesium Plasma, mM/L	0,84	0,78	**1,27**	0,45	0,067	0,690	6,88	0,001	0,809	0,88
Phosphates Plasma, mM/L	0,84	1,11	**1,19**	0,46	0,078	0,596	10,4	10^{-4}	0,630	0,72
Calcium Excretion, µM/100 g•24h	2,60	4,17	**4,27**	2,89	0,050	0,926	1,23	0,308	0,275	2,90
Potassium Plasma, mM/L	3,63	3,37	**3,87**	3,25	0,061	0,767	4,66	0,006	0,642	4,23
Phosphates Excretion, µM/100 g•24h	9,0	**12,7**	10,4	9,3	0,052	0,895	1,80	0,160	0,229	9,4
Urea Excretion µM/100 g•24h	231	**264**	224	144	0,054	0,865	2,39	0,081	0,151	169
Variables	**S+**	**Sn+**	**Sn**	**S-**	Wil-	Parti-	F to	p-	Tole-	**Norm**

currently not in the model	Un+ (9)	U± (19)	Un+ (17)	Un- (15)	ks' Λ	al Λ	enter	level	rancy	(10)
Uricosuria, µM/100 g•24h	7,00	6,63	5,46	3,31	0,047	0,999	0,01	0,999	0,478	5,72
Osmolality Urine, mOsm/L	611	550	523	530	0,046	0,986	0,21	0,889	0,729	559
Sodium Excretion, µM/100 g•24h	201	184	149	118	0,046	0,996	0,07	0,977	0,517	135
Chloride Excretion, µM/100 g•24h	213	190	136	154	0,046	0,984	0,24	0,867	0,692	144
Creatinine Plasma, µM/L	50	81	97	81	0,044	0,942	0,92	0,439	0,219	73
Potassium Excretion, µM/100 g•24h	193	214	182	185	0,044	0,950	0,79	0,503	0,283	189
Magnesium Excretion, µM/100 g•24h	2,81	3,62	4,56	5,02	0,046	0,989	0,17	0,915	0,557	3,30
Sodium Erythrocytes, mM/L	23,1	23,6	23,1	20,4	0,045	0,969	0,47	0,703	0,588	22,0
Sodium Plasma, mM/L	129	129	131	127	0,046	0,978	0,33	0,802	0,746	128,6
Calcium Plasma, mM/L	2,92	2,69	2,41	2,78	0,044	0,943	0,91	0,445	0,783	3,35
Chloride Plasma, mM/L	93,8	92,0	94,8	90,7	0,045	0,958	0,65	0,587	0,639	94,3

Table 2.32. Standardized and raw coefficients and constants for discriminant metabolic variables

Variable	Standardized Coefficients		
	Root 1	Root 2	Root 3
Uricemia	-0,975	-0,230	0,094
Magnesium Plasma	-0,267	0,589	-0,682
Phosphates Plasma	-0,539	0,711	0,593
Phosphates Excretion	0,078	0,117	1,408
Potassium Plasma	-0,447	0,548	0,167
Urea Plasma	0,162	0,624	0,042
Potassium Erythrocytes	-0,386	-0,333	0,127
Creatinine Excretion	-0,099	0,359	-0,736
Glucose Plasma	-0,147	-0,320	0,002
Urea Excretion	-0,963	-0,206	-0,629
Calcium Excretion	0,527	0,159	0,310

Variable	Raw Coefficients		
	Root 1	Root 2	Root 3
Uricemia	-0,0040	-0,0010	0,0004
Magnesium Plasma	-0,6112	1,3477	-1,5617
Phosphates Plasma	-1,2330	1,6275	1,3584
Phosphates Excretion	0,0149	0,0223	0,2690
Potassium Plasma	-0,5778	0,7096	0,2156
Urea Plasma	0,0577	0,2219	0,0150
Potassium Erythrocytes	-0,0617	-0,0532	0,0202
Creatinine Excretion	-0,0214	0,0774	-0,1585
Glucose Plasma	-0,1864	-0,4069	0,0028
Urea Excretion	-0,0056	-0,0012	-0,0036
Calcium Excretion	0,2278	0,0689	0,1339
Constant	12,9270	-0,7885	-3,6300

The identifying information contained in the 11 discriminant variables is condensed into three roots. The first root contains 71,9% of the discriminant power (r*=0,915; Wilks' Λ=0,047; $\chi^2_{(33)}$=158; p<10^{-6}), second - 24,0% (r*=0,795; Wilks' Λ=0,286; $\chi^2_{(20)}$=65; p=10^{-6}), and the third only 4,1% and, moreover, is insignificant (r*=0,474; Wilks' Λ=0,775; $\chi^2_{(9)}$=13; p=0,158).

Further, on the basis of the coefficients given in the Table 2.32, the individual root values were calculated with subsequent visualization of cluster members in their information field.

In the Table 2.33 metabolic parameters are grouped and ranked according to their structural coefficients, and together with discriminant variables, variables that did not enter the model, but still carry recognizable information, are also considered.

Table 2.33. Correlations between metabolic variables and roots, centroids of clusters and Z-values of clusters

	Correlations Variables-Roots			S+Un+	Sn+U±	SnUn+	S-Un-
Root 1 (71,9%)	Root 1	Root 2	Root 3	**-3,39**	**-1,05**	**+0,06**	**+3,30**
Uricemia	**-,663**	-,325	,101	**+2,10**	+0,59	-0,32	**-1,18**
Uricosuria	currently not in the model			**+0,24**	+0,17	-0,05	**-0,45**
Creatinine Excretion	**-,133**	,168	,077	**+0,74**	+0,90	+0,88	**-0,03**
Potassium Erythrocytes	**-,102**	-,057	-,006	**+0,38**	+0,04	-0,12	**-0,29**
Glucose Plasma	**-,047**	-,077	-,150	**+0,62**	+0,29	+0,31	**+0,30**
Sodium Erythrocytes	currently not in the model			**+0,23**	+0,35	+0,24	**-0,37**
Sodium Excretion	currently not in the model			**+0,79**	+0,59	+0,17	**-0,19**
Chloride Excretion	currently not in the model			**+0,70**	+0,47	-0,09	**+0,10**
Osmolality Urine	currently not in the model			**+0,37**	-0,06	-0,26	**-0,21**
Urea Plasma	**,170**	,235	,262	**-1,24**	+0,78	+1,09	**+1,15**
Magnesium Excretion	currently not in the model			**-0,24**	+0,15	+0,61	**+0,83**
Root 2 (24,0%)	Root 1	Root 2	Root 3	-1,88	+0,28	**+1,63**	-1,08
Magnesium Plasma	-,142	**,426**	-,585	-0,07	-0,17	**+0,64**	-0,72
Phosphates Plasma	-,193	**,411**	,132	+0,28	+0,85	**+1,02**	-0,57
Calcium Excretion	-,023	**,225**	,195	-0,20	+0,83	**+0,90**	-0,01
Potassium Plasma	-,094	**,183**	-,017	-0,85	-0,69	**-0,51**	-1,39
Creatinine Plasma	currently not in the model			-0,93	+0,35	**+1,02**	+0,34
Sodium Plasma	currently not in the model			+0,16	+0,02	**+0,43**	-0,23
Chloride Plasma	currently not in the model			-0,08	-0,33	**+0,07**	-0,50
Calcium Plasma	currently not in the model			-0,42	-0,65	**-0,92**	-0,56
Root 3 (4,1%)	Root 1	Root 2	Root 3	-0,53	**+0,71**	-0,48	-0,03
Phosphates Excretion	-,038	,108	**,446**	-0,06	**+0,52**	+0,16	-0,02
Urea Excretion	-,101	,085	**,199**	+0,46	**+0,71**	+0,41	-0,19
Potassium Excretion	currently not in the model			+0,03	**+0,21**	-0,05	-0,03

Fig. 2.19 shows that the extreme left zone of the first root axis is occupied by members of the **S+Un+** cluster. Such localization reflects the combination of hyperuricemia with increased (and maximal for the sample) levels of creatinine excretion, erythrocyte potassium and glycemia, and a reduced level of urea in the plasma. Worthy of attention are the maximum normal levels of uricosuria, erythrocyte natriuresis, and urine osmolality for the sample, and elevated levels of natriuria and chlorideuria, instead of minimal normal magniuria. The opposite polar position is occupied by the members of the **S-Un-** cluster, which are characterized by a combination of hypouricemia with a reduced content of potassium in erythrocytes, normal, but minimal for the sample, uricosuria, creatinineuria, and glycemia, instead, maximally elevated levels of urea in plasma and magnesia. Members of the other two clusters occupy an intermediate position along the axis of the first radical and are partially mixed.

Mixing also takes place along the axis of the second radical, but to a lesser extent. At the same time, members of the **SnUn+** cluster are characterized by maximally increased levels of magnesium, phosphatemia, and calciuria (as well as abnormal creatinineemia and natriemia) in combination with minimally reduced potassium (as well as maximally reduced calcium).

An additional unclear demarcation of these clusters occurs along the axis of the third radical, due to the maximally increased excretion of phosphates and urea (as well as potassium) in the members of the **Sn+U±** cluster.

Despite the visual mixing, in the information space of the three discriminant roots, the last two clusters are statistically significantly separated from each other, which is confirmed by the calculation of the squares of the Mahalanobis distances between them, not to mention even the visually clear separation of the first two clusters (Table 2.34).

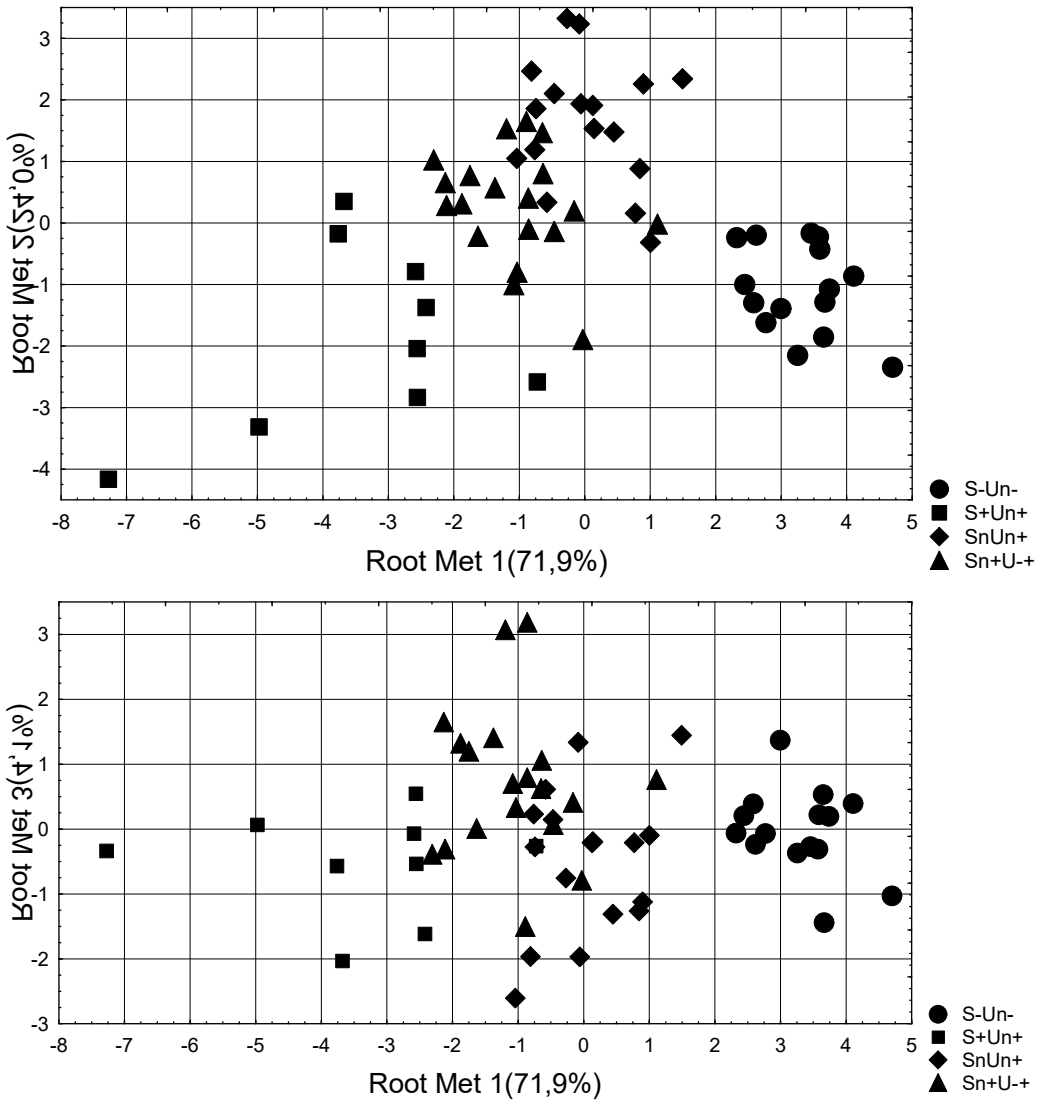

Fig. 2.19. Scattering of individual values of the discriminant metabolic roots of rats of different clusters

Table 2.34. Squares of Mahalanobis distances between clusters (above the diagonal) and F-criteria (df=11,5) and p-levels (below the diagonal)

Clusters	S-Un-	S+Un+	SnUn+	Sn+U±
S-Un-	0	46	18	21
S+Un+	19,2 10^{-6}	0	24	12
SnUn+	10,7 10^{-6}	10,6 10^{-6}	0	5
Sn+U±	13,3 10^{-6}	3,6 10^{-4}	3,0 0,005	0

The application of classification functions (Table 2.35) enables the retrospective identification of the first two clusters without error, and the other two with 1 and 2 errors, which gives a total accuracy of 95,0% (Table 2.36).

Table 2.35. Coefficients and constants of classification functions for metabolic accompaniment of clusters of uric acid metabolism

Variable	S-Un- p=,250	S+Un+ p=,150	SnUn+ p=,283	Sn+U-+ p=,317
Uricemia	0,032	0,060	0,043	0,049
Magnesium Plasma	0,443	4,229	6,779	3,770
Phosphates Plasma	15,39	21,65	23,18	23,98
Phosphates Excretion	1,478	1,226	1,369	1,644
Potassium Plasma	11,63	14,81	15,32	15,27
Urea Plasma	0,059	-0,512	0,466	0,122
Potassium Erythrocytes	2,858	3,304	2,905	3,069
Creatinine Excretion	-1,476	-1,316	-1,126	-1,396
Glucose Plasma	11,99	13,56	11,49	12,25
Urea Excretion	0,044	0,084	0,060	0,064
Calcium Excretion	-1,650	-3,296	-2,263	-2,446
Constant	-182,7	-268,9	-220,4	-237,3

Table 2.36. Classification matrix for uric acid exchange clusters
Rows: observed classifications; columns: predicted classifications

Clusters	Percent Correct	S+Un+ p=,150	Sn+U± p=,317	SnUn+ p=,283	S-Un- p=,250
S+Un+	100	**9**	0	0	0
Sn+U±	94,7	0	**18**	**1**	0
SnUn+	88,2	0	**2**	**15**	0
S-Un-	100	0	0	0	**15**
Total	95,0	9	20	16	15

At the last stage, we will analyze the connections between the parameters of uric acid and electrolyte&nitrogen exchanges. The correlation matrix shows that uricemia is significantly associated with plasma levels of urea and creatinine and excretion of magnesia (Table 2.37).

Table 2.37. Matrix of correlations between parameters of uric acid and electrolyte&nitrogen exchanges

Variable	Uricemia	Uricosuria
CrE	0,15	0,39
Diur	0,09	0,54
CrP	-0,28	0,13
KE	0,09	0,46
MgE	-0,30	-0,06
CaE	-0,03	0,33
PE	0,02	0,50
UreaE	0,12	0,35
UreaP	-0,31	0,06
KP	0,05	0,20

However, when constructing a regression model by stepwise exclusion, the program left creatinineuria in the model, excluding creatinineemia. As a result, the determination rate was 26% (Table 2.38).

Table 2.38. Regression model for metabolic parameters and uricemia

N=60	R= 0,50 9; R^2=0,259 ; Adjusted R ^2=0,219 ; F(3,6)=6,5 ; p=0 ,0007					
	Beta	St. Err. of Beta	B	St. Err. of B	t(56)	p-value
Intercpt			926,31	179,17	5,17	0,000003
Cr E	0,353	0,127	31,84	11,41	2,79	0,007176
Mg E	-0,394	0,128	-60,43	19,55	-3,09	0,003108
Urea P	-0,282	0,117	-39,98	16,62	-2,41	0,019495

Instead, the connections of uricosuria are more numerous and stronger. The descending series consists of: daily diuresis, urinary excretion of phosphates, potassium, creatinine, urea and calcium. Interestingly, with stepwise elimination, the last two parameters were not included in the regression model, while plasma potassium was. The rate of determination of the listed parameters by uricosuria is 39% (Table 2.39).

Table 2.39. Regression model for metabolic parameters and uricosuria

N=60	R= 0,62 1; R^2=0,386 ; Adjusted R ^2=0,32 9 F(5,5)=6,8 ; p=0,00006					
	Beta	St. Err. of Beta	B	St. Err. of B	t(54)	p-value
Intercpt			-0,071	1,853	-0,04	0,969
Cr Excr	-0,404	0,238	-0,268	0,158	-1,70	0,096
Diurese	1,023	0,452	4,301	1,900	2,26	0,028
K Excr	0,338	0,144	0,011	0,005	2,34	0,023
P Excr	-0,388	0,350	-0,234	0,211	-1,11	0,272
K Plasma	0,123	0,111	0,496	0,450	1,10	0,275

According to the results of the canonical correlation analysis, the total determining influence of the parameters of uric acid exchange (due to the significant advantage of uricosuria over uricemia) on the constellation of parameters of electrolyte and nitrogen exchange reaches 56% (Fig. 2.20).

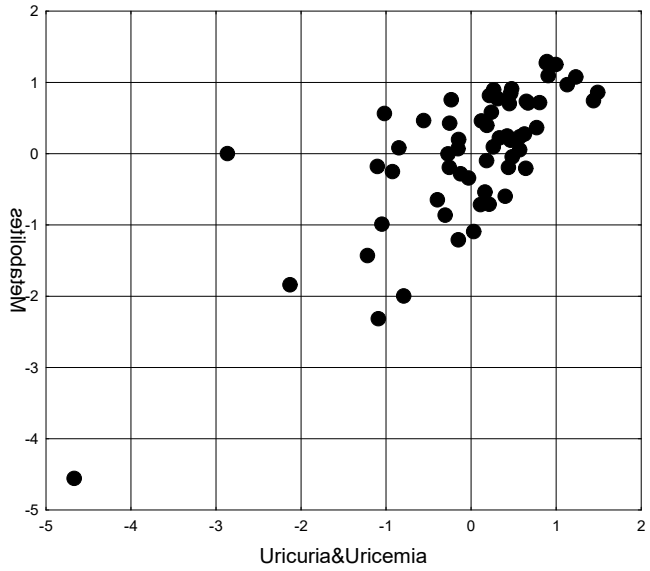

$R=0,751$; $R^2=0,563$; $\chi^2_{(20)}=65$; $p<10^{-6}$; Λ Prime=0,292

Fig. 2.20. Scatterplot of canonical correlation between uricosuria and uricemia (X axis) and metabolic parameters (Y axis) of female rats

The factor loadings on the metabolic canonical root indicate that diuresis and excretion of phosphates and potassium are the most positively determined; calcium, creatinine and urea excretion are less determined; creatinine, urea and potassium levels in plasma are even less determined, and magnesiumuria is the least determined (Table 2.40).

Table 2.40. Factor structure of canonical roots of uric acid and other metabolites

	left set
Variable	R
Uricosuria	-0,910
Uricemia	-0,070

	right set
Variable	R
Creatinine Excretion	-0,490
Diurese	-0.765
Creatinine Plasma	-0,373
Potassium Excretion	-0,639
Magnesium Excretion	-0,098
Calcium Excretion	-0,519
Phosphates Excretion	-0,745
Urea Excretion	-0,460
Urea Plasma	-0,289
Potassium Plasma	-0,278

2.6. FEATURES OF THE STATE OF NEURO-ENDOCRINE-IMMUNE COMPLEX AND ELECTROLITHE&NITROGENOUS EXCHANGE UNDER DIFFERENT VARIANTS OF URIC ACID EXCHANGE

It is known that autonomic, endocrine and immune parameters interact with each other within the neuro-endocrine-immune complex (NEIC) [Popovych IL et al, 2020; 2022]. The purpose of last subdivision is to find out exactly which parameters of the NEIC reflect the specificity of quantitative and qualitative clusters of uric acid metabolism.

As a result of the discriminant analysis, 30 recognition parameters were included in the model (Tables 2.41 and 2.41). In addition to, by definition, uricemia and uricosuria, they represent **neuro-endocrine** (6) and **immune** (11) systems as well as **electrolytes** (9) and **nitrogenous** metabolites (2) of blood and urine.

The identifying information contained in the 30 discriminant variables is condensed into three roots. The first root contains 56,0% of the discriminant power (r^*=0,963; Wilks' Λ=0,002; $\chi^2_{(90)}$=260; $p<10^{-6}$), second - 25,6% (r^*=0,924; Wilks' Λ=0,028; $\chi^2_{(58)}$=150; $p<10^{-3}$), third - 18,4% (r^*=0,899; Wilks' Λ=0,192; $\chi^2_{(28)}$=69; $p<10^{-4}$).

Calculation of the values of the discriminant roots for each animal as the sum of the products of raw coefficients on the individual values of the discriminant variables together with a constant (Table 2.43) make it possible to visualize each rat in the information space of the roots.

Table 2.41. Summary of the stepwise analysis of NEIC and metabolic parameters, ranked according to the Λ criterion

Variable enter	F to enter	p-value	Lambda	F-value	p-value
Uricemia	45,6	10^-6	0,290	45,6	0,000000
Parathyroid Activity	10,2	10^-4	0,187	24,1	0,000000
Magnesium Plasma	5,61	0,002	0,142	18,0	0,000000
Macrophages Thymus	4,05	0,012	0,116	14,7	0,000000
Creatinine Excretion	4,62	0,006	0,091	13,2	0,000000
MxDMn as Vagal tone	3,43	0,024	0,076	12,0	0,000000
0 Lymphocytes Blood	3,31	0,027	0,063	11,1	0,000000
Phosphates Excretion	2,80	0,050	0,054	10,3	0,000000
Macrophages Spleen	2,50	0,071	0,047	9,7	0,000000
T helper Lymphocytes	2,71	0,056	0,040	9,2	0,000000
Urea Plasma	2,32	0,088	0,035	8,8	0,000000
Potassium Erythrocytes	1,86	0,149	0,031	8,3	0,000000
Phosphates Plasma	1,93	0,139	0,027	8,0	0,000000
Potassium Plasma	3,01	0,041	0,023	7,9	0,000000
B Lymphocytes Blood	1,80	0,163	0,020	7,6	0,000000
Entropy Splenocytogram	1,63	0,198	0,018	7,3	0,000000
17-Ketosteroides Excretion	1,80	0,162	0,016	7,1	0,000000
Corticosterone	1,53	0,222	0,014	6,9	0,000000
(Ca/K)^0,5 Plasma	1,49	0,232	0,013	6,7	0,000000
Calcium Excretion	1,92	0,144	0,011	6,6	0,000000
Leukocytes Blood	1,41	0,255	0,010	6,4	0,000000
Plasmocytes Thymus	1,91	0,146	0,008	6,3	0,000000
Microphages Spleen	1,70	0,185	0,007	6,2	0,000000
Spleen Mass Index	1,43	0,251	0,006	6,1	0,000000
Mineralocorticoid Activity	1,75	0,177	0,006	6,0	0,000000
Sodium Excretion	4,10	0,015	0,004	6,4	0,000000
Lymphoblastes Thymus	2,04	0,129	0,003	6,4	0,000000
Uricosuria	1,89	0,153	0,003	6,4	0,000000
Chloride Plasma	1,27	0,305	0,002	6,3	0,000000
Sodium Plasma	1,62	0,208	0,002	6,3	0,000000

Table 2.42. Summary of the analysis of discriminant functions for NEIC and metabolic parameters, ranked by structural coefficient

Step 30, N of vars in model: 30; Grouping: 4 grps; Wilks' Λ: 0,0021; approx. $F_{(91)}$=6,3; $p<10^{-6}$

	Clusters of Uric acid Exchange (n)				Parameters of Wilks' Statistics					
Variables currently in the model	S- Un- (15)	Sn+ U± (19)	Sn Un+ (17)	S+ Un+ (9)	Wil-ks' Λ	Parti-al Λ	F-re-move	p-level	Tole-rancy	Norm (10)
Uricemia, µM/L	**259**	865	554	**1379**	0,007	0,290	22,0	10^{-6}	0,380	662
Uricosuria, µM/100g•d	**3,31**	6,63	5,46	**7,00**	0,002	0,838	1,74	0,182	0,236	5,72
MxDMn HRV, msec	**26**	39	45	**101**	0,003	0,753	2,96	0,050	0,219	53
0- Lymphocytes, %	**15,5**	22,8	21,8	**23,1**	0,002	0,748	3,03	0,047	0,430	22,2
K Erythrocyt, mM/L	**85,0**	87,3	86,2	**89,6**	0,002	0,826	1,89	0,155	0,439	87,0
Na Excr, µM/100 g•d	**118**	184	149	**201**	0,003	0,620	5,52	0,004	0,104	135
Urea Plasma, mM/L	**9,39**	8,76	9,29	**5,29**	0,003	0,690	4,04	0,017	0,255	7,42
Plasmocytes Thym, %	**2,40**	1,83	1,88	**1,67**	0,002	0,748	3,03	0,046	0,414	1,80
Macrophages Thy, %	3,07	**3,56**	2,88	2,11	0,003	0,714	3,61	0,026	0,347	2,70
Macrophags Spleen,%	7,87	**9,11**	8,18	7,89	0,002	0,925	0,73	0,544	0,204	7,90

Phosph E, µM/100 g•d	9,3	12,7	10,4	9,0	0,003	0,720	3,49	0,029	0,061	9,4
17-KS, nM/100g•24h	55	83	69	62	0,002	0,886	1,16	0,344	0,067	61
Creatin. E, µM/100g•d	8,6	12,6	12,6	11,9	0,002	0,863	1,43	0,257	0,115	8,7
T helper Lymphoc, %	30,5	32,0	31,3	28,4	0,003	0,665	4,54	0,010	0,419	31,5
Entropy Splenocytogr	0,752	0,761	0,751	0,741	0,003	0,716	3,57	0,027	0,389	0,753
Microphag Spleen, %	13,8	11,8	13,1	13,9	0,003	0,635	5,16	0,006	0,352	13,0
B Lymphocytes, %	16,3	15,1	16,4	16,3	0,003	0,592	6,20	0,002	0,324	16,0
Mineralocort Activity	3,12	2,83	3,09	3,03	0,004	0,490	9,36	10^{-4}	0,081	2,73
Mg Plasma, mM/L	0,45	0,78	1,27	0,84	0,003	0,677	4,29	0,013	0,360	0,88
Phosphat Plas, mM/L	0,46	1,11	1,19	0,84	0,002	0,827	1,89	0,155	0,105	0,72
Corticosterone, nM/L	437	422	532	321	0,003	0,677	4,28	0,013	0,225	482
Spleen MI, µg/g BM	264	287	321	304	0,003	0,793	2,35	0,095	0,403	312
Ca Excr, µM/100 g•d	2,89	4,17	4,27	2,60	0,002	0,864	1,42	0,259	0,151	2,90
K Plasma, mM/L	3,25	3,37	3,87	3,63	0,002	0,834	1,79	0,172	0,208	4,23
Na Plasma, mM/L	127,4	128,7	130,8	129,4	0,002	0,848	1,63	0,208	0,042	128,6
Cl Plasma, mM/L	90,7	92,0	94,8	93,8	0,003	0,802	2,22	0,109	0,036	94,3
Lymphoblasts Thy, %	7,27	7,06	7,41	6,67	0,002	0,861	1,45	0,251	0,443	7,40
Leukocytes Blood,G/L	11,35	11,40	11,98	11,56	0,002	0,843	1,68	0,195	0,425	12,68
Parathyroid Activity	2,15	1,71	1,55	1,93	0,002	0,866	1,39	0,267	0,077	2,08
$(Cap/Kp)^{0,5}$ as S/V bal	0,92	0,85	0,79	0,91	0,002	0,872	1,32	0,289	0,125	0,89

Table 2.43. Standardized and raw coefficients and constants for NEIC and metabolic parameters included in the discriminant model

Coefficients	Standardized			Raw		
Variables	Root 1	Root 2	Root 3	Root 1	Root 2	Root 3
Uricemia	1,303	0,429	-0,408	0,0054	0,0018	-0,0017
Parathyroid Activity	-0,690	-0,101	1,262	-2,055	-0,299	3,756
Magnesium Plasma	0,080	0,415	0,959	0,184	0,950	2,195
Macrophages Thymus	-0,716	0,271	-0,597	-0,679	0,256	-0,566
MxDMn as Vagal tone	0,796	-0,778	0,171	0,0201	-0,0197	0,0043
0 Lymphocytes Blood	0,648	0,434	0,208	0,094	0,063	0,030
Phosphates Excretion	0,335	2,273	-0,243	0,064	0,434	-0,047
Macrophages Spleen	-0,212	0,456	-0,429	-0,121	0,261	-0,245
T helper Lymphocytes	-0,505	0,755	0,310	-0,140	0,209	0,086
Urea Plasma	-0,785	0,622	0,626	-0,279	0,221	0,223
Potassium Erythrocytes	-0,053	0,363	-0,589	-0,0085	0,0580	-0,0941
Phosphates Plasma	-0,141	0,084	1,422	-0,322	0,193	3,255
Potassium Plasma	0,537	0,057	0,811	0,694	0,074	1,049
B Lymphocytes Blood	0,703	-0,819	0,533	0,223	-0,259	0,169
Entropy Splenocytogram	-0,212	0,495	-0,770	-9,673	22,53	-35,07
17-Ketosteroides Excretion	0,215	-1,362	-0,327	0,0054	-0,0341	-0,0082
Creatinine Excretion	0,452	0,415	1,026	0,097	0,089	0,221
Corticosterone	0,723	-0,968	0,432	0,0044	-0,0058	0,0026
$(Ca/K)^{0,5}$ Plasma	0,111	-0,371	-1,052	0,683	-2,277	-6,449
Calcium Excretion	-0,280	-0,526	0,855	-0,121	-0,227	0,370
Leukocytes Blood	0,512	0,316	0,229	0,1095	0,0676	0,0490
Plasmocytes Thymus	-0,017	-0,834	0,138	-0,022	-1,042	0,172
Microphages Spleen	0,499	-0,880	0,420	0,262	-0,462	0,220
Spleen Mass Index	0,459	-0,551	0,272	0,0071	-0,0085	0,0042
Mineralocorticoid Activity	1,473	-2,235	-0,045	1,534	-2,328	-0,047
Sodium Excretion	1,047	-1,758	-0,069	0,0061	-0,0102	-0,0004
Lymphoblastes Thymus	-0,309	0,442	0,267	-0,315	0,451	0,272
Uricosuria	-0,697	0,436	-0,301	-0,236	0,148	-0,102
Chloride Plasma	0,696	-0,993	-2,268	0,110	-0,157	-0,358
Sodium Plasma	-0,450	0,560	1,991	-0,083	0,103	0,367
			Constants	-3,586	-13,865	-2,813
			Eigenvalues	12,73	5,824	4,194
		Cumulative Proportions		0,560	0,816	1

Table 2.44 demonstrates that the characteristic features of the **S-Un** cluster are a combination of moderate hypouricemia and lower borderline uricosuria with reduced vagal tone and the level of 0-lymphocytes in the blood, lower borderline potassium level and a normal, but minimal for the sample, level of natriuria, on the other hand, a moderately increased percentage of plasma cells in the thymus and a maximum for a sample elevated level of urea in the plasma. Such a constellation of parameters is visualized by the localization of cluster members in the extreme left zone of the first root axis (Fig. 2.21). At the opposite pole of the axis are members of the **S+Un+** cluster, which are characterized by a combination of pronounced hyperuricemia and normal, but maximal for the sample, uricosuria with moderately increased levels of vagal tone and natriuria and normal, but maximal for the sample, levels of 0-lymphocytes in the blood and potassium in erythrocytes, instead, a moderately reduced level of urea in the plasma and a normal, but minimal for sampling content of plasma cells in the thymus. Members of the other two clusters occupy an intermediate position along the axis of the first root and are mixed. Their separation occurs along the axis of the second root. The top position is occupied by the rats of the **Sn+U±** cluster, in which the upper limit level of uricemia is combined with the maximum for the sample upper limit levels of macrophages in the thymus and spleen as well as urinary excretion of phosphates, creatinine and 17-ketosteroids while normal levels of T-helpers and splenocytogram entropy. Instead, they have a reduced level of macrophages in the spleen, and the level of B-lymphocytes in the blood and mineralocorticoid activity are normal, but minimal for the sample, while in the members of the **SnUn+** cluster, the lower borderline level of uricemia is accompanied to a greater or lesser extent by lower/higher levels of the listed parameters. Additional delimitation of these clusters occurs along the axis of the third root. The top position is occupied by rats of the **SnUn+** cluster, which reflects their upper limit plasma levels of magnesium, phosphates, corticosterone and calcium excretion as well as normal, but maximum for the sample, levels of chloride in the plasma, leukocytes in the blood, lymphoblastes in the thymus, and mass index of the spleen in combination with the maximally reduced electrolyte markers of parathyroid activity and sympatho-vagal balance, while the rats placed below the **Sn+U±** cluster are characterized to a greater or lesser extent by lower/higher levels of the listed parameters.

Table 2.44. Structural coefficients of NEIC and metabolism parameters, their average Z-values and centroids of discriminant roots for clusters

	Correlations Variables-Roots			**S-Un-**	**Sn+U±**	**SnUn+**	**S+Un+**
Root 1 (56,0%)	Root 1	Root 2	Root 3	**-4,30**	**-0,43**	**+0,63**	**6,88**
Uricemia	**,393**	,191	-,250	**-1,18**	+0,59	-0,32	**+2,10**
Uricosuria	**,106**	,126	-,010	**-0,45**	+0,17	-0,05	**+0,24**
MxDMn as Vagal tone	**,168**	-,057	-,055	**-0,63**	-0,34	-0,18	**+1,18**
0 Lymphocytes Blood	**,097**	,122	,044	**-1,08**	-0,10	-0,07	**+0,15**
Potassium Erythrocytes	**,062**	,024	-,040	**-0,29**	+0,04	-0,12	**+0,38**
Sodium Excretion	**,040**	,041	-,023	**-0,19**	+0,59	+0,17	**+0,79**
Urea Plasma	**-,125**	,039	,116	**+1,15**	+0,78	+1,09	**-1,24**
Plasmocytes Thymus	**-,081**	-,067	-,027	**+0,76**	+0,04	+0,10	**-0,17**
Root 2 (25,6%)	Root 1	Root 2	Root 3	-2,40	**+3,25**	-0,46	-1,99
Macrophages Thymus	-,086	**,137**	-,003	+0,27	**+0,64**	+0,16	-0,44
Macrophages Spleen	-,004	**,129**	-,012	-0,02	**+0,76**	+0,17	-0,01
Phosphates Excretion	-,009	**,120**	,006	-0,02	**+0,52**	+0,16	-0,06
17-Ketosteroides Excretion	,013	**,114**	,014	-0,11	**+0,40**	+0,14	+0,02
Creatinine Excretion	,065	**,104**	,076	-0,03	**+0,90**	+0,88	+0,74
T helper Lymphocytes	-,052	**,101**	,062	-0,31	**+0,14**	-0,07	-0,99
Entropy Splenocytogram	-,051	**,100**	-,002	-0,03	**+0,25**	-0,08	-0,43
Microphages Spleen	,010	**-,188**	-,010	+0,56	**-0,82**	+0,08	+0,63
B Lymphocytes Blood	,007	**-,075**	,032	+0,09	**-0,32**	+0,12	+0,11
Mineralocorticoid Activity	-,005	**-,053**	,022	+0,50	**+0,12**	+0,46	+0,39
Root 3(18,4%)	Root 1	Root 2	Root 3	-1,23	-0,89	**+3,10**	-1,93
Magnesium Plasma	,098	,050	**,300**	-0,72	-0,17	**+0,64**	-0,07
Phosphates Plasma	,086	,196	**,203**	-0,57	+0,85	**+1,02**	+0,28

Corticosterone	-,051	,008	**,187**	-0,36	-0,47	**+0,40**	-1,28
Spleen Mass Index	,062	,012	**,126**	-0,48	-0,25	**+0,09**	-0,08
Calcium Excretion	-,008	,097	**,103**	-0,01	+0,83	**+0,90**	-0,20
Potassium Plasma	,048	,076	**,099**	-1,39	-0,69	**-0,51**	-0,85
Sodium Plasma	,039	,010	**,096**	-0,23	+0,02	**+0,43**	+0,16
Chloride Plasma	,049	-,004	**,095**	-0,50	-0,33	**+0,07**	-0,08
Lymphoblastes Thymus	-,048	-,010	**,094**	-0,16	-0,41	**+0,01**	-0,87
Leukocytes Blood	,006	-,004	**,026**	-0,22	-0,21	**-0,12**	-0,19
Parathyroid Activity	-,068	-,166	**-,260**	+0,13	-0,75	**-1,08**	-0,31
$(Ca/K)^{0,5}$ Plasma	-,012	-,068	-,144	+0,17	-0,27	**-0,58**	+0,11

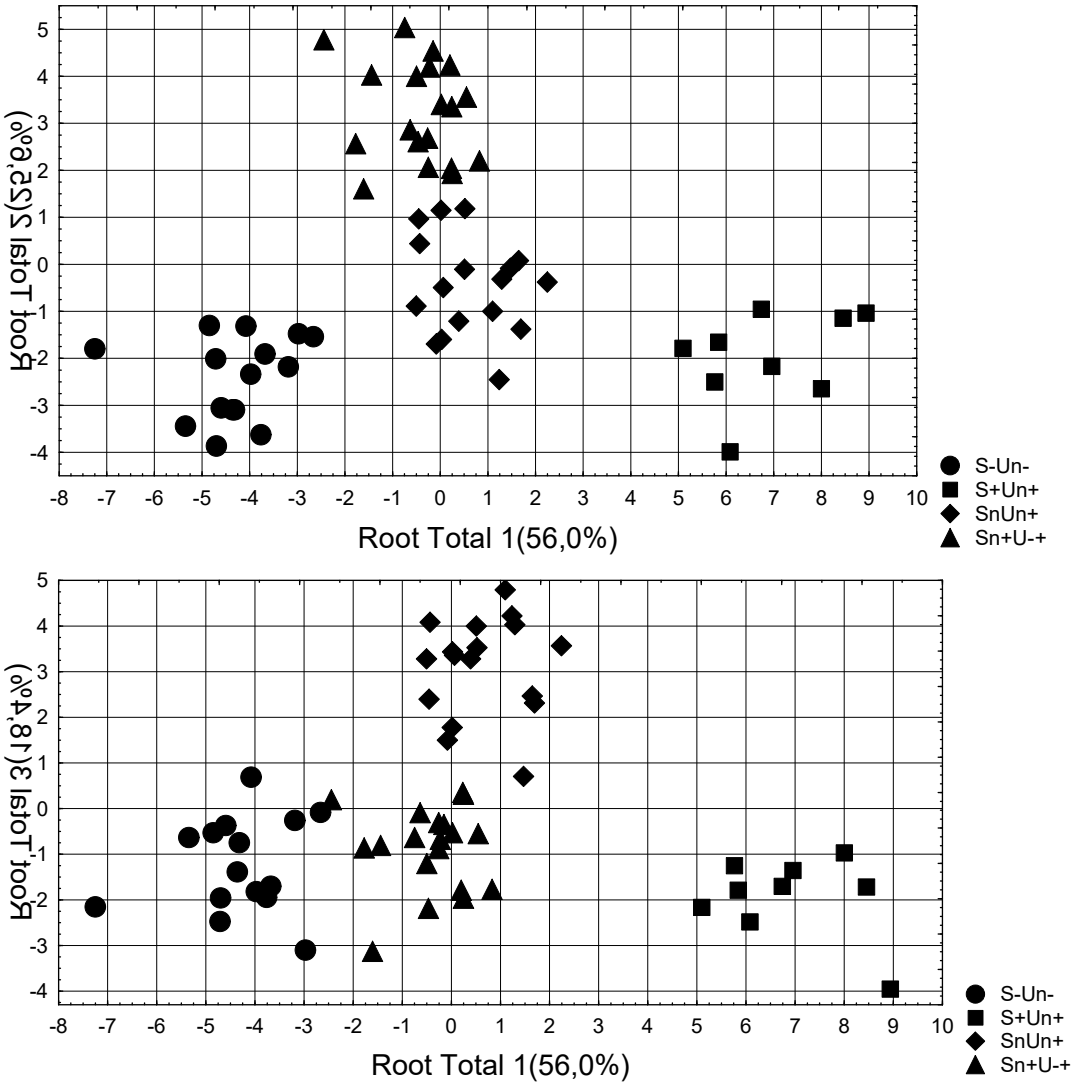

Fig. 2.21. Scattering of individual values of the discriminant roots of rats of different clusters

The apparent clarity of the demarcation of the four clusters in the information space of the three canonical discriminant roots is documented by the calculation of the Mahalanobis distances between the clusters (Table 2.45).

Table 2.45. Squares of Mahalanobis distances between clusters (above the diagonal) and F-criteria (df=30,3) and p-levels (below the diagonal)

Clusters	S-Un-	S+Un+	SnUn+	Sn+U±
S-Un-	0	126	47	47
S+Un+	11,4 10^{-6}	0	67	82
SnUn+	6,0 10^{-5}	6,3 10^{-5}	0	31

Sn+U±	6,3 10^{-5}	8,0 10^{-6}	4,4 10^{-4}	0

The use of classification functions (Table 2.46) enables error-free retrospective identification of all members of the four clusters (Table 2.47).

Table 2.46. Coefficients and constants of classification functions for neuroendocrine-immune and metabolic support of uric acid metabolism clusters

Variable	S-Un- p=,250	S+Un+ p=,150	SnUn+ p=,283	Sn+U-+ p=,317
Uricemia	0,051	0,114	0,074	0,082
Parathyroid Activity	-88,49	-114,23	-82,93	-96,85
Magnesium Plasma	80,91	81,80	93,16	87,73
Macrophages Thymus	22,98	15,89	17,68	21,61
Creatinine Excretion	-16,21	-15,24	-14,60	-15,25
MxDMn as Vagal tone	-0,229	-0,015	-0,150	-0,261
0 Lymphocytes Blood	1,55	2,61	2,27	2,28
Phosphates Excretion	12,19	13,12	13,15	14,88
Macrophages Spleen	-9,45	-10,52	-10,60	-8,53
T helper Lymphocytes	3,39	1,85	3,48	4,06
Urea Plasma	-5,03	-8,21	-5,01	-4,78
Potassium Erythrocytes	7,07	7,06	6,73	7,33
Phosphates Plasma	-90,20	-96,01	-77,31	-89,24
Potassium Plasma	62,32	69,37	70,43	65,78
B Lymphocytes Blood	-2,62	-0,36	-1,30	-3,17
Entropy Splenocytogram	2911	2837	2755	2989
17-Ketosteroides Excretion	0,209	0,261	0,134	0,034
Corticosterone	-0,0231	0,0214	-0,0017	-0,0383
(Ca/K)^0,5 Plasma	329,6	340,8	300,6	317,1
Calcium Excretion	2,45	0,74	3,01	0,82
Leukocytes Blood	1,19	2,41	2,07	2,01
Plasmocytes Thymus	-6,59	-7,38	-7,98	-12,50
Microphages Spleen	5,91	8,49	7,26	4,39
Spleen Mass Index	0,05	0,12	0,09	0,31
Mineralocorticoid Activity	45,31	61,53	48,14	38,07
Sodium Excretion	0,076	0,140	0,085	0,042
Lymphoblastes Thymus	5,25	1,73	5,75	6,67
Uricosuria	-6,30	-8,80	-7,61	-6,41
Chloride Plasma	-30,20	-28,78	-31,51	-30,78
Sodium Plasma	40,36	39,21	41,74	40,75
Constant	-2895	-2954	-2944	-2981

Table 2.47. Classification matrix for uric acid metabolism clusters
Rows: observed classifications; columns: predicted classifications

Clusters	Percent Correct	S+Un+ p=,150	Sn+U± p=,317	SnUn+ p=,283	S-Un- p=,250
S+Un+	100	9	0	0	0
Sn+U±	100	0	19	0	0
SnUn+	100	0	0	17	0
S-Un-	100	0	0	0	15
Total	100	9	19	17	15

So, the state of uric acid exchange is closely related to the state of the neuro-endocrine-immune complex and electrolithes&nitrogene exchange. A detailed discussion will be conducted after the publication of the results of a similar study in humans.

CHAPTER 3

CLINICAL-PHYSIOLOGICAL OBSERVATIONS

According to the classic motto "*Ex experimentum ad inhaero*" ("From experiment to clinic" in Latine), the purpose of next chapter was to clarify such relationships in patients with neuroendocrine-immune complex dysfunction on the background of chronic pyelonephritis combined with cholecystitis in remission.

Accordance to ethics standards. Tests in patients are conducted in accordance with positions of Helsinki Declaration 1975, revised and complemented in 2002, and directive of National Committee on ethics of scientific researches. During realization of tests from all participants the informed consent is got and used all measures for providing of anonymity of participants.

Study designe. The object of observation were 34 men and 10 women aged 24-70 years old, who came to the Truskavets' spa for the treatment of chronic pyelonephritis in remission. The survey was conducted twice, before and after ten-day balneotherapy (drinking Naftussya bioactive water three times a day, ozokerite applications, mineral baths every other day) [Popovych IL, 2011; Popovych IL et al, 2022].

Daily urine was collected the day before, in which the concentration of uric acid, creatinine, urea, glucose, calcium, magnesium, phosphates, chloride, sodium and potassium was determined by the mentioned methods.

In the morning, under basal conditions, the mucous membrane of the cheeks was scraped with a cotton swab for microelectrophoretic examination of the cells of the buccal epithelium, during which the electrokinetic potential of cell nuclei (zeta potential) was determined, the marker of which is the electrokinetic index, that is, the percentage of electronegative nuclei that move during electrophoresis [Shakhbasov VH et al, 1986; Honcharenko MS et al, 1992, 2011]. The device "Biotest" (manufactured by Kharazin University, Kharkiv) and a light microscope were used.

Then we recorded electrocardiogram in II lead to assess the parameters of heart rate variability (HRV) [Heart Rate Variability, 1996; Berntson GG et al., 1997; Baevskiy RM & Ivanov GG, 2001] (software and hardware complex "CardioLab+HRV" produced by "KhAI-MEDICA", Kharkiv, Ukraine). For further analysis the following parameters were selected. Baevskiy's RM parameters: heart rate (HR), Mo, AMo, MxDMn. Temporal parameters (Time Domain Methods): the standart deviation of all NN intervals (SDNN), the square root of the mean of the sum of the squares of differences between adjacent NN intervals (RMSSD), the percent of interval differences of successive NN intervals greater than 50 msec (pNN_{50}); triangular index (TNN). Spectral parameters (Frequency Domain Methods): power spectral density (PSD) bands of HRV - high-frequency (HF, range 0,4÷0,15 Hz), low-frequency (LF, range 0,15÷0,04 Hz), very low-frequency (VLF, range 0,04÷0,015 Hz) and ultralow-frequency (ULF, range 0,015÷0,003 Hz). We calculated classical indexes LF/HF, LFnu=100%•LF/(LF+HF), (VLF+LF)/HF as Centralization Index as well as Baevskiy's Stress Index (BSI) and Activity of Regulatory Systems Index (BARSI).

Simultaneosly recorded EEG (hardware-software complex "NeuroCom Standard", KhAI Medica, Kharkiv, Ukraine) monopolar in 16 loci (Fp1, Fp2, F3, F4, F7, F8, C3, C4, T3, T4, P3, P4, T5, T6, O1, O2) by 10-20 international system, with the reference electrodes A and Ref on the tassels of ears. Two minutes after the eyes had been closed, 25 sec of artifact free EEG data were collected by computer. Among the options considered the average EEG amplitude (μV), average frequency (Hz), frequency deviation (Hz), index (%), coefficient of asymmetry (%) as well as absolute (μV^2/Hz) and relative (%) spectral power density (SPD) in the standard frequency bands: β (35÷13 Hz), α (13÷8 Hz), θ (8÷4 Hz) and δ (4÷0,5 Hz) in all loci, according to the instructions of the device.

In addition, calculated coefficient of Asymmetry (As) and Laterality Index (LI) for PSD each Rhythm using formulas [Newberg AB et al., 2001]:

As, % = 100•(Max – Min)/Min; LI, % = Σ [200•(Right – Left)/(Right + Left)]/8.

We calculated also for HRV and each locus EEG the Entropy (h) of normalized PSD using Popovych's IL [Popadynets OO et al, 2020; Gozhenko ai et al, 2021; Popovych IL et al., 2022] formulas based on classic Shannon's CE [1948] formula:

$hHRV = - [SPDHF \bullet \log_2 SPDHF + SPDLF \bullet \log_2 SPDLF + SPDVLF \bullet \log_2 SPDVLF + SPDULF \bullet \log_2 SPDULF]/\log_2 4;$
$hEEG = - [SPD\alpha \bullet \log_2 SPD\alpha + SPD\beta \bullet \log_2 SPD\beta + SPD\theta \bullet \log_2 SPD\theta + SPD\delta \bullet \log_2 SPD\delta]/\log_2 4$

Finally, the battery of tests included the good old Kerdö's Vegetative Index [Kerdö I, 1966; Fajda OI et al, 2015] and $(Cap/Kp)^{0,5}$ ratio [Fajda OI et al, 2016] as markers of Sympathetic/Vagal balance.

The previously listed metabolites and hormones were determined in venous blood samples. Among hormones determined Cortisol, Aldosterone, Testosterone, Triiodothyronine, Parathyroid hormone and Calcitonin (by the ELISA with the use of analyzers "Tecan" and "RT-2100C" and corresponding sets of reagents from "Алкор Био", XEMA Co, Ltd and DRG International Inc).

In portion of the capillary blood we counted up Leukocytogram (LCG) (Eosinophils, Stub and Segmentonucleary Neutrophils, Lymphocytes and Monocytes) and calculated two variants of Adaptation Index as well as two variants of Strain Index by Popovych IL [Popovych IL et al, 2000; 2022]. We remind that the algorithm of quantization of the Popovych's indexes is based on the proposed Garkavi LKh et al [1990; 1998] ranges of relative content in the Leukocytogram of lymphocytes, which determines the type of General Adaptation Reaction of Organism as well as other components of Leukocytogram and total leukocyte levels indicating harmonic or disharmonious character of GARO.

Table 3.1. The first scale for the quantitative assessment of pathological, disharmonious and harmonious GARO and the formula for calculating the Strain Index of the leukocytogram [Popovych IL et al, 2000; Kostyuk PG et al, 2006].

Leukocyto-gram Lymphocy-tes level, %	**G**eneral **A**daptation **R**eaction of **O**rganism	Eosinophiles and Stub Neutrophiles: 1÷6 %; Monocytes: 4÷7 %; Leukocytes: 4÷8 G/l	Eosinophiles and Stub Neutrophiles: <1; >6; Monocytes: <4; >7; Leukocytes: <4; >8 G/l
<21	Stress	**1,22**	**0,02**
21÷27	Training	**1,46**	**0,74**
28÷33	Quiet Activation	**1,95**	**0,98**
34÷43,5	Heightened Activation	**1,70**	**0,50**
≥44	Overactivation	**0,26**	

Strain Index-1 = $[(Eo/3,5\text{-}1)^2 + (SN/3,5\text{-}1)^2 + (Mon/5,5\text{-}1)^2 + (Leu/6\text{-}1)^2]/4$.

Later, Garkavi LKh et al [2000] proposed some other boundaries of ranges, on the basis of which Popovych IL [Popadynets OO et al, 2020; Popovych IL et al, 2022] calculated the second version of the indices.

Table 3.2. The second scale for the quantitative assessment of pathological, disharmonious and harmonious GARO and the formula for calculating the Strain Index of the leukocytogram

Leukocyto-gram Lymphocy-tes level, %	**G**eneral **A**daptation **R**eaction of **O**rganism	Eosinophiles: 1÷4,5 %; Stub Neutrophiles: 3÷5,5 %; Monocytes: 5÷7 %; Leukocytes: 4÷6 G/l	Eosinophiles: <1;>4,5% Stub Neutrophiles: <3; >5,5; Monocytes: <5; >7; Leukocytes: <4; >6 G/l
<21	Stress	**1,22**	**0,02**
21÷27	Training	**1,46**	**0,74**
28÷33	Quiet Activation	**1,95**	**0,98**
34÷43,5	Heightened Activation	**1,70**	**0,50**
≥44	Overactivation	**0,26**	

Strain Index-2 = $[(Eo/2,75\text{-}1)^2 + (SN/4,25\text{-}1)^2 + (Mon/6\text{-}1)^2 + (Leu/5\text{-}1)^2]/4$.

The informativeness of these indices was demonstrated by other authors [Barylyak LG et al, 2013; Petsyukh SV et al, 2016].

Immune status evaluated on a set of I and II levels recommended by the WHO as described in the manual [Lapovets LYe et Lutsyk BD, 2004]. For phenotyping subpopulations of lymphocytes used the methods of rosette formation with sheep erythrocytes on which adsorbed monoclonal antibodies against receptors CD3, CD4, CD8, CD22 and CD56 from company "Granum" (Kharkiv) with visualization under light microscope with immersion system. Subpopulation of T cells with receptors high affinity determined by test of “active” rosette formation. The state of humoral immunity judged by the concentration in serum of Immunoglobulins classes G, A, M (ELISA, analyser “Immunochem”, USA) and circulating immune complexes (by polyethylene glycol precipitation method). In addition, the saliva level of secretory IgA, IgA and IgG was determined as well as Lysozime (by bacteriolysis of Micrococcus lysodeikticus).

We calculated also the Entropy (h) of Immunocytogram (ICG) and Leukocytogram (LCG) using Popovych’s IL formulas [Popadynets OO et al, 2020; Gozhenko AI et al, 2021; Popovych IL et al, 2022]:

$$hICG = - [CD4 \bullet \log_2 CD4 + CD8 \bullet \log_2 CD8 + CD22 \bullet \log_2 CD22 + CD56 \bullet \log_2 CD16] / \log_2 4;$$
$$hLCG = - [Lym \bullet \log_2 Lym + Mon \bullet \log_2 Mon + Eo \bullet \log_2 Eo + SNN \bullet \log_2 SNN + StubN \bullet \log_2 StubN] / \log_2 5.$$

Parameters of phagocytic function of neutrophils estimated as described by Douglas SD and Quie PG [1981] with moderately modification by Kovbasnyuk MM [Kulchynskyi AB et al, 2016]. To do this, 5 drops of blood immediately after collection, made in glass centrifuge tubes with 2 ml of 4% solution of sodium citrate. Blood samples were stored in a refrigerator at a temperature of 4^0C. Further samples were centrifuged (5000 rev/min for 5 min). The supernatant was removed with the help of the Pasteur’s pipette. We used a fraction of leukocytes with traces of erythrocytes. The objects of phagocytosis served daily cultures of Staphylococcus aureus (ATCC N 25423 F49) as typical specimen for Gram-positive Bacteria and Escherichia coli (O55 K59) as typical representative of Gram-negative Bacteria. Both cultures obtained from Laboratory of Hydro-Geological Regime-Operational Station JSC “Truskavets’kurort”. To prepare the suspension microbes did wipes with relevant shoal sterile saline, immersed tubes in boiling water for 3 seconds, cooled to room temperature. Integrity microbes controlled with the aid of a microscope. To do this, drop the suspension of microbes applied to skimmed substantive piece of glass, fixed in alcohol lamp flame. Ready preparations stained by Papenheim, microscoped during immersion, lense h90, eyepiece x10. The test samples were prepared as follows. In Vidal’s plastic tubes made in the following order of 0,05 mL of heparin, 0,05 mL of sterile saline, 0,1 mL suspension of leukocytes, 0,05 mL suspension of microbial bodies. Samples shaked and placed in thermostat at 37^0C for 30 min, shaking them with every 10 mins. Then, to stop phagocytosis, the sample was cooled under running water for 10 min. In further samples are centrifuged (5000 rev/min, for 5 min), the supernatant removed with the help of the Pasteur’s pipette. From the suspension of leukocytes (with traces of red blood cells) prepared strokes, dried in air at room temperature and stained by Papenheim. Microscoped during immersion lens h90, x10 eyepiece. Take into account the following parameters of phagocytosis: activity as percentage of neutrophils, in which found microbes - Hamburger’s Phagocytic Index; intensity as number of microbes absorbed one phagocytes - Microbial Count (MC) or Right’s Index; completeness as percentage of dead microbes - Killing Index (KI). Microbial number and index their digestion is determined for each phagocyte and fixed in phagocytic frame.

On the basis of the recorded partial parameters of Phagocytosis, taking into account the Neutrophils (N) content of 1 L blood, we calculated the integral parameter such as Bactericidal Capacity of Neutrophils (BCCN) by the formula:

$$BCCN\ (10^9\ Bact/L) = N\ (10^9/L) \bullet PhI\ (\%) \bullet MC\ (Bact/Phag) \bullet KI\ (\%) \bullet 10^{-4}.$$

In addition, the blood level of cytokines IL-1, IL-6 and TNF-α as well as C-Reactive Protein was determined (by the ELISA with the use of analyzer "RT-2100C" and corresponding sets of reagents from "Diactone", France).

The condition of Microbiota is evaluated on the results of sowing of feces and urine.

Reference (norm) values are taken from the instructions and database of the Truskavetsian Scientific School of Balneology.

3.1. VARIANTS OF URIC ACID EXCHANGE

First of all, we consider it necessary to determine the standards of uric acid exchange parameters. It is generally accepted that they are determined by sex and age, however, the specific values, according to different sources, do not match. In particular, differences between uricemia rates for different age groups are 5% for men and 21% for women, and gender differences range from 13-42% [review: Ivassivka SV et al, 2004). We have adopted the following uricemia standards for gender and age (Table 3.3).

Table 3.3. Uricemia standards for age and gender

	Serum Uric Acid, mM/L	
Age	Males	Females
23-29	0,375	0,290
30-39	0,390	0,275
40-49	0,392	0,278
50-59	0,388	0,305
60-69	0,385	0,333
>69	0,380	0,310

With regard to uricosuria standards, the situation is less ambiguous, as various authors do not consider gender differences to be significant. We have adopted as a standard the average of 3,0 mM/24h (range 1,5÷4,5 mM/24h, which is very close to the average literary range of 1,80÷4,46 mM/24h [review: Ivassivka SV et al, 2004].

A preliminary examination revealed a wide variance in both serum uric acid concentrations and urinary excretion. This prompted us to apply cluster analysis again (k-mean clustering method). As a result, four groups of persons were created, significantly different from each other in parameters of Uric Acid exchange (Table 3.4), while the differences between the members of each group were much smaller (Table 3.5).

Table 3.4. Cluster Means and Euclidean Distances between Clusters

Distances below diagonal, Squared distances above diagonal

	Cluster No. 1 (21)	Cluster No. 2 (15)	Cluster No. 3 (30)	Cluster No. 4 (22)
Serum Uric Acid, Z	+0,09	-1,89	-0,53	-0,70
Uric Acid Excretion, Z	+1,26	+1,17	-0,97	+3,87
No. 1	0,00	1,95	2,68	3,71
No. 2	1,40	0,00	3,21	4,34
No. 3	1,64	1,79	0,00	11,72
No. 4	1,93	2,08	3,42	0,00

Table 3.2. Members of Clusters and Distances from Respective Cluster Center

Cluster Number 1 contains 21 cases

	Case No.	Case No.	Case No.	Case No.	Case No.	Case No.	Case No.	Case No.	Case No.	Case No.	Case No.	Case No.	Case No.	Case No.	Case No.	Case No.
	C_22	C_26	C_29	C_31	C_34	C_36	C_40	C_50	C_51	C_54	C_58	C_59	C_73	C_78	C_79	C_80
Distance	,58	,81	1,18	,97	,22	,38	,57	,31	,80	,79	,51	,76	,91	,69	,52	,81

	Case No.	Case No.	Case No.	Case No.	Case No.
	C_7	C_10	C_13	C_15	C_17
Distance	,52	,78	,46	,40	,49

Cluster Number 2 contains 15 cases

	Case No.	Case No.	Case No.	Case No.	Case No.	Case No.	Case No.	Case No.	Case No.	Case No.	Case No.	Case No.	Case No.	Case No.	Case No.
	C_2	C_3	C_21	C_24	C_27	C_30	C_39	C_43	C_46	C_47	C_56	C_65	C_72	C_85	C_87
Distance	,53	,32	1,04	,66	,48	,95	,68	,64	,51	,31	,69	,49	,73	,40	,64

Cluster Number 3 contains 30 cases

	Case No.	Case No.	Case No.	Case No.	Case No.	Case No.	Case No.	Case No.	Case No.	Case No.	Case No.	Case No.	Case No.	Case No.	Case No.
	C_52	C_53	C_60	C_62	C_63	C_64	C_66	C_74	C_75	C_76	C_77	C_81	C_82	C_83	C_84
Distance	,67	,86	,42	,52	,67	,64	,33	,97	,78	,62	,41	,92	,69	,49	1,11

	Case No.	Case No.	Case No.	Case No.	Case No.	Case No.	Case No.	Case No.	Case No.	Case No.	Case No.	Case No.	Case No.	Case No.	Case No.
	C_4	C_6	C_8	C_9	C_12	C_16	C_18	C_19	C_23	C_32	C_33	C_38	C_41	C_42	C_48
Distance	1,15	,61	,78	2,19	,38	1,30	,90	,74	,67	,57	,08	1,01	,91	,81	1,30

Cluster Number 4 contains 22 cases

	Case No.	Case No.	Case No.	Case No.	Case No.	Case No.	Case No.	Case No.	Case No.	Case No.	Case No.	Case No.	Case No.	Case No.	Case No.
	C_1	C_5	C_11	C_14	C_20	C_25	C_28	C_35	C_37	C_44	C_45	C_49	C_55	C_57	C_61
Distance	,92	,88	,75	,61	,92	,73	,72	,60	1,03	2,15	1,17	,33	,80	1,50	2,02

	Case No.	Case No.	Case No.	Case No.	Case No.	Case No.	Case No.
	C_67	C_68	C_69	C_70	C_71	C_86	C_88
Distance	,85	,58	,56	,81	,65	,88	1,77

The entire observed sample is visualized in fig. 3.1.

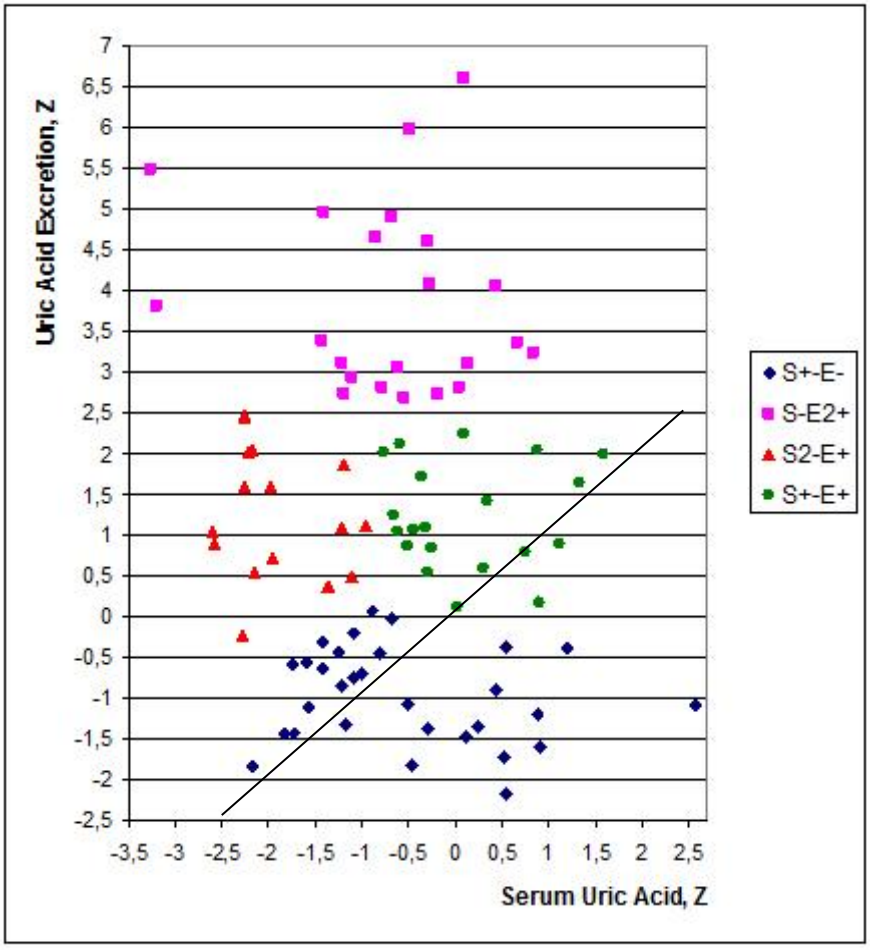

Fig. 3.1. Normalized levels (Z-scores) of uricemia (X-line) and uricosuria (Y-line) in patients of different clusters

As in healthy female rats, in humans of both sexes, patients with chronic pyelonephritis in the phase of remission, four variants of uric acid exchange were found. In 34% (20 men and 10 women), moderate hypouricosuria is combined with lower borderline uricemia (cluster **S±E-**). In 24% (16 men and 5 women), moderately increased uricosuria is associated with normal uricemia

(cluster S±E+). In 17% (14 men and 1 woman), moderately increased uricosuria is combined with pronounced hypouricemia (cluster S2-E+). Finally, in 25% of patients (18 men and 4 women), subliminal uricemia is accompanied by marked hyperuricosuria (cluster S-E2+).

The clearance of uric acid in members of the first cluster is normal, in the next two it is moderately increased, and in the last one it is drastically increased

3.2. IMMUNE AND MICROBIOTIC ACCOMPANIMENTS OF VARIANTS OF URIC ACID EXCHANGE

In order to identify exactly those parameters of immunity and microbiota, according to the constellation of which the four clusters differ from each other, discriminant analysis was again carried out. The program included in the discriminant model, in addition, by definition, uricemia and uricosuria, 8 immune parameters of **blood**, 2 of **saliva**, 2 so-called **informational** parameters, 2 parameters of **feces microbiota** and 3 parameters of **urine** that characterize chronic pyelonephritis (Table 3.3).

Table 3.3. Discriminant Function Analysis Summary for Variables of Uric Acid Exchange, Immunity and Microbiota

Step 21, N of vars in model: 19; Grouping: 4 grps; Wilks' Λ: 0,00478; approx. $F_{(57)}$=17,3; $p<10^{-6}$

Variables currently in the model	Clusters of Uric Acid Exchange (n)				Parameters of Wilks' Statistics					
	S±E-III (30)	S2-E+ II (15)	S±E+ I (21)	S-E2+ IV (22)	Wilks Λ	Par-tial Λ	F-re-move (3,7)	p-le-vel	Tole ran-cy	Norm Cv/σ (30)
Serum Uric Acid, mM/L	0,322	0,249	0,371	0,316	,0063	,758	7,0	10^{-3}	,658	0,365
Z	-0,53	-1,89	+0,09	-0,70						0,116
Uric Acid Excr, mM/24 h	2,27	3,88	3,94	5,94	,0390	,123	157	10^{-6}	,647	3,00
Z	-0,97	+1,17	+1,26	+3,87						0,250
Popovych's Strain Index-1, points	0,13	0,16	0,25	0,13	,0050	,953	1,1	,362	,754	0,067 0,722
Killing Index vs *Staph. aureus*, %	47,9	47,9	53,0	49,5	,0049	,980	,4	,720	,312	58,9 0,142
Lysozime Saliva, mg/L	171	171	172	167	,0059	,804	5,4	,002	,249	180 0,168
Phagocytose Index vs *Staph. aureus*, %	98,96	99,00	99,00	98,54	,0057	,843	4,1	,010	,318	98,3 0,018
Pan-Lymphocytes of Blood, %	33,9	35,8	31,7	34,6	,0055	,868	3,3	,025	,306	32,0 0,174
Phagocytose Index vs *E. coli*, %	99,43	98,80	99,13	98,40	,0057	,845	4,0	,011	,295	98,3 0,012
Erythrocyturia, points	0,12	0,08	0,07	0,12	,0051	,935	1,5	,212	,662	0 **0,10**
IgA Saliva, mg/L	144	142	135	118	,0054	,887	2,8	,047	,215	415 0,241
***Bifidobacteria* faeces, lg CFU/g**	5,66	5,40	5,49	5,74	,0055	,867	3,4	,023	,016	6,94 0,011
***Lactobacilli* faeces, lg CFU/g**	6,38	6,14	6,31	6,48	,0053	,902	2,4	,078	,015	8,10 0,015
Leukocyturia, lg/mL	3,44	3,19	3,26	3,44	,0056	,855	3,7	,015	,237	3,00 0,070
IgG Serum, g/L	15,6	14,5	15,1	14,4	,0053	,911	2,2	,101	,694	12,75 0,206
Bacteriuria, points	0,27	0,43	0,22	0,28	,0054	,881	3,0	,037	,243	0 **0,24**
Bactericidity vs *Staph. aureus*, 10^9 Bacteria/L	94,5	90,6	103,0	93,8	,0055	,877	3,1	,034	,233	105,7 0,100
Entropy of Immunocytogram	0,956	0,964	0,967	0,967	,0052	,927	1,7	,171	,459	0,960 0,059
Interleukin-6,	5,49	5,27	5,20	5,44	,0051	,929	1,7	,182	,202	4,25

ng/L										0,324
Microbial Count vs *E. coli*, Bacteria/Phagocyte	64,6	62,8	65,3	63,5	,0051	,938	1,5	,233	,320	54,7 0,194

Note. For some variables instead Cv is **SD**.

Outside the model appeared 8 variables of Leukocytogram and Phagocytosis (Table 3.4), 6 of Humoral Immunity (Table 3.5), 5 of Cellular Immunity (Table 3.6), 3 Proinflammatory factors (Table 2.7), 4 Informational variables (Table 3.8), as well as 6 variables of feces and urine Microbiota (Table 3.9).

Table 3.4. Variables of Leukocytogram and Phagocytosis, currently not in the model

Variables	Clusters of Uric Acid Exchange (n)				Parameters of Wilks' Statistics					
	S±E- III (30)	S2-E+ II (15)	S±E+ I (21)	S-E2+ IV (22)	Wilks Λ	Par-tial Λ	F-re-move (3,7)	p-le-vel	Tole ran-cy	Norm Cv/σ (30)
Leukocytes of Blood, 10^9/L	5,67	5,48	5,55	5,91	,0048	,993	,14	,93	,257	5,00 0,100
Polymorphonucleary Neutrophiles of Blood, %	54,6	52,7	55,8	53,2	,0048	,995	,10	,96	,073	55,0 0,100
Stubnucleary Neutrophiles of Blood, %	2,78	2,56	2,54	2,69	,0047	,987	,29	,83	,469	4,25 0,147
Eosinophiles of Blood, %	3,30	2,97	3,80	3,25	,0046	,972	,63	,60	,624	2,75 0,318
Monocytes of Blood, %	5,40	6,00	6,18	6,32	,0047	,990	,23	,88	,689	6,0 0,083
Microbial Count vs *Staph. aur*, Bact/Phagoc.	62,0	64,0	63,1	60,7	,0048	,994	,14	,94	,275	61,6 0,160
Killing Index vs *E. coli*, %	45,9	44,0	51,0	48,8	,0048	,996	,09	,96	,114	62,0 0,156
Bactericidity vs *E. coli*, 10^9 Bacteria/L	94	80	100	97	,0048	,997	,06	,98	,075	99 0,100

Table 3.5. Variables of Humoral Immunity, currently not in the model

Variables	Clusters of Uric Acid Exchange (n)				Parameters of Wilks' Statistics					
	S±E- III (30)	S2-E+ II (15)	S±E+ I (21)	S-E2+ IV (22)	Wilks Λ	Par-tial Λ	F-re-move (3,7)	p-le-vel	Tole ran-cy	Norm Cv/σ (30)
$CD22^+$ B-Lymphocytes, %	22,7	23,9	23,8	24,5	,0047	,991	,20	,90	,363	20,0 0,175
Circulating Immune Complexes, units	35	33	40	35	,0047	,986	,32	,81	,729	45 0,389
IgA Serum, g/L	1,85	1,64	1,85	1,67	,0047	,977	,51	,67	,485	1,875 0,167
IgM Serum, g/L	1,50	1,40	1,47	1,40	,0047	,976	,52	,67	,718	1,15 0,239
Secretory IgA Saliva, mg/L	496	496	503	472	,0047	,978	,49	,69	,189	622 0,153
IgG Saliva, mg/L	42,2	42,8	41,6	41,3	,0046	,967	,73	,54	,227	36 0,222

Table 3.6. Variables of Cellular Immunity, currently not in the model

Variables	Clusters of Uric Acid Exchange (n)				Parameters of Wilks' Statistics					
	S±E- III (30)	S2-E+ II (15)	S±E+ I (21)	S-E2+ IV (22)	Wilks Λ	Par-tial Λ	F-re-move (3,7)	p-le-vel	Tole ran-cy	Norm Cv/σ (30)
CD4⁺CD3⁺ T-helper Lymphocytes, %	32,6	32,3	30,0	28,3	,0046	,967	,73	,54	,001	39,5 0,082
CD8⁺CD3⁺ T-cytolytic Lymphocytes, %	23,3	21,2	23,4	23,7	,0047	,983	,37	,78	,613	23,5 0,138
CD3⁺ T-active Lymphocytes, %	29,0	29,7	28,4	28,6	,0047	,978	,50	,69	,648	30,0 0,167
CD56⁺ Natural Killer Lymphocytes, %	18,9	20,7	20,4	21,2	,0047	,982	,40	,76	,240	17,0 0,172
0-Lymphocytes of Blood, %	2,5	1,8	2,4	2,3	,0048	,996	,09	,97	,295	0 **5,56**

Table 3.7. Variables of Proinflammatory factors, currently not in the model

Variables	Clusters of Uric Acid Exchange (n)				Parameters of Wilks' Statistics					
	S±E- III (30)	S2-E+ II (15)	S±E+ I (21)	S-E2+ IV (22)	Wilks Λ	Par-tial Λ	F-re-move (3,7)	p-le-vel	Tole ran-cy	Norm Cv/σ (30)
Interleukin-1, ng/L	4,58	5,34	4,74	4,81	,0047	,975	,56	,65	,522	4,51 0,173
Tumor Necrosis Factor-α, ng/L	6,21	5,87	5,76	6,13	,0046	1,00	,00	1,00	,648	4,90 0,326
C-Reactive Protein, µg/L	2,60	2,46	2,41	2,57	,0047	1,00	,00	1,00	,485	2,18 0,324

Table 3.8. Informational Variables, currently not in the model

Variables	Clusters of Uric Acid Exchange (n)				Parameters of Wilks' Statistics					
	S±E- III (30)	S2-E+ II (15)	S±E+ I (21)	S-E2+ IV (22)	Wilks Λ	Par-tial Λ	F-re-move (3,7)	p-le-vel	Tole ran-cy	Norm Cv/σ (30)
Entropy of Leukocytogram	0,647	0,653	0,651	0,660	,0048	,997	,07	,98	,659	0,681 0,070
Popovych's Strain Index-2, points	0,18	0,21	0,39	0,18	,0047	,978	,50	,69	,088	0,065 0,618
Popovych's Adaptation Index-1, points	1,17	1,16	1,07	1,06	,0047	,980	,45	,72	,469	1,70 0,147
Popovych's Adaptation Index-2, points	0,84	0,82	0,81	0,77	,0046	,971	,64	,59	,524	1,70 0,147

Table 3.9. Variables of Microbiota, currently not in the model

Variables	Clusters of Uric Acid Exchange (n)				Parameters of Wilks' Statistics					
	S±E- III (30)	S2-E+ II (15)	S±E+ I (21)	S-E2+ IV (22)	Wilks Λ	Par-tial Λ	F-re-move (3,7)	p-le-vel	Tole ran-cy	Norm Cv/σ (30)
Common *E. coli* faeces, lg CFU/g	8,28	8,28	8,23	8,28	,0048	1,00	,00	1,00	,613	8,66 0,030
Attenuated *E. coli* faeces, %	60	66	53	56	,0048	,997	,08	,97	,110	17,4 1,0
Hemolytic *E. coli* faeces, %	13	26	20	10	,0047	,976	,52	,67	,432	0 **25**
Klebsiela&Proteus faeces, %	11,2	8,8	18,2	13,1	,0047	,982	,40	,75	,146	0 11
Bacteriuria, lg CFU/mL	1,19	1,79	1,05	1,21	,0047	,976	,53	,67	,077	0 **0,98**

Leukocyturia, points	0,15	0,10	0,15	0,19	,0047	,977	,50	,68	,162	0 **0,15**
Erhytrocyturia, lg/mL	3,09	3,01	2,94	3,13	,0047	,982	,40	,75	,172	2,70 0,095

The discriminant variables are ranked by criterion Lambda (Table 3.10).

Table 3.10. Summary of Stepwise Analysis for Variables of Uric Acid Exchange, Immunity and Microbiota

Variables currently in the model	F to enter	p-level	**Λ**	F-value	p-level
Uric Acid excretion, Z-score	154	10^{-6}	,154	154	10^{-6}
Serum Uric Acid level, Z-score	13,5	10^{-6}	,104	58,3	10^{-6}
Popovych's Strain Index-1, points	2,3	,079	,095	36,1	10^{-6}
Killing Index vs *Staphylococcus aureus*, %	2,1	,108	,089	26,8	10^{-6}
Lysozime Saliva, mg/L	2,2	,096	,082	21,8	10^{-6}
Phagocytose Index vs *Staphylococcus aureus*, %	2,3	,084	,075	18,6	10^{-6}
Pan-Lymphocytes of Blood, %	2,2	,090	,069	16,4	10^{-6}
Phagocytose Index vs *Escherichia coli*, %	2,0	,119	,064	14,7	10^{-6}
Erythrocyturia, points	2,2	,096	,059	13,5	10^{-6}
IgA Saliva, mg/L	1,6	,208	,056	12,3	10^{-6}
***Bifidobacteria* faeces, lg CFU/g**	1,7	,167	,052	11,5	10^{-6}
***Lactobacilli* faeces, lg CFU/g**	1,6	,194	,049	10,7	10^{-6}
Leukocyturia, lg/L	1,4	,254	,046	10,0	10^{-6}
IgG Serum, g/L	1,3	,290	,044	9,4	10^{-6}
Bacteriuria, points	1,8	,161	,041	9,0	10^{-6}
Bactericidity vs *Staphyl. aureus*, 10^9 Bacteria/L	2,8	,046	,036	8,8	10^{-6}
Entropy of Immunocytogram	1,1	,338	,005	19,0	10^{-6}
Interleukin-6, ng/L	1,5	,210	,005	18,1	10^{-6}
Microbial Count vs *E. coli*, Bacteria/Phagocyte	1,5	,233	,005	17,3	10^{-6}

Next, the 19-dimensional space of discriminant variables transforms into 3-dimensional space of canonical roots. The canonical correlation coefficient is for Root 1 0,950 (Wilks' Λ=0,030; $\chi^2_{(57)}$=264; $p<10^{-6}$), for Root 2 0,678 (Wilks' Λ=0,312; $\chi^2_{(36)}$=88; $p<10^{-5}$) and for Root 3 0,650 (Wilks' Λ=0,577; $\chi^2_{(17)}$=41; p=0,0008). The major root contains 85,4% of discriminative properties, the second 8,0% and the third 6,6%.

Table 3.11 presents standardized (normalized) and raw (actual) coefficients for discriminant variables. The calculation of the discriminant root values for each person as the sum of the products of raw coefficients to the individual values of discriminant variables together with the constant enables the visualization of each patient in the information space of the roots.

Table 3.11. Standardized and Raw Coefficients and Constants for Variables of Uric Acid exchange, Immunity and Microbiota

Coefficients	**Standardized**			**Raw**		
Variables	Root 1	Root 2	Root 3	Root 1	Root 2	Root 3
Uric Acid excretion, Z-score	1,223	,017	,043	1,523	,021	,054
Serum Uric Acid level, Z-score	,083	-,832	-,123	,088	-,889	-,131
Popovych's Strain Index-1, points	,002	-,242	-,280	,012	-1,292	-1,493
Killing Index vs Staph. aureus, %	,062	-,356	-,074	,007	-,042	-,009
Lysozime Saliva, mg/L	,204	-,140	-1,296	,030	-,021	-,193
Phagocytose Index vs Staph. aur,, %	,563	,247	-,683	,478	,210	-,580
Pan-Lymphocytes of Blood, %	-,661	,239	,188	-,086	,031	,025
Phagocytose Index vs E. coli, %	-,327	-,061	,931	-,247	-,046	,703
Erythrocyturia, points	-,049	-,148	,455	-,493	-1,506	4,621
IgA Saliva, mg/L	-,704	,399	,060	-,020	,012	,002
Bifidobacterium faeces, lg CFU/g	-1,357	,214	4,010	-1,165	,184	3,443
Lactobacillus faeces, lg CFU/g	1,355	-,150	-3,680	,949	-,105	-2,577
Leukocyturia, lg/L	-,381	-,056	,987	-,571	-,084	1,479

IgG Serum, g/L	-,301	-,203	,238	-,081	-,055	,064
Bacteriuria, points	-,051	,937	-,463	-,210	3,855	-1,903
Bactericidity vs Staph. aur, 10^9 Bac/L	-,279	,689	-,766	-,011	,028	-,031
Entropy of Immunocytogram	-,344	,274	-,095	-12,89	10,26	-3,568
Interleukin-6, ng/L	-,475	,365	,522	-1,808	1,389	1,986
Microbial Count vs E. coli, Bact/Phag	,072	,091	,654	,008	,011	,077
			Constants	7,317	-38,51	-3,494
			Eigenvalues	9,266	,850	,732
		Cumulative Proportions		,854	,933	1,000

Table 3.12 shows the correlation coefficients of discriminant variables with canonical discriminant Roots, the cluster centroids of Roots, and the normalized values of the discriminant variables as well as variables currently not in the model but worth the attention.

Table 3.12. Correlations Variables-Canonical Roots, Means of Roots and Z-scores of Variables of Uric Acid exchange, Immunity and Microbiota

Variables	Correlations Variables-Roots			S±E- III (30)	S2-E+ II (15)	S±E+ I (21)	S-E2+ IV (22)
Root 1 (85,4%)	**R 1**	**R 2**	**R 3**	**-3,51**	-0,09	+0,61	**4,27**
Uric Acid excretion	**,768**	,130	,161	**-0,97**	+1,17	+1,26	**+3,87**
Entropy of Immunocytogram	**,057**	-,013	-,099	**-0,07**	+0,07	+0,13	**+0,13**
Monocytes	currently not in model			**-1,22**	0,00	+0,36	**+0,65**
Phagocytose Index vs E. coli	**-,097**	-,106	-,048	**+0,96**	+0,42	+0,70	**+0,09**
IgA Saliva	**-,095**	,061	-,108	**-2,71**	-2,73	-2,80	**-2,97**
Lysozime Saliva	**-,073**	-,042	-,180	-0,28	-0,31	-0,27	**-0,42**
Phagocytose Index vs Staph. aureus	**-,043**	,009	-,121	+0,37	+0,40	+0,39	**+0,14**
IgG Serum	**-,041**	-,075	,023	**+1,10**	+0,65	+0,89	**+0,64**
$CD4^+CD3^+$ T-helper Lymphocytes	currently not in model			**-2,12**	-2,21	-2,93	**-3,47**
Root 2 (8,0%)	**R 1**	**R 2**	**R 3**	-0,18	**+1,82**	**-0,99**	-0,04
Uric Acid Serum	-,008	**-,743**	-,050	-0,53	**-1,89**	**+0,09**	-0,70
Killing Index vs Staph. aureus	,033	**-,181**	-,186	-1,25	**-1,32**	**-0,70**	-1,12
Bactericidity vs Staph. aureus	,003	**-,163**	-,118	-1,06	**-1,43**	**-0,25**	-1,12
Bactericidity vs E. coli	currently not in model			-0,50	**-1,92**	**+0,14**	-0,20
$CD8^+CD3^+$ T-cytolytic Lymphocytes	currently not in model			-0,06	**-0,71**	**-0,04**	+0,06
Microbial Count vs E. coli	-,014	**-,103**	-,026	+0,94	**+0,76**	**+0,99**	+0,83
Leukocyturia, lg	-,004	**-,061**	,177	+0,89	**+0,39**	**+0,51**	+0,88
Lactobacillus faeces	,008	**-,050**	,069	-1,19	**-1,35**	**-1,24**	-1,12
Bifidobacterium faeces	,002	**-,043**	,106	-1,13	**-1,35**	**-1,27**	-1,09
Bacteriuria, points	,003	**,308**	-,033	+1,11	**+1,75**	**+0,93**	+1,17
Bacteriuria, lg	currently not in model			+1,21	**+1,82**	**+1,07**	+1,23
Attenuated E. coli faeces	currently not in model			+2,47	**+2,79**	**+2,07**	+2,21
Interleukin-1	currently not in model			+0,09	**+1,06**	**+0,29**	+0,38
Pan-Lymphocytes	,005	**,175**	,095	+0,34	**+0,68**	**-0,05**	+0,40
Root 3 (6,6%)	**R 1**	**R 2**	**R 3**	+0,59	-0,74	**-1,16**	+0,81
Popovych's Strain Index-1	,010	-,135	**-,287**	+1,29	+1,87	**+3,83**	+1,28
Klebsiela&Proteus faeces	currently not in model			+1,02	+0,80	**+1,65**	+1,19
Erythrocyturia, points	-,006	-,023	**,271**	+1,22	+0,80	**+0,75**	+1,23
Interleukin-6	,014	-,061	**,112**	+0,90	+0,74	**+0,69**	+0,86
Tumor Necrosis Factor-α	currently not in model			+0,82	+0,62	**+0,54**	+0,77
C-Reactive Protein	currently not in model			+0,60	+0,39	**+0,32**	+0,55

As we can see, the major root is uniquely interpreted as uricosuria. Together with it, the root condenses information on the entropy of the immunocytogram (ICG) and, in the reverse way, the intensity of phagocytosis by neutrophils of both bacteria, the content of IgA and lysozyme in saliva and IgG in serum. Such uricous-immune relationships are visualized (Fig. 3.2) by the localization of members of the **S±E-** cluster in the negative zone of the root axis, reflecting the combination of hypouricosuria with a slight neg-entropy of ICG, on the one hand, and maximally for sampling increased phagocytosis activity against E. coli and IgG content in serum while minimally for sampling reduced IgA content in saliva, on the other hand.

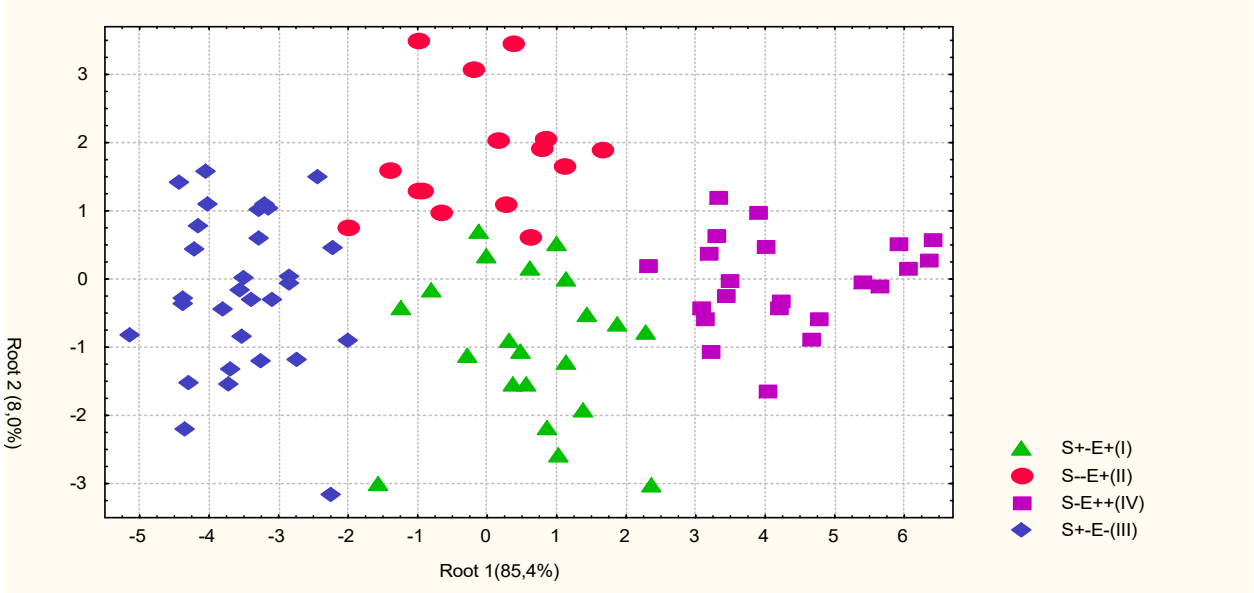

Fig. 3.2. Scatterplot of patients from differ clusters in space of first and second Roots

Instead, in the positive zone of the axis localized members of the cluster **S-E2+**, in which hyperuricosuria is accompanied by a slightly increased ICG entropy, minimal for the sample increase in serum IgG, lack of activation of phagocytosis and maximum for the sample decrease in IgA and lysozyme saliva content.

The members of the other two clusters with equally moderate hyperuricosuria occupy an intermediate quasi-zero zone of the axis, reflecting the intermediate state of these immune parameters.

By adding monocytes and T-helper cells not included in the model, we obtain **immuno-enhancing** and **immuno-suppressive** patterns for uricosuria (Fig. 3.3).

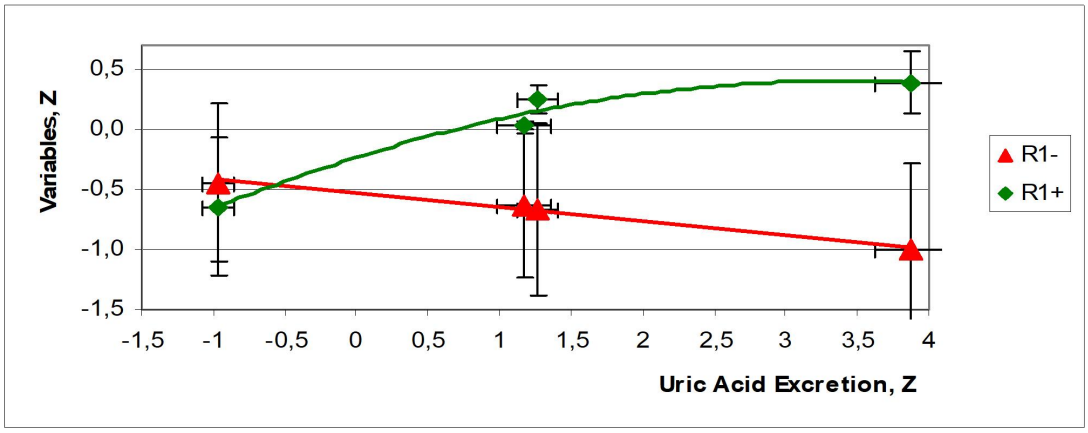

Fig. 3.3. Patterns of Immunity parameters, the information of which is condensed in the first Root

The separation of the last two clusters occurs along the axis of the second root, which represents inverted uricemia. The upper position of the members of the **S2-E+** cluster reflects a combination of hypouricemia in them with a maximum for sampling inhibition of the completion of Staph. aureus phagocytosis, a minimum of Leukocyturia and activation of the intensity of E. coli phagocytosis, as well as maximum reduction in the microbiota of beneficial Lactobacilli and Bifidobacteria, which are inversely related to the root. Instead, bacteriuria (estimated on a one-point scale) and pan-lymphocytes levels, which are directly related to the root, are maximal for sampling.

The lower position of the **S±E+** cluster members reflects a combination of normal uricemia with normal or less reduced/elevated levels of the listed immunity parameters and microbiota negatively/positively associated with the second root.

Taking into account not included in the model T-cytolytic lymphocytes, bactericidal activity against E. coli, row bacteriuria, relative content of E. coli with impaired enzymatic activity in the microbiota and plasma IL-1 level, we have formed **immuno-enhancing** and **immuno-suppressive** patterns of uricemia (Fig. 3.4).

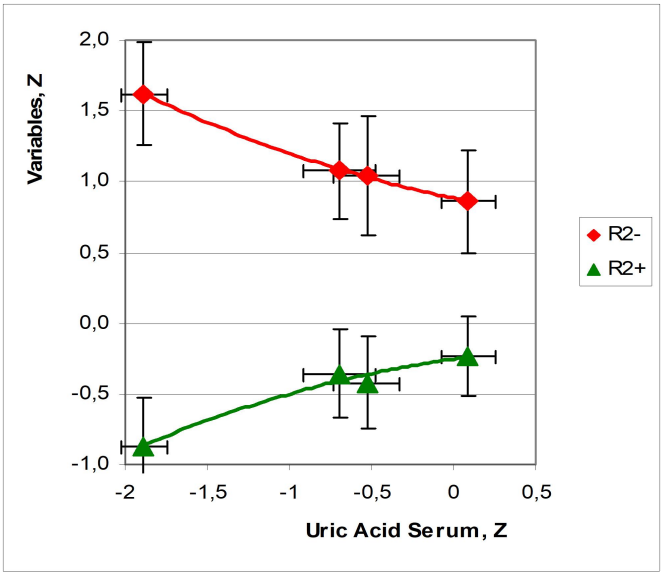

Fig. 3.4. Patterns of Immunity parameters, the information of which is condensed in the second Root

In the information space of the two roots, which together condense 93,4% of the discriminatory information, all four clusters are visually clearly separated, with some exceptions (Fig. 3.2).

Additional delimitation of the members of the **S±E+** cluster occurs along the axis of the third root, due to the maximum elevated Popovych's Strain Index-1, the relative content in microbiota of the Klebsiela&Proteus and Erythrocyturia, instead of the minimally increased levels of proinflammatory factors (Figs. 3.5 and 3.6).

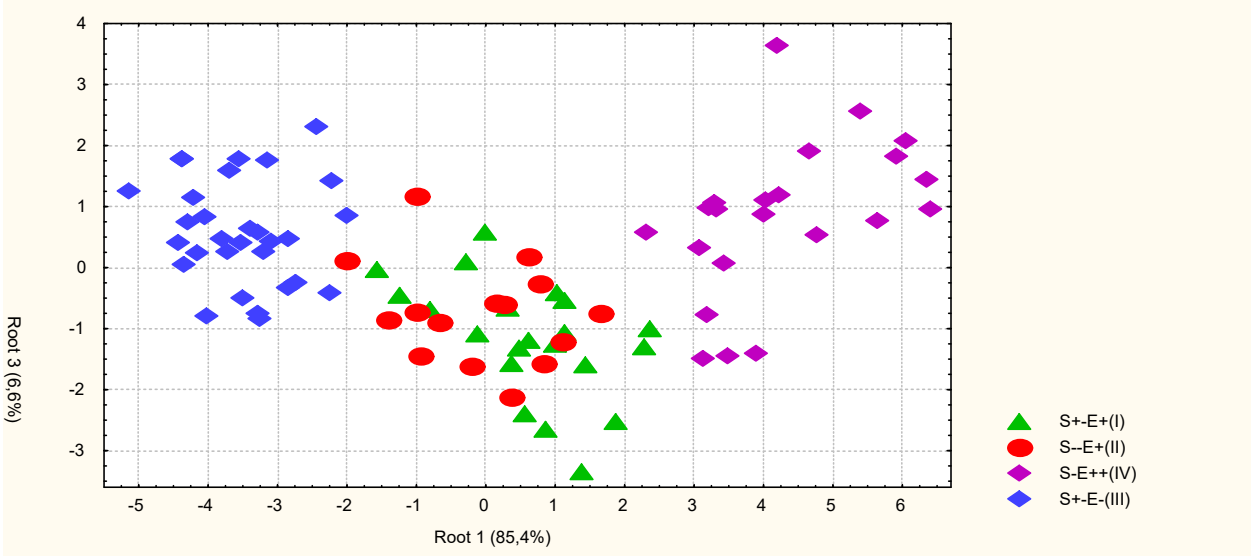

Fig. 3.5. Scatterplot of patients from differ clusters in space of first and third Roots

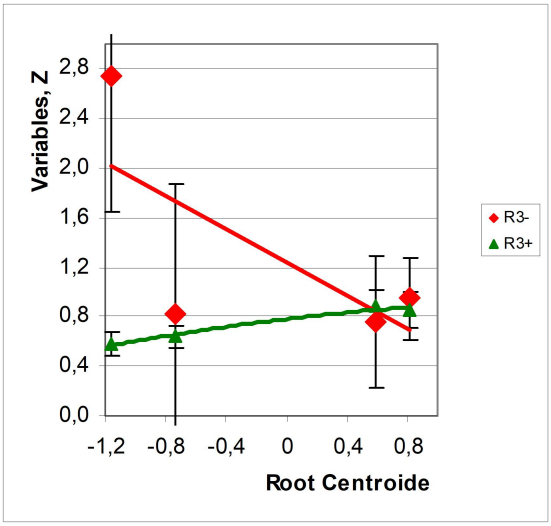

Fig. 3.6. Patterns of Immunity parameters, the information of which is condensed in the third Root

In general, cluster delineation is highly reliable (Table 3.13).

Table 3.13. Squared Mahalanobis Distances between Clusters, F-values (df=19,7) and p-levels

Clusters	S±E+ I	S2-E+ II	S-E2+ IV	S±E- III
S±E+ I (21)	0	9,1	19,5	21,7
S2-E+ II (15)	3,1 10^{-3}	0	26,2	18,3
S-E2+ IV (22)	8,3 10^{-6}	9,1 10^{-6}	0	63,7
S±E- III (30)	10,6 10^{-6}	7,1 10^{-6}	32,1 10^{-6}	0

The same discriminant variables can be used to identify the belonging of one or another person to one or another cluster. This purpose of discriminant analysis is realized with the help of classifying functions (Table 3.14).

Table 3.14. Coefficients and Constants for Classification Functions of Clusters

Clusters	S±E+ I	S2-E+ II	S-E2+ IV	S±E- III
Variables	p=,239	p=,170	p=,250	p=,341
Uric Acid excretion, Z-score	-5,524	-6,483	,233	-11,67
Serum Uric Acid level, Z-score	-66,14	-68,88	-67,14	-67,53
Popovych's Strain Index-1, points	-67,95	-72,32	-72,26	-71,73
Killing Index vs Staph. aureus, %	6,538	6,410	6,506	6,458
Lysozime Saliva, mg/L	-,192	-,363	-,499	-,678
Phagocytose Index vs Staph. aureus, %	118,4	118,5	119,3	115,7
Pan-Lymphocytes of Blood, %	-5,873	-5,732	-6,143	-5,459
Phagocytose Index vs E. coli, %	69,08	69,51	69,67	71,34
Erythrocyturia, points	-150,3	-152,2	-144,3	-141,3
IgA Saliva, mg/L	-1,631	-1,588	-1,699	-1,537
Bifidobacterium faeces, lg CFU/g	-12,09	-9,259	-9,291	-1,077
Lactobacillus faeces, lg CFU/g	-13,36	-15,21	-14,74	-21,76
Leukocyturia, lg/L	238,1	239,0	239,1	243,0
IgG Serum, g/L	,326	,271	,129	,739
Bacteriuria, points	138,8	149,4	138,7	139,7
Bactericidity vs Staph. aureus, 10^9 Bacteria/L	-1,871	-1,796	-1,948	-1,856
Entropy of Immunocytogram	3605	3637	3552	3658

Interleukin-6, ng/L	580,9	586,6	579,1	592,8
Microbial Count vs E. coli, Bacter/Phagocyte	-6,096	-6,036	-5,897	-5,985
Constants	-13393	-13514	-13427	-13468

We can retrospectively recognize members of III cluster unmistakably, of IV cluster with one error, but of I and II clusters with two errors (Table 3.15).

Table 3.15. Classification Matrix for Clusters
Rows: Observed classifications; Columns: Predicted classifications

	Percent	S±E+ I	S2-E+ II	S-E2+ IV	S±E- III
Clusters	correct	p=,239	p=,170	p=,250	p=,341
I	90,5	**19**	**2**	0	0
II	86,7	**1**	**13**	0	**1**
IV	95,5	**1**	0	**21**	0
III	100	0	0	0	**30**
Total	94,3	21	15	21	31

3.3. RELATIONSHIPS BETWEEN PARAMETERS OF URIC ACID EXCHANGE AND IMMUNITY&MICROBIOTA

Correlation links screening has found, first, their complete absence between uricemia and uricosuria (Table 3.16). Second, raw uricemia levels are more closely related to Immunity and Microbiota parameters than levels standardized by sex and age. Third, uricosuria was significantly associated with only 5 parameters of immunity.

Table 3.16. Matrix of correlations between parameters of Uric acid exchange and Immunity as well as Microbiota (color-coded significant links)

N=88 $_{0,05}\|r\|\geq 0,21$	UAS raw	UAS standard	UA Excretion
UAS raw	1,00	**,87**	-,03
UAS standardised by sex&age	**,87**	1,00	-,09
UA Excretion	-,03	-,09	1,00
CD4⁺ Lymphocytes	**-,38**	-,13	**-,23**
Killing Index vs E. coli	**,38**	**,23**	,11
Attenuated E. coli feces	**-,38**	**-,22**	-,12
Killing Index vs Staph. aureus	**,36**	**,24**	,16
IgA Saliva	**-,34**	-,10	**-,27**
Monocytes	**,27**	,02	,20
Bactericidal Capacity vs E. coli	**,26**	**,28**	,06
IgG Saliva	**-,27**	,11	,13
Lactobacilli feces	**,27**	,14	,09
Bifidobacteria feces	**,25**	,12	,08
Polymorphonucleary Neutrophils	**-,22**	-,00	-,15
Entropy Immunocytogram	**,22**	,08	**,24**
Microbial Count vs Staph. aureus	**,21**	,20	-,09
Bacteriuria, lg CFU	**-,20**	**-,24**	-,02
Bacteriuria, points	**-,20**	**-,23**	-,01
Bactericidal Capacity vs Staph. aur.	,20	**,22**	,04
CD56⁺ Lymphocytes	,20	-,06	,17
Phagocytose Index vs Staph. aureus	,14	**,25**	**-,22**
CD8⁺ Lymphocytes	,14	**,25**	,02
Microbial Count vs E. coli	,12	**,22**	-,10
Phagocytose Index vs E. coli	,03	,16	**-,27**
Pan-Lymphocytes	,19	-,01	,10
E. coli feces	,19	,02	,05
Popovych Adaptation Index-1	-,18	-,13	-,08
0-Lymphocytes	,17	,00	-,01
IgA Serum	-,15	,07	-,18

Hemolytica E. coli feces	-,15	-,05	-,05
Active T-Lymphocytes	-,14	-,02	-,02
CIC Serum	,13	,17	-,01
Entropy Leukocytogram	,12	-,02	,17
Leukocyturia raw	-,12	,04	-,02
Klebsiela&Proteus feces	,04	,16	-,04
Leukocyturia points	,01	,12	,06
IgM Serum	,06	,06	-,16
$CD22^+$ Lymphocytes	,02	,03	,16
Leukocytes Blood	,00	-,04	,16
Eosinophils	-,09	,03	,01
Stubnucleary Neutrophils	-,08	,01	-,03
Popovych Strain Index-2	-,06	,02	,01
Erythrocyturia points	,03	,08	-,01
Popovych Adaptation Index-2	-,03	-,02	-,11
TNF-α	,03	,03	,03
IL-6	,03	,03	,03
C-RP	,03	,03	,03
IL-1	,02	,02	,07
IgG Serum	,00	,01	-,07
Erythrocyturia raw	-,02	,01	,04
Popovych Strain Index-1	-,01	,02	-,01

Note: for a sample with n=88, the critical level |r| at p<0,05 (t>2,00) is 0,21, at p<0,02 (t>2,39) is 0.25, at p<0,01 (t>2,66) is 0,28, at p<0,001 (t>3,46) is 0,36.

By stepwise exclusion, 9 Immunity parameters were included in the regression model for raw uricemia, as well as bacteriuria and E. coli content, despite very low correlation coefficients, while some parameters with significant coefficients were found outside the model. Such constellation of parameters of Immunity and Microbiota is determined by raw uricemia by 37% (Table 3.17 and Fig. 3.7).

Table 3.17. Regression Summary for Serum Uric Acid raw level
R=0,611; R^2=0,374; Adjusted R^2=0,283; $F_{(12)}$=4,1; $p<10^{-4}$

		Beta	St. Err. of Beta	B	SE of B	$t_{(76)}$	p-level
Variables	r		Intercpt	1,533	,5238	2,93	,005
$CD4^+$ Lymphocytes, %	**-,38**	-,299	,196	-,0031	,0021	-1,53	,130
IgG Saliva, mg/L	**-,27**	-,217	,139	-,0075	,0048	-1,56	,122
Polymorphonucleary Neutrophils, %	**-,22**	-,394	,312	-,0040	,0032	-1,26	,211
Bacteriuria, points	-,20	-,336	,151	-,1094	,0492	-2,22	,029
Killing Index vs Staph. aureus, %	**,36**	,555	,153	,0053	,0015	3,62	,001
Microbial Count vs Staph. aur, Bac/Phag	**,21**	,371	,130	,0037	,0013	2,86	,006
Bactericidal Capacity vs St. aur., 10^9 B/L	,20	-,397	,197	-,0013	,0007	-2,01	,048
$CD56^+$ Lymphocytes, %	,20	-,233	,161	-,0030	,0021	-1,45	,152
Pan-Lymphocytes, %	,19	-,443	,341	-,0047	,0036	-1,30	,199
E. coli feces, lg CFU	,19	-,271	,147	-,0848	,0459	-1,85	,069
0-Lymphocytes, %	,17	,166	,134	,0024	,0020	1,24	,220

Interestingly, uricemia standardized by sex and age determines another constellation of Immunity and Microbiota parameters, but at almost the same rate as the actual one (Table 3.18 and Fig. 3.8).

Table 3.18. Regression Summary for Serum Uric Acid level standardized by Sex and Age
R=0,565; R^2=0,319; Adjusted R^2=0,250; $F_{(8,8)}$=4,6; p=0,0001

		Beta	St. Err. of Beta	B	St. Err. of B	$t_{(79)}$	p-level
Variables	r		Intercpt	-23,6	10,3	-2,30	,024
$CD8^+$ Lymphocytes, %	**,25**	,159	,098	,036	,022	1,61	,111

Phagocytose Index vs Staph. aureus, %	**,25**	,232	,115	,221	,110	2,01	,048
Killing Index vs Staph. aureus, %	**,24**	,278	,132	,036	,017	2,10	,039
Killing Index vs E. coli, %	**,23**	-,476	,284	-,041	,025	-1,67	,098
Microbial Count vs E. coli, Bact/Phag	**,22**	,162	,121	,022	,016	1,34	,184
CIC Serum, units	,17	,137	,098	,010	,007	1,40	,164
Klebsiela&Proteus feces, %	,16	,346	,120	,026	,009	2,89	,005
Attenuated E. coli feces, %	**-,22**	-,698	,294	-,028	,012	-2,38	,020

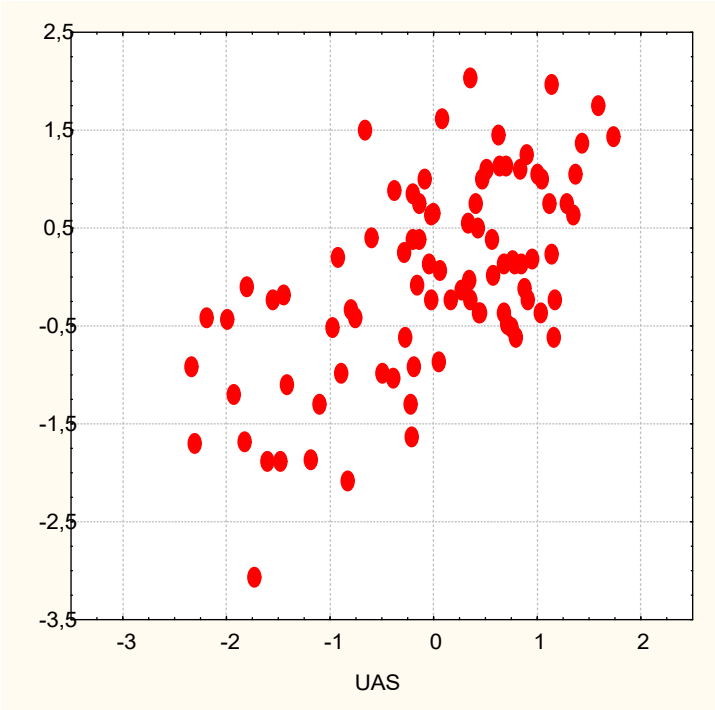

R=0,611; R^2=0,374; $\chi^2_{(11)}$=38; p<10^{-4}; Λ Prime=0,626

Fig. 3.7. Scatterplot of canonical correlation between Serum Uric Acid raw level (X-line) and parameters of Immunity and Microbiota (Y-line)

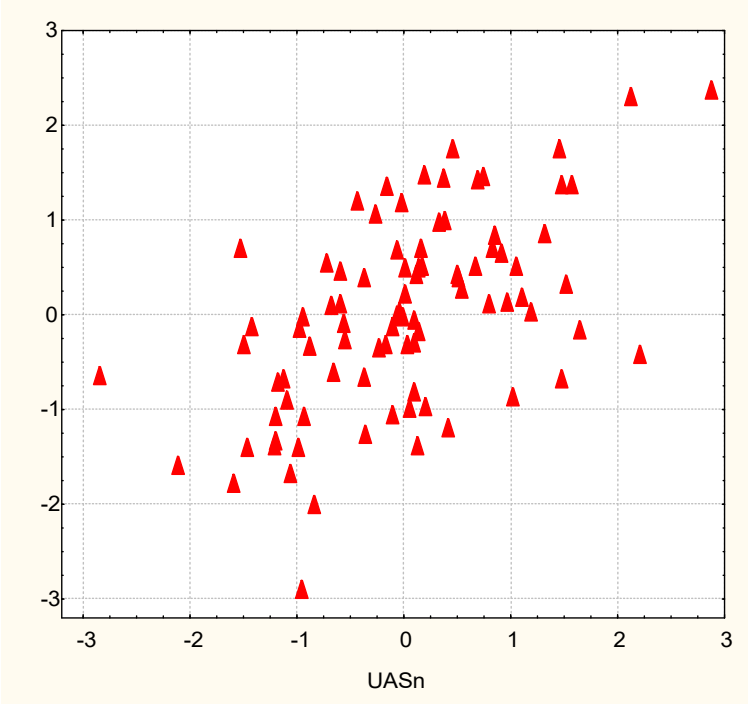

R=0,565; R^2=0,319; $\chi^2_{(8)}$=31,5; p=0,0001; Λ Prime=0,681

Fig. 3.8. Scatterplot of canonical correlation between Serum Uric Acid level standardized by sex and age (X-line) and parameters of Immunity and Microbiota (Y-line)

Instead, uricosuria slightly determines only four Immunity parameters and is only 16% but statistically significant (Table 3.19 and Fig. 3.9).

Table 3.19. Regression Summary for Uric Acid Urinary Excretion
R=0,395; R^2=0,156; Adjusted R^2=0,115; $F_{(4,8)}$=3,8; p=0,007

		Beta	St. Err. of Beta	B	St. Err. of B	$t_{(83)}$	p-level
Variales	r		Intercpt	12,63	19,01	,66	,508
Phagocytose Index vs E. coli	**-,27**	-,203	,105	-,30	,15	-1,94	,056
IgM Serum	-,16	-,139	,103	-,94	,69	-1,35	,179
Entropy Immunocytogram	**,24**	,184	,104	13,89	7,87	1,77	,081
Entropy Leukocytogram	,17	,198	,102	9,44	4,85	1,95	,055

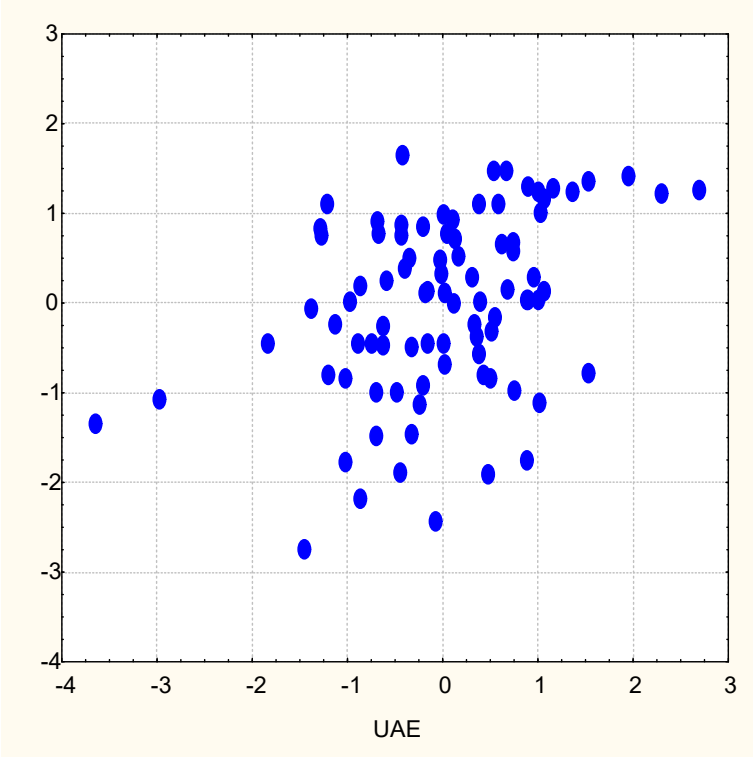

R=0,395; R^2=0,156; $\chi^2_{(4)}$=14,2; p=0,007; Λ Prime=0,844
Fig. 3.9. Scatterplot of canonical correlation between Uric Acid Excretion (X-line) and parameters of Immunity (Y-line)

In the final stage of the analysis, the relationship between the three parameters of Uric acid metabolism, on the one hand, and the parameters of Immunity and Microbiota, on the other, was clarified. Taken together, they have a more significant effect on Immunity and the Microbiota than taken separately (Table 3.20 and Fig. 3.10).

Table 3.20. Factor structure of canonical correlation between parameters of Uric Acid exchange and parameters of Immunity and Microbiota

Right set	**R**
Uric Acid Serum raw, mM/L	**-,890**
Uric Acid Serum standardized by sex&age, Z	**-,599**
Uric Acid Excretion, mM/24h	**-,293**
Left set	**R**
$CD4^+$ Lymphocytes, %	**,724**
Attenuated E. coli feces, %	**,593**
Polymorphonucleary Neutrophils, %	**,490**
IgG Saliva, mg/L	**,489**
Phagocytose Index vs E. coli, %	**,187**
Bacteriuria, points	**,187**

Klebsiela&Proteus feces, %	,072
Phagocytose Index vs Staph. aureus, %	,038
Killing Index vs E. coli, %	-,581
Killing Index vs Staph. aureus, %	-,556
$CD56^+$ Lymphocytes, %	-,504
Entropy Immunocytogram	-,457
Pan-Lymphocytes, %	-,421
E. coli feces, lgCFU	-,370
0-Lymphocytes, %	-,326
Entropy Leukocytogram	-,325
Bactericidal Capacity vs Staph. aur., 10^9 B/L	-,208
Microbial Count vs Staph. aur., Bact/Phagoc	-,202
CIC Serum, units	-,099
$CD8^+$ Lymphocytes, %	-,060
IgM Serum, g/L	-,008
Microbial Count vs E. coli, Bacter/Phagocyte	-,003

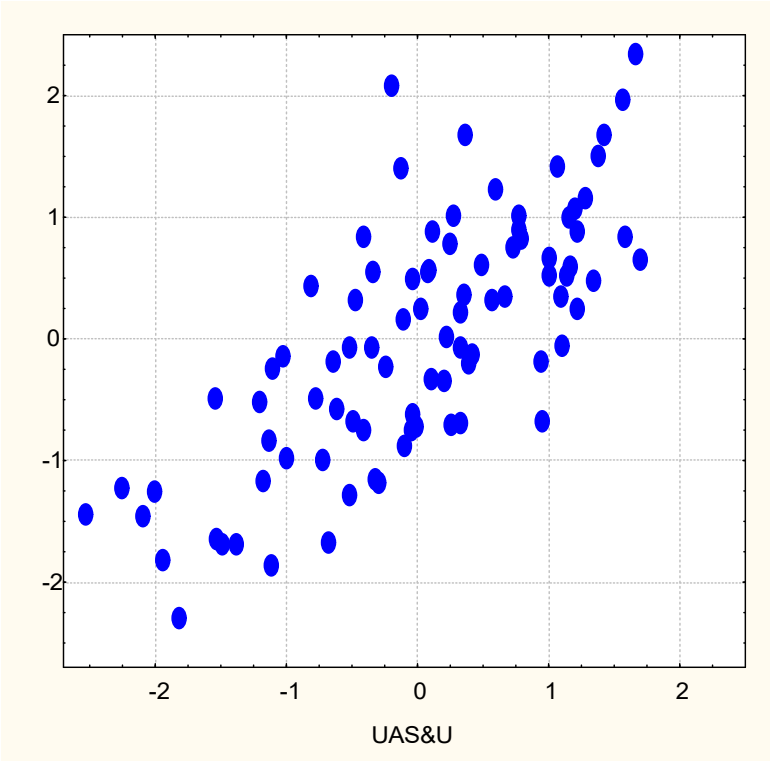

R=0,747; R^2=0,559; $\chi^2_{(66)}$=108; p=0,0008; Λ Prime=0,231

Fig. 3.10. Scatterplot of canonical correlation between parameters of Uric Acid exchange (X-line) and parameters of Immunity and Microbiota (Y-line)

Judging by factor loadings, the major targets of Uric acid suppressor activity are $CD4^+$ Lymphocytes and Polymorphonucleary Neutrophils levels in the blood as well as IgG levels in saliva, to a lesser extent E. coli and Staph. aureus Phagocytosis Activity. Instead, the impact on both the Intensity and, in particular, the Completion of Phagocytosis by neutrophils of both bacterial species, blood levels of Natural and T-killers, as well as serum levels of CIC and IgM is enhancing.

Now let's analyze the connections between changes in two sets of parameters caused by balneotherapy.

Based on the results of the screening, a correlation matrix is created (Table 3.21). For comparison, we present the correlation matrix from the previous analysis. We draw attention to the difference between the critical levels of the coefficient modules, which is caused by twice the difference of the samples.

Table 3.21. Correlation matrix for changes in parameters of Uric Acid metabolism and Immunity

	N=44; $_{0,05}\|r\|\geq 0,30$		N=88; $_{0,05}\|r\|\geq 0,21$		
Variables	Change in UA Serum raw	Change in UA Excretion	UA Serum raw	UA Serum standard	UA Excretion
Uric Acid Serum	1,00	-,05	1,00	**,87**	-,03
UAS standardized by sex&age			**,87**	1,00	-,09
Uric Acid Excretion	-,05	1,00	-,03	-,09	1,00
$CD4^+$ Lymphocytes	**-,49**	,29	**-,38**	-,13	**-,23**
IgA Saliva	**-,36**	,11	**-,34**	-,10	**-,27**
IgG Saliva	-,25	,04	**-,27**	,11	,13
Tumor Necrosis Factor-α	**-,30**	,08	,03	,03	,03
IL-6	**-,31**	,08	,03	,03	,03
C-Reactive Protein	**-,30**	,08	,03	,03	,03
Monocytes	**,34**	-,07	**,27**	,02	,20
Circulating Immune Complexes	**,33**	,04	,13	,17	-,01
$CD8^+$ Lymphocytes	,26	-,17	,14	**,25**	,02
Microbial Count vs Staph. aureus	-,06	-,28	**,21**	,20	-,09
IgG Serum	,06	,23	,00	,01	-,07

Note: for a sample of n=44 critical value |r| at p<0,05 (t>2,02) is 0,30, at p<0,02 (t>2,42) is 0,35, at p<0,01 (t>2,70) is 0,39, at p<0,001 (t>3,55) is 0,50.

First of all, it is found that individual **changes** in uricemia correlate inversely with **changes** in the level of T-helpers in blood (Fig. 3.11) as well as IgA and IgG in saliva while positively with **changes** in the level of Monocytes with the almost same force as their **static** levels.

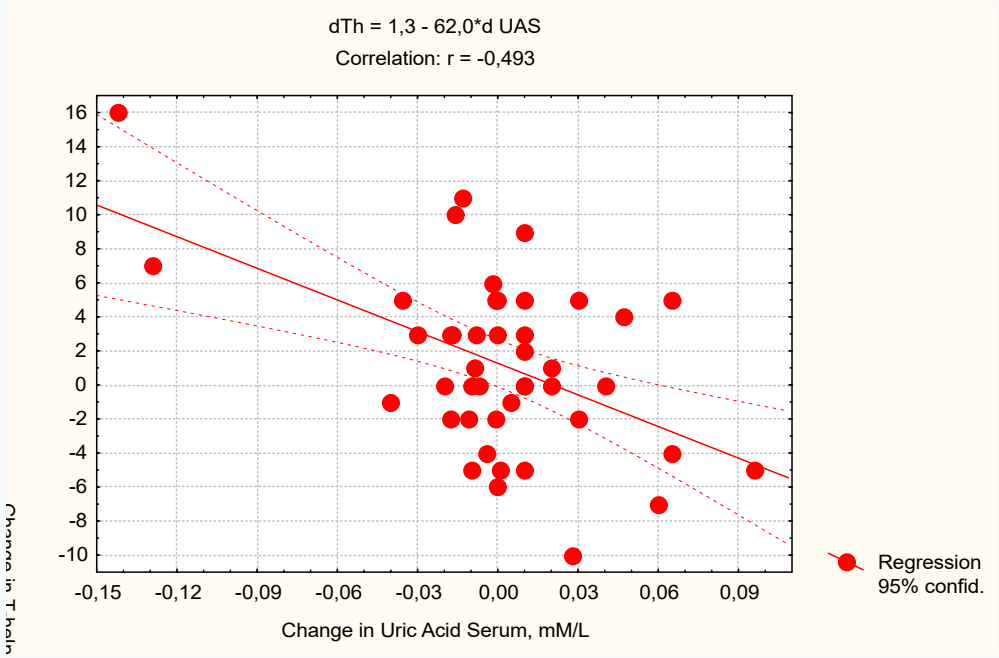

Fig. 3.11. Scatterplot of correlation between changes in Uric Acid Serum (X-line) and T-helpers (Y-line)

Instead, inverse links with changes in inflammatory markers and positive connections with changes in CIC and T-killers that are absent with respect to static parameters are revealed. However, no association was found between changes in uricemia and the intensity of Staph. aureus phagocytosis by blood neutrophils.

Changes in uricosuria correlate with changes in only three immune parameters, and even at the limit of significance. Note the opposite signs of the correlation coefficients for T-helpers and T-killers, on the one hand, and uricemia and uricosuria, on the other. This is due to the inverse

nature of the association between changes in the blood content of these subpopulations of T lymphocytes (Fig. 3.12).

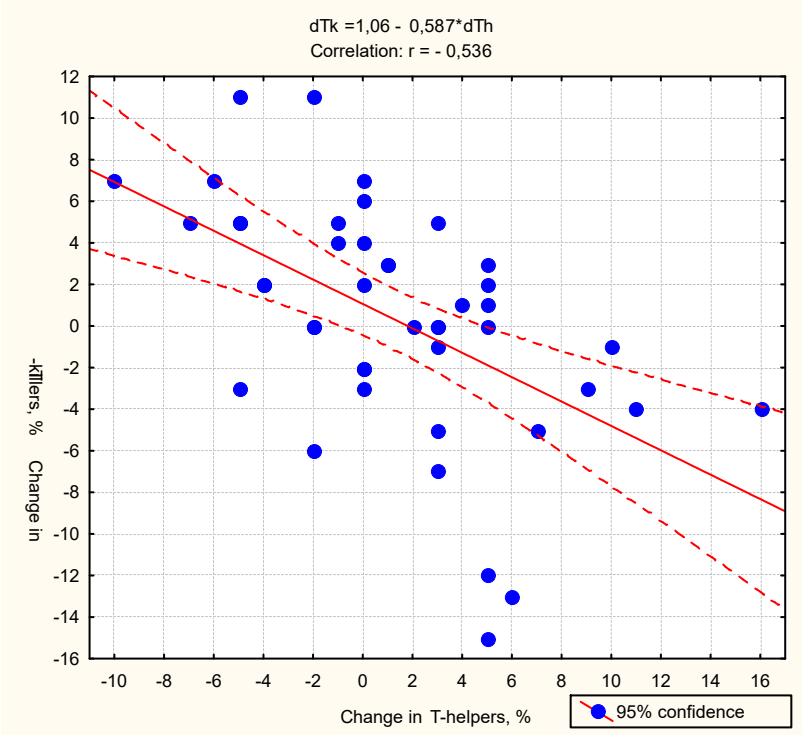

Fig. 3.12. Scatterplot of correlation between changes in T-helpers (X-line) and T-killers (Y-line)

By stepwise exclusion, 4 Immunity parameters were included in the regression model for change in uricemia, while some 3 parameters with significant coefficients were found outside the model. Such constellation of change in parameters of Immunity is determined by change in uricemia by 55% (Table 3.22 and Fig. 3.13).

Table 3.22. Regression Summary for change in Serum Uric Acid level
R=0,740; R^2=0,547; Adjusted R^2=0,500; $F_{(4,4)}$=11,8; $p<10^{-5}$

		Beta	St. Err. of Beta	B	St. Err. of B	$t_{(39)}$	p-level
Change in	r		Intercpt	,0013	,0047	,27	,788
T-helpers	**-0,49**	-,420	,11	-,0033	,0009	-3,70	,001
TNF-α	**-0,31**	-,249	,11	-,0057	,0026	-2,17	,036
Monocytes	**0,34**	,386	,11	,0069	,0019	3,56	,001
CIC	**0,33**	,399	,11	,0008	,0002	3,66	,001

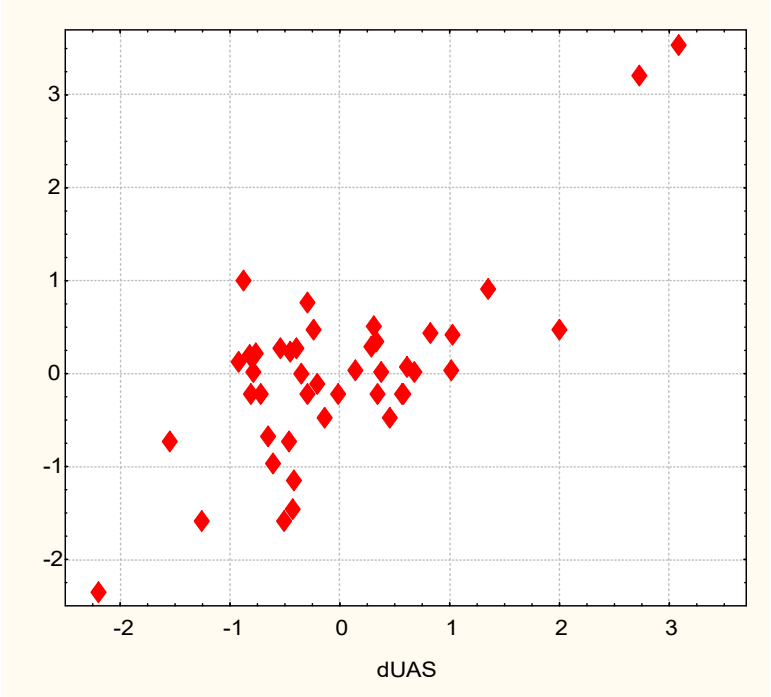

R=0,740; R^2=0,547; $\chi^2_{(4)}$=32; p<10^{-5}; Λ Prime=0,453

Fig. 3.13. Scatterplot of canonical correlation between changes in Uric Acid Serum (X-line) and Immunity parameters (Y-line)

Instead, change in uricosuria slightly determines only three Immunity parameters and is only 21% but statistically significant (Table 3.23 and Fig. 3.14).

Table 3.23. Regression Summary for change in Uric Acid Excretion
R=0,459; R^2=0,211; Adjusted R^2=0,152; $F_{(3,4)}$=3,6; p=0,022

		Beta	St. Err. of Beta	B	St. Err. of B	$t_{(40)}$	p-level
Change in	r		Intercpt	,017	,252	,07	,948
T-helpers	0,29	,284	,146	,095	,049	1,94	,059
IgG Serum	0,23	,177	,145	,070	,057	1,22	,230
MC St. aur.	-0,28	-,319	,142	-,060	,026	-2,25	,030

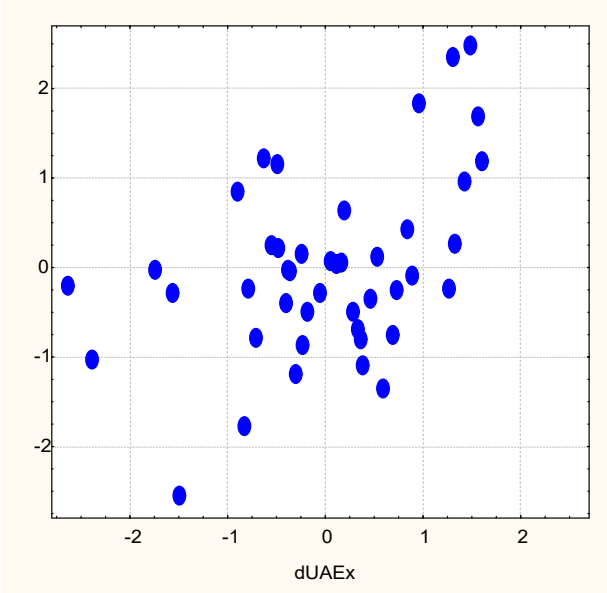

R=0,459; R^2=0,211; $\chi^2_{(3)}$=9,6; p=0,022; Λ Prime=0,789

Fig. 3.14. Scatterplot of canonical correlation between changes in Uric Acid Excretion (X-line) and Immunity parameters (Y-line)

It is interesting that changes in the content of T-helpers in the blood are positively determined by changes in uricosuria, but negatively by changes in uricemia. The determination rate is 34% (Fig. 3.15).

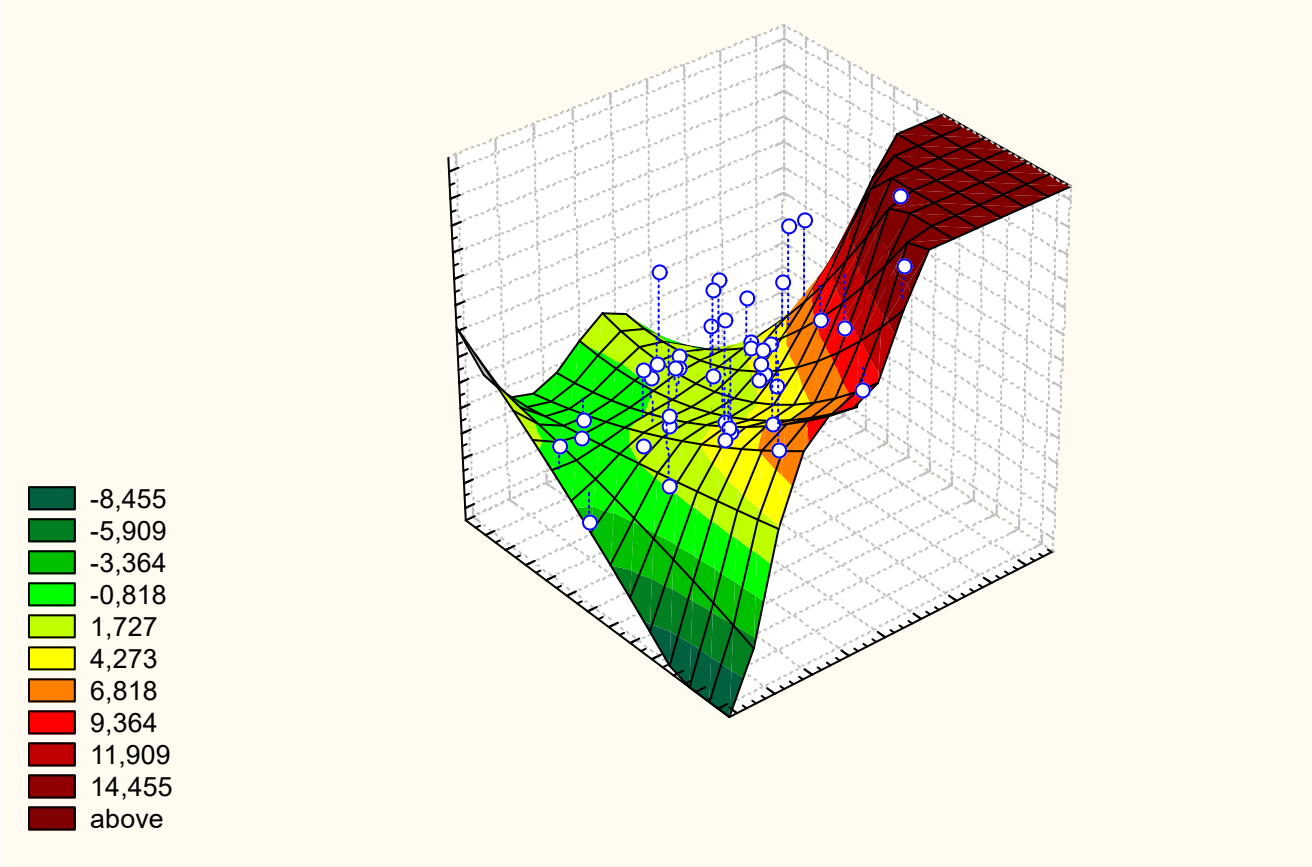

dTh(%) = 1,28 – 60,18•dUAS(mM/L) + 0,874•dUAE(mM/24h)
R=0,582; R^2=0,338; Adjusted R^2=0,305; $F_{(2,4)}$=10,2; p=0,0003

Fig. 3.15. Scatterplot of correlation between changes in Uric Acid Excretion (X-line), Uric Acid Serum (Y-line) and T-helpers blood level (Z-line)

Uricosuria also positively determines the level of serum IgG, while the intensity of phagocytosis of Staphylococcus aureus is negatively determined; uricemia causes downregulation of TNF-alpha and upregulation of monocyte and CIC levels.

Taking into account other relationships, we find that balneotherapy-induced changes in uricemia and uricosuria determine changes in immune status by 60% (Table 3.24 and Fig. 6).

Table 3.24. Factor structure of canonical correlation between changes in parameters of Uric Acid exchange and parameters of Immunity

Right set	R
Uric Acid Serum	**-,945**
Uric Acid Excretion	**,374**
Left set	R
T-helpers	**,716**
TNF-α	**,408**
Monocytes	**-,440**
CIC	**-,379**
Microbial Count St. aur.	**-,050**
IgG Serum	**,025**

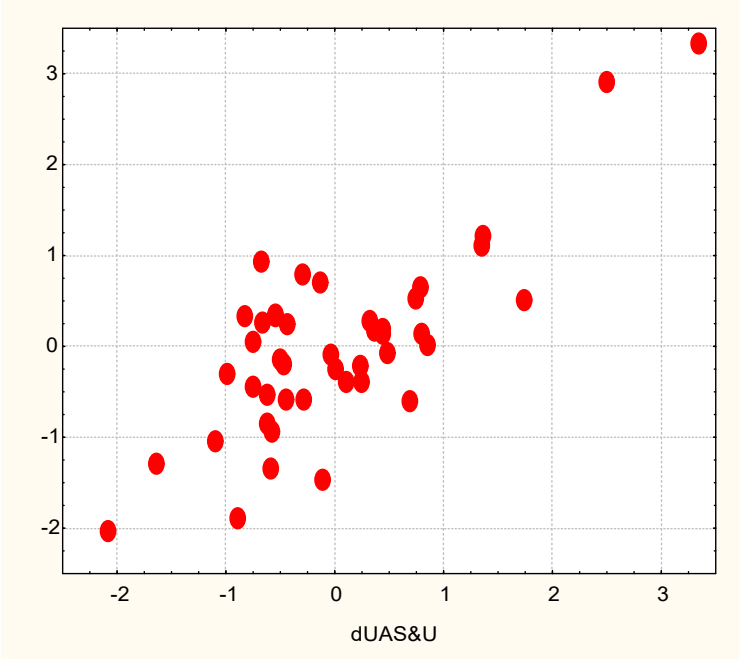

R=0,772; R^2=0,596; $\chi^2_{(12)}$=42; p<10^{-4}; Λ Prime=0,334

Fig. 3.16. Scatterplot of canonical correlation between changes in Uric Acid Exchange parameters (X-line) and Immunity parameters (Y-line)

Despite expectations, no significant telationships was found regarding microbiota parameters. We explain this too short observation period (10 days). However, the hope is that there are negative links with inflammatory markers.

3.4. AUTONOMOUS AND ENDOCRINE ACCOMPANIMENTS OF VARIANTS OF URIC ACID EXCHANGE

The purpose of this section is to clarify the connections between uricemia and uricosuria - on the one hand, and the main attributes of general adaptation reactions - on the other hand. As the latter, we chose the plasma levels of classical adaptogenic hormones – cortisol, aldosterone, triiodothyronine and testosterone [Garkavi LCh et al, 1990], as well as calcitonin and PTH and HRV markers of sympathetic and vagal tone [Gozhenko AI et al, 2017; 2019]. At the same time, the vegetative index of Kerdö and the Ca/K index of blood plasma were included in the battery of tests as hemodynamic [Kerdoe I, 1966; Fajda OI et al, 2015] and electrolyte [Fajda OI et al, 2016] markers of sympatho-vagal balance, respectively.

At the first stage, we will find out which constellation of neuro-endocrine adaptation factors is recognizable. The discriminant analysis program included in the model, in addition to three parameters of uric acid exchange, 4 indices of sympatho-vagal balance as well as triiodothyronine, cortisol, calcitonin and testosterone, and the level of the latter is not row, but normalized by sex and age (Table 3.25). Row level of testosterone, which is drastically different for sex, was left out of the model, as was sex-normalized calcitonin. Aldosterone, PTH and HRV parameters were also not included in the model (Table 3.26).

Table 3.25. Discriminant Function Analysis Summary for Variables of Uric Acid Exchange and Neuro-endocrine adaptation factors

Step 11, N of vars in model: 11; Grouping: 4 grps; Wilks' Λ: 0,0568; approx. $F_{(33)}$=10,9; p<10^{-6}

Variables currently in the model	**Clusters of Uric Acid Exchange (Males/Females)**				**Parameters of Wilks' Statistics**					
	S-E2+ IV (18/4)	**S±E+ I (16/5)**	**S2-E+ II (14/1)**	**S±E- III (20/10)**	Wilks Λ	Partial Λ	F-remove (3,7)	p-level	Tolerancy	Norm Cv/**σ** (30)
Uric Acid Excretion,	5,94	3,94	3,88	2,27	0,416	0,137	156	10^{-6}	0,812	3,00

mM/24 h										0,250
Serum Uric Acid, mM/L	0,316	0,371	0,249	0,322	0,067	0,842	4,62	0,005	0,232	0,365 0,116
Serum Uric Acid normalized, Z-score	-0,70	+0,09	-1,89	-0,53	0,061	0,935	1,72	0,170	0,211	0
Kerdö Vegetative Index, units	-24	-13	-27	-20	0,063	0,907	2,54	0,063	0,826	-20 **23,6**
$(Ca/K)^{0,5}$ Plasma as Symp/Vagal balance	0,71	0,71	0,69	0,73	0,063	0,907	2,52	0,064	0,776	0,71 0,104
AMo/MxDMn as Symp/Vagal balance	218	394	234	236	0,065	0,881	3,34	0,024	0,222	251 0,303
Baevskiy Stress Index, ln units	4,81	5,09	4,66	4,78	0,062	0,913	2,35	0,079	0,197	4,91 0,166
Triiodothyronine, nM/L	1,86	2,17	2,02	1,96	0,059	0,955	1,16	0,331	0,805	2,20 0,227
Cortisol, nM/L	531	475	432	563	0,060	0,940	1,57	0,205	0,816	405 0,524
Calcitonin, ng/L	6,45	7,21	8,76	7,50	0,064	0,888	3,11	0,031	0,732	12,03 0,493
Males, ng/L	6,65	7,76	8,64	8,80						13,95
Females, ng/L	5,55	5,48	10,39	4,90						5,50
Testosterone normalized by Sex&Age, Z	-0,12	+0,55	+1,03	+0,22	0,059	0,956	1,13	0,344	0,915	0
Males, Z-score	-0,31	+0,62	+1,09	+0,18						0
Females, Z-score	+0,70	+0,22	+0,12	+0,29						0

Table 3.26. Variables of Neuro-endocrine adaptation factors currently not in the model

Variables	**Clusters of Uric Acid Exchange (n)**				**Parameters of Wilks' Statistics**						
	S-E2+ IV (22)	**S± E+ I (21)**	**S2-E+ II (15)**	**S± E- III (30)**	Wilks Λ	Partial Λ	F to enter	p-level	Tolerancy	Reference mean (88)	Cv
Baevski Stress Index	156	259	145	137	0,056	0,991	0,232	0,874	0,036	136	,417
Baevski ARS Index	3,42	3,54	3,09	2,20	0,056	0,985	0,363	0,780	0,529	0 ÷ 3	
Mode HRV, msec	833	808	885	883	0,055	0,970	0,749	0,526	0,376	875	,116
AMo HRV, %	43,0	49,7	42,4	43,4	0,056	0,979	0,515	0,673	0,127	39,2	,298
MxDMn HRV, msec	226	196	229	213	0,055	0,976	0,602	0,616	0,097	162	,293
TNN HRV, units	11,3	10,0	12,0	10,8	0,056	0,978	0,537	0,659	0,216	11,2	,217
SDNN HRV, msec	55,4	43,7	51,7	45,9	0,056	0,993	0,173	0,914	0,165	56,2	,516
RMSSD HRV, msec	30,6	27,4	32,6	26,1	0,056	0,981	0,469	0,707	0,417	28,8	,486
pNN_{50} HRV, %	10,4	9,5	12,6	6,9	0,055	0,976	0,589	0,624	0,455	9,0	,820
ULF HRV, $msec^2$	71	103	99	98	0,055	0,972	0,706	0,552	0,778	122	,892
VLF HRV, $msec^2$	1259	1007	1319	1133	0,056	0,991	0,221	0,881	0,270	1250	,572
LF HRV, $msec^2$	1233	834	1192	594	0,055	0,977	0,584	0,627	0,422	625	,482
HF HRV, $msec^2$	426	549	526	395	0,056	0,991	0,232	0,874	0,452	350	,713
LF/HF	4,59	4,55	6,02	3,37	0,056	0,980	0,492	0,689	0,743	2,86	,709
LFnu, %	73,6	71,2	74,0	67,1	0,056	0,992	0,205	0,892	0,798	64,2	,201
(VLF+LF)/HF	9,4	11,6	15,4	13,7	0,057	0,995	0,121	0,948	0,730	6,82	,554
Entropy HRV	0,721	0,733	0,733	0,698	0,055	0,973	0,678	0,568	0,758	0,806	,114
PTH, pM/L	4,35	3,98	3,74	3,24	0,056	0,981	0,472	0,703	0,924	3,75	,230
Aldosterone, pM/L	224	228	218	235	0,055	0,975	0,630	0,598	0,580	238	,187
Calcitonin normd, Z	-0,87	-0,69	-0,60	-0,57	0,056	0,993	0,179	0,910	0,135	0	
Males, Z-score	-1,07	-0,90	-0,78	-0,75						0	
Females, Z-score	+0,02	-0,01	+1,08	-0,22						0	
Testosterone, nM/L	12,0	14,5	17,6	9,9	0,056	0,989	0,266	0,849	0,233		
Testost Males, nM/L	14,0	17,2	18,7	13,5						14,8	,407
Test Females, nM/L	3,26	2,61	2,47	2,70						2,30	,600
Sex Ind (M=1, F=2)	1,18	1,24	1,07	1,33						1,23	
Age, years	44,6	49,0	51,5	53,1						49,7	,256

Table 3.27. Summary of Stepwise Analysis for Variables of Uric Acid Exchange and Neuro-endocrine adaptation factors

Variables currently in the model	F to enter	p-level	Λ	F-value	p-level
Uric Acid Excretion, mM/24 h	154	10^{-6}	0,154	154	10^{-6}
Serum Uric Acid, Z	13,5	10^{-6}	0,104	58,3	10^{-6}
Calcitonin, ng/L	3,08	0,032	0,093	36,7	10^{-6}
Kerdö Vegetative Index, units	2,55	0,061	0,085	27,5	10^{-6}
Testosterone, Z	1,91	0,135	0,079	22,3	10^{-6}
Triiodothyronine, nM/L	1,41	0,247	0,075	18,6	10^{-6}
$(Ca/K)^{0,5}$ Plasma	1,46	0,232	0,071	16,1	10^{-6}
AMo/MxDMn, units	1,22	0,306	0,068	14,2	10^{-6}
Baevskiy Stress Index, ln units	1,76	0,163	0,064	12,9	10^{-6}
Serum Uric Acid, mM/L	1,32	0,273	0,060	11,8	10^{-6}
Cortisol, nM/L	1,57	0,205	0,057	10,92	10^{-6}

Following the algorithm, we transform the 11-dimensional space of discriminant variables into the 3-dimensional space of canonical roots. The canonical correlation coefficient for the first root is 0,935 (Wilks' Λ=0,057; $\chi^2_{(33)}$=228; $p<10^{-6}$), for the second 0,643 (Wilks' Λ=0,449; $\chi^2_{(20)}$=64; $p<10^{-5}$), for the third 0,484 (Wilks' Λ=0,766; $\chi^2_{(9)}$=21; p=0,012). The major root contains 87,2% of the discriminant possibilities, second - 8,9% and minor - 3,9%.

Calculation of the discriminant values of the roots for each person based on raw coefficients and constants (Table 3.28) allows us to visualize each patient in the information space of these roots.

Table 3.28. Standardised and raw coefficients and constants for for variables of Uric Acid Exchange and Neuro-endocrine adaptation factors

Coefficients	Standardized			Raw		
Variables	Root 1	Root 2	Root 3	Root 1	Root 2	Root 3
Uric Acid Excretion, mM/24 h	-1,103	-0,038	-0,018	-1,831	-0,064	-0,029
Serum Uric Acid, Z	-0,103	-1,064	-0,924	-0,110	-1,136	-0,987
Calcitonin, ng/L	0,414	0,086	-0,053	0,092	0,019	-0,012
Kerdö Vegetative Index, units	-0,143	-0,425	0,296	-0,0072	-0,0213	0,0149
Testosterone normalized, Z	0,102	0,115	0,377	0,063	0,071	0,233
Triiodothyronine, nM/L	-0,144	-0,243	0,237	-0,177	-0,300	0,293
$(Ca/K)^{0,5}$ Plasma	-0,064	-0,332	-0,548	-1,151	-5,935	-9,784
AMo/MxDMn, units	0,354	-0,249	1,313	0,0016	-0,0011	0,0058
Baevskiy Stress Index, ln units	-0,401	0,168	-1,110	-0,530	0,222	-1,467
Serum Uric Acid, mM/L	-0,047	0,147	1,128	-0,647	2,034	15,57
Cortisol, nM/L	0,092	-0,134	-0,499	0,00030	-0,00044	-0,00165
		Constants		9,510	2,534	7,581

Table 3.29 shows the correlation coefficients of the discriminant variables with canonical discriminant roots, cluster centroids and normalized values of the discriminant variables, as well as variables not included in the model, but worth noting.

Table 3.29. Correlations Variables-Canonical Roots, Means of Roots and Z-scores of Variables of Uric Acid exchange and Neuro-endocrine adaptation factors

Variables	Correlations Variables-Roots			S-E2+ IV (22)	S±E+ I (21)	S2-E+ II 15)	S±E- III (30)
Root 1 (87,2%)	**R 1**	**R 2**	**R 3**	**-3,87**	-0,31	+0,38	**+2,87**
Uric Acid excretion	**-0,890**	0,202	0,104	**+3,87**	+1,26	+1,17	**-0,97**
PTH				**+0,70**	+0,27	-0,01	**-0,60**
Calcitonin	**0,038**	0,132	0,146	**-0,87**	-0,69	-0,60	**-0,57**
Root 2 (8,9%)	**R 1**	**R 2**	**R 3**	+0,04	**-0,99**	**+1,60**	-0,14
Uric Acid Serum	0,004	**-0,817**	-0,017	-0,70	**+0,09**	**-1,89**	-0,53
AMo/MxDMn HRV	0,004	**-0,248**	0,432	-0,07	**+1,63**	**-0,47**	-0,34
Kerdö Vegetative Index	0,021	**-0,244**	0,172	-0,18	**+0,29**	**-0,29**	0,00
Baevskiy Stress Index, ln	-0,013	**-0,203**	0,172	-0,05	**+0,22**	**-0,35**	-0,20

$(Ca/K)^{0,5}$ Plasma	0,051	**-0,154**	-0,266	-0,01	**+0,01**	**-0,23**	+0,27
Cortisol	0,015	**-0,074**	-0,269	+0,59	**+0,33**	**+0,13**	+0,75
Aldosterone	currently not in model			-0,32	**-0,23**	**-0,44**	-0,07
AMo HRV	currently not in model			+0,35	**+0,90**	**+0,27**	+0,36
Testosterone	0,033	**0,126**	0,367	-0,12	**+0,55**	**+1,03**	+0,22
HF HRV	currently not in model			+0,38	**+0,38**	**+0,71**	+0,22
RMSSD HRV	currently not in model			+0,23	**-0,31**	**+0,38**	-0,01
pNN_{50} HRV	currently not in model			+0,10	**0,00**	**+0,60**	-0,23
Mode HRV	currently not in model			-0,33	**-0,65**	**+0,05**	+0,05
Root 3 (3,9%)	**R 1**	**R 2**	**R 3**	-0,46	**+0,71**	+0,56	-0,44
Triiodothyronine	0,014	-0,062	**0,224**	-0,67	**-0,06**	-0,36	-0,49

Characteristic features of members of the **S-E2+** cluster are a combination of pronounced hyperuricosuria with the maximum for sample level of PTH in plasma and the minimum level of calcitonin, which is visualized by the localization of the cluster in the extreme left zone of the axis of the first root (Fig. 3.17).

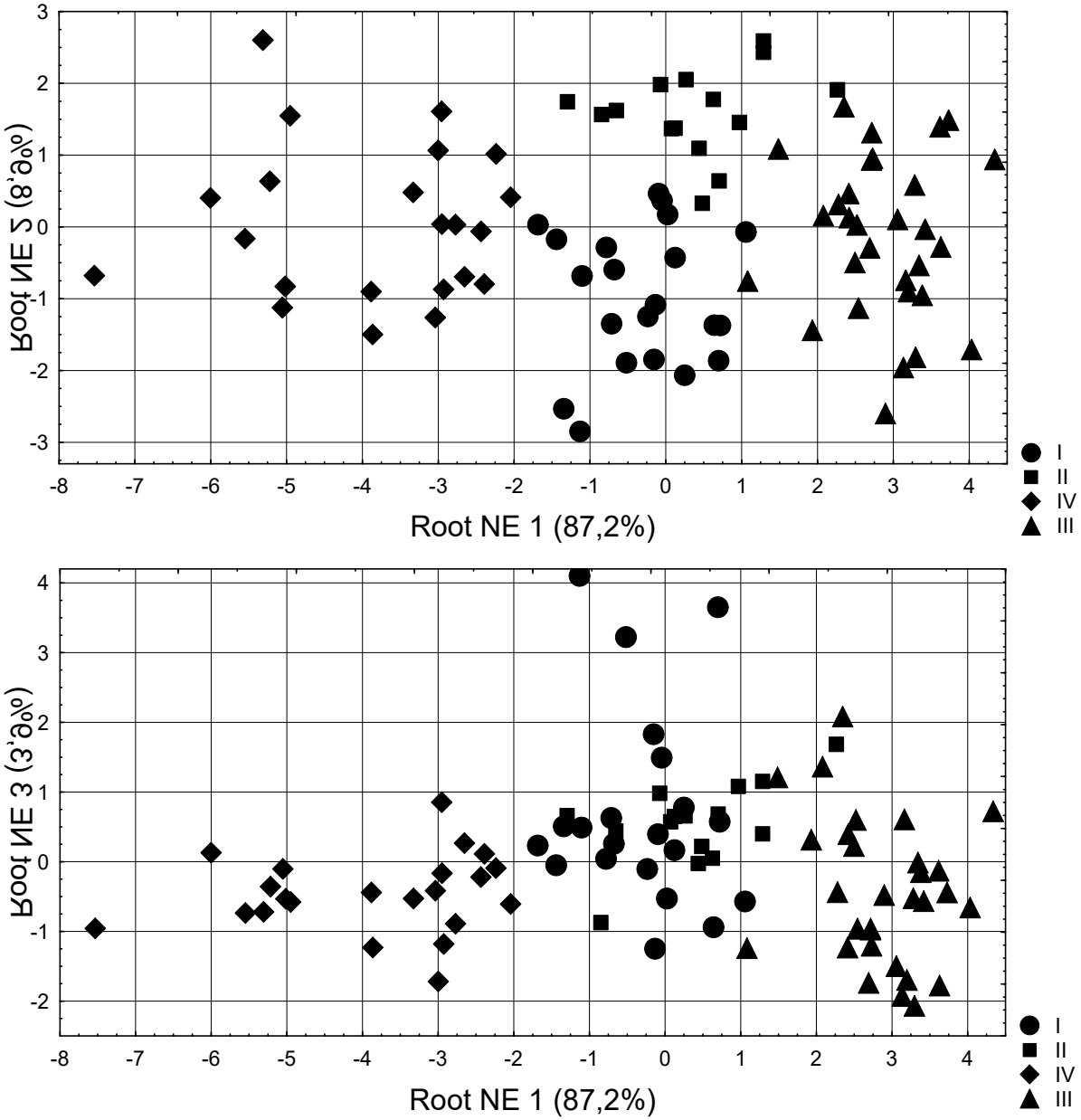

Fig. 3.17. Scattering of individual values of discriminant neuro-endocrine roots of patients of different clusters

Instead, the polar position of the **S±E-** cluster reflects the combination of hypouricosemia in its members with a reduced PTH level and the maximum for the sample calcitonin level (minimally reduced). The other two clusters occupy an intermediate position along the axis of the first root and are intermingled, but are separated along the axis of the second root. The top position of the members of the **S2-E+** cluster reflects a combination of pronounced hypouricemia with a moderate vagotonic shift in the sympatho-vagal balance (it is important that according to various markers: HRV, hemodynamic and calcium-potassium), normal, but minimal for the sample cortisolemia, aldosteronemia and sympathetic tone, and maximal for sample testosterone (normalized by sex&age) and HRV-markers of vagal tone. Instead, the lower localization along the axis of members of the **S±E+** cluster reflects the combination of a normal level of uricemia with a sympathotonic shift in the sympatho-vagal balance, maximal levels of sympathetic tone and circulating catecholamines (minimum Mode HRV) and higher/lower levels of other parameters correlated with the second root negatively/positively respectively. Additional demarcation of the **S±E+** cluster occurs along the axis of the third root, reflecting a normal average level of triiodothyronine against the background of its decrease in other clusters.

In the three-dimensional information space of canonical roots, all four clusters are delimited by the set of discriminant variables quite clearly (Table 3.30).

Table 3.30. Squared Mahalanobis Distances between Clusters, F-values (df=11,7) and p levels

Clusters	S±E+ I	S2-E+ II	S-E2+ IV	S±E- III
S±E+ I (21)	0	7,2	15,1	12,1
S2-E+ II (15)	**5,0** 10^{-6}	0	21,5	10,2
S-E2+ IV (22)	**13,3** 10^{-6}	**15,3** 10^{-6}	0	45,4
S±E- III (30)	**12,0** 10^{-6}	**8,2** 10^{-6}	**46,1** 10^{-6}	0

With the help of classification functions (Table 3.31), it is possible to identify whether a person belongs to a particular cluster.

Table 3.31. Coefficients and constants for classification functions

Clusters	S±E+ I	S2-E+ II	S-E2+ IV	S±E- III
Variables	p=,239	p=,170	p=,250	p=,341
Uric Acid Excretion, mM/24 h	19,43	18,01	25,91	13,59
Serum Uric Acid, Z	1,756	-1,100	2,135	1,579
Calcitonin, ng/L	-0,193	-0,078	-0,487	0,130
Kerdö Index, units	0,018	-0,045	0,004	-0,040
Testosterone, Z	0,845	1,035	0,422	0,837
Triiodothyronine, nM/L	13,86	12,92	13,84	12,71
$(Ca/K)^{0,5}$ Plasma	289,2	274,5	298,6	291,7
AMo/MxDMn, units	-0,107	-0,110	-0,121	-0,110
Baevskiy Stress Ind, ln units	39,43	39,87	43,27	39,62
Serum Uric Acid, mM/L	19,92	22,31	6,075	1,698
Cortisol, nM/L	0,0173	0,0168	0,0179	0,0199
Constants	-244,2	-233,3	-291,1	-223,6

That is, in retrospect, it is possible to recognize members of the II and IV clusters without error, and the other two - with two errors, so that the classification accuracy is 95.5% (Table 3.32).

Table 3.32. Classification matrix for clusters
Rows: observed classifications; columns: predicted classifications

Clusters	Percent correct	S±E+ I p=,239	S2-E+ II p=,170	S-E2+ IV p=,250	S±E- III p=,341
I	90,5	**19**	**1**	0	**1**
II	100	0	**15**	0	0
IV	100	0	0	**22**	0
III	93,3	0	**2**	0	**28**
Total	95,5	19	18	22	29

3.5. RELATIONSHIPS BETWEEN PARAMETERS OF URIC ACID EXCHANGE AND NEURO-ENDOCRINE ADAPTATION FACTORS

Now we will consider relationships between parameters of uric acid exchange and neuro-endocrine factors of adaptation. Table 3.33 shows that uricemia correlates negatively with HRV-markers of vagal tone (TNN, MxDMn, SDNN, TP, VLF, LF), but positively - with HRV-markers of sympathetic tone (AMo) and sympatho-vagal balance (AMo/MxDMn and ln AMo/2MxDMn•Mo). The latter also includes the Ca/K plasma index. Therefore, blood uric acid manifests itself as a sympathoactivating and vagoinhibitory factor. However, uricemia is negatively correlated with the plasma level of triiodothyronine.

After stepwise exclusion, 9 parameters remained in the regression model, the constellation of which is determined by uricemia by 35% (Table 3.34 and Fig. 3.18).

Table 3.33. Correlation matrix for uric acid parameters and adaptation

Variable	Uricemia	Uricosuria
TNN HRV	-0,35	0,04
AMo	0,32	0,00
MxDMn	-0,37	0,09
AMo/MxDMn	0,25	-0,00
ln Stress Index	0,34	0,01
SDNN	-0,31	0,14
Total Power	-0,30	0,16
VLF	-0,31	0,09
LF	-0,37	0,30
LF/TP	-0,12	0,38
Parathyroid hor	0,19	0,46
Triiodothyronine	-0,23	-0,08
Ca/K	0,19	-0,15

Table 3.34. Regression model for adaptation factors and uricemia

N=88	R=0,594; R^2=0,353; Adjusted R^2=0,278; F(9,8)=4,7; p<10^-4					
	Beta	St. Err. of Beta	B	St. Err. of B	t(78)	p-value
Intercpt			-0,18140	0,26150	-0,69	0,4899
Parathyroid hor	0,190	0,094	0,05332	0,02643	2,02	0,0471
Triiodothyronine	-0,143	0,103	-0,01439	0,01038	-1,39	0,1694
Ca/K Plasma	0,137	0,094	0,19707	0,13499	1,46	0,1484
MxDMn	-0,330	0,263	-0,00037	0,00030	-1,26	0,2125
AMo/MxDMn	-0,440	0,196	-0,00015	0,00007	-2,24	0,0279
In Stress Index	0,726	0,349	0,07759	0,03727	2,08	0,0406
Total Power	1,652	0,406	0,00007	0,00002	4,07	0,0001
VLF	-0,401	0,225	-0,00004	0,00002	-1,78	0,0785
LF	-0,990	0,241	-0,00009	0,00002	-4,11	0,0001

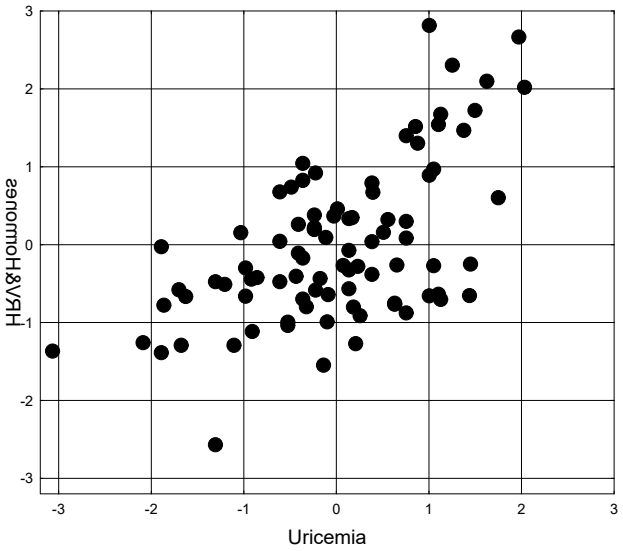

R=0,594; R^2=0,353; $\chi^2_{(9)}$=35; p<10^{-4}; Lambda Prime=0,647

Fig. 3.18. Scatterplot of canonical correlation between Uricemia (X-line) and adaptation factors (Y-line)

Uricosuria significantly correlates with the absolute and relative PSD of the LF band of HRV (in this situation, it is a marker of vagal tone, but not sympatho-vagal modulation), as well as PTH level. The measure of their determination is similar (Table 3.35 and Fig. 3.19).

Table 3.35. A regression model for adaptation factors and uricosuria

N=88	R=0,591; R^2=0,349; Adjusted R^2=0,326; F(3,8)=15,0; p<10^-5					
	Beta	St. Err. of Beta	B	St. Err. of B	t(84)	p-value
Intercpt			0,530	0,529	1,00	0,31926
PTH	0,419	0,089	0,559	0,118	4,72	0,00001
LF	0,188	0,094	0,000	0,000	2,00	0,04881
LF%	0,265	0,095	0,028	0,010	2,80	0,00638

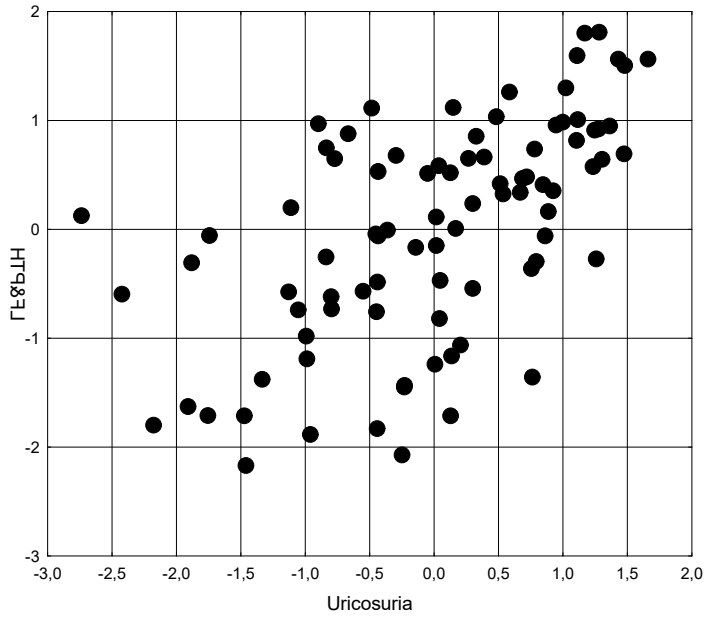

$R=0,591$; $R^2=0,349$; $\chi^2_{(3)}=36,3$; $p<10^{-5}$; Λ Prime=0,651

Fig. 3.19. Scatterplot of canonical correlation between Uricosuria (X-line) and adaptation factors (Y-line)

Canonical correlation analysis proves that the causal root receives the maximum factor load from uricosuria, which positively regulates vagal tone and PTH level, while the effect of uricemia is much weaker and oppositely directed. Taken together, uricosuria and uricemia determine neuro-endocrine adaptation factors by 44% (Table 3.36 and Fig. 3.20).

Table 3.36. Factor structure of canonical roots of parameters of uric acid exchange and neuro-endocrine adaptation factors

Variable	R
Uricosuria	-0,950
Uricemia	0,342

Variable	R
PTH	-0,574
Cap/Kp	0,308
TNN	-0,229
MxDMn	-0,299
SDNN	-0,345
TP	-0,375
VLF	-0,277
LF	-0,604
LF%	-0,596

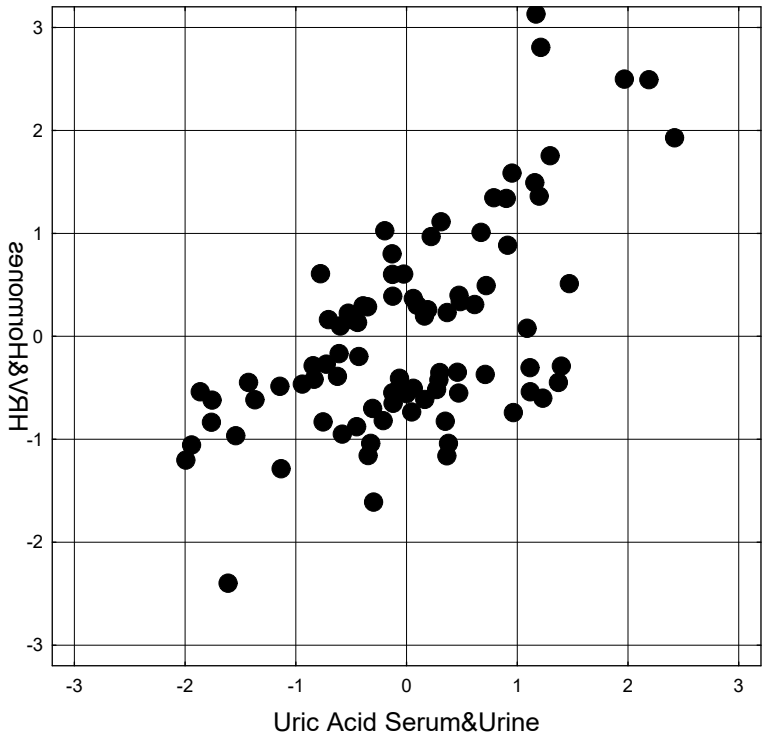

R=0,661; R^2=0,437; $\chi^2_{(20)}$=73; p<10^{-6}; Lambda Prime=0,405

Fig. 3.20. Scatterplot of canonical correlation between Uricemia&Uricosuria (X-line) and neuro-endocrine adaptation factors (Y-line)

Now we will consider the connections between caused by the course of adaptogenic therapy **changes** in the parameters of uric acid exchange, on the one hand, and neuro-endocrine factors of adaptation, on the other.

At the preparatory stage, a correlation matrix was created (Table 3.36).

Table 3.36. Matrix of correlations between changes in parameters of uric acid exchange and neuro-endocrine adaptation factors

Variable	Uricemia	Uricosuria
Kerdo e Vegetative Index	-0,19	-0,50
Ca/Kp Plasma	0,26	-0,15
Parathyroid hormone	-0,14	0,40
Triiodothyronine	-0,08	0,17
Cortisol	-0,22	-0,17
Calcitonin	-0,23	0,10
Testosterone actual	0,06	-0,20
Testosterone normalized	0,20	0,01
Baevski ARS Index	-0,16	0,32
1/ Mode HRV	-0,02	-0,34
AMo/MxDMn HRV	0,14	0,04
SDNN HRV	-0,02	0,25
RMSSD HRV	-0,02	0,26
PNN50 HRV	0,11	0,29
Total Power HRV	-0,04	0,24
VLF Power	-0,04	0,18
LF Power	-0,02	0,38
HF Power	-0,03	0,13
LF /TP	0,10	0,23

Table 3.37. Regressive model for changes in neuro-endocrine adaptation factors and uricosuria

N=44	R=0,720; R^2=0,518; Adjusted R^2=0,440 F(6,4)=6,6; p<0,0001 Beta	St. Err. of Beta	B	St. Err. of B	t(37)	p-value
Intercpt			-0,048	0,248	-0,20	0,846
Kerdo	-0,308	0,132	-0,031	0,013	-2,34	0,025
PTH	0,375	0,117	0,541	0,168	3,22	0,003
IARS	0,154	0,139	0,107	0,096	1,11	0,272
1/Mode	-0,228	0,133	-0,004	0,002	1,71	0,095
SDNN	-0,291	0,204	-0,025	0,018	-1,43	0,161
LF	0,348	0,220	0,001	0,000	1,58	0,123

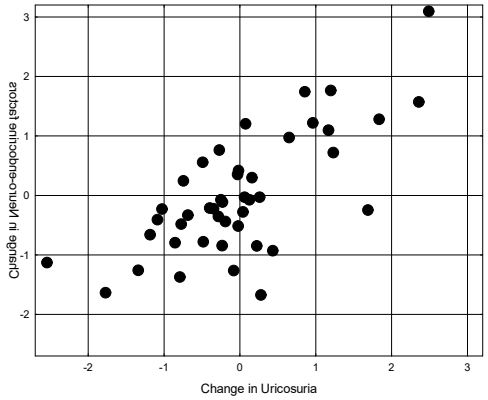

R=0,720; R^2=0,518; $\chi^2_{(6)}$=28,5; p<0,0001; Lambda Prime=0,482

Fig. 3.21. Scatterplot of canonical correlation between changes in Uricosuria (X-line) and neuro-endocrine adaptation factors (Y-line)

The regression model built on the basis of the matrix demonstrates that changes in uricosuria upregulate changes in PTH and markers of vagal tone, but downregulate changes in the index of sympatho-vagal balance and level of circulating catecholamines. The rate of determination of changes in neuro-endocrine factors of adaptation is 52% (Table 3.37 and Fig. 3.21).

Instead, the degree of determining influence of uricemia is twice as weak (26%) and is manifested in upregulation of changes in sympatho-vagal balance and level of testosterone, but downregulation of changes in levels of cortisol and calcitonin (Table 3.38 and Fig. 3.22).

Table 3.38. Regressive model for changes in neuro-endocrine adaptation factors and uricemia

N=44	R=0,509; R^2=0,259; Adjusted R^2=0,162 F(5,4)=2,7; p=,037 Beta	St. Err. of Beta	B	St. Err. of B	t(38)	p-value
Intercpt			0,0193	0,0087	2,23	0,032
Ca/Kp	0,273	0,151	0,1620	0,0896	1,81	0,078
Cortisol	-0,305	0,145	-0,0001	0,0000	-2,10	0,042
Calcitonin	-0,236	0,149	-0,0016	0,0010	-1,58	0,123
Testost Z	0,185	0,141	0,0078	0,0060	1,31	0,197
IVB	0,210	0,144	0,0001	0,0000	1,46	0,153

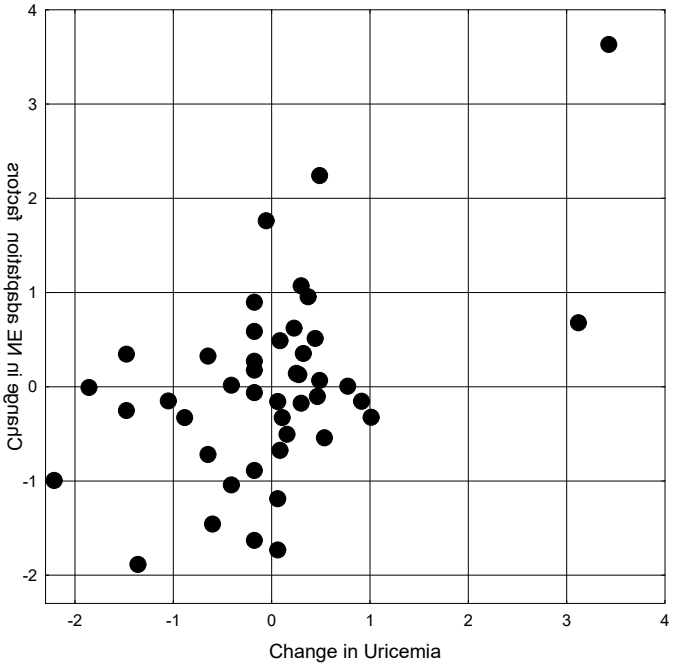

R=0,509; R^2=0,259; $\chi^2_{(5)}$=11,9; p=0,037; Lambda Prime=0,741

Fig. 3.22. Scatterplot of canonical correlation between changes in Uricemia (X-line) and neuro-endocrine adaptation factors (Y-line)

When assessing the combined effect of changes in both parameters of uric acid on changes in neuro-endocrine factors of adaptation, it was found that the uricosic canonical root receives the lion's share of the factor load from changes in uricosuria, while the contribution of uricemia is negligible and in the opposite direction. The neuro-endocrine canonical root reflects changes in PTH, triiodothironine and vagal tone, subject to upregulation, and changes in Kerdö's index, sympathetic tone, catecholamines, cortisol and raw testosterone, subject to downregulation by uricosuria, as well as upregulation of Ca/K-index and downregulation of raw calcitonin and cortisol by uricemia. The expressed dominance of the influence of uricosuria in the end gives an increase in the combined influence of both parameters of uric acid by only 3% (Table 3.39 and Fig. 3.23).

Table 3.39. Factor structure of canonical roots of changes in uric acid exchange parameters and neuro-endocrine adaptation factors

Root Variable	Root 1
Uricemia	-0,161
Uricosuria	0,989

Root Variable	Root 1
Kerdo	-0,633
Ca/Kp	-0,248
PTH	0,566
T3	0,246
Cortisol	-0,183
Calcitonin	0,175
Testoster	-0,277
BARS	0,460
1/Mode	-0,463
SDNN	0,234
RMSSD	0,278
PNN50	0,368
LF	0,516

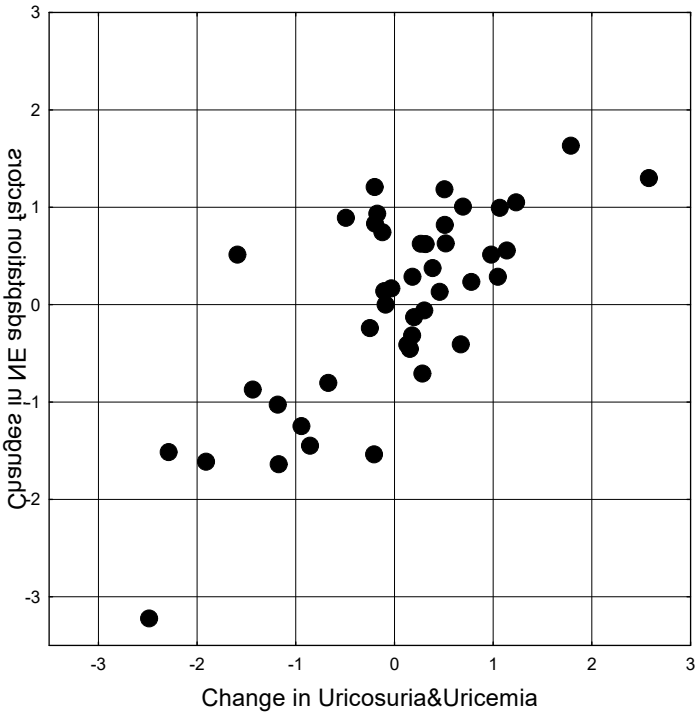

R=0,739; R^2=0,547; $\chi^2_{(26)}$=43; p=0,020; Lambda Prime=0,249

Fig. 3.23. Scatterplot of canonical correlation between changes in Uricemia&Uricosuria (X-line) and neuro-endocrine adaptation factors (Y-line)

3.6. ELECTROENCEPHALOGRAM ACCOMPANIMENT OF VARIANTS OF URIC ACID EXCHANGE

The electroencephalogram reflects the activity of cortical and subcortical structures that have bilateral connections with vagal and sympathetic nuclei of brainstem and medulla. Therefore, the study of the relationships between parameters of EEG and uric acid exchange is very appropriate.

Following the pre-accepted algorithm, the recorded UA&EEG parameters were subjected to discriminant analysis. The forward stepwise program identified 12 parameters as characteristic of uric acid exchange clusters. In addition to uric acid parameters by default, 4 **delta-rhythm**, 2 **theta-rhythm**, 1 **alpha-rhythm** and 3 **entropy** parameters are included in the discriminant model (Tables 3.40 and 3,41).

Another 42 EEG parameters (19 **delta-rhythm**, 8 **theta-rhythm**, 3 **alpha-rhythm** and **entropy** as well as 9 **beta-rhythm**) were found to be out of the model, despite the clear recognition ability (Tables 3.42-3.45).

Table 3.40. Summary of Stepwise Analysis for Uric acid and EEG Variables, ranked by criterion Λ

Variables currently in the model	F to enter	p-level	**Λ**	F-value	p-level
Uricosuria	154	10^{-6}	0,154	154	10^{-6}
Uricemia normalized	13,46	10^{-6}	0,104	58,3	10^{-6}
PSD T4-δ, μV²/Hz	3,96	0,011	0,090	37,4	10^{-6}
PSD O2-θ, %	3,51	0,019	0,080	28,6	10^{-6}
Laterality δ, %	3,40	0,022	0,071	23,7	10^{-6}
PSD C4 Entropy	1,94	0,129	0,066	20,1	10^{-6}
PSD C3-δ, %	2,58	0,060	0,060	17,8	10^{-6}
PSD F4 Entropy	2,02	0,118	0,056	15,9	10^{-6}
PSD T6-α, %	1,72	0,171	0,052	14,4	10^{-6}
PSD F7-θ, μV²/Hz	1,89	0,139	0,049	13,3	10^{-6}
PSD T4 Entropy	1,45	0,235	0,046	12,2	10^{-6}
PSD C3-δ, μV²/Hz	1,30	0,281	0,044	11,4	10^{-6}

Table 3.41. Discriminant Function Analysis Summary for Uric acid and EEG Variables, their actual levels for Clusters as well as Reference levels and Coefficients of Variability
Step 12, N of vars in model: 12; Grouping: 4 grps; Wilks' Λ: 0,0435; appr. $F_{(36)}$=11,4; $p<10^{-6}$

Variables currently in the model	Clusters of Uric Acid Exchange (Males/Females)				Parameters of Wilks' Statistics					
	S-E2+ IV (18/4)	S± E+ I (16/5)	S2-E+ II (14/1)	S± E- III (20/10)	Wilks' Λ	Partial Λ	F-remove	p-level	Tolerancy	Reference Cv/σ (112)
Uricosuria, mM/24 h	5,94	3,94	3,88	2,27	0,274	0,159	129	10^{-6}	0,893	3,00 0,250
Uricemia normalized, Z	-0,70	+0,09	-1,89	-0,53	0,070	0,619	15,0	10^{-6}	0,835	0
Laterality δ, %	-9,6	-24,9	-27,5	+6,8	0,048	0,913	2,31	0,083	0,779	+2,5 **39,8**
PSD T4-δ, μV²/Hz	57	354	94	161	0,050	0,864	3,84	0,013	0,181	92 1,091
PSD C3-δ, %	25,7	42,1	32,4	30,5	0,046	0,939	1,59	0,199	0,282	28,0 0,602
PSD C3-δ, μV²/Hz	91	315	259	166	0,046	0,949	1,30	0,281	0,234	108 0,774
PSD O2-θ, %	6,3	5,1	5,3	9,1	0,054	0,803	5,96	0,001	0,642	7,1 0,554
PSD F7-θ, μV²/Hz	15,8	42,7	29,1	28,3	0,047	0,922	2,07	0,112	0,254	18,2 0,843
PSD T6-α, %	37,8	27,3	24,4	28,0	0,047	0,921	2,10	0,106	0,591	35,5 0,502
PSD C4 Entropy	0,83	0,87	0,80	0,85	0,049	0,881	3,30	0,025	0,317	0,867 0,109
PSD F4 Entropy	0,81	0,71	0,80	0,81	0,046	0,938	1,60	0,197	0,374	0,851 0,139
PSD T4 Entropy	0,84	0,76	0,82	0,82	0,047	0,930	1,84	0,147	0,342	0,844 0,137
Variable currently not in model					Wilks' Λ	Partial Λ	F to en-ter	p-level	Tolerancy	Reference (112)
Uricemia, mM/L	0,316	0,371	0,249	0,322	0,043	0,979	0,52	0,668	0,213	0,365 0,116

Table 3.42. Parameters of EEG delta-rhythm not included in the model

Variables	Clusters of Uric Acid Exchange (Males/Females)				Parameters of Wilks' Statistics					
	S-E2+ IV (18/4)	S± E+ I (16/5)	S2-E+ II (14/1)	S± E- III (20/10)	Wilks Λ	Partial Λ	F to enter	p-level	Tolerancy	Reference Cv (112)
Amplitude δ, μV	13,2	29,5	18,9	20,4	0,043	0,994	0,15	0,927	0,482	14,9 0,431
PSD Fp1-δ, %	19,8	40,5	24,4	29,3	0,043	0,994	0,15	0,932	0,486	23,6 0,687
PSD Fp1-δ, μV²/Hz	39	560	63	102	0,043	0,986	0,35	0,790	0,734	58 1,132
PSD Fp2-δ, %	20,5	40,0	26,5	32,7	0,043	0,991	0,23	0,878	0,531	26,5 0,687
PSD Fp2-δ, μV²/Hz	39	636	71	119	0,043	0,983	0,42	0,737	0,717	74 1,260
PSD F4-δ, μV²/Hz	111	424	204	215	0,043	0,981	0,46	0,711	0,270	115 1,014

PSD F7-δ, %	22,5	53,2	32,3	35,1	0,043	0,982	0,44	0,724	0,625	31,4 0,706
PSD F7-δ, μV²/Hz	47	1309	128	151	0,043	0,989	0,26	0,857	0,722	80 1,759
PSD F8-δ, %	27,6	53,3	40,8	40,7	0,043	0,981	0,46	0,710	0,640	35,2 0,656
PSD F8-δ, μV²/Hz	59	579	129	194	0,043	0,998	0,05	0,983	0,584	92 1,642
PSD T3-δ, %	26,6	45,3	38,0	31,7	0,043	0,993	0,16	0,920	0,527	28,6
PSD T3-δ, μV²/Hz	73	368	215	146	0,043	0,992	0,19	0,905	0,413	86 1,055
PSD T4-δ, %	24,7	45,9	29,0	36,7	0,043	0,998	0,04	0,988	0,223	31,0 0,615
PSD C4-δ, μV²/Hz	94	250	193	197	0,043	0,990	0,25	0,864	0,124	114 0,813
PSD T5-δ, %	25,7	45,0	33,0	32,2	0,043	0,983	0,42	0,736	0,729	26,3 0,696
PSD T6-δ, %	21,3	38,3	35,1	33,9	0,043	0,989	0,26	0,857	0,470	26,1 0,626
PSD T6-δ, μV²/Hz	45	420	124	159	0,043	0,996	0,09	0,963	0,607	74 1,110
PSD P4-δ, μV²/Hz	81	203	193	180	0,043	0,982	0,44	0,726	0,564	107 0,886
PSD O2-δ, μV²/Hz	78	548	188	318	0,043	0,978	0,54	0,654	0,672	95 0,965

Table 3.43. Parameters of EEG theta-rhythm not included in the model

Variables	**Clusters of Uric Acid Exchange (Males/Females)**				**Parameters of Wilks' Statistics**					
	S-E2+ IV (18/4)	**S±E+ I (16/5)**	**S2-E+ II (14/1)**	**S±E- III (20/10)**	Wilks Λ	Par-tial Λ	F to enter	p-level	Tole-ran-cy	Refe-rence Cv/**σ** (112)
Amplitude θ, μV	7,4	10,0	8,9	9,1	0,042	0,972	0,69	0,564	0,341	7,75 0,376
Laterality θ, %	-13,1	-20,7	-43,4	-6,8	0,043	0,982	0,43	0,729	0,577	-4,9 **38,9**
PSD Fp1-θ, %	10,3	7,8	9,4	11,5	0,043	0,996	0,11	0,957	0,658	10,4 0,588
PSD F7-θ, %	9,5	7,4	10,2	9,2	0,043	0,990	0,24	0,871	0,528	10,0 0,458
PSD T3-θ, μV²/Hz	25	58	57	42	0,043	0,982	0,44	0,721	0,339	30 1,077
PSD T4-θ, μV²/Hz	21	44	28	40	0,043	0,991	0,22	0,885	0,294	28 1,114
PSD T6-θ, %	9,6	7,6	6,6	9,9	0,043	0,998	0,05	0,985	0,202	8,6 0,474
PSD T5-θ, %	11,4	8,9	7,7	9,9	0,043	0,998	0,06	0,981	0,201	9,7 0,471

Table 3.44. Parameters of EEG alpha-rhythm and entropy not included in the model

Variables	Clusters of Uric Acid Exchange (Males/Females)				Parameters of Wilks' Statistics					
	S-E2+IV (18/4)	S±E+I (16/5)	S2-E+II (14/1)	S±E-III (20/10)	Wilks Λ	Partial Λ	F to enter	p-level	Tolerancy	Reference Cv/σ (112)
Laterality α, %	-1,2	-14,6	-29,1	-9,6	0,043	0,997	0,07	0,977	0,580	-1,1 **34,2**
PSD F7-α, %	32,0	18,8	26,0	22,5	0,043	0,989	0,27	0,850	0,423	27,6 0,522
PSD C4-α, %	37,9	31,7	30,3	31,3	0,043	0,991	0,21	0,890	0,256	34,8 0,432
PSD Fp1 Entropy	0,83	0,74	0,80	0,82	0,043	0,979	0,52	0,669	0,567	0,848 0,116
PSD F7 Entropy	0,83	0,69	0,80	0,76	0,043	0,991	0,22	0,883	0,583	0,821 0,187
PSD F8 Entropy	0,80	0,66	0,70	0,77	0,042	0,961	0,98	0,407	0,584	0,815 0,202
PSD O2 Entropy	0,75	0,68	0,72	0,81	0,043	0,996	0,10	0,961	0,430	0,776 0,178

Table 3.45. Parameters of EEG beta rhythms not included in the model

Variables	Clusters of Uric Acid Exchange (Males/Females)				Parameters of Wilks' Statistics					
	S-E2+IV (18/4)	S±E+I (16/5)	S2-E+II (14/1)	S±E-III (20/10)	Wilks Λ	Partial Λ	F to enter	p-level	Tolerancy	Reference Cv (112)
Asymmetry β, %	22,1	17,7	17,9	25,6	0,042	0,968	0,79	0,504	0,677	23,4 0,679
PSD Fp2-β, %	33,6	22,2	34,4	27,6	0,043	0,987	0,31	0,815	0,682	30,7 0,504
PSD F3-β, %	22,8	17,4	26,4	23,8	0,043	0,979	0,53	0,665	0,601	26,7 0,463
PSD F7-β, %	36,1	20,6	31,5	33,1	0,043	0,981	0,46	0,712	0,710	31,0 0,558
PSD T3-β, %	31,6	18,9	24,1	32,2	0,043	0,999	0,02	0,995	0,670	30,7 0,462
PSD T4-β, %	31,4	21,4	36,8	28,3	0,043	0,990	0,25	0,860	0,567	30,4 0,483
PSD C3-β, %	25,6	17,6	24,8	25,4	0,043	1,000	0,01	0,999	0,432	25,5 0,420
PSD C4-β, %	25,1	21,4	28,1	22,9	0,043	0,985	0,37	0,775	0,407	25,9 0,405
PSD O1-β, %	27,8	17,0	24,5	25,3	0,043	0,983	0,42	0,737	0,734	26,3 0,542

Next, the 12-dimensional space of discriminant variables transforms into 3-dimensional space of a canonical roots. For Root 1 r*=0,929 (Wilks' Λ=0,044; $\chi^2_{(36)}$=248; $p<10^{-6}$), for Root 2 r*=0,706 (Wilks' Λ=0,317; $\chi^2_{(22)}$=91; $p<10^{-6}$), for Root 3 r*=0,607 (Wilks' Λ=0,631; $\chi^2_{(10)}$=36; $p<10^{-4}$). The major root contains 79,9% of discriminative opportunities, the second 12,6%, the minor 7,5%.

The calculation of the discriminant root values for each person as the sum of the products of raw coefficients to the individual values of discriminant variables together with the constant (Table 3.46) enables the visualization of each patient in the information space of the roots.

Table 3.46. Standardized and Raw Coefficients and Constants for Uric acid and EEG Variables

Coefficients	Standardized	Raw

Variables	Root 1	Root 2	Root 3	Root 1	Root 2	Root 3
Uricosuria	-1,044	-0,022	0,082	-1,733	-0,037	0,136
Uricemia normalized	-0,198	0,878	0,326	-0,211	0,937	0,348
PSD T4-δ, μV²/Hz	-0,215	1,099	0,552	-0,001	0,005	0,002
PSD O2-θ, %	0,088	-0,104	0,894	0,023	-0,027	0,237
Laterality δ, %	0,082	-0,126	0,514	0,002	-0,004	0,015
PSD C4 Entropy	-0,184	0,465	-0,806	-1,523	3,847	-6,660
PSD C3-δ, %	-0,267	0,386	-0,472	-0,014	0,021	-0,025
PSD F4 Entropy	-0,057	-0,488	0,344	-0,366	-3,126	2,204
PSD T6-α, %	-0,221	0,387	0,220	-0,015	0,026	0,015
PSD F7-θ, μV²/Hz	0,247	-0,290	-0,761	0,007	-0,008	-0,022
PSD T4 Entropy	-0,214	0,434	0,443	-1,768	3,584	3,657
PSD C3-δ, μV²/Hz	0,046	-0,606	-0,296	0,0002	-0,002	-0,001
		Constants		10,20	-4,279	-0,091
		Eigenvalues		6,283	0,992	0,584
	Cumulative proportions			0,799	0,926	1

At the next stage of the analysis, the actual values of the parameters were normalized and grouped into three discriminant roots based on structural coefficients that reflect the strength and nature of the connection between the variable and the root. In addition, the table includes parameters that did not enter the discriminant model due to duplication/redundancy of information (Table 3.47).

Table 3.47. Correlations Variables-Canonical Roots, Means of Roots and Z-scores of Uric acid and EEG Variables

Variables	Correlations Variables-Roots			S-E2+ IV (22)	S±E+ I (21)	S2-E+ II (15)	S±E- III (30)
Root 1 (79,9%)	**R 1**	**R 2**	**R 3**	**-3,61**	-0,44	+0,31	**+2,80**
Uricosuria	**-0,932**	-0,192	-0,004	**+3,87**	+1,26	+1,17	**-0,97**
Root 2 (12,6%)	**R 1**	**R 2**	**R 3**	-0,21	**+1,36**	-1,70	+0,05
Uricemia normalized	0,002	**0,678**	0,161	-0,70	**+0,09**	-1,89	-0,53
PSD C4 Entropy	0,025	**0,149**	0,017	-0,44	**+0,07**	-0,67	-0,14
PSD T4-δ, μV²/Hz	0,039	**0,298**	-0,243	-0,35	**+2,60**	+0,02	+0,69
PSD F7-δ, μV²/Hz	currently not in model			-0,23	**+8,79**	+0,35	+0,51
PSD Fp1-δ, μV²/Hz	currently not in model			-0,29	**+7,69**	+0,08	+0,68
PSD Fp2-δ, μV²/Hz	currently not in model			-0,38	**+6,04**	-0,03	+0,48
PSD F8-δ, μV²/Hz	currently not in model			-0,22	**+3,22**	+0,25	+0,68
PSD C3-δ, %	0,020	**0,139**	-0,245	-0,14	**+0,83**	+0,26	+0,26
PSD F7-θ, μV²/Hz	0,037	**0,112**	-0,194	-0,16	**+1,59**	+0,71	+0,66
Amplitude θ, μV	currently not in model			-0,12	**+0,76**	+0,38	+0,45
PSD F8-δ, %	currently not in model			-0,33	**+0,78**	+0,24	+0,24
PSD T5-δ, %	currently not in model			-0,03	**+1,02**	+0,36	+0,32
Amplitude δ, μVz	currently not in model			-0,26	**+2,29**	+0,62	+0,87
PSD F4-δ, μV²/Hz	currently not in model			-0,03	**+2,66**	+0,76	+0,86
PSD T6-δ, μV²/Hz	currently not in model			-0,35	**+4,23**	+0,62	+1,05
PSD O2-δ, μV²/Hz	currently not in model			-0,19	**+4,92**	+1,00	+2,41
PSD Fp2-δ, %	currently not in model			-0,33	**+0,74**	0,00	+0,34
PSD T4-θ, μV²/Hz	currently not in model			-0,22	**+0,50**	+0,01	+0,39
PSD T4-δ, %	currently not in model			-0,33	**+0,78**	-0,11	+0,30
PSD F7-δ, %	currently not in model			-0,40	**+0,98**	+0,04	+0,17
PSD Fp1-δ, %	currently not in model			-0,23	**+1,05**	+0,05	+0,35
PSD F4 Entropy	0,006	**-0,146**	0,189	-0,31	**-1,20**	-0,44	-0,38
PSD T4 Entropy	-0,010	**-0,118**	0,163	-0,05	**-0,70**	-0,24	-0,21
PSD F7 Entropy	currently not in model			+0,07	**-0,83**	-0,12	-0,41
PSD Fp1 Entropy	currently not in model			-0,14	**-1,14**	-0,52	-0,24
PSD Fp1-θ, %	currently not in model			-0,02	**-0,43**	-0,17	+0,17
PSD F7-θ, %	currently not in model			-0,12	**-0,58**	+0,04	-0,17
PSD T4-β, %	currently not in model			+0,07	**-0,61**	+0,43	-0,14
PSD Fp2-β, %	currently not in model			+0,19	**-0,55**	+0,24	-0,20
PSD C4-β, %	currently not in model			-0,08	**-0,43**	+0,21	-0,29

PSD C3-β, %	currently not in model			+0,01	**-0,74**	-0,06	-0,01
PSD F3-β, %	currently not in model			-0,32	**-0,76**	-0,03	-0,23
PSD F7-β, %	currently not in model			+0,30	**-0,60**	+0,03	+0,13
PSD O1-β, %	currently not in model			+0,10	**-0,65**	-0,12	-0,07
PSD F7-α, %	currently not in model			+0,31	**-0,61**	-0,11	-0,35
Root 3 (7,5%)	**R 1**	**R 2**	**R 3**	+0,66	**-0,82**	**-1,00**	+0,59
Laterality δ, %	0,077	0,026	**0,406**	-0,30	**-0,69**	**-0,75**	+0,11
PSD O2-θ, %	0,112	0,007	**0,391**	-0,18	**-0,49**	**-0,45**	+0,52
PSD T6-α, %	-0,080	0,022	**0,210**	+0,13	**-0,46**	**-0,63**	-0,42
Laterality α, %	currently not in model			0,00	**-0,39**	**-0,82**	-0,25
Laterality θ, %	currently not in model			-0,21	**-0,41**	**-0,99**	-0,05
PSD T5-θ, %	currently not in model			+0,38	**-0,17**	**-0,42**	+0,04
PSD T6-θ, %	currently not in model			+0,25	**-0,24**	**-0,48**	+0,31
Asymmetry β, %	currently not in model			-0,08	**-0,36**	**-0,35**	+0,14
PSD T3-β, %	currently not in model			+0,07	**-0,83**	**-0,46**	+0,10
PSD F8 Entropy	currently not in model			-0,07	**-0,95**	**-0,69**	-0,26
PSD O2 Entropy	currently not in model			-0,17	**-0,71**	**-0,38**	+0,25
PSD C3-δ, μV^2/Hz	0,026	**0,069**	**-0,311**	-0,20	**+2,47**	**+1,80**	+0,70
PSD T3-δ, μV^2/Hz	currently not in model			-0,14	**+3,12**	**+1,43**	+0,67
PSD C4-δ, μV^2/Hz	currently not in model			-0,22	**+1,46**	**+0,86**	+0,90
PSD T6-δ, %	currently not in model			-0,30	**+0,75**	**+0,55**	+0,47
PSD P4-δ, μV^2/Hz	currently not in model			-0,27	**+1,01**	**+0,91**	+0,77
PSD T3-δ, %	currently not in model			-0,12	**+0,98**	**+0,55**	+0,18
PSD T3-θ, μV^2/Hz	currently not in model			-0,17	**+0,86**	**+0,84**	+0,37

The result of the analysis is the visualization of each patient in the information space of discriminant roots (Fig. 3.24).

Patients with **hypouricosuria** are located in the extreme right zone of the axis of the first root. Instead, patients with pronounced **hyperuricosuria** are located at the opposite pole of the axis. An intermediate position is occupied by patients of I and II clusters with moderately increased excretion of uric acid, while both the average levels and their dispersion are practically the same.

The delimitation of these clusters occurs along the axis of the second root. The top position of the members of the I cluster reflects their **normal**, but maximum for the sample levels of **uricemia** and EEG entropy in the C4 locus, as well as to one degree or another increased levels of 16 parameters of the delta-rhythm and 3 parameters of the theta-rhythm, on the one hand, instead, the maximum for sample reduced entropy levels in loci F4, T4, F7 and Fp1, as well as 7 parameters of beta-, 2 theta- and one alpha-rhythms - on the other hand. In members of the II cluster, against the background of **hypouricemia**, the levels of the listed parameters are lower/higher, respectively.

In addition, both clusters, taken together, are separated from IV and III clusters along the axis of the third root. Their common lowest position reflects the maximum for the sample left-sided asymmetry of delta-, alpha- and theta-rhythms, maximally reduced entropy in loci F8 and O2, as well as levels of 3 parameters of theta-, 2 beta- and one alpha-rhythms, on the one hand, instead, the maximally increased levels of 6 parameters of delta-rhythm and one parameter of theta-rhythm - on the other hand.

The apparent clear demarcation of all four clusters in the information space of the three roots is documented by the calculation of Mahalanobis distances (Table 3.48).

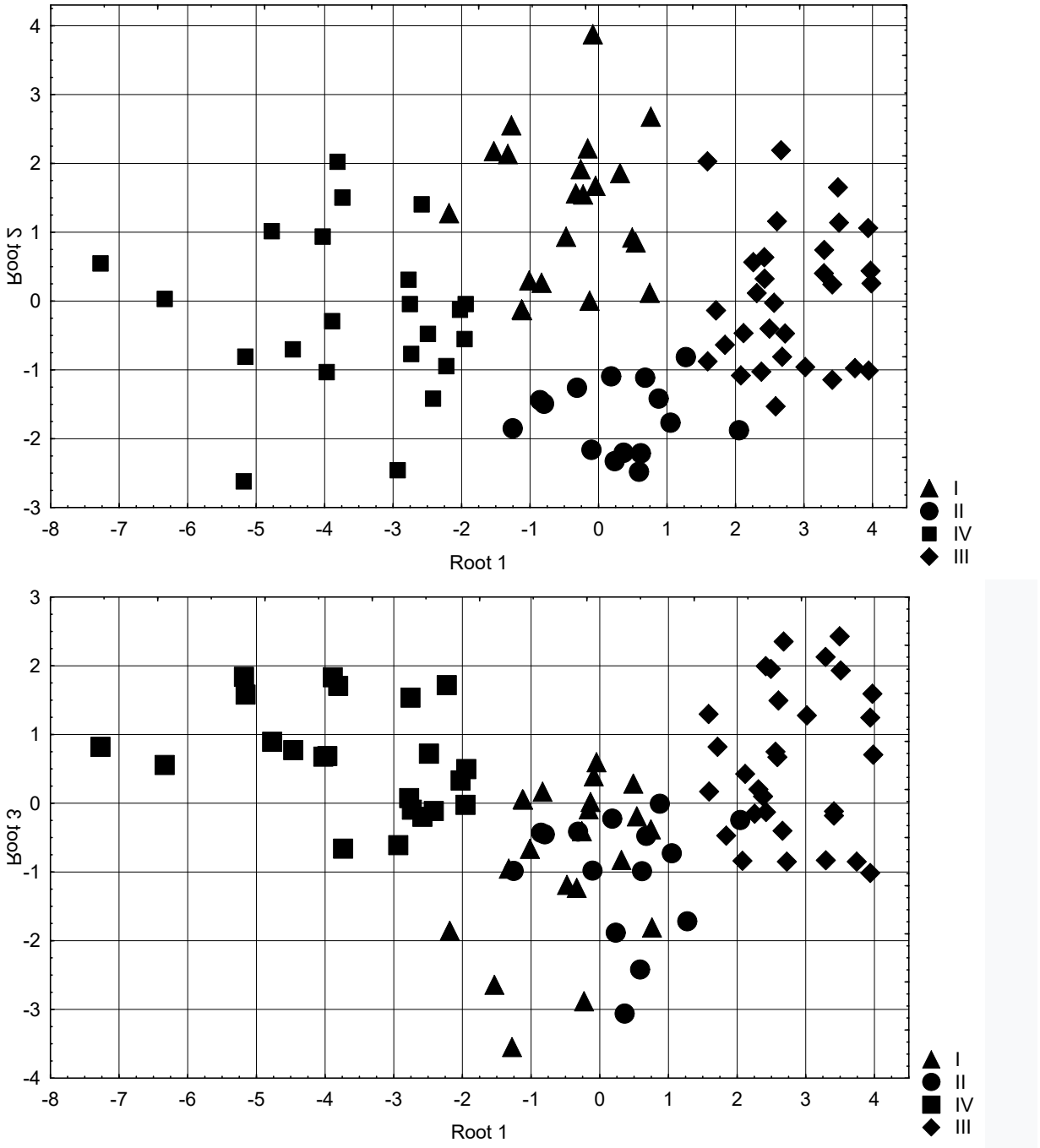

Fig. 3.24. Scattering of individual values of the discriminant UA&EEG roots of patients of different uric acid clusters

Table 3.48. Squared Mahalanobis Distances between Clusters, F-values (df=12,7) and p levels

Clusters	S±E+ I	S2-E+ II	S-E2+ IV	S±E- III
S±E+ I (21)	0	9,97	14,7	14,2
S2-E+ II (15)	6,3 10^{-5}	0	20,3	11,8
S-E2+ IV (22)	11,4 10^{-6}	13,1 10^{-6}	0	41,2
S±E- III (30)	12,7 10^{-6}	8,6 10^{-6}	24,1 10^{-6}	0

Another result of discriminant analysis is the possibility of retrospective identification of members of different clusters by calculating individual discriminant functions according to the coefficients and constants given in the Table 3.49.

Table 3.49. Coefficients and Constants for Classification Functions for Uric acid Clusters

Clusters	S±E+ I	S2-E+ II	S-E2+ IV	S±E- III
Variables	p=,239	p=,170	p=,250	p=,341
Uricosuria	17,83	16,62	23,58	12,45
Uricemia normalized	4,851	1,759	4,562	3,422
PSD T4-δ, μV²/Hz	0,058	0,043	0,057	0,052
PSD O2-θ, %	0,073	0,130	0,392	0,517
Laterality δ, %	-0,165	-0,155	-0,145	-0,132
PSD C4 Entropy	96,79	85,11	85,74	77,43
PSD C3-δ, %	0,478	0,409	0,454	0,370
PSD F4 Entropy	-15,04	-6,147	-5,710	-9,013
PSD T6-α, %	0,549	0,457	0,576	0,488
PSD F7-θ, μV²/Hz	-0,286	-0,251	-0,328	-0,283
PSD T4 Entropy	101,7	88,71	107,1	96,38
PSD C3-δ, μV²/Hz	-0,011	-0,003	-0,009	-0,008
Constants	-133,3	-113,5	-164,4	-97,11

Taking into account all features enables the retrospective recognition of members of all clusters with one error: the classification accuracy is 98,9% (Table 3.50).

Table 3.50. Classification matrix for clusters

Rows: observed classifications; columns: predicted classifications

Clusters	Percent correct	S±E+ I	S2-E+ II	S-E2+ IV	S±E- III
		p=,239	p=,170	p=,250	p=,341
S±E+ I	100	**20**	0	0	0
S2-E+ II	93,3	0	**14**	0	**1**
S-E2+ IV	100	0	0	**22**	0
S±E- III	100	0	0	0	**30**
Total	98,9	20	16	22	30

3.7. RELATIONSHIPS BETWEEN PARAMETERS OF URIC ACID EXCHANGE AND ELECTROENCEPHALOGRAM

Two approaches were used to clarify the relationships between uric acid and EEG parameters. In the first approach, the object of analysis was the average values of clusters grouped into patterns. The linear nature of the relationship was revealed only in relation to the entropy of the PSD in the C4 locus (Fig. 3.25). Constellations of other EEG parameters are related to uric acid in a non-linear manner. In 4 constellations, which contain 31 EEG parameters, the coefficients of their determination by uricemia significantly outweigh those by uricosuria: 0,987÷0,758 vs 0,543÷0,332 (Figs. 3.26-3.31 and 3.34-3.35). In 2 constellations, which contain 18 EEG parameters, the coefficients of their determination by uricemia and uricosuria are equally high (Figs. 3.32-3.33 and 3.36-3.37). It is interesting that in all cases the curves of uricemia and uricosuria are quasi-mirror, and there is no correlation between them (Fig. 3.38).

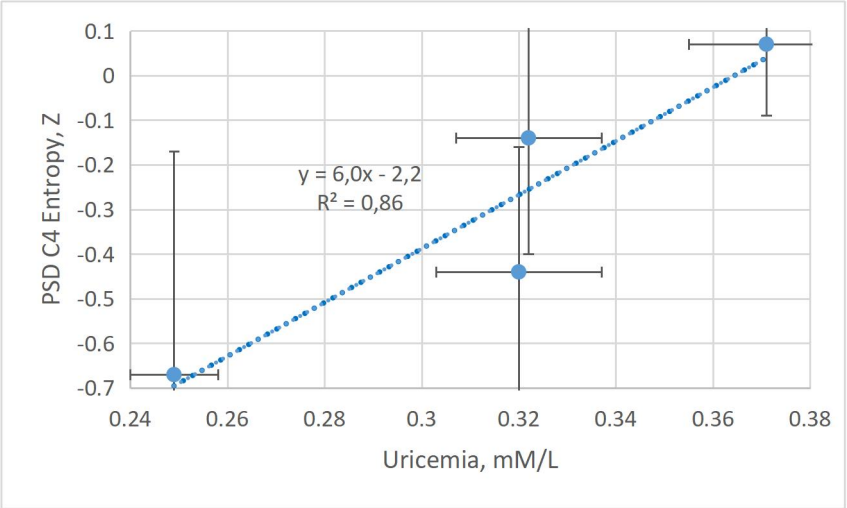

Fig. 3.25. Linear relationship between uricemia and entropy of PSD at the C4 locus

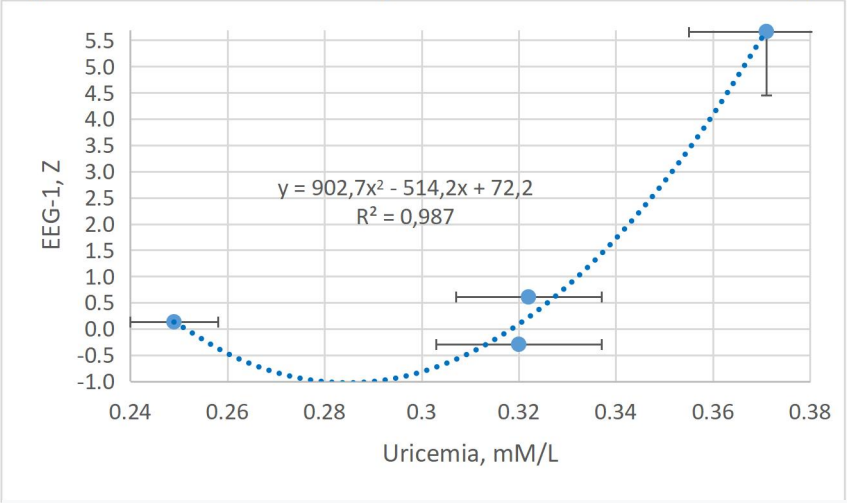

Fig. 3.26. Nonlinear relationship between uricemia and PSD delta-rhythm in loci Fp1, Fp2, F7, F8 and T4

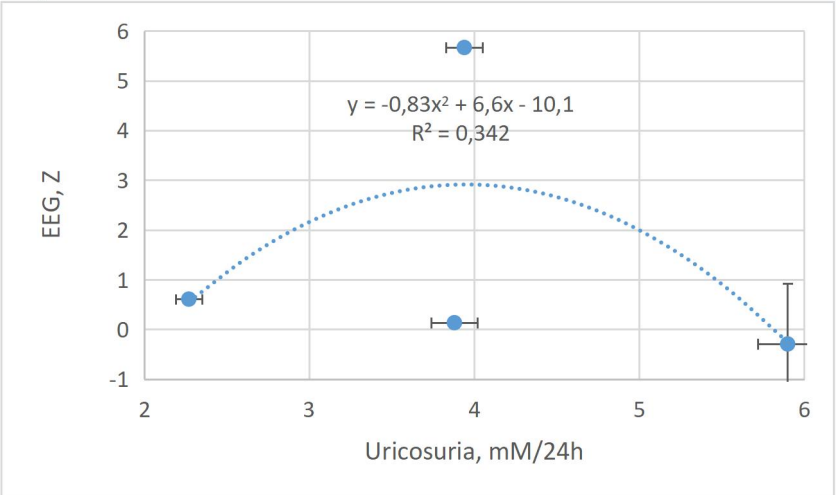

Fig. 3.27. Non-linear relationship between uricosuria and PSD delta rhythm in loci Fp1, Fp2, F7, F8 and T4

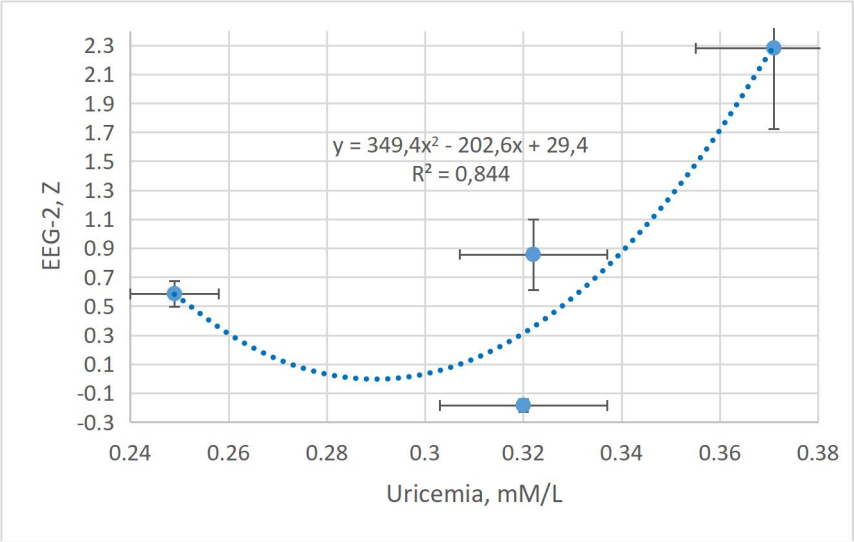

Fig. 3.28. Non-linear relationship between uricemia and PSD delta-rhythm in loci F4, F8%, T5%, T6, O2 and its amplitude; PSD of the theta-rhythm at the F7 locus and its amplitude

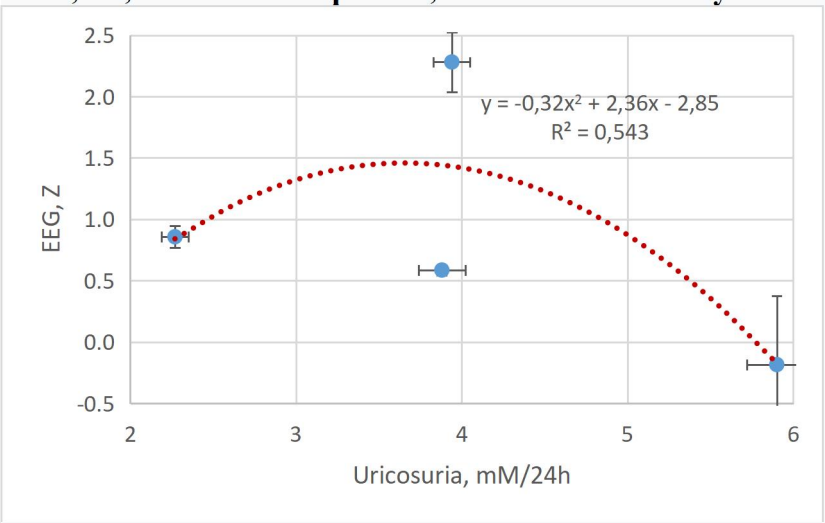

Fig. 3.29. Non-linear relationship between uricosuria and delta-rhythm PSD in loci F4, F8%, T5%, T6, O2 and its amplitude; PSD of the theta-rhythm in the F7 locus and its amplitude

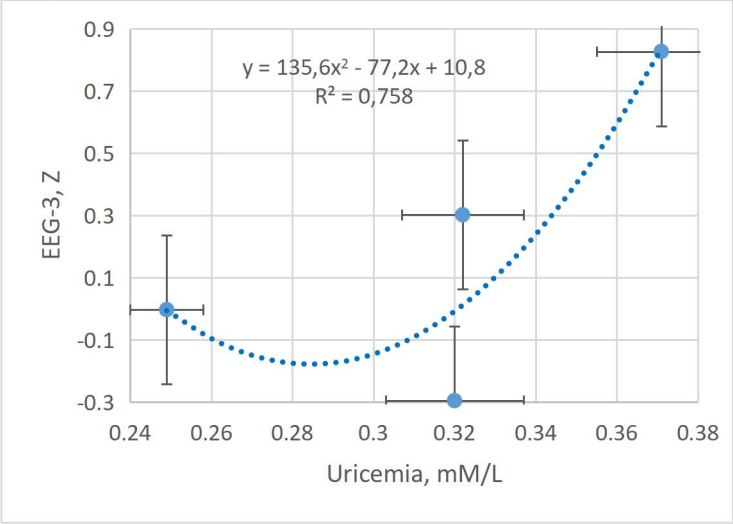

Fig. 3.30. Nonlinear relationship between uricemia and PSD of the delta-rhythm in the Fp1%, F7%, T4% loci and theta-rhythm in the T4 locus

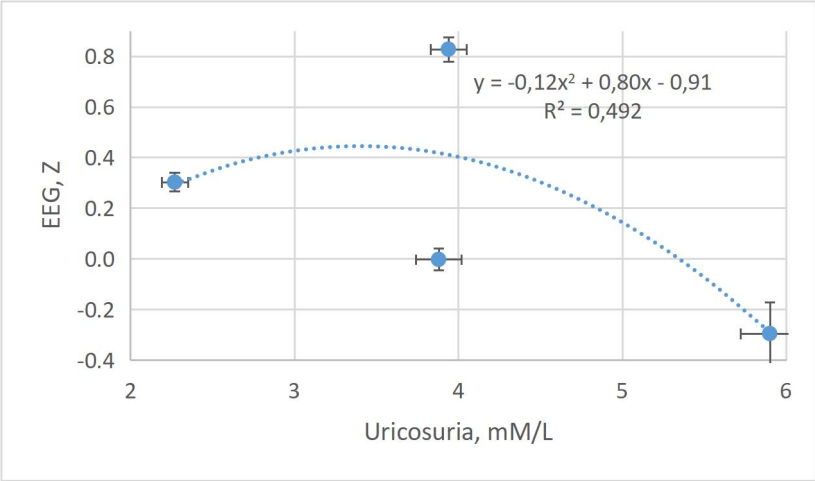

Fig. 3.31. Nonlinear relationship between uricosuria and PSD of the delta-rhythm in the Fp1%, F7%, T4% loci and theta-rhythm in the T4 locus

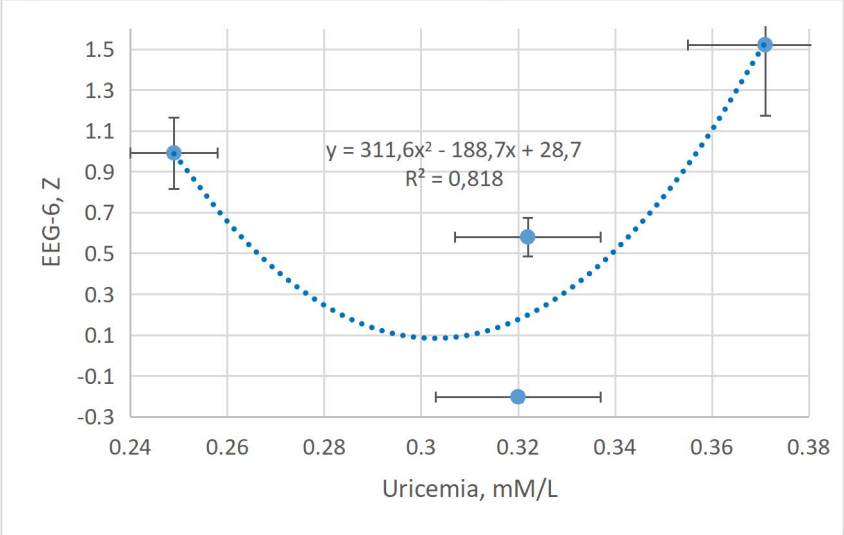

Fig. 3.32. Nonlinear relationship between uricemia and PSD of the delta-rhythm in the T3%, T3, C3, C4, T6%, P4 loci and theta-rhythm in the T3 locus

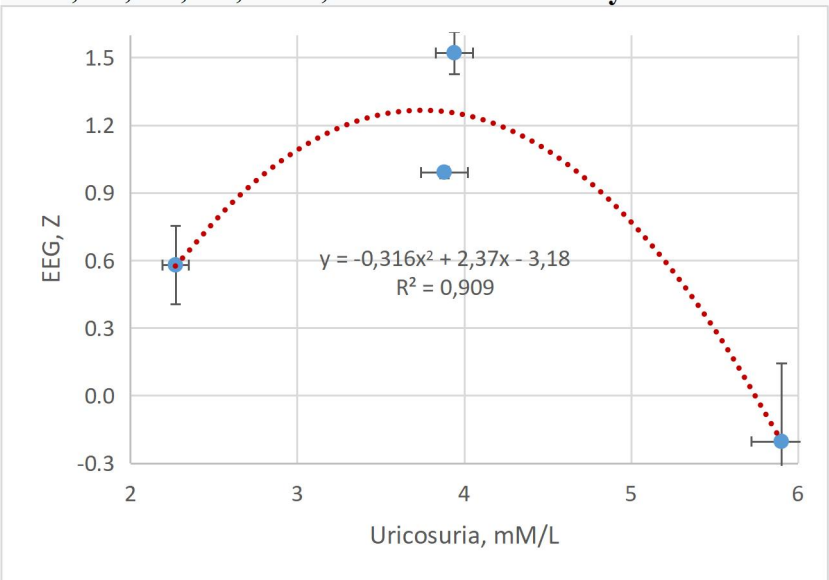

Fig. 3.33. Nonlinear relationship between uricosuria and PSD of the delta-rhythm in the T3%, T3, C3, C4, T6%, P4 loci and theta-rhythm in the T3 locus

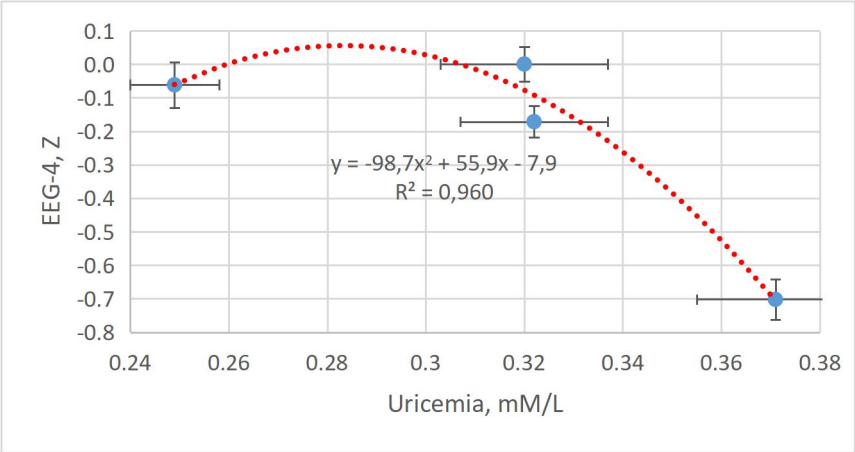

Fig. 3.34. Nonlinear relationship between uricemia and PSD beta-rhythm in loci Fp2%, F3%, F7%, T4%, C3%, C4%, O1%; theta-rhythm in the Fp1% and F7% loci; alpha-rhythm in the F7% locus and PSD entropy in the Fp1, F4, F7 and T4 loci

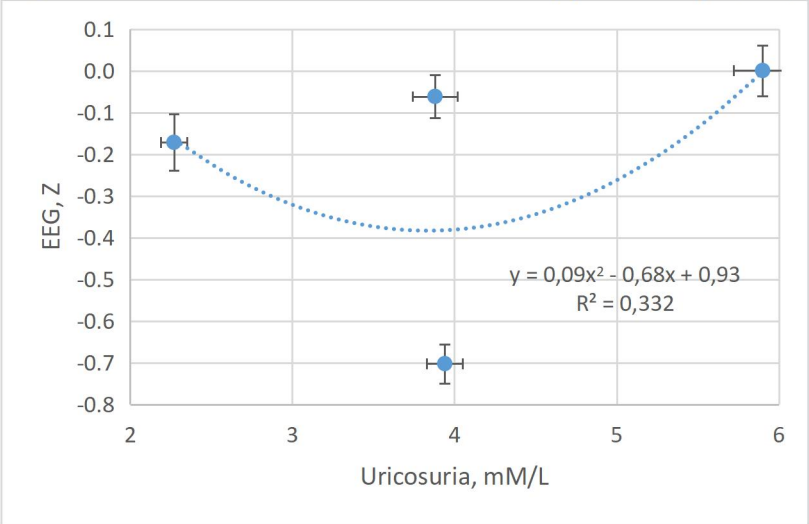

Fig. 3.35. Non-linear relationship between uricosuria and beta-rhythm PSD in loci Fp2%, F3%, F7%, T4%, C3%, C4%, O1%; theta-rhythm in the Fp1% and F7% loci; of the alpha-rhythm in the F7% locus and the entropy of the PSD in the Fp1, F4, F7 and T4 loci

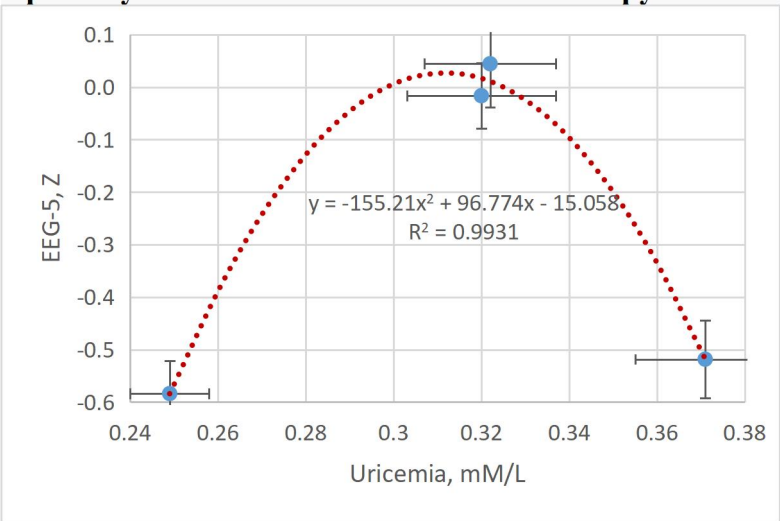

Fig. 3.36. Non-linear relationship between uricemia and PSD theta-rhythm in loci T5, T6, O2% and its lateralization; alpha-rhythm in the T6% locus and its lateralization; beta-rhythm in the T3% locus and its asymmetry; lateralization of the delta-rhythm, as well as PSD entropy in the F8 and O2 loci

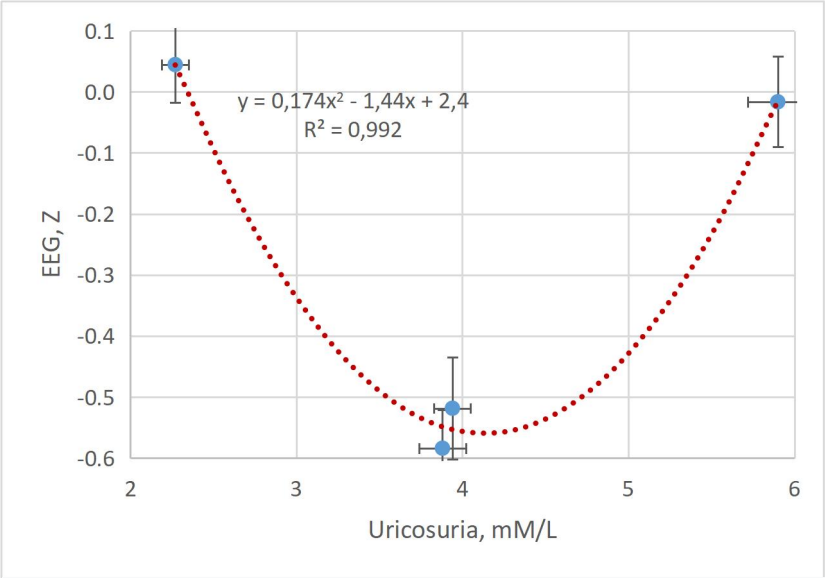

Fig. 3.37. Non-linear relationship between uricosuria and PSD theta-rhythm in loci T5, T6, O2% and its lateralization; alpha-rhythm in the T6% locus and its lateralization; beta-rhythm in the T3% locus and its asymmetry; lateralization of the delta-rhythm, as well as PSD entropy in the F8 and O2 loci

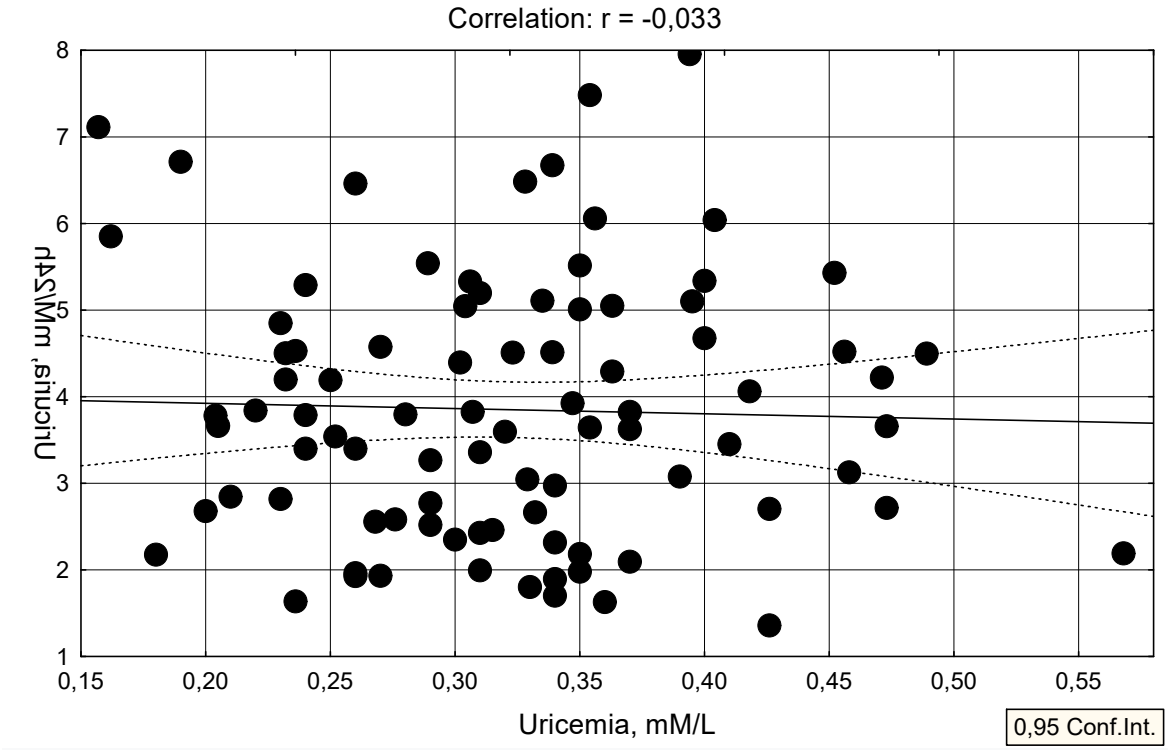

Fig. 3.38. Lack of linear relationship between uricemia and uricosuria

In the second approach, the object of analysis was individual parameters of uric acid metabolism and EEG. As a result of the screening, a correlation matrix was created (Table 3.51). Since it turned out that the relationships with EEG parameters of sex- and age-normalized levels of uricemia are weaker than those of actual uricemia or even insignificant, the canonical correlation was calculated only in relation to the latter.

Table 3.51. Correlation matrix for parameters of uric acid metabolism and EEG

Variable	Correlations N=74		
	UaS	UaSz	UaEx
UaS	1,00	0,85	-0,05
UaSz	0,85	1,00	-0,08
UaEx	-0,05	-0,08	1,00
DT	0,01	0,02	0,30
IRB	-0,27	-0,23	-0,02
LID	-0,03	-0,04	-0,23
FP2H	-0,24	-0,15	-0,04
FP2T%	-0,22	-0,09	-0,09
FP2D%	-0,02	0,10	-0,24
F3T	-0,21	-0,09	-0,14
F4B%	0,20	0,01	0,11
F7H	-0,34	-0,24	0,09
F7T%	-0,24	-0,08	0,02
F7B	0,07	0,04	-0,20
F8H	-0,27	-0,14	0,05
F8B%	0,21	0,07	0,11
F8A%	-0,06	-0,05	0,27
F8D%	-0,08	-0,02	-0,23
T3B%	0,20	0,06	-0,05
T3T%	-0,23	-0,12	-0,00
T4B%	0,23	0,05	0,09
T4A%	0,08	0,04	0,25
T4D%	-0,19	-0,05	-0,21
C3T	-0,20	-0,06	-0,05
T5H	-0,20	-0,15	0,01
T5T%	-0,23	-0,05	0,06
T5D	0,22	0,22	0,03
T6H	-0,35	-0,24	-0,02
T6A%	-0,04	-0,03	0,21
T6T%	-0,23	-0,03	-0,10
T6D%	-0,05	0,02	-0,23
T6B	0,29	0,29	-0,10
P3H	-0,21	-0,18	-0,11
P3B%	-0,01	-0,20	0,03
P3A%	0,30	0,24	0,04
P3T%	-0,31	-0,18	-0,07
P3D%	-0,23	-0,09	-0,04
P4A%	0,27	0,20	0,07
P4T%	-0,26	-0,10	-0,13
P4D%	-0,25	-0,10	-0,16
O2T%	-0,15	0,05	-0,29

It was found that uricemia is significantly ($|r| \geq 0,23$) or borderline negatively correlated with 18 EEG parameters and positively with 8. After stepwise exclusion, 14 parameters remained in the regression model, the constellation of which is determined by uricemia by 53% (Table 3.52 and Fig. 3.39).

Table 3.52. Regressive model for uricemia and EEG parameters

N=74	R=,729; R^2=,531; Adjusted R^2=,420; F(14)=4,8; p<,00001; Std.Error of estimate:,062					
	Beta	St. Err. of Beta	B	St. Err. of B	t(59)	p-value
Intercpt			0,1780	0,2058	0,87	0,390
IRB	-0,330	0,115	-0,0020	0,0007	-2,86	0,006
F4B%	-0,467	0,195	-0,0025	0,0011	-2,40	0,020
F7H	-0,143	0,128	-0,0585	0,0522	-1,12	0,267
F8H	-0,214	0,133	-0,0797	0,0497	-1,61	0,114
T3B%	0,196	0,132	0,0010	0,0007	1,49	0,143
T4B%	0,571	0,183	0,0028	0,0009	3,12	0,003
C3T	-0,180	0,113	-0,0002	0,0002	-1,59	0,117
T6H	-0,355	0,178	-0,1746	0,0878	-1,99	0,051
T6T%	0,417	0,152	0,0067	0,0024	2,74	0,008
T6B	0,172	0,111	0,0002	0,0001	1,55	0,126
P3H	0,381	0,168	0,2367	0,1046	2,26	0,027
P3A%	1,180	0,323	0,0048	0,0013	3,65	0,001
P3D%	0,850	0,291	0,0036	0,0012	2,92	0,005
P4D%	-0,243	0,166	-0,0011	0,0007	-1,46	0,149

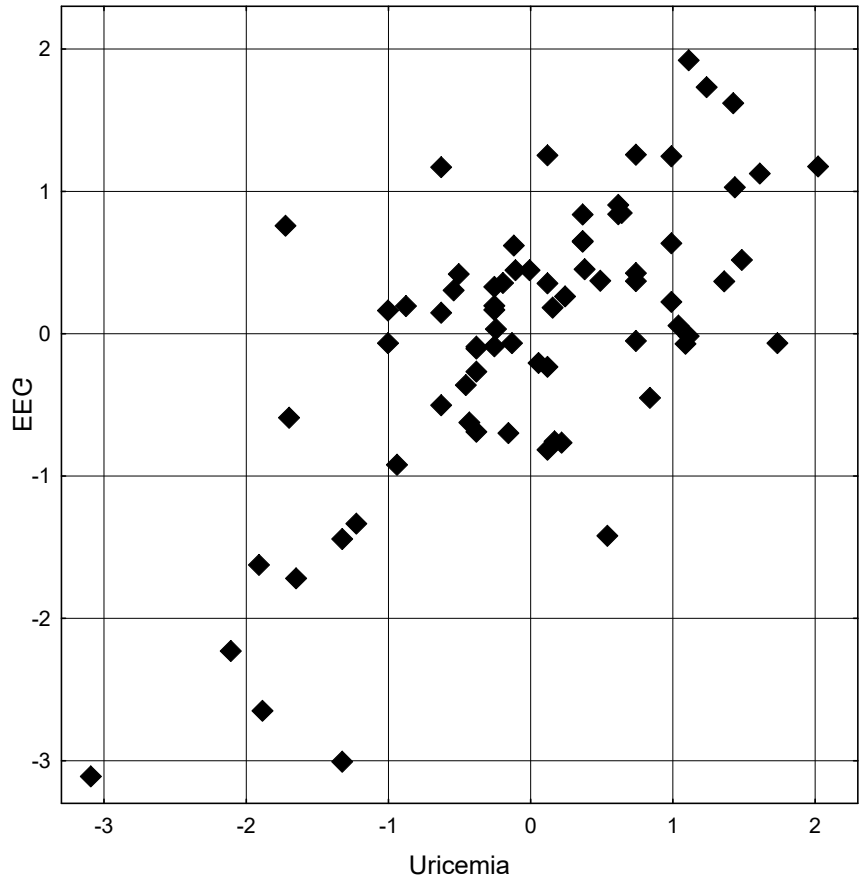

R=0,729; R^2=0,531; $\chi^2_{(14)}$=42; p=10^{-4}; Λ Prime=0,521

Fig. 3.39. Scatterplot of canonical correlation between Uricemia (X-line) and EEG parameters (Y-line)

Instead, the connections of uricosuria with EEG parameters are less numerous and generally weaker (Table 3.51). After a step-by-step exclusion of 11 parameters in the regression model, 6 remained, the constellation of which is determined by uricosuria by 31% (Table 3.53 and Fig. 3.40).

Table 3.53. Regressive model for uricosuria and EEG parameters

N=74	R=,55 3; R^2=,306 ; Adjusted R ^2=,24 4; F(6,7)=4,9 ; p<,0003 ; Std.Error of estimate:1,25					
	Beta	St. Err. of Beta	B	St. Err. of B	t(67)	p-value
Intercpt			3,2034	0,6825	4,69	0,00001
DT	0,346	0,105	1,0857	0,3290	3,30	0,00155
LID	-0,239	0,105	-0,0087	0,0038	-2,28	0,02609
F7B	-0,133	0,107	-0,0032	0,0026	-1,24	0,21753
F8A%	0,146	0,123	0,0133	0,0112	1,19	0,23963
T6D%	-0,127	0,118	-0,0085	0,0079	-1,08	0,28581
O2T%	-0,174	0,107	-0,0575	0,0354	-1,62	0,10941

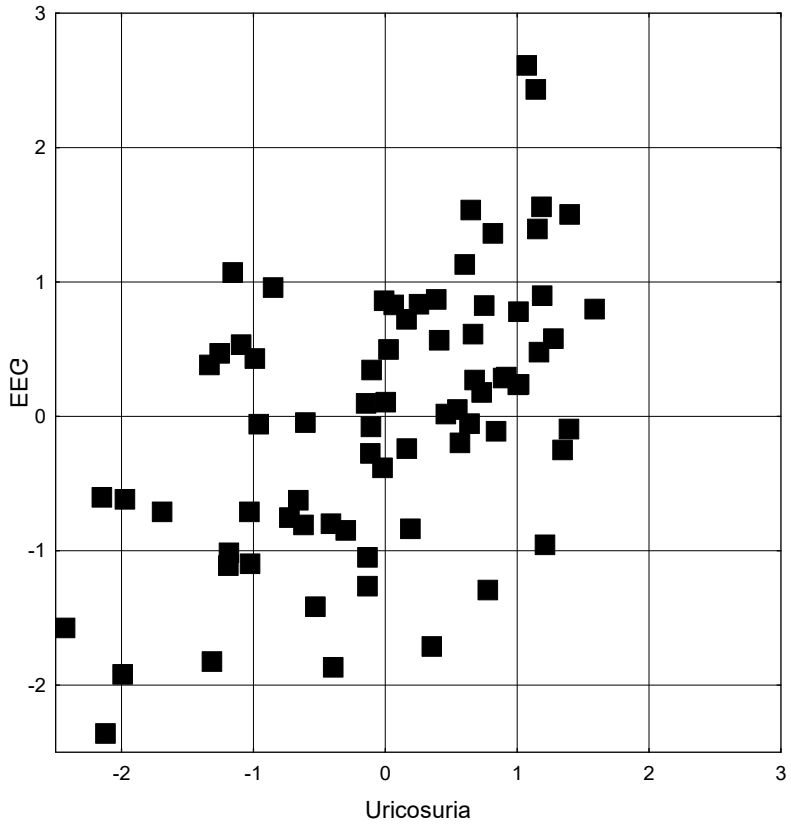

R=0,553; R^2=0,306; $\chi^2_{(6)}$=25; p=0,0003; Λ Prime=0,694

Fig. 3.40. Scatterplot of canonical correlation between Uricosuria (X-line) and EEG parameters (Y-line)

The combined effect of uricemia and uricosuria on EEG parameters does not differ from that of uricemia alone (Table 3.54 and Fig. 3.41).

Table 3.54. Factor structure of canonical roots of parameters of uric acid metabolism and EEG

Left set	R
Uricemia	-0,939
Uricosuria	0,394
Right set	R
PSD F7 Entropy	0,482
PSD F8 Entropy	0,369
PSD T5 Entropy	0,259
PSD P3 Entropy	0,208
PSD T5-θ, %	0,323

PSD C3-θ, μV^2/Hz	0,234
PSD P3-δ, %	0,280
PSD P4-δ, %	0,240
Index β, %	0,342
PSD T6-β, μV^2/Hz	-0,425
PSD T3-β, %	-0,279
PSD T4-β, %	-0,251
PSD F4-β, %	-0,199
PSD P3-α, %	-0,366
PSD F8-α, %	0,210
Deviation θ, Hz	0,133
PSD F7-β, μV^2/Hz	-0,183
PSD O2-θ, %	0,052
PSD T6-δ, %	-0,048
Laterality δ, %	-0,075

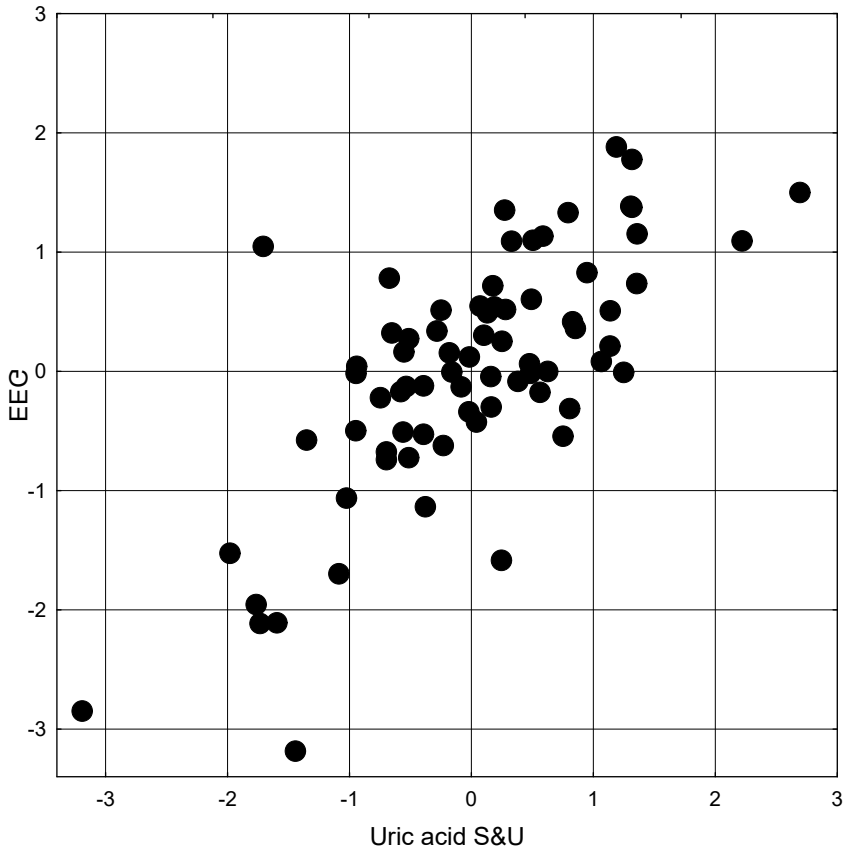

R=0,721; R^2=0,520; $\chi^2_{(40)}$=74; p=0,0008; Λ Prime=0,300

Fig. 3.41. Scatterplot of canonical correlation between Uricemia&Uricosuria (X-line) and EEG parameters (Y-line)

Next, the relationships between changes in uric acid parameters and EEG under the influence of balneotherapy were analyzed. Following the previous algorithm, a correlation matrix was first created from significant (|r|≥0,33) and marginal coefficients (Table 3.55).

Table 3.55. Matrix of correlations between changes in parameters of uric acid and EEG

Variable	Correlations N=35	
	UaS	UaEx
AF	0,05	-0,35
BF	0,02	-0,28
IRA	0,23	-0,30
AT	-0,33	0,18
AA	-0,28	-0,01
LIT	0,13	-0,37
FP2B%	-0,29	0,16
FP2B	-0,28	-0,06
F7H	-0,33	0,22
F7B%	-0,01	0,28
F7A%	-0,29	0,06
F8H	-0,31	-0,09
F8D	0,36	-0,05
T3B%	-0,43	0,05
T3T%	0,11	0,38
T3B	-0,44	0,08
T4B%	-0,53	0,20
T4B	-0,54	0,08
C3H	0,14	0,36
C3B%	-0,31	0,24
C4B%	-0,32	0,31
T5A%	-0,30	0,05
T5D%	0,29	-0,15
T6B%	-0,42	0,29
T6D%	0,29	-0,16
P3B%	-0,58	0,17
P3A	0,29	-0,03
P4B%	-0,51	0,37
P4A	0,31	-0,12
O1T%	-0,36	0,30
O2B%	-0,00	0,41
O2T%	-0,28	-0,11
O2D	0,36	0,02

Inverse relationships between changes in uricemia and beta-rhythm PSD in the P3 (Fig. 3.42) and T4 (Fig. 3.43) loci turned out to be the closest, and among the direct relationships, the correlation with the dynamics of alpha-rhythm PSD in the P3 locus is noteworthy (Fig. 3.44).

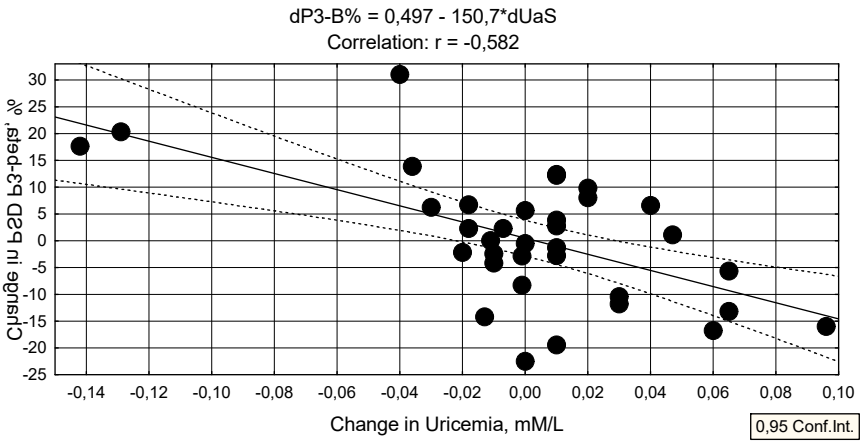

Fig. 3.42. Scatterplot of correlation between changes in Uricemia (X-line) and PSD P3-beta (Y-line)

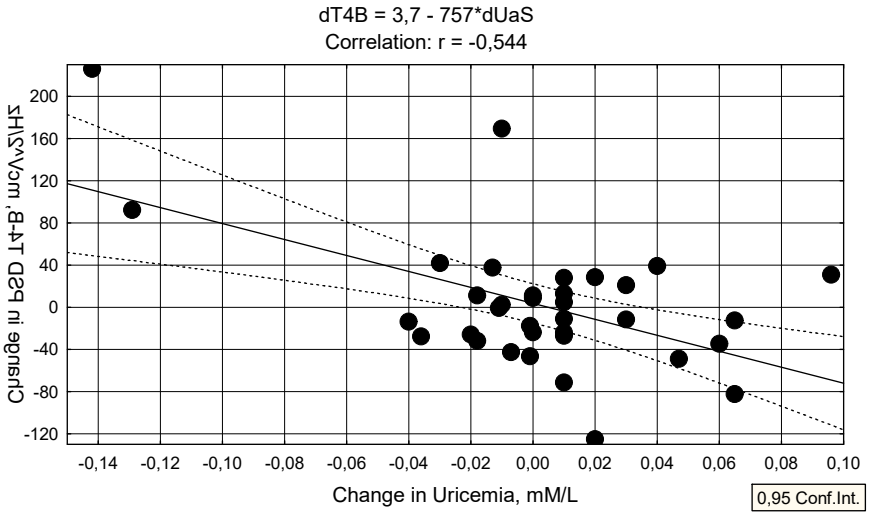

Fig. 3.43. Scatterplot of correlation between changes in Uricemia (X-line) and PSD T4-beta (Y-line)

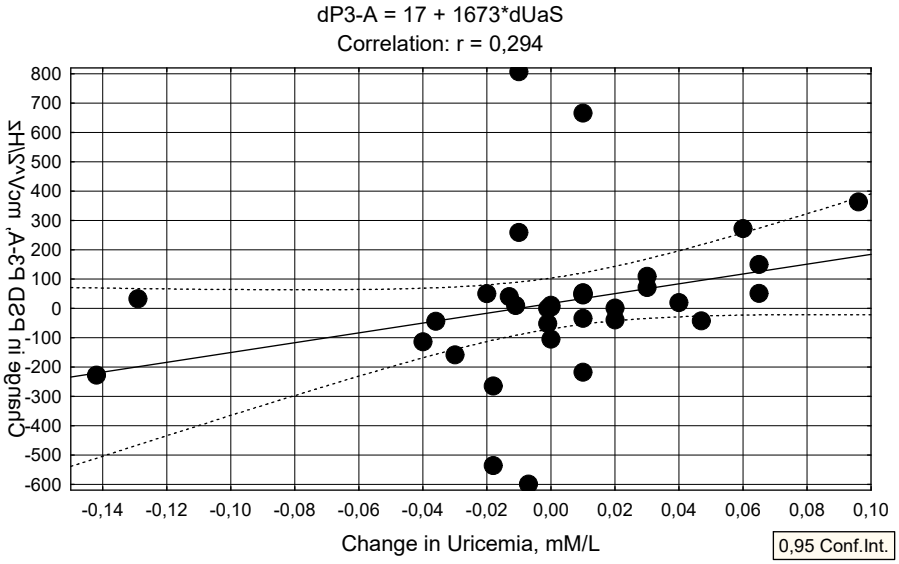

Fig. 3.44. Scatterplot of correlation between changes in Uricemia (X-line) and PSD P3-alpha (Y-line)

It was found that changes in the level of uricemia determine changes in 9 EEG parameters by 81% (Table 3.56 and Fig. 3.45).

Table 3.56. Regressive model for uricemia and EEG parameters

N=35	R=,901; R^2=,812; Adjusted R^2=,745; F(9,3)=12,0; p<,00000; Std.Error of estimate:,023					
	Beta	St. Err. of Beta	B	St. Err. of B	t(25)	p-value
Intercpt			0,00728	0,00421	1,73	0,09579
AA	-0,382	0,098	-0,00096	0,00025	-3,92	0,00062
T4B	-0,560	0,098	-0,00040	0,00007	-5,74	0,00001
C3B%	0,352	0,169	0,00104	0,00050	2,08	0,04823
C4B%	-0,330	0,151	-0,00098	0,00045	-2,20	0,03764
T5A%	-0,642	0,271	-0,00191	0,00080	-2,37	0,02599
T5D%	-0,665	0,295	-0,00090	0,00040	-2,26	0,03303
P3B%	-0,612	0,144	-0,00236	0,00056	-4,25	0,00026
P3A	0,584	0,212	0,00010	0,00004	2,76	0,01074
P4A	-0,391	0,203	-0,00009	0,00005	-1,93	0,06526

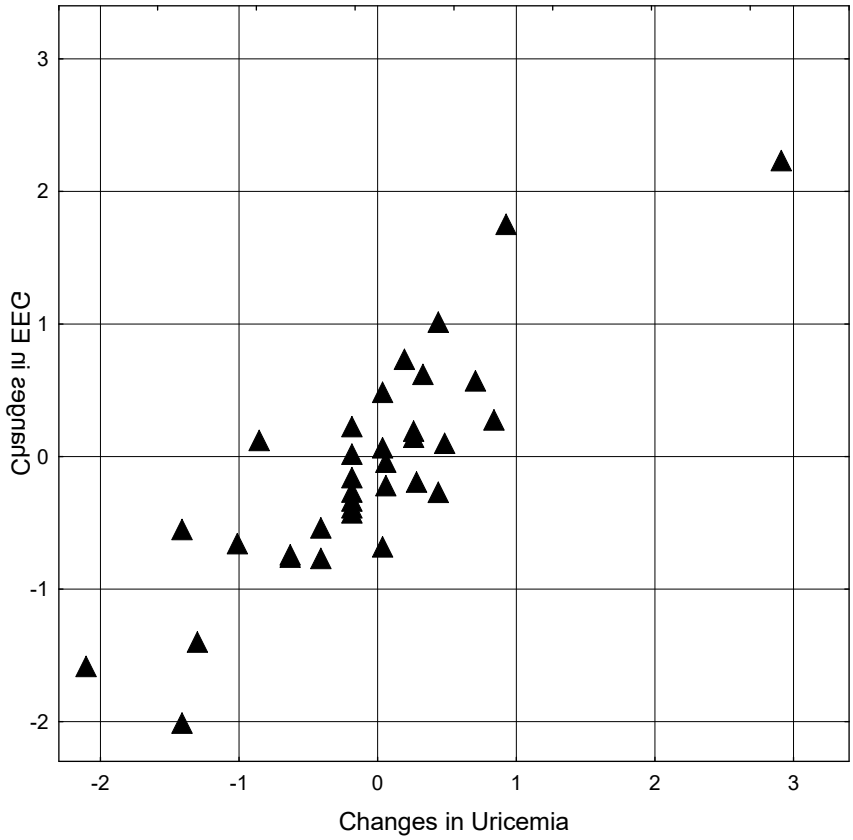

R=0,901; R^2=0,812; $\chi^2_{(9)}$=48; p=10^{-6}; Λ Prime=0,187

Fig. 3.45. Scatterplot of canonical correlation between changes in Uricemia (X-line) and EEG parameters (Y-line)

Neurotropic determination from the side of uricosuria is much weaker and amounts to 46,5% (Table 3.57 and Fig. 3.46).

Table 3.57. Regressive model for uricosuria and EEG parameters

N=35	R=,682; R^2=,465; Adjusted R^2=,326; F(7,3)=3,4; p<,0106; Std.Error of estimate:1,30					
	Beta	St. Err. of Beta	B	St. Err. of B	t(27)	p-value
Intercpt			-0,109	0,246	-0,44	0,661
IRA	-0,236	0,197	-0,014	0,012	-1,20	0,242
LIT	-0,358	0,156	-0,011	0,005	-2,29	0,030
T3T%	0,176	0,165	0,058	0,054	1,07	0,296
C3H	0,222	0,159	2,012	1,443	1,39	0,174
T6B%	-0,420	0,328	-0,033	0,025	-1,28	0,210
P4B%	0,381	0,276	0,047	0,034	1,38	0,180
O2B%	0,232	0,211	0,024	0,022	1,10	0,282

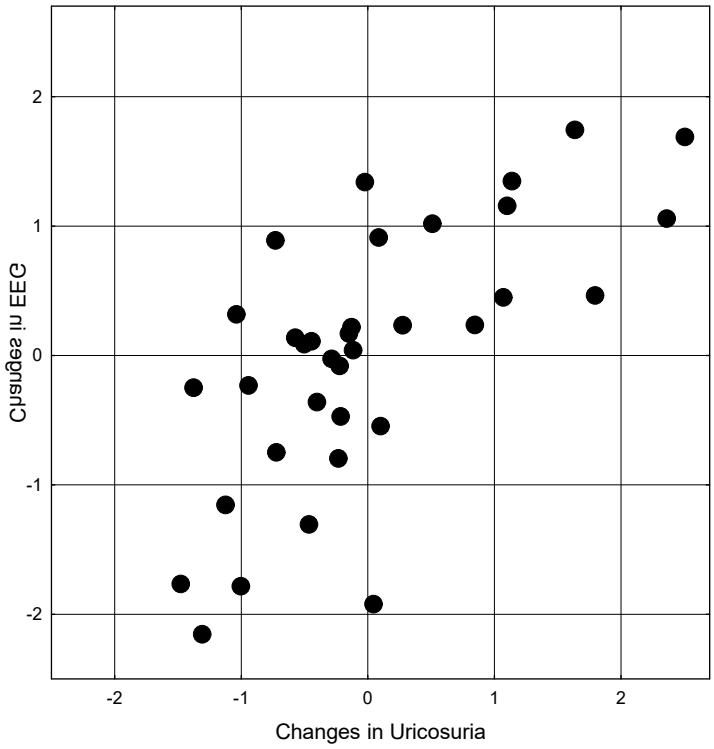

R=0,682; R^2=0,465; $\chi^2_{(7)}$=18; p=0,010; Λ Prime=0,535

Fig. 3.46. Scatterplot of canonical correlation between changes in Uricosuria (X-line) and EEG parameters (Y-line)

Finally, the canonical correlation between **changes** in both parameters of uric acid exchange, on the one hand, and EEG parameters, on the other, was analyzed.

The lion's share of the factor load on the causal canonical root belongs to uricemia (Table 3.58). The factor structure of the neural root is represented, first of all, by the PSD beta-rhythm in the P3, T4, C4 and C3 loci, as well as the alpha-rhythm in the T5 locus and its asymmetry, which are subject to downregulation by uricemia.

PSD of the beta-rhythm in the P4 and T6 loci are subject to both downregulation by uricemia and upregulation by uricosuria. On the other hand, PSDs of the delta-rhythm in the T5 locus, as well as the alpha-rhythm in the P4 and P3 loci are upregulated by uricemia. Alpha-rhythm index and theta-rhythm lateralization are subject to significant downregulation by uricosuria and weak upregulation by uricemia.

Finally, PSD of theta-rhythm in the T3 locus and beta-rhythm in the O2 locus, as well as entropy in the C3 locus are subject to significant upregulation by uricosuria and weak upregulation by uricemia.

Table 3.58. Factor structure of the canonical roots of changes in parameters of uric acid metabolism and EEG

Left set	**R**
Uricemia	**-0,984**
Uricosuria	**0,209**
Right set	**R**
PSD P3-β, %	**0,643**
PSD T4-β, μV²/Hz	**0,585**
PSD C4-β, %	**0,395**
PSD C3-β, %	**0,371**
PSD T5-α, %	**0,323**
Asymmetry α, %	**0,292**
PSD P4-β, %	**0,608**
PSD T6-β, %	**0,494**
PSD T5-δ, %	**-0,336**

PSD P4-α, μV²/Hz	-0,344
PSD P3-α, μV²/Hz	-0,313
Index α, %	-0,301
Laterality θ, %	-0,209
PSD T3-θ, %	-0,044
PSD C3 Entropy	-0,079
PSD O2-β, %	0,079

Taken together, changes in the parameters of uric acid exchange determine changes in the listed EEG parameters by 87% (Fig. 3.47).

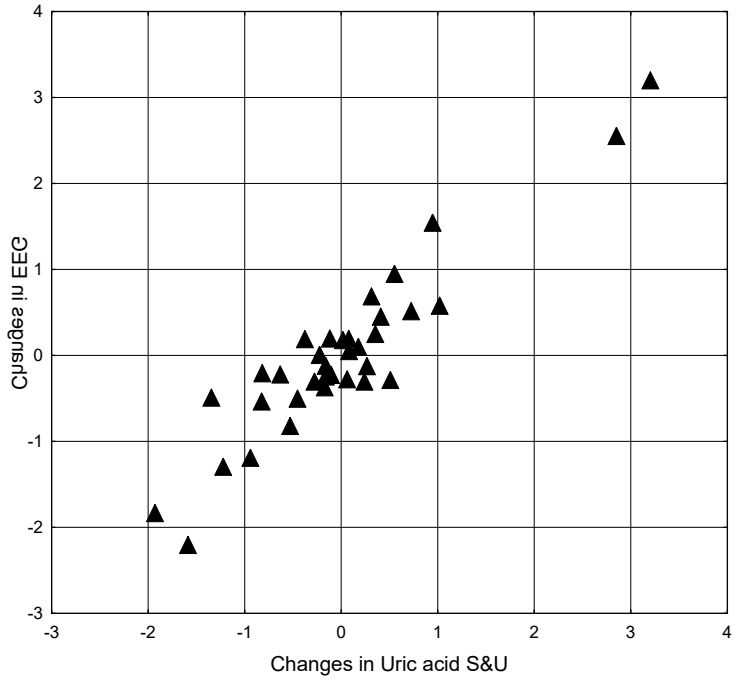

R=0,934; R^2=0,872; $\chi^2_{(32)}$=70; p=0,0001; Λ Prime=0,058

Fig. 3.47. Scatterplot of canonical correlation between changes in Uricemia&Uricosuria (X-line) and EEG parameters (Y-line)

3.8. METABOLIC ACCOMPANIMENTS OF VARIANTS OF URIC ACID EXCHANGE

It is obvious that uric acid is related to the metabolism of other biochemical ingredients. Discriminant analysis was used to identify the specific metabolic accompaniment of clusters of uric acid exchange. From among all the registered parameters, the forward stepwise program selected 12 as identifiers for the four variants of uric acid metabolism. The discriminant model includes (Tables 3.59 and 3.60), in addition to uricosuria and uricemia by definition, plasma **electrolytes** magnesium, potassium and phosphates, **non-electrolytes** glucose, urea and creatinine and urine creatinine, as well as **integral** markers of metabolism such as body mass index and electrokinetic index and sex as a metabolotropic factor.

Table 3.59. Summary of discriminant function analysis for metabolic parameters exchange
Step 12, N of vars in model: 12; Grouping: 4 grps; Wilks' Λ: 0,0570; approx. $F_{(36)}$=9,8; $p<10^{-6}$

Variables currently in the model	Clusters of Uric Acid Exchange (n)				Parameters of Wilks' Statistics					
	S-E2+IV (22)	S±E+I (21)	S2-E+II (15)	S±E-III (30)	Wilks Λ	Partial Λ	F-remove (3,7)	p-level	Tolerancy	Norm Cv (30)
Uricosuria, mM/24 h	5,94	3,94	3,88	2,27	0,289	0,197	98,9	10^{-6}	0,865	3,00 0,250
Uricemia, mM/L	0,316	0,371	0,249	0,322	0,079	0,723	9,31	10^{-4}	0,679	0,365 0,116
Sex Index (M=1; F=2)	1,18	1,24	1,07	1,33	0,065	0,872	3,57	0,018	0,610	1,23 0,344
Magnesium Plasma, mM/L	0,826	0,856	0,831	0,822	0,067	0,849	4,32	0,007	0,812	0,90 0,056
Electrokinetic Index, %	48,3	43,6	42,7	40,4	0,063	0,906	2,52	0,064	0,684	40,9 0,250
Body Mass Index, kg/m²	27,5	28,1	25,9	26,9	0,061	0,929	1,873	0,142	0,651	24,2 0,133
Glucose Plasma, mM/L	4,57	4,11	4,94	4,69	0,061	0,930	1,84	0,147	0,843	4,70 0,160
Phosphates Plasma, mM/L	0,96	0,97	1,09	1,06	0,061	0,937	1,64	0,188	0,884	1,20 0,167
Potassium Plasma, mM/L	4,40	4,40	4,50	4,19	0,063	0,906	2,53	0,064	0,762	4,55 0,104
Urea Plasma, mM/L	6,13	6,22	6,09	5,70	0,061	0,936	1,663	0,182	0,572	5,0 0,330
Creatininuria, mM/24 h	9,43	9,27	7,21	6,71	0,061	0,928	1,874	0,141	0,682	11,0 0,330
Creatinine Plasma, µM/L	85,6	87,4	88,1	84,0	0,061	0,940	1,56	0,207	0,396	77,5 0,172

Table 3.60. Summary of forward stepwise analysis of metabolic parameters

Variables currently in the model	F to enter	p-level	Λ	F-value	p-level
Uricosuria, mM/24 h	154	10^{-6}	0,154	154	10^{-6}
Uricemia, mM/L	8,47	10^{-4}	0,118	52,9	10^{-6}
Sex Index (M=1; F=2)	3,93	0,011	0,103	34,3	10^{-6}
Magnesium Plasma, mM/L	3,41	0,021	0,091	26,3	10^{-6}
Electrokinetic Index, %	1,62	0,191	0,086	21,1	10^{-6}
Body Mass Index, kg/m²	1,51	0,219	0,082	17,7	10^{-6}
Glucose Plasma, mM/L	1,76	0,161	0,076	15,5	10^{-6}
Phosphates Plasma, mM/L	1,41	0,246	0,072	13,7	10^{-6}
Potassium Plasma, mM/L	1,56	0,205	0,068	12,4	10^{-6}
Urea Plasma, mM/L	1,27	0,291	0,065	11,3	10^{-6}
Creatininuria, mM/24 h	1,72	0,169	0,061	10,5	10^{-6}
Creatinine Plasma, µM/L	1,56	0,207	0,057	9,84	10^{-6}

Instead, urinary excretion of urea and all registered electrolytes, lithogenicity of urine, as well as age, despite their obvious recognition ability, were outside the discriminant model, apparently due to duplication/redundancy of information (Table 3.61).

Table 3.61. Parameters of metabolism, not included in the model

Variables	Clusters of Uric Acid Exchange (n)				Parameters of Wilks' Statistics						
	S-E2+ IV (22)	S±E+ I (21)	S2-E+ II (15)	S±E- III (30)	Wilks Λ	Partial Λ	F to enter	p-level	Tolerancy	Reference mean (30)	Cv
Urea Excretion, mM/24 h	796	566	548	407	0,055	0,967	0,81	0,491	0,520	458	0,186
Diurese, L/24 h	2,59	2,00	2,05	1,51	0,055	0,966	0,85	0,469	0,515	1,40	0,274
Calcium Excretion, mM/24 h	6,37	5,23	5,13	3,96	0,055	0,963	0,92	0,438	0,748	4,38	0,214
Magnesium Excretion, mM/24 h	5,74	5,13	4,31	3,68	0,056	0,977	0,56	0,641	0,718	4,10	0,266
Phosphates Excretion, mM/24 h	30,5	25,7	23,3	18,1	0,056	0,980	0,50	0,683	0,707	25,2	0,294
Chloride Excretion mM/24 h	277	214	208	156	0,056	0,988	0,30	0,834	0,766	167,5	0,172
Sodium Excretion, mM/24 h	262	211	218	179	0,056	0,978	0,55	0,652	0,738	154	0,211
Potassium Excretion, mM/24 h	87	71	65	66	0,055	0,971	0,70	0,552	0,484	65	0,269
$(UA \bullet Ca)/(Cr \bullet Mg)^{0,25}$ Lithogenicity Urine	0,93	0,83	0,91	0,78	0,055	0,973	0,66	0,581	0,368	0,73	0,300
Age, Years	44,6	48,9	57,5	53,1	0,056	0,980	0,49	0,687	0,046	49,7	0,256
Calcium Plasma, mM/L	2,20	2,21	2,16	2,21	0,056	0,988	0,28	0,837	0,699	2,30	0,065
Chloride Plasma, mM/L	100	103	99,5	105	0,055	0,964	0,90	0,445	0,776	101,5	0,032
Sodium Plasma, mM/L	141	144	140	146	0,055	0,964	0,90	0,445	0,776	145	0,034

Following the algorithm, we transform the 12-dimensional space of discriminant variables into the 3-dimensional space of canonical roots. The canonical correlation coefficient for the first root is 0,928 (Wilks' Λ=0,057; $\chi^2_{(36)}$=226; $p<10^{-6}$), for the second 0,679 (Wilks' Λ=0,412; $\chi^2_{(22)}$=70; $p=10^{-6}$), for the third 0,487 (Wilks' Λ=0,763; $\chi^2_{(10)}$=21; p=0,019). The major root contains 84,2% of the discriminant possibilities, the second – 11,6%, and the minor - only 4,2%. Calculating the values of the discriminant roots for each person based on raw coefficients and constants (Table 3.62) allows to visualize each patient in the information space of these roots.

Table 3.62. Standardized and raw coefficients and constants for metabolic parameters

Coefficients	Standardized			Raw		
Variables	Root 1	Root 2	Root 3	Root 1	Root 2	Root 3
Uricosuria, mM/24 h	-1,030	0,104	0,197	-1,710	0,172	0,327
Uricemia, mM/L	-0,094	-0,897	0,350	-1,304	-12,39	4,833
Sex Index (M=1; F=2)	-0,035	-0,535	0,569	-0,084	-1,281	1,360
Magnesium Plasma, mM/L	-0,089	-0,124	-0,852	-2,376	-3,326	-22,81
Electrokinetic Index, %	-0,314	-0,333	-0,075	-0,0267	-0,0282	-0,0064
Body Mass Index, kg/m^2	-0,070	-0,468	0,139	-0,020	-0,133	0,039
Glucose Plasma, mM/L	0,167	0,273	0,328	0,181	0,297	0,357
Phosphates Plasma, mM/L	-0,052	0,372	-0,150	-0,261	1,887	-0,760
Potassium Plasma, mM/L	0,035	0,353	-0,525	0,064	0,643	-0,958
Urea Plasma, mM/L	0,158	-0,421	-0,191	0,138	-0,367	-0,166
Creatininuria, mM/24 h	-0,016	-0,154	-0,629	-0,0045	-0,043	-0,177
Creatinine Plasma, µM/L	-0,069	0,397	-0,564	-0,005	0,030	-0,042
			Constants	9,602	6,431	23,08

At the next stage of the analysis, the actual values of the parameters were normalized and grouped into three discriminant roots based on the structural coefficients (Table 3.63). In addition to discriminant variables, the table also presents variables that are not included in the model, but are still informal carriers of identifying information.

Table 3.63. Correlations of variables with canonical roots, root mean values and Z-values of metabolic parameters

Variables	Correlations Variables-Roots			S-E2+ IV (22)	S±E+ I (21)	S2-E+ II (15)	S±E- III (30)
Root 1 (84,2%)	**R 1**	**R 2**	**R 3**	**-3,60**	-0,36	+0,19	**+2,80**
Uricosuria	**-0,939**	0,140	0,037	**+3,87**	+1,26	+1,17	**-0,97**
Creatininuria	**-0,126**	-0,175	-0,131	-0,47	-0,52	-1,15	**-1,30**
Electrokinetic Index	**-0,118**	-0,031	0,056	**+0,73**	+0,26	+0,17	**-0,05**
Urea Plasma	**-0,061**	-0,017	-0,211	+0,69	+0,74	+0,66	**+0,42**
Potassium Plasma	**-0,059**	0,084	-0,253	-0,32	-0,31	-0,10	**-1,55**
Creatinine Plasma	**-0,019**	0,029	-0,195	+1,18	+1,33	+1,38	**+1,09**
Phosphates Excretion	currently not in model			**+0,71**	+0,06	-0,26	**-0,96**
Urea Excretion	currently not in model			**+3,96**	+1,27	+1,06	**-0,60**
Calcium Excretion	currently not in model			**+2,13**	+0,91	+0,81	**-0,44**
Magnesium Excretion	currently not in model			**+1,56**	+0,99	+0,20	**-0,40**
Chloride Excretion	currently not in model			**+3,82**	+1,61	+1,42	**-0,38**
Sodium Excretion	currently not in model			**+3,31**	+1,75	+1,97	**+0,76**
Potassium Excretion	currently not in model			**+1,25**	+0,36	+0,01	**+0,06**
Lithogenicity Urine	currently not in model			**+0,89**	+0,44	+0,79	**+0,23**
Diurese	currently not in model			**+3,11**	+1,56	+1,70	**+0,28**
Age	currently not in model			**-0,40**	-0,06	+0,14	**+0,27**
Root 2 (11,6%)	**R 1**	**R 2**	**R 3**	+0,05	**-1,13**	**+1,73**	-0,11
Uricemia	-0,012	**-0,587**	-0,049	-0,70	**+0,09**	**-1,89**	-0,53
Body Mass Index	-0,033	**-0,213**	-0,021	+1,02	**+1,21**	**+0,52**	+0,83
Magnesium Plasma	-0,029	**-0,206**	-0,553	-1,47	**-0,87**	**-1,36**	-1,35
Sex Index	0,055	**-0,161**	0,196	-0,11	**+0,02**	**-0,39**	+0,24
Sodium Plasma	currently not in model			-0,86	**-0,11**	**-1,01**	+0,27
Calcium Plasma	currently not in model			-0,69	**-0,60**	**-0,94**	-0,61
Chloride Plasma	currently not in model			-0,45	**+0,46**	**-0,63**	+0,92
Glucose Plasma	0,030	**0,303**	0,206	-0,17	**-0,78**	**+0,32**	-0,01
Phosphates Plasma	0,088	**0,213**	-0,004	-1,21	**-1,17**	**-0,53**	-0,69
Root 3 (4,2%)	**R 1**	**R 2**	**R 3**	+0,49	-0,69	-0,60	+0,42

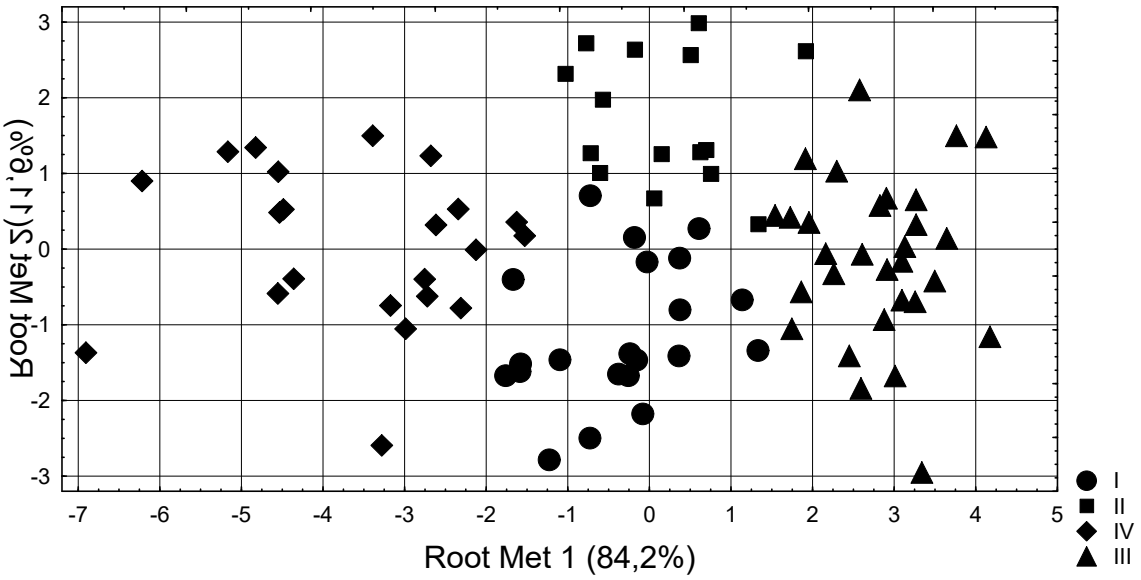

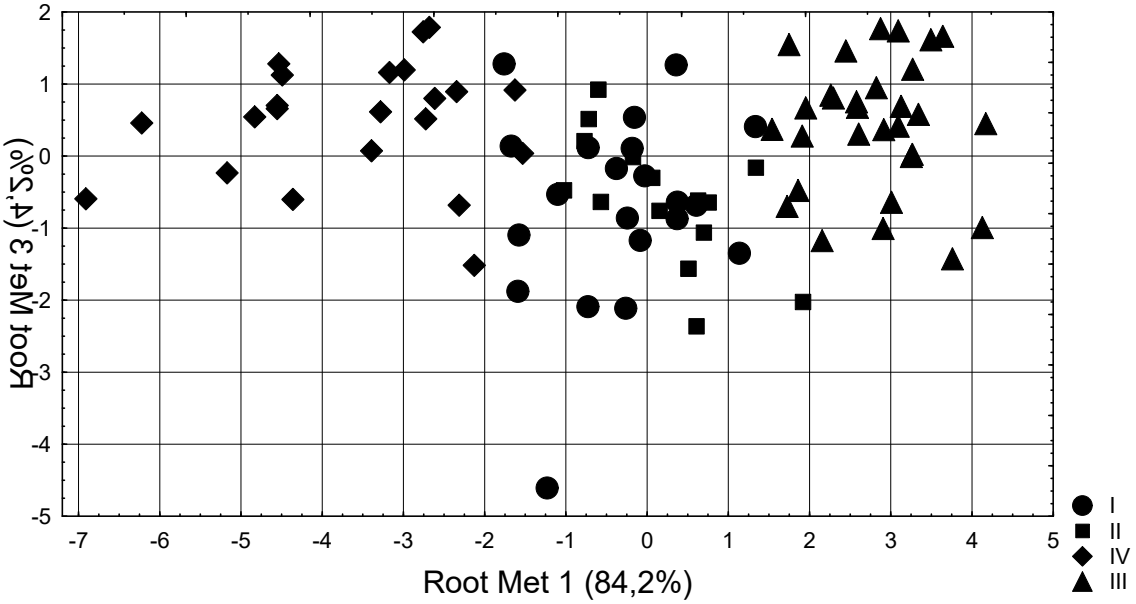

Fig. 3.48. Scattering of individual values of the first and second (top) and first and third (bottom) discriminant metabolic roots of patients from different clusters

As we can see in Fig. 3.48, members of the **S±E** cluster most clearly stand out from others, the characteristic features of which are a combination of hypouricosuria with hypokalemia and hypocreatininuria, while the level of creatinine in the plasma is elevated to the minimum extent for the sample, and the level of urea is at the upper limit and also minimal. Another characteristic feature is the normal, but minimal for the sample electrokinetic index. It is worth noting a number of parameters that were left out of the model, probably due to duplication and redundancy of recognition information. In particular, these are hypophosphaturia, lower limit levels of excretion of urea, calcium, magnesium and chloride, normal, but minimal for the sample, levels of natriuria, kaliuria and diuresis, as well as lithogenicity of urine. Instead, the members of this cluster were on average the oldest in the sample.

At the other pole of the axis of the first root are members of the **S-E2+** cluster, in which hyperuricosuria is accompanied by higher levels of the already mentioned parameters, as well as maximally increased electrokinetic index, diuresis, excretion of urea, chloride, calcium, magnesium, sodium and potassium, and lithogenicity of urine. In addition, the members of this cluster were on average the youngest in the sample.

Members of the other two clusters occupy an intermediate position along the axis of the first root and are mutually mixed. Instead, they are quite clearly demarcated along the axis of the second root. The top position of patients of the **S2-E+** cluster reflects the combination of hypouricemia with hypomagnesemia and, maximally for the sample, reduced levels in plasma of sodium, calcium, and chloride and a normal body mass index, instead, maximally for the sample, normal glycemia and low-limit phosphateemia. At the same time, there is only one woman among the 15 members of the cluster. In the members of the **S±E+** cluster located below, the listed parameters are significantly **higher**/**lower**, and among 16 people, there are 5 women.

The third discriminant root carries no additional information. So that all four clusters are quite clearly demarcated by the set of discriminant variables in the information space of even two roots (Table 3.64).

Table 3.64. Squares of Mahalanobis distances between clusters, F-criterions (df=12,7) and p-levels

Clusters	S±E+ I	S2-E+ II	S-E2+ IV	S±E- III
S±E+ I (21)	0	8,4	13,3	12,2
S2-E+	5,3	0	18,3	11,2

II (15)	10^{-5}			
S-E2+ IV (22)	**10,3** 10^{-6}	**11,8** 10^{-6}	0	40,9
S±E- III (30)	**10,9** 10^{-6}	**8,1** 10^{-6}	**37,6** 10^{-6}	0

With the help of classification functions (Table 3.65), we will find out the possibility of identifying the belonging of this or that person to this or that cluster.

Table 3.65. Coefficients and constants for cluster classification functions

Clusters	S±E+ I	S2-E+ II	S-E2+ IV	S±E- III
Variables	p=,239	p=,170	p=,250	p=,341
Uricosuria, mM/24 h	9,453	9,042	15,58	4,600
Uricemia, mM/L	47,74	12,13	43,09	36,42
Sex Index (M=1; F=2)	-4,855	-8,430	-4,484	-4,908
Magnesium Plasma, mM/L	808,0	795,1	784,8	771,7
Electrokinetic Index, %	1,438	1,342	1,484	1,318
Body Mass Index, kg/m^2	2,996	2,610	2,950	2,843
Glucose Plasma, mM/L	0,426	1,405	0,610	1,697
Phosphates Plasma, mM/L	62,97	68,15	65,15	63,22
Potassium Plasma, mM/L	19,24	21,03	18,66	19,04
Urea Plasma, mM/L	5,491	4,503	4,415	5,368
Creatininuria, mM/24 h	2,460	2,317	2,214	2,204
Creatinine Plasma, µM/L	0,892	0,970	0,894	0,859
Constants	-586,8	-562,2	-588,6	-527,0

As you can see, in retrospect, it is possible to recognize members of the most numerous **S±E-** cluster without error, and others - with 1-2 errors, so that the classification accuracy is 94,3% (Table 3.66).

Table 3.66. Classification matrix for clusters
Rows: observed classifications; columns: predicted classifications

Clusters	Percent correct	S±E+ I	S2-E+ II	S-E2+ IV	S±E- III
		p=,239	p=,170	p=,250	p=,341
I	90,5	**19**	**1**	0	**1**
II	93,3	0	**14**	0	**1**
IV	90,9	**2**	0	**20**	0
III	100	0	0	0	**30**
Total	94,3	21	15	20	32

3.9. RELATIONSHIPS BETWEEN PARAMETERS OF URIC ACID AND OTHER METABOLITES EXCHANGE

Now let's consider correlations between parameters of uric acid metabolism, on the one hand, and electrolytes, non-electrolytes, and metabolic markers - on the other hand (Table 3.67).

Table 3.67. Correlation matrix for uric acid and other metabolites parameters

	Uricemia raw	Uricemia normalized	Uricosuria
Sex Index	-0,29	0,20	-0,15
Age	0,02	-0,03	-0,19
Electrokinetic Index	-0,09	-0,02	0,22
Body Mass Index	0,13	0,09	0,10
Creatinine Plasma	0,23	0,02	0,07
Urea Plasma	0,02	-0,10	0,22
Glucose Plasma	-0,35	-0,28	-0,01
Calcium Plasma	0,28	0,22	-0,03
Phosphates Plasma	-0,04	-0,06	-0,23

Magnesium Plasma	0,11	0,23	0,04
Potassium Plasma	-0,04	0,08	0,16
Chloride Plasma	0,32	0,38	-0,28
Sodium Plasma	0,32	0,38	-0,28
Diuresis	0,12	0,01	0,65
Creatininuria	-0,04	0,10	0,30
Urea Excretion	0,12	0,02	0,71
Calcium Excretion	0,12	0,03	0,38
Phosphates Excretion	0,18	0,10	0,37
Magnesium Excretion	0,16	0,14	0,44
Potassium Excretion	0,14	0,08	0,27
Chloride Excretion	-0,06	-0,07	0,51
Sodium Excretion	0,04	0,00	0,36
Lithogenicity Urine	-0,04	-0,23	0,42

It was found that uricosuria has more numerous and closer correlations with metabolic parameters than uricemia. First of all, this concerns the excretion of urea (Fig. 3.49) and chloride (Fig. 3.50).

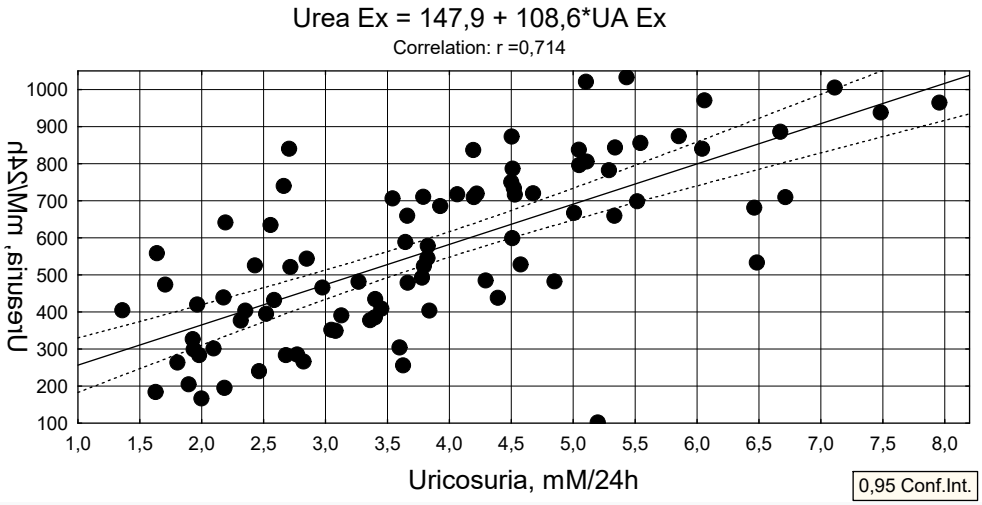

Fig. 3.49. Scatterplot of the correlation between uricosuria (line X) and ureauria (line Y)

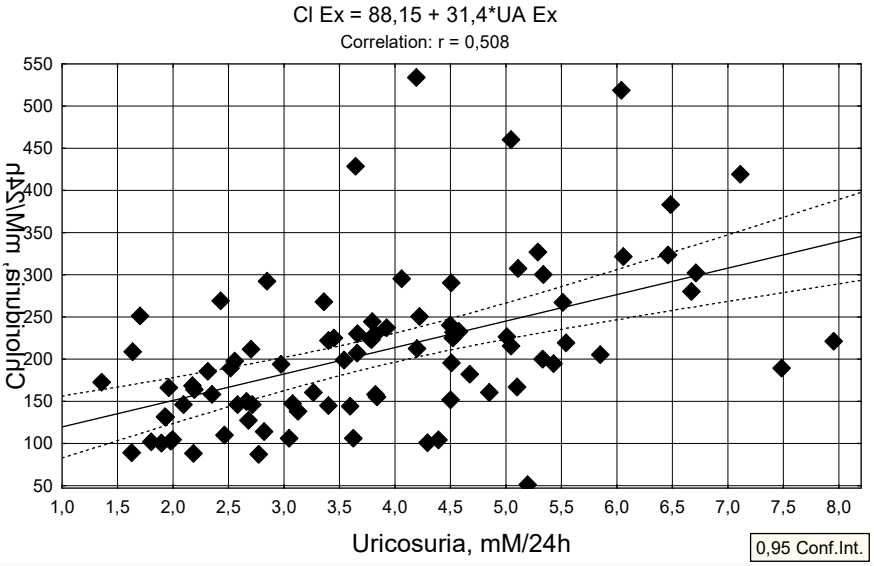

Fig. 3.50. Scatterplot of the correlation between uricosuria (line X) and chloriduria (line Y)

In the regression model, after stepwise exclusion, in addition to these parameters, chloridemia and kaliemia, excretion of creatinine, calcium and magnesium, as well as caused by

them the lithogenicity of urine, were found. This metabolic constellation is determined by uricosuria by 83% (Table 3.68 and Fig. 3.51).

Table 3.68. Regression model for metabolic parameters and uricosuria

N=88	R=0,911 ; R^2=0,830; Adjusted R^2=0,813; F(8,8)=48; p<10^-6					
	Beta	St. Err. of Beta	B	St. Err. of B	t(79)	p-value
Intercpt			-5,387	1,509	-3,57	0,000612
Creatinine E	0,475	0,068	0,193	0,028	6,94	0,000000
Ca E	-0,594	0,091	-0,290	0,044	-6,56	0,000000
Mg E	0,371	0,095	0,286	0,073	3,91	0,000197
Cl E	0,159	0,065	0,003	0,001	2,45	0,016523
Lithogenicity	0,798	0,078	7,856	0,772	10,17	0,000000
Cl P lasma	-0,083	0,049	-0,018	0,011	-1,70	0,093951
Urea E	0,412	0,073	0,003	0,000	5,61	0,000000
K Plasma	0,076	0,049	0,209	0,134	1,57	0,121253

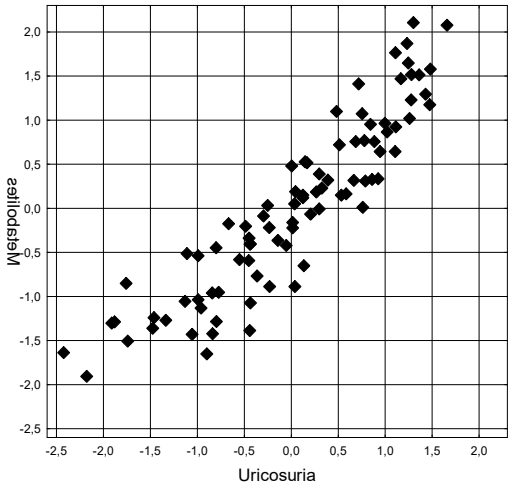

$R=0,911$; $R^2=0,830$; $\chi^2_{(8)}=146$; $p<10^{-6}$; Lambda Prime=0,170

Fig. 3.51. Scatterplot of the canonical correlation between uricosuria (line X) and other metabolic parameters (line Y)

It is interesting that magnesiumuria was included in the regression model for uricemia, and other components of the model were glycemia, chlorideemia, calciumemia, and creatinineemia. This metabolic constellation is determined by uricemia by 36% (Table 3.69 and Fig. 3.52).

Table 3.69. Regression model for metabolic parameters and raw uricemia

N=88	R=0,630; R^2=0,397; Adjusted R^2=0,360; F(5,8)=10,8; p<10^-5					
	Beta	St. Err. of Beta	B	St. Err. of B	t(82)	p-value
Intercpt			-0,5184	0,1736	-2,99	0,00372
Glucose	-0,278	0,089	-0,0238	0,0076	-3,13	0,00240
Ca P	0,315	0,091	0,1432	0,0413	3,46	0,00085
Cl P	0,393	0,089	0,0046	0,0010	4,42	0,00003
Cr P	0,247	0,086	0,0015	0,0005	2,86	0,00535
Mg E	0,163	0,086	0,0067	0,0036	1,89	0,06216

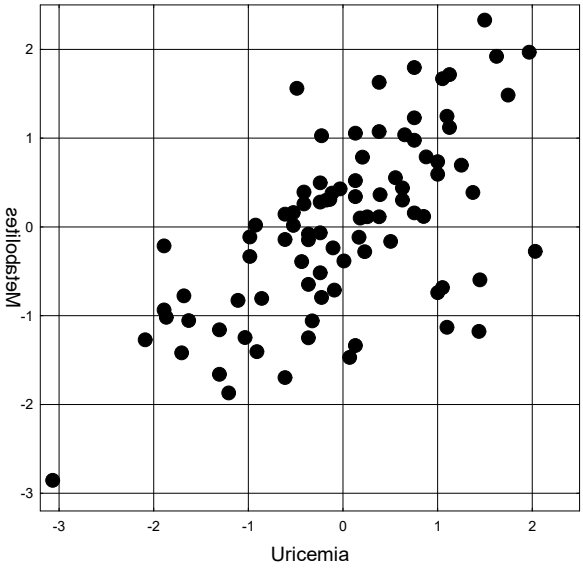

R=0,630; R^2=0,397; $\chi^2_{(5)}$=42; $p<10^{-6}$; Lambda Prime=0,603

Fig. 3.52. Scatterplot of canonical correlation between Uricemia (X-line) and other metabolic parameters (Y-line)

The same 4 parameters appeared in the regression model for uricemia, normalized by sex and age, together with magnesiumemia and urinary lithogenicity, but without creatinineemia. Such a metabolic constellation is determined by normalized uricemia by 38% (Table 3.70 and Fig. 3.53).

Table 3.70. Regression model for metabolic parameters and normalized uricemia

N=88	R=0,617; R^2=0,381; Adjusted R^2=0,335; F(6,8)=8,3; p<10^-6					
	Beta	St. Err. of Beta	B	St. Err. of B	t(81)	p-value
Intercpt			-14,162	3,343	-4,24	0,00006
Glucose	-0,213	0,091	-0,252	0,108	-2,34	0,02184
Ca P	0,305	0,093	1,911	0,582	3,28	0,00152
Cl P	0,358	0,095	0,058	0,015	3,76	0,00032
Mg E	0,180	0,089	0,103	0,051	2,02	0,04625
Lithogenicity	-0,173	0,093	-1,263	0,677	-1,87	0,06574
Mg P	0,216	0,090	6,153	2,571	2,39	0,01902

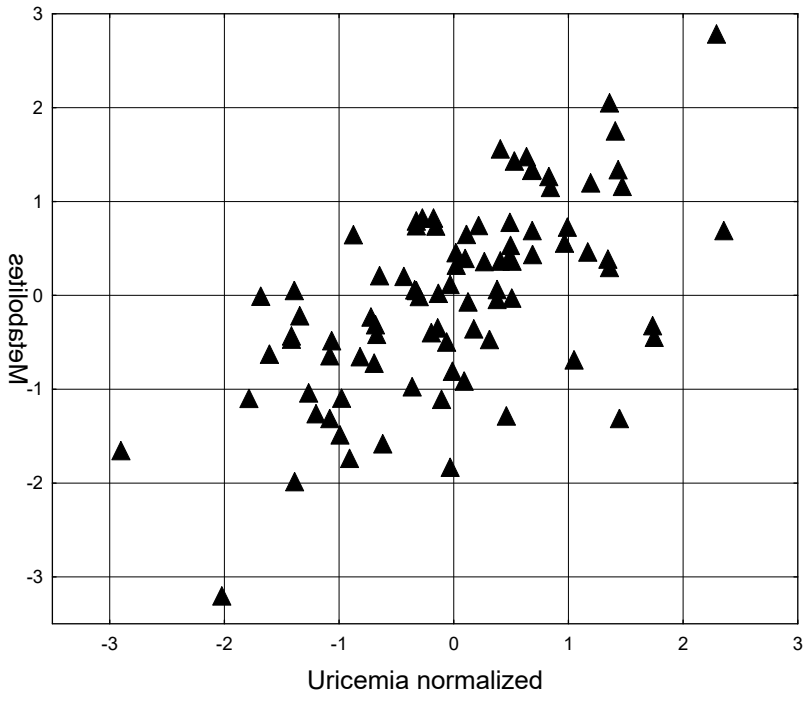

R=0,617; R^2=0,381; $\chi^2_{(6)}$=40; $p<10^{-6}$; Lambda Prime=0,619

Fig. 3.53. Scatterplot of canonical correlation between normalized Uricemia (X-line) and other metabolic parameters (Y-line)

According to the results of the canonical correlation analysis, two pairs of canonical roots were formed. The uric acid root of the first pair mainly represents uricosuria. The metabolic canonical root receives the maximum positive factor load from ureauria, then there is a constellation of parameters with smaller, approximately equal burdens - chlorideuria, magnesiria, calciuria, creatinineuria and the associated lithogenicity of urine, and the minimum load on the root is given by potassiumemia. Instead, chloridemia gives a negative load on the metabolic root (Table 3.71). Uricose determination of this metabolic constellation is 85% (Fig. 3.54).

Table 3.71. Factor structure of the canonical roots of parameters of uric acid and other metabolites exchange

	left set	
Variable	Root 1	Root
Uricosuria	0,995	0,038
Uricemia raw	-0,083	0,987
Uricemia norm	-0,176	0,783

Variable	right set	
	Root 1	Root 2
Glucose	0,007	-0,514
Urea Excr	0,772	0,261
Ca P	-0,045	0,428
Mg P	0,015	0,099
K P	0,145	-0,108
Cl P	-0,335	0,408
Creatinine P	0,096	0,424
Ca Excr	0,412	0,247
Mg Excr	0,455	0,274
Cl Excr	0,548	-0,040
Lithogenicity	0,493	0,067
Creatininuria	0,301	-0,097

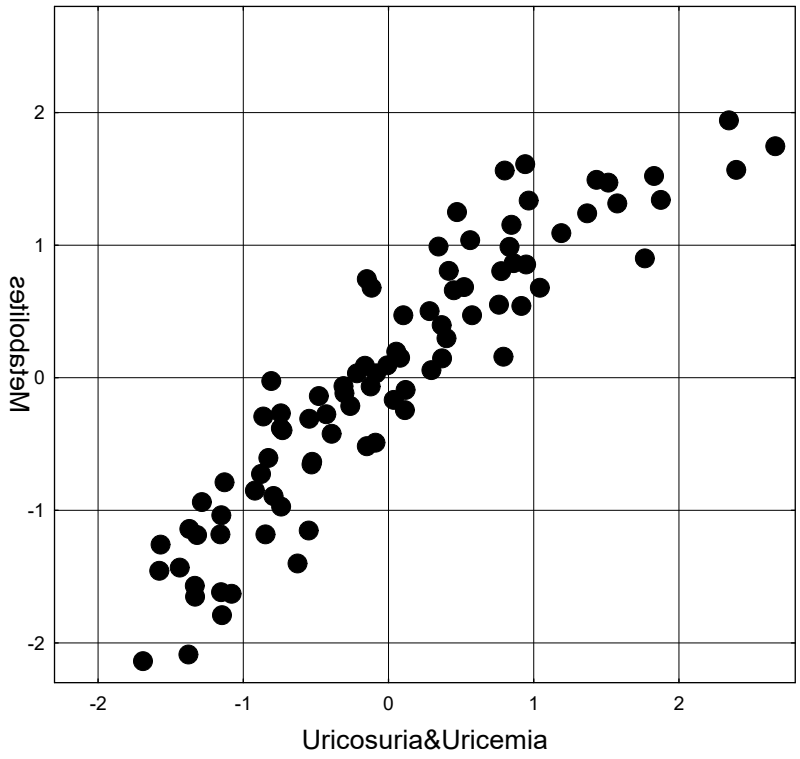

R=0,920; R^2=0,847; $\chi^2_{(36)}$=227; $p<10^{-6}$; Lambda Prime=0,056

Fig. 3.54. Scatterplot of canonical correlation between parameters of Uric acid exchange (X-line) and other metabolic parameters exchange (Y-line). First pair of Roots

The uric acid root of the second pair mainly represents uricemia. The metabolic canonical root receives the maximum inverse factor load from glycemia, smaller unidirectional loads with uricemia - from calciumemia, creatinineemia, and chloridemia, and minimum - from the excretion of magnesium, urea, and calcium. This metabolic constellation is determined by uric acid by 46% (Fig. 3.55).

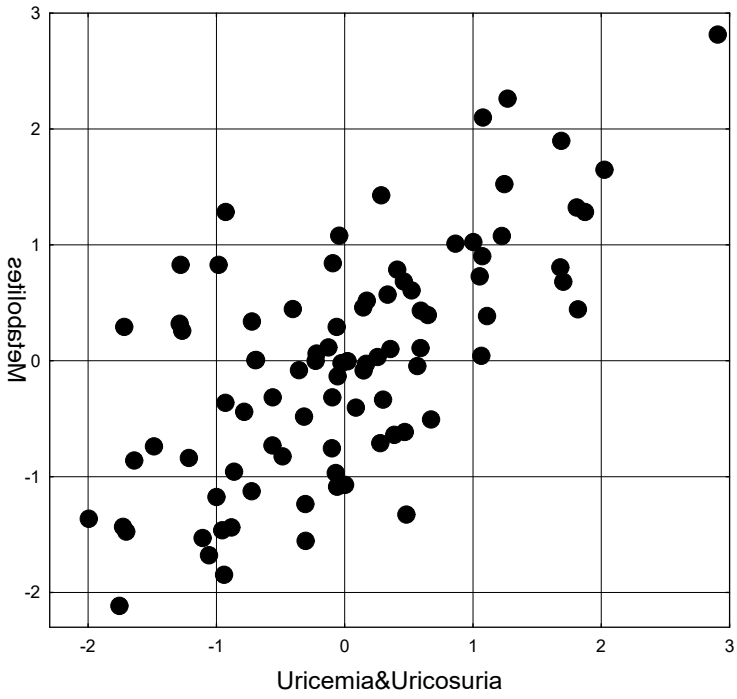

R=0,675; R^2=0,456; $\chi^2_{(22)}$=79; $p<10^{-6}$; Lambda Prime=0,369

Fig. 3.55. Scatterplot of canonical correlation between parameters of Uric acid exchange (X-line) and other metabolic parameters exchange (Y-line). Second pair of Roots

It is time to move on to considering the relationship between the **changes** in the parameters of uric acid and other metabolites caused by the course of adaptogenic balneotherapy. The screening result is shown in the Table 3.72.

As we can see, the dynamics of uricosuria is closely related to the dynamics of daily diuresis and excretion of urea and creatinine. Magnesiuria, calciuria, phosphaturia and chlorideuria, as well as the lithogenicity of urine caused by them, are the second constellation of parameters with the strongest connections. Instead, changes in natriuria and kaliuria correlate with changes in uricosuria very weakly, as do changes in plasma levels of creatinine, urea, and potassium.

Table 3.72. Correlation matrix for changes in uric acid and other metabolites parameters

Variable	Uricemia	Uricosuria
Cr P	0,23	-0,25
Diurese	-0,03	0,79
Cr E	-0,02	0,60
Ca E	-0,20	0,36
Pi E	-0,15	0,34
Mg E	-0,04	0,38
K E	0,03	0,20
Cl E	0,12	0,32
Na E	0,14	0,15
Lithogenicity	-0,19	0,31
Ca P	0,28	0,06
Mg P	0,18	0,03
K P	-0,09	0,18
Cl P	0,26	-0,10
Na P	0,26	-0,10
Urea E	-0,06	0,77
Urea P	0,07	0,20

However, after step-by-step exclusion, the dynamics of kaliemia remained in the regression model, while the dynamics of chloriduria was left out of the model (Table 3.73).

Table 3.73. Regression model for changes in metabolic parameters and uricosuria

N=44	R=0,940; R^2=0,884; Adjusted R^2=0,853; F(9,3)=28; p<10^-5					
	Beta	St. Err. of Beta	B	St. Err. of B	t(34)	p-value
Intercpt			-0,5510	0,1268	-4,35	0,000119
Diurese	0,228	0,114	0,6896	0,3448	2,00	0,053533
Cr E	0,358	0,090	0,1553	0,0392	3,97	0,000356
Ca E	-0,593	0,128	-0,2604	0,0563	-4,62	0,000053
Pi E	0,186	0,082	0,0185	0,0082	2,26	0,030115
Mg E	0,245	0,100	0,2089	0,0853	2,45	0,019580
K E	0,178	0,103	0,0064	0,0037	1,73	0,092282
Lithogenicity	0,625	0,096	6,4268	0,9898	6,49	0,000000
K P	0,227	0,109	0,6315	0,3044	2,07	0,045666
Urea E	0,350	0,108	0,0030	0,0009	3,25	0,002624

The dynamics of this constellation of metabolic parameters is determined by the dynamics of uricosuria by 88% (Fig. 3.56).

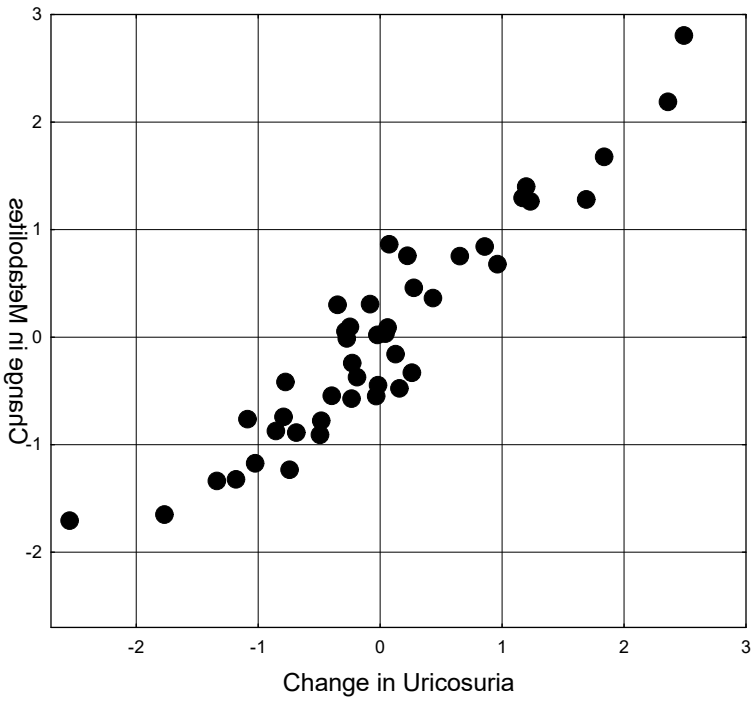

$R=0,940$; $R^2=0,884$; $\chi^2_{(9)}=81$; $p<10^{-6}$; Lambda Prime=0,116

Fig. 3.56. Scatterplot of canonical correlation between changes in Uricosuria (X-line) and other metabolic parameters (Y-line)

Instead, the dynamics of uricemia is related to the dynamics of metabolic parameters much weaker. It is surprising that in the process of step-by-step exclusion, the program left chlorideuria, natriuria, lithogenicity, and magnesiumemia in the regression model, while natriemia and creatinineemia were left out of the model. Obviously, this circumstance explains the significant difference (11,4%) between the actual and adjusted coefficients of determination (Table 3.74 and Fig. 3.57).

Table 3.74. Regression model for changes in metabolic parameters and uricemia

N=44	R=0,544; R^2=0,295; Adjusted R^2=0,181; F(6,4)=2,6; p=0,034					
	Beta	St. Err. of Beta	B	St. Err. of B	t(37)	p-value
Intercpt			-0,00365	0,00705	-0,52	0,608
Cl E	0,250	0,179	0,00009	0,00007	1,40	0,171
Na E	-0,345	0,213	-0,00015	0,00009	-1,62	0,114
Lithogenicity	-0,325	0,157	-0,08307	0,04025	-2,06	0,046
Ca P	0,453	0,152	0,10625	0,03556	2,99	0,005
Mg P	0,199	0,155	0,17439	0,13606	1,28	0,208
Cl P	0,349	0,154	0,00145	0,00064	2,27	0,029

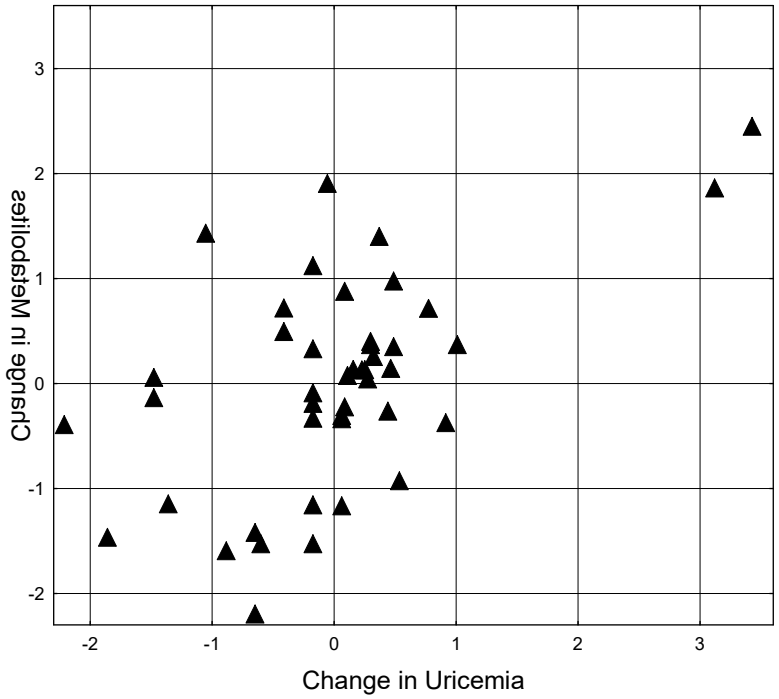

R=0,543; R^2=0,295; $\chi^2_{(6)}$=13,7; p=0,034; Lambda Prime=0,705

Fig. 3.57. Scatterplot of canonical correlation between changes in Uricemia (X-line) and other metabolic parameters (Y-line)

It is natural that according to the results of the canonical correlation analysis, the combined determination of the dynamics of metabolic parameters from the side of uricosuria and uricemia exceeds the effect of uricosuria itself by only 10% (Table 3.75 and Fig. 3.58).

Table 3.75. Factor structure of the canonical roots of changes in parameters of uric acid and other metabolites exchange

Root	left set
Variable	R
Uricemia	-0,058
Uricosuria	0,999

Root Variable	right set R
Cl E	0,333
Na E	0,185
Lithogenicity	0,341
Ca P	0,055
Mg P	0,020
Cl P	-0,115
Diurese	0,834
Cr E	0,637
Ca E	0,386
Pi E	0,371
Mg E	0,405
K E	0,207
K P	0,197
Urea E	0,813

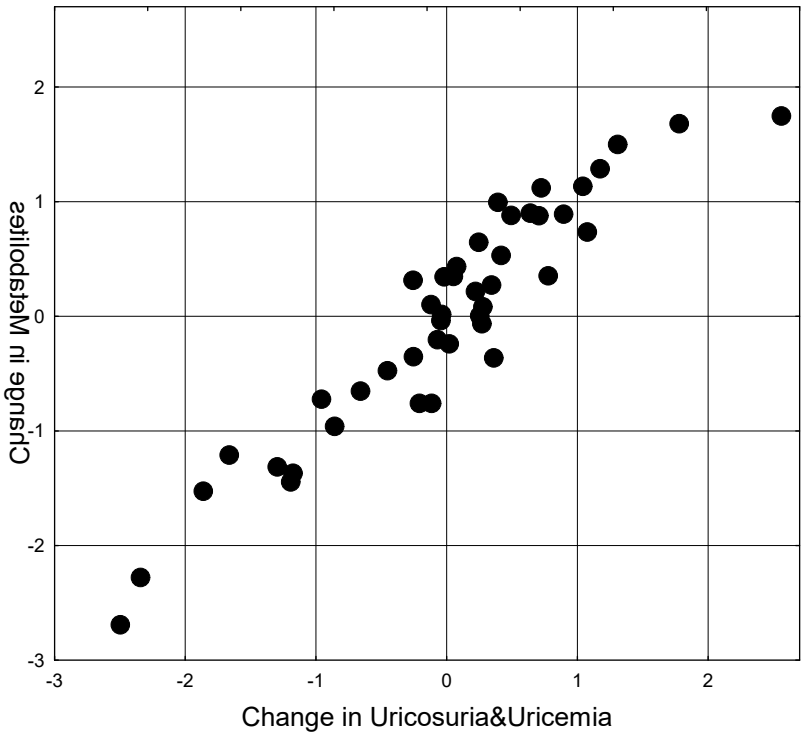

R=0,946; R^2=0,894; $\chi^2_{(28)}$=93; $p<10^{-6}$; Lambda Prime=0,068

Fig. 3.58. Scatterplot of canonical correlation between changes in Uricosuria&Uricemia (X-line) and other metabolic parameters (Y-line)

Therefore, the exchange of uric acid is closely related to the exchange of other metabolites, at least electrolytes and nitrogenous compounds. A detailed analysis of the mechanisms of such connections will be carried out in the conclusion. Spoiler. Mediators are neuro-endocrine effects of uric acid.

3.10. URIC ACID AND NEUROENDOCRINE-IMMUNE COMPLEX&METABOLISM

It's time to collect all the puzzles and create a complete picture.

From among all the registered parameters, the forward stepwise program selected 28 as identifiers for the four variants of uric acid metabolism. The discriminant model includes (Tables 3.76 and 3.77), in addition to uricosuria and uricemia by definition, 10 **neuroendocrine** parameters (6 EEG, vagal tone, indices of sympatho-vagal balance of Kerdö and Baevskyi,

calcitonin), 5 parameters of **immunity** (activity and completion of phagocytosis by neutrophils of gram-positive bacteria, the level of total lymphocytes and IgG in the blood and IgA in saliva), two **informational** parameters (Popovych's strain index of the leukocytogram and the entropy of the immunocytogram), 6 parameters of **metabolism** (serum magnesium, potassium, phosphates and creatinine, creatinineuria, body mass index), as well as markers of chronic pyelonephritis (**bacteriuria**) and microbiota (***Bifidobacteria***).

Table 3.76. Summary of stepwise analysis of parameters of uric acid exchange, metabolism and neuroendocrine-immune complex, ranked by Λ criterium

Variables currently in the model	F to enter	p-level	Λ	F-value	p-level
Uricosuria, mM/24 h	154	0	0,154	154	10^{-6}
Uricemia normalized, Z	13,5	10^{-6}	0,104	58,3	10^{-6}
PSD T4-δ, μV^2/Hz	3,96	0,011	0,090	37,4	10^{-6}
PSD O2-θ, %	3,51	0,019	0,080	28,6	10^{-6}
Laterality δ, %	3,40	0,022	0,071	23,7	10^{-6}
Calcitonin, ng/L	3,01	0,035	0,064	20,5	10^{-6}
Phagocytose Index vs Staphylococcus aureus, %	2,37	0,077	0,058	18,1	10^{-6}
Bacteriuria, points	3,11	0,031	0,052	16,5	10^{-6}
PSD C4 Entropy	2,25	0,090	0,048	15,1	10^{-6}
PSD F4 Entropy	2,70	0,052	0,043	14,1	10^{-6}
Pan-Lymphocytes of Blood, %	2,36	0,078	0,039	13,2	10^{-6}
Kerdö Vegetative Index, units	3,08	0,033	0,035	12,7	10^{-6}
Bactericidity vs Staphyl. aureus, 10^9 Bacteria/L	3,97	0,011	0,030	12,4	10^{-6}
IgA Saliva, mg/L	3,54	0,019	0,026	12,2	10^{-6}
IgG Serum, g/L	2,06	0,114	0,024	11,6	10^{-6}
PSD C3-δ, %	1,68	0,180	0,022	11,1	10^{-6}
Popovych's Strain Index-1, points	2,12	0,106	0,020	10,7	10^{-6}
AMo/MxDMn as Sympatho-vagal balance Index	1,90	0,138	0,019	10,4	10^{-6}
Body Mass Index, kg/m^2	2,21	0,096	0,017	10,1	10^{-6}
Magnesium Plasma, mM/L	1,84	0,149	0,016	9,80	10^{-6}
Phosphates Plasma, mM/L	1,46	0,235	0,015	9,46	10^{-6}
Potassium Plasma, mM/L	1,77	0,162	0,014	9,20	10^{-6}
Uricemia, mM/L	1,69	0,179	0,013	8,96	10^{-6}
RMSSD, msec	1,69	0,179	0,012	8,75	10^{-6}
***Bifidobacteria* faeces, lg CFU/g**	2,85	0,045	0,010	8,75	10^{-6}
Entropy of Immunocytogram	1,22	0,312	0,010	8,48	10^{-6}
Creatinine Plasma, μM/L	1,21	0,313	0,009	8,24	10^{-6}
Creatininuria, mM/24 h	1,18	0,327	0,008	8,00	10^{-6}

Table 3.77. Summary of discriminant function analysis for parameters of uric acid exchange, metabolism and neuroendocrine-immune complex

Step 28, N of vars in model: 28; Grouping: 4 grps; Wilks' Λ: 0,0085; approx. $F_{(84)}$=8,0; $p<10^{-6}$

Variables currently in the model	Clusters of Uric Acid Exchange (Males/Females)				Parameters of Wilks' Statistics					
	S-E2+ IV (18/4)	S±E+ I (16/5)	S2-E+ II (14/1)	S±E- III (20/10)	Wilks Λ	Partial Λ	F-remove	p-level	Tolerancy	Reference Cv/σ
Uricosuria, mM/24 h	5,94	3,94	3,88	2,27	0,076	0,112	150	10^{-6}	0,396	3,00 0,250
Uricemia, mM/L	0,316	0,371	0,249	0,322	0,010	0,864	2,99	0,038	0,109	0,365 0,116
Uricemia normalized, Z-score	-0,70	+0,09	-1,89	-0,53	0,009	0,897	2,17	0,101	0,155	0 **0,5**
PSD T4-δ, μV^2/Hz	57	354	94	161	0,009	0,984	0,31	0,818	0,543	92 1,091
PSD O2-θ, %	6,3	5,1	5,3	9,1	0,010	0,864	3,00	0,038	0,538	7,1 0,554

Laterality δ, %	-9,6	-24,9	-27,5	+6,8	0,010	0,891	2,33	0,084	0,610	+2,5 **39,8**
Calcitonin, ng/L	6,45	7,21	8,76	7,50	0,010	0,878	2,65	0,058	0,639	12,03
Calcitonin Males, ng/L	6,65	7,76	8,64	8,80						13,95 0,493
Calcitonin Females, ng/L	5,55	5,48	10,39	4,90						5,05 0,490
Phagocytose Index vs Staph. aureus, %	98,54	99,00	99,00	98,96	0,010	0,852	3,31	0,026	0,431	98,3 0,018
Bacteriuria, points	0,28	0,22	0,43	0,27	0,010	0,810	4,45	0,007	0,290	0 **0,24**
PSD C4 Entropy	0,83	0,87	0,80	0,85	0,014	0,623	11,5	10^{-5}	0,222	0,867 0,109
PSD F4 Entropy	0,81	0,71	0,80	0,81	0,010	0,822	4,12	0,010	0,295	0,851 0,139
Pan-Lymphocytes of Blood, %	34,6	31,7	35,8	33,9	0,012	0,683	8,84	10^{-4}	0,166	32,0 0,174
Kerdö Vegetative Index, units	-24	-13	-27	-20	0,013	0,640	10,7	10^{-5}	0,484	-20 **23,6**
Bactericidity vs Staph. aureus, 10^9 Bacteria/L	93,8	103,0	90,6	94,5	0,010	0,813	4,37	0,008	0,322	105,7 0,100
IgA Saliva, mg/L	118	135	142	144	0,010	0,882	2,53	0,066	0,239	163 0,241
IgG Serum, g/L	14,4	15,1	14,5	15,6	0,009	0,930	1,42	0,246	0,602	12,75 0,206
PSD C3-δ, %	25,7	42,1	32,4	30,5	0,010	0,850	3,35	0,025	0,407	28,0 0,602
Popovych's Strain Index-1, points	0,13	0,25	0,16	0,13	0,009	0,975	0,48	0,699	0,479	0,067 0,722
AMo/MxDMn as Symp/Vagal balance	218	394	234	236	0,009	0,943	1,15	0,338	0,374	251 0,303
Body Mass Index, kg/m^2	27,5	28,1	25,9	26,9	0,010	0,855	3,22	0,029	0,461	24,2 0,133
Magnesium Plasma, mM/L	0,826	0,856	0,831	0,822	0,010	0,889	2,37	0,080	0,512	0,90 0,056
Phosphates Plasma, mM/L	0,96	0,97	1,09	1,06	0,009	0,895	2,23	0,094	0,581	1,20 0,167
Potassium Plasma, mM/L	4,40	4,40	4,50	4,19	0,010	0,893	2,27	0,091	0,570	4,55 0,104
RMSSD HRV, msec	30,6	27,4	32,6	26,1	0,010	0,869	2,87	0,044	0,291	28,8 ,486
***Bifidobacteria* faeces, lg CFU/g**	5,74	5,49	5,40	5,66	0,010	0,885	2,48	0,070	0,398	6,94 0,011
Entropy of Immunocytogram	0,967	0,967	0,964	0,956	0,009	0,910	1,88	0,143	0,486	0,960 0,059
Creatinine Plasma, µM/L	85,6	87,4	88,1	84,0	0,009	0,924	1,55	0,211	0,363	77,5 0,172
Creatininuria, mM/24 h	9,43	9,27	7,21	6,71	0,009	0,942	1,18	0,327	0,448	11,0 0,330

Note. For four variables, SD is given instead of Cv.

Instead, a number of parameters, despite their obvious recognition ability, were outside the discriminant model, apparently due to duplication/redundancy of information (Table 3.78).

Next, we transform the 28-dimensional space of discriminant variables into the 3-dimensional space of canonical roots. The canonical correlation coefficient for the first root is 0,969 (Wilks' Λ=0,008; $\chi^2_{(84)}$=339; $p<10^{-6}$), for the second 0,837 (Wilks' Λ=0,140; $\chi^2_{(54)}$=139; $p<10^{-6}$), for the third 0,729 (Wilks' Λ=0,469; $\chi^2_{(26)}$=54; p=0,001). The major root contains 81,7% of the discriminant possibilities, the second – 12,3% and the minor - 6,0%.

Table 3.78. Parameters of neuroendocrine-immune complex and metabolism, not included in the model

Variables	Clusters of Uric Acid Exchange (Males/Females)				Parameters of Wilks' Statistics					
	S-E2+IV (18/4)	S±E+I (16/5)	S2-E+II (14/1)	S±E-III (20/10)	Wilks Λ	Partial Λ	F to enter	p-level	Tolerancy	Reference Cv/σ
PSD C3-δ, μV^2/Hz	91	315	259	166	0,008	0,968	0,63	0,601	0,251	108 0,774
PSD T6-α, %	37,8	27,3	24,4	28,0	0,008	0,955	0,88	0,455	0,431	35,5 0,502
PSD F7-θ, μV^2/Hz	15,8	42,7	29,1	28,3	0,008	0,979	0,40	0,752	0,302	18,2 0,843
PSD T4-δ, %	24,7	45,9	29,0	36,7	0,008	0,985	0,28	0,839	0,272	31,0 0,615
$(Ca/K)^{0,5}$ Plasma as Symp/Vagal balance	0,71	0,71	0,69	0,73	0,008	0,987	0,25	0,865	0,186	0,71 0,104
Triiodothyronine, nM/L	1,86	2,17	2,02	1,96	0,008	0,985	0,29	0,832	0,431	2,20 0,227
Cortisol, nM/L	531	475	432	563	0,008	0,952	0,94	0,430	0,750	405 0,524
PTH, pM/L	4,35	3,98	3,74	3,24	0,008	0,980	0,50	0,875	0,100	3,75 0,230
Sex Index (M=2; F=1)	1,82	1,76	1,93	1,67	0,008	0,991	0,18	0,913	0,035	1,23 0,344
Testosterone normalized by sex&age, Z	-0,12	+0,55	+1,03	+0,22	0,008	0,985	0,28	0,837	0,581	0 **0,5**
Males, Z-score	-0,31	+0,62	+1,09	+0,18						0
Females, Z-score	+0,70	+0,22	+0,12	+0,29						0
Calcitonin normalized by sex, Z	-0,87	-0,69	-0,60	-0,57	0,008	0,988	0,23	0,877	0,107	0 **0,5**
Males, Z-score	-1,07	-0,90	-0,78	-0,75						0
Females, Z-score	+0,02	-0,01	+1,08	-0,22						0
Interleukin-1, ng/L	4,81	4,74	5,34	4,58	0,008	0,974	0,50	0,685	0,651	4,51 0,173
Killing Index vs Staph. aureus, %	49,5	53,0	47,9	47,9	0,008	0,991	0,16	0,922	0,350	58,9 0,142
$CD4^+CD3^+$ T-helper Lymphocytes, %	28,3	30,0	32,3	32,6	0,008	0,978	0,42	0,737	0,168	39,5 0,082
$CD8^+CD3^+$ T-cytolytic Lymphocytes, %	23,7	23,4	21,2	23,3	0,008	0,974	0,50	0,684	0,629	23,5 0,138
Leukocyturia, lg/mL	3,44	3,26	3,19	3,44	0,008	0,965	0,69	0,564	0,453	3,00 0,070
Lactobacilli faeces, lg CFU/g	6,48	6,31	6,14	6,38	0,008	0,963	0,72	0,543	0,016	8,10 0,015
Age, years	44,6	49,0	51,5	53,1	0,008	0,991	0,17	0,918	0,456	49,7 0,256
Electrokinetic Index, %	48,3	43,6	42,7	40,4	0,015	0,993	0,13	0,940	0,497	40,9 0,250
Glucose Plasma, mM/L	4,57	4,11	4,94	4,69	0,008	0,972	0,54	0,658	0,748	4,70 0,160

Table 3.79 presents the standardized and raw coefficients for the discriminant variables needed to calculate the values of the discriminant roots for each person as the sum of the products of the raw coefficients by the individual values of the discriminant variables together with a constant.

At the next stage of the analysis, the actual values of the parameters were normalized and grouped into three discriminant roots based on the structural coefficients (Table 3.80). In

addition to discriminant variables, the table also presents variables that are not included in the model, but are still informal carriers of identifying information.

Table 3.79. Standardized and raw coefficients and constants for parameters of uric acid exchange, metabolism and neuroendocrine-immune complex

Coefficients	Standardized			Raw		
Variables	Root 1	Root 2	Root 3	Root 1	Root 2	Root 3
Uricosuria, mM/24 h	1,529	-0,181	0,204	2,539	-0,300	0,338
Uricemia, mM/L	1,003	0,485	-0,520	13,85	6,694	-7,174
Uricemia normalized, Z	-0,332	0,345	0,943	-0,355	0,368	1,007
PSD T4-δ, μV²/Hz	-0,133	0,091	-0,116	-0,0006	0,0004	-0,0005
PSD O2-θ, %	-0,356	0,042	0,501	-0,094	0,011	0,132
Laterality δ, %	-0,151	-0,104	0,531	-0,004	-0,003	0,015
Calcitonin, ng/L	-0,447	0,021	-0,085	-0,099	0,005	-0,019
Phagocytose Index vs Staph. aur., %	0,497	-0,395	-0,065	0,422	-0,336	-0,056
Bacteriuria, points	-0,210	-0,858	-0,427	-0,865	-3,527	-1,758
PSD C4 Entropy	0,808	1,203	-0,374	6,676	9,945	-3,092
PSD F4 Entropy	0,028	-0,886	0,319	0,179	-5,678	2,041
Pan-Lymphocytes of Blood, %	-1,371	-0,464	0,032	-0,179	-0,061	0,004
Kerdö Vegetative Index, units	0,668	0,679	0,033	0,034	0,034	0,002
Bactericidity vs Staph. aur., 10^9 Bac/L	-0,660	-0,395	-0,341	-0,027	-0,016	-0,014
IgA Saliva, mg/L	-0,710	-0,122	-0,116	-0,021	-0,005	-0,003
IgG Serum, g/L	-0,346	0,012	0,073	-0,094	0,003	0,020
PSD C3-δ, %	0,432	0,407	-0,380	0,023	0,022	-0,020
Popovych's Strain Index-1, points	0,022	0,214	-0,186	0,206	1,981	-1,722
AMo/MxDMn as SV balance Index	-0,379	-0,152	-0,046	-0,0017	-0,0007	-0,0002
Body Mass Index, kg/m²	0,395	0,449	0,225	0,112	0,127	0,064
Magnesium Plasma, mM/L	-0,139	0,282	-0,518	-3,728	7,560	-13,86
Phosphates Plasma, mM/L	-0,310	-0,294	-0,239	-1,570	-1,492	-1,214
Potassium Plasma, mM/L	-0,018	-0,304	-0,479	-0,032	-0,554	-0,874
RMSSD, msec	0,435	0,549	-0,342	0,025	0,032	-0,020
Bifidobacteria faeces, lg CFU/g	-0,426	-0,4041	0,094	-0,366	-0,347	0,080
Entropy of Immunocytogram	-0,169	0,372	-0,341	-6,341	13,94	-12,77
Creatinine Plasma, μM/L	-0,068	0,015	-0,619	-0,005	0,001	-0,046
Creatininuria, mM/24 h	-0,138	0,188	-0,406	-0,039	0,053	-0,114
			Constants	-37,08	14,51	42,59
			Eigenvalues	15,51	2,340	1,134
			Cumulative Proportio	,817	,940	1,000

Table 3.80. Correlations of variables with canonical roots, root mean values and Z-values of parameters of uric acid exchange, metabolism and neuroendocrine-immune complex

Variables	Correlations Variables-Roots			S± E- III (30)	S2- E+ II (15)	S± E+ I (21)	S- E2+ IV (22)
Root 1 (81,7%)	**R 1**	**R 2**	**R 3**	**-4,42**	-1,17	+1,43	**+5,45**
Uricosuria	**0,583**	-0,309	-0,016	**-0,97**	+1,17	+1,26	**+3,87**
Creatininuria	**0,085**	0,084	-0,025	**-1,30**	-1,15	-0,52	**-0,47**
Entropy of Immunocytogram	**0,045**	0,013	-0,076	**-0,07**	+0,07	+0,13	**+0,13**
Electrokinetic Index	currently not in model			**-0,05**	+0,17	+0,26	**+0,73**
PTH	currently not in model			**-0,60**	-0,01	+0,27	**+0,70**
IgG Serum	**-0,029**	0,047	0,046	**+1,10**	+0,65	+0,89	**+0,64**
Phagocytose Index vs St. aureus	**-0,033**	0,032	-0,088	**+0,40**	+0,39	+0,39	**+0,14**
IgA Saliva	**-0,075**	-0,014	-0,088	**-0,48**	-0,53	-0,71	**-1,15**
Calcitonin	**-0,027**	-0,044	0,107	**-0,57**	-0,60	-0,69	**-0,87**
$CD4^+CD3^+$ T-helper Lymphocyte	currently not in model			**-2,12**	-2,21	-2,93	**-3,47**
Age	currently not in model			**+0,27**	+0,14	-0,06	**-0,40**
Root 2 (12,3%)	**R 1**	**R 2**	**R 3**	+0,11	-2,26	**+2,25**	-0,77
Uricemia	0,018	**0,423**	0,204	-0,53	-1,89	**+0,09**	-0,70
PSD C4 Entropy	-0,011	**0,099**	0,032	-0,14	-0,67	**+0,07**	-0,44

Kerdö Vegetative Index	-0,006	**0,150**	-0,028	0,00	-0,29	**+0,29**	-0,18
Triiodothyronine	currently not in model			-0,49	-0,36	**-0,06**	-0,67
Bactericidity vs Staph. aureus	0,008	**0,114**	-0,035	-1,06	-1,43	**-0,25**	-1,12
PSD T4-δ, μV^2/Hz	-0,015	**0,215**	-0,134	+0,69	+0,02	**+2,60**	-0,35
PSD C3-δ, μV^2/Hz	currently not in model			+0,70	+1,80	**+2,47**	-0,20
PSD F7-θ, μV^2/Hz	currently not in model			+0,66	+0,71	**+1,59**	-0,16
PSD C3-δ, %	-0,007	**0,110**	-0,155	+0,15	+0,26	**+0,83**	-0,14
PSD T4-δ, %	currently not in model			+0,30	-0,11	**+0,78**	-0,33
AMo/MxDMn HRV	0,009	**0,176**	-0,154	-0,34	-0,47	**+1,63**	-0,07
Popovych's Strain Index-1	0,011	**0,111**	-0,197	+1,29	+1,87	**+3,83**	+1,28
Body Mass Index	0,028	**0,117**	0,040	+0,83	+0,52	**+1,21**	+1,02
Magnesium Plasma	0,028	**0,166**	-0,230	-1,55	-1,36	**-0,87**	-1,47
Killing Index vs Staph. aureus	currently not in model			-1,25	-1,32	**-0,70**	-1,12
Bacteriuria	-0,008	**-0,164**	-0,125	+1,11	+1,75	**+0,93**	+1,17
Pan-Lymphocytes	-0,002	**-0,118**	0,013	+0,34	+0,68	**-0,05**	+0,40
PSD F4 Entropy	-0,009	**-0,106**	0,115	-0,38	-0,44	**-1,20**	-0,31
Phosphates Plasma	-0,062	**-0,101**	-0,052	-0,69	-0,53	**-1,17**	-1,21
Glucose Plasma	currently not in model			-0,01	+0,32	**-0,78**	-0,17
Root 3 (6,0%)	**R 1**	**R 2**	**R 3**	+0,82	**-1,64**	-0,92	+0,89
Laterality δ, %	-0,049	0,003	**0,291**	+0,11	**-0,75**	-0,69	-0,30
PSD O2-θ, %	-0,072	-0,001	**0,277**	+0,52	**-0,45**	-0,44	-0,18
PSD T6-α, %	currently not in model			-0,43	**-0,63**	-0,46	+0,13
$CD8^+CD3^+$ T-cytolytic Lymphoc	currently not in model			-0,06	**-0,71**	-0,04	+0,06
Bifidobacteria faeces	0,002	0,001	**0,092**	-1,13	**-1,35**	-1,27	-1,09
Lactobacilli faeces	currently not in model			-1,19	**-1,35**	-1,24	-1,12
$(Ca/K)^{0,5}$ Plasma	currently not in model			+0,27	**-0,23**	+0,01	-0,01
Cortisol	currently not in model			+0,75	**+0,13**	+0,33	+0,59
Leukocyturia	currently not in model			+0,89	**+0,39**	+0,51	+0,88
Creatinine Plasma	0,012	-0,002	**-0,105**	+1,09	**+1,38**	+1,33	+1,18
Interleukin-1	currently not in model			+0,09	**+1,06**	+0,29	+0,38
Testosterone	currently not in model			+0,22	**+1,03**	+0,55	-0,12
Sex Index (M=2;F=1)	currently not in model			-0,24	**+0,39**	-0,02	+0,11
Potassium Plasma	0,035	-0,038	**-0,148**	-1,55	**-0,10**	-0,31	-0,32
RMSSD HRV	0,021	-0,070	**-0,058**	-0,01	**+0,38**	-0,31	+0,23

The result of the analysis is the visualization of each patient in the information space of discriminant roots (Fig. 3.59).

The localization of members of the **S±E-** cluster in the extreme left zone of the axis of the first root reflects the combination of **hypouricosuria** with hypocreatininuria, decreased level of PTH and normal, but **minimal** for the samples, levels of entropy of the immunocytogram and the electrokinetic index - on the one hand; and with **maximally** for the sample elevated levels of serum IgG and phagocytosis activity, minimally for the sample reduced levels of salivary IgA, T-helpers, and calcitonin, as well as the maximum average age of patients, on the other hand. At the opposite pole, members of the **S-E2+** cluster are located, in which pronounced **hyperuricosuria** is combined with the **maximum** for the sample levels of the parameters **inversely** related to the root, and the **minimum** for the sample levels of the parameters **directly** related to the root. In addition, the members of this cluster are on average the youngest in the sample.

The members of the other two clusters occupy intermediate positions and are partially mixed, which reflects the absence of significant differences between the parameters of the mentioned constellation of parameters.

However, these clusters are clearly demarcated along the axis of the second root. At the same time, the top position (centroid: +2,25) is occupied by members of the **S±E+** cluster, which are characterized, firstly, by a normal, but **maximum** for the sample, level of **uricemia** in combination with such EEG entropy in the C4 locus, Kerdö autonomic index, triiodothyronine and bactericidal activity of blood neutrophils against Staphylococcus aureus; secondly, by the **maximally** increased PSD of the delta-rhythm in the T4 and C3 loci and theta-rhythm in the F7

locus, Baevsky's sympatho-vagal balance index and Popovych's strain index, as well as body mass index; thirdly, by minimally reduced levels of the killing index of Staphylococcus aureus and the plasma magnesium, that is, the **maximum** for the sample. On the other hand, the members of this cluster have **minimal** for the sample bacteriuria and a normal level of pan-lymphocytes, and maximally reduced levels of EEG entropy in the F4 locus, as well as phosphatemia and glycemia.

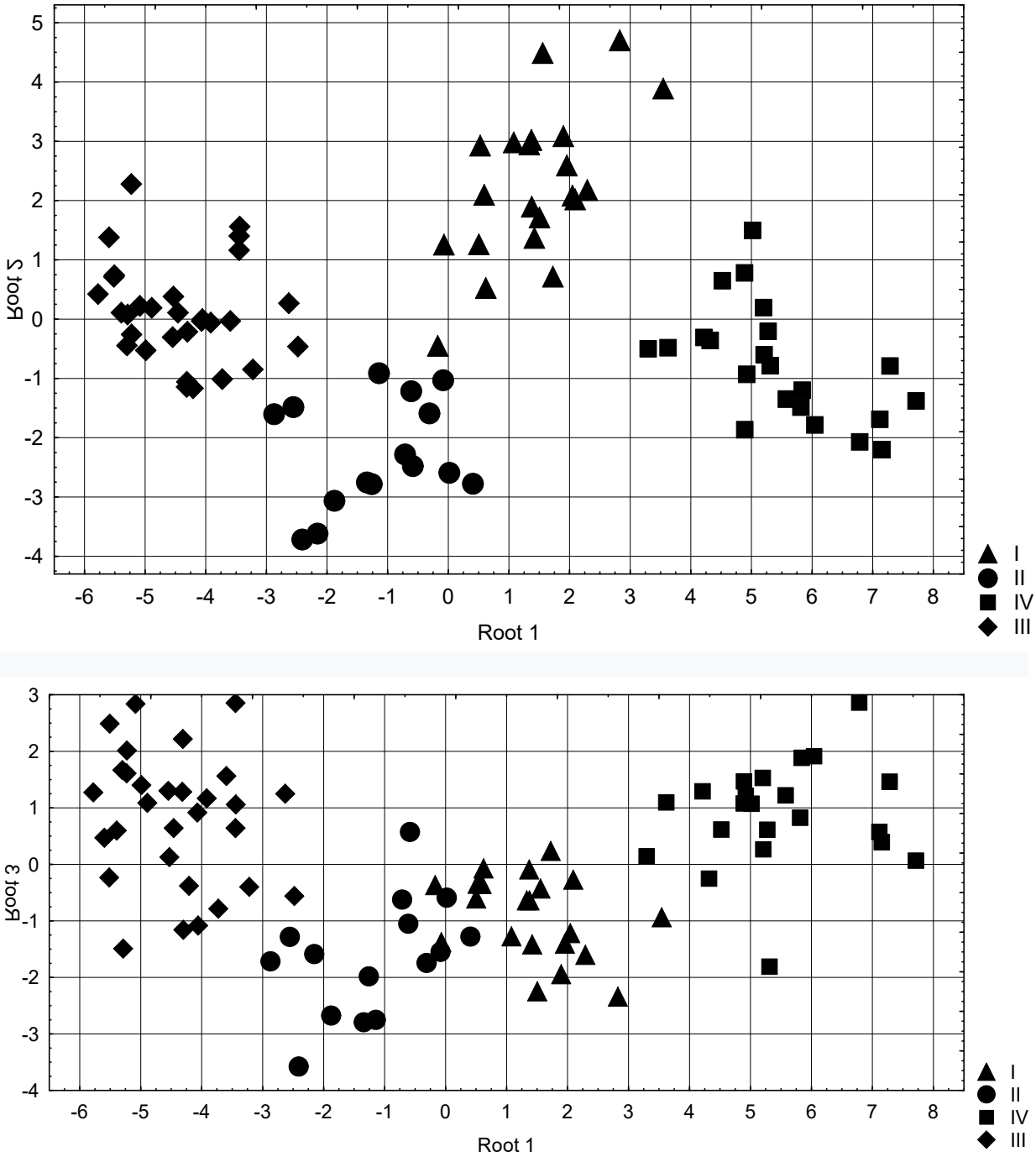

Fig. 3.59. Scattering of individual values of the integral discriminant roots of patients from different clusters

Additional demarcation of the members of the **S2-E+** cluster occurs along the axis of the third root, which reflects, firstly, their left lateralization of the delta-rhythm and **maximally reduced** PSD of the theta-rhythm in the O2 locus and alpha-rhythm in the T6 locus, the content of T-killers in the blood and favorable acidophilic microflora in feces; secondly, normal, but

minimal for the sample levels of cortisolemia, Ca/K-marker of sympathetic-vagal balance and leukocyturia. On the other hand, among the members of this cluster, the **maximum** percentage of men and the **maximally** elevated plasma levels of testosterone, creatinine, and IL-1 and normal, but **maximal** for the sample, levels of plasma potassium and vagotonia.

The apparent clear demarcation of all four clusters is documented by the calculation of Mahalanobis distances (Table 3.81).

Table 3.81. Squares of Mahalanobis distances between clusters, F-criterions (df=28,6) and p-levels

Clusters	S±E+ I	S2-E+ II	S-E2+ IV	S±E- III
S±E+ I (21)	0	27,6	28,6	41,7
S2-E+ II (15)	5,9 10^{-6}	0	52,5	22,2
S-E2+ IV (22)	7,4 10^{-6}	11,3 10^{-6}	0	98,2
S±E- III (30)	12,5 10^{-6}	5,4 10^{-6}	30,2 10^{-6}	0

Another result of discriminant analysis is the possibility of retrospective identification of members of different clusters by calculating individual discriminant functions according to the coefficients and constants given in the Table 3.82.

Table 3.82. Coefficients and constants for cluster classification functions

Clusters	S±E+ I	S2-E+ II	S-E2+ IV	S±E- III
Variables	p=,239	p=,170	p=,250	p=,341
Uricosuria, mM/24 h	89,13	83,64	100,9	75,51
Uricemia, mM/L	194,2	133,3	216,8	86,54
Uricemia normalized, Z	-62,88	-64,34	-63,60	-59,85
PSD T4-δ, $\mu V^2/Hz$	-0,148	-0,148	-0,153	-0,146
PSD O2-θ, %	-6,565	-6,466	-6,739	-5,808
Laterality δ, %	0,897	0,911	0,916	0,956
Calcitonin, ng/L	-1,975	-1,723	-2,423	-1,435
Phagocytose Index vs Staph. aur., %	154,3	154,8	156,9	152,5
Bacteriuria, points	74,64	94,07	78,63	84,19
PSD C4 Entropy	160,1	100,1	151,4	94,44
PSD F4 Entropy	-194,0	-170,3	-172,5	-179,4
Pan-Lymphocytes of Blood, %	-14,62	-13,89	-15,15	-13,44
Kerdö Vegetative Index, units	2,699	2,457	2,734	2,433
Bactericidity vs Staph. aur., 10^9 Bac/L	-0,870	-0,717	-0,956	-0,701
IgA Saliva, mg/L	-1,785	-1,713	-1,864	-1,663
IgG Serum, g/L	-4,180	-3,966	-4,532	-3,604
PSD C3-δ, %	1,097	0,954	1,089	0,882
Popovych's Strain Index-1, points	-226,0	-234,2	-234,2	-234,4
AMo/MxDMn as SV balance Index	0,108	0,116	0,103	0,119
Body Mass Index, kg/m^2	9,098	8,187	9,280	8,282
Magnesium Plasma, mM/L	211,3	196,9	148,4	192,9
Phosphates Plasma, mM/L	64,89	76,58	60,88	75,16
Potassium Plasma, mM/L	-5,639	-2,424	-5,675	-5,781
RMSSD, msec	3,845	3,651	3,815	3,597
Bifidobacteria faeces, lg CFU/g	-5,063	-2,605	-5,345	-2,042
Entropy of Immunocytogram	3460	3423	3369	3445
Creatinine Plasma, µM/L	4,455	4,497	4,348	4,403
Creatininuria, mM/24 h	6,295	6,240	5,773	6,211
Constants	-9544	-9545	-9672	-9291

Taking into account all features enables the retrospective recognition of members of all clusters almost without error: the classification accuracy is 98,9% (Table 3.83).

Table 3.83. Classification matrix for clusters
Rows: observed classifications; columns: predicted classifications

	Percent	S±E+ I	S2-E+ II	S-E2+ IV	S±E- III
Clusters	correct	p=,239	p=,170	p=,250	p=,341
I	95,2	**20**	1	0	0
II	100	0	**15**	0	0
IV	100	0	0	**22**	0
III	100	0	0	0	**30**
Total	98,9	20	16	22	30

In order to study the relationship between parameters of uric acid exchange and all other parameters registered in this study, a canonical correlation analysis procedure was performed. The program selects two almost equal pairs of canonical roots. The uric acid root of the first pair represents, mainly, uricosuria, while actual and normalized uricemia give significantly smaller and opposite factor loads on the root (Table 3.84). The factor structure of the resulting root is represented, almost entirely, by parameters that are subject to upregulation by uricosuria. These are 4 HRV-markers of vagal tone, EEG entropy in the F7 and F8 loci, PSD of alpha-rhythm in the F7 locus and theta-rhythm in the T5 locus, as well as metabolic parameters: excretion of urea, chloride, sodium and creatinine as well as lithogenicity of urine. On the other hand, beta-rhythm PSD in the T6 locus was subject to upregulation by uricemia, and in the F7 locus - to downregulation by uricosuria. In general, uric acid determines this constellation of parameters by 88% (Fig. 3.60).

Table 3.84. Factor structure of the first pair of canonical roots of parameters of uric acid exchange (left set) and EEG&HRV and metabolic parameters (right set)

Left set	***Root 1***
Uricosuria, mM/24 h	**-0,886**
Uricemia, mM/L	**0,493**
Uricemia normalized, Z-score	**0,472**
Right set	**Root 1**
LF Power HRV, msec^2	**-0,466**
LF Power HRV, %	**-0,411**
PTH	**-0,400**
MxDMn HRV as Vagal tone	**-0,268**
VLF Power HRV, msec^2	**-0,244**
PSD F7 Entropy	**-0,231**
PSD F8 Entropy	**-0,170**
PSD F8-α, %	**-0,251**
PSD T5-θ, %	**-0,162**
PSD T6-β, μV^2/Hz	**0,216**
PSD F7-β, μV^2/Hz	**0,196**
Urea Excretion, mM/24 h	**-0,603**
(Cau•UAu/Mgu•Cru)^{0,25} as Urolithogenicity, un	**-0,404**
Chloride Excretion, mM/24 h	**-0,317**
Sodium Excretion, mM/24 h	**-0,319**
Creatininuria, mM/24 h	**-0,309**

Instead, the uric acid root of the second pair (Table 3.85) is mainly represented by uricemia, both actual (to a greater extent) and normalized (to a lesser extent). Uricosuria gives a smaller factor load on the root, but unidirectional, which simplifies the interpretation of uric acid

determination of parameters, information about which is condensed in the resulting canonical root.

Downregulation of 7 EEG parameters, 3 HRV-markers of vagal tone and triiodothyronine level was revealed by uric acid, instead of upregulation of 4 EEG parameters and HRV-marker of sympatho-vagal balance. Such a neuro-endocrine pattern is accompanied by downregulation of the relative levels of T-helpers and polymorphonuclear neutrophils in the blood, the concentration of IgG in saliva, and the content of Escherichia coli with weakened enzymatic activity in feces, instead by a upregulation of the completion of phagocytosis by blood neutrophils of representatives of gram-positive and gram-negative microbes, the relative level of lymphocytes in the blood in general and the population of natural killers in particular, as well as the entropy of the immunocytogram. The metabolic effects of uric acid are manifested by a positive effect on the excretion of urea, chloride and sodium, the lithogenicity of urine, the plasma levels of creatinine and calcium, but a negative effect on glycemia. This constellation of parameters is determined by uric acid by 77% (Fig. 3.61).

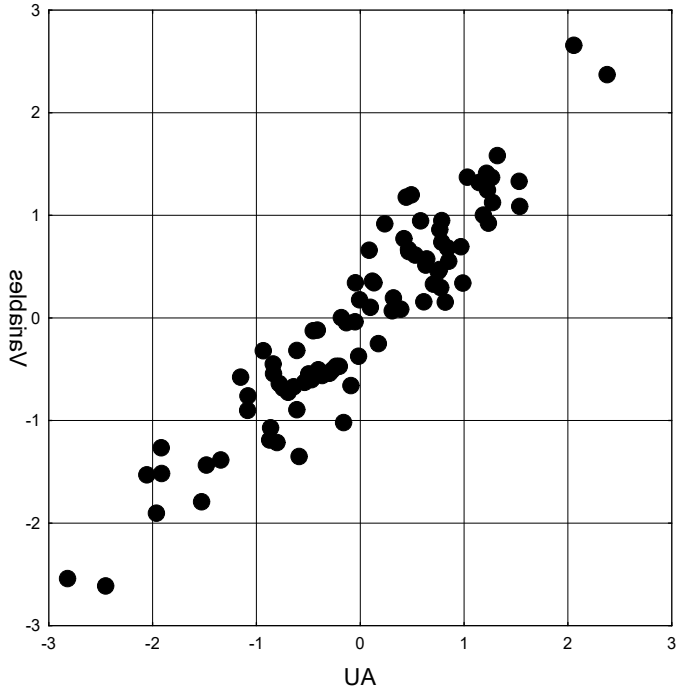

R=0,940; R^2=0,883; $\chi^2_{(117)}$=293; $p<10^{-6}$; Lambda Prime=0,011

Fig. 3.60. Scatterplot of the canonical correlation between parameters of uric acid exchange (line X) and neural and metabolic parameters (line Y). The first pair of roots

Table 3.85. Factor structure of the second pair of canonical roots of parameters of uric acid exchange (left set) and neuro-endocrine, immune and metabolic parameters (right set)

Left set	**Root 2**
Uricemia, mM/L	**-0,689**
Uricosuria, mM/24 h	**-0,382**
Uricemia normalized, Z-score	**-0,283**
Right set	**Root 2**
PSD P4-δ, %	**0,389**
PSD T5-θ, %	**0,333**
PSD P3-δ, %	**0,324**
PSD C3-θ, μV^2/Hz	**0,312**
PSD F7 Entropy	**0,303**
PSD F8 Entropy	**0,300**
Index β, %	**0,221**
MxDMn HRV as Vagal tone	**0,383**
VLF Power HRV, $msec^2$	**0,374**
LF Power HRV, $msec^2$	**0,292**

Triiodothyronine, nM/L	0,315
PSD T4-β, %	-0,394
PSD F4-β, %	-0,386
PSD T3-β, %	-0,281
PSD P3-α, %	-0,266
Baevski Stress Index HRV, ln units	-0,192
$CD4^+CD3^+$ T-helper Lymphocytes, %	0,673
IgG Saliva, mg/L	0,653
Polymorphonucleary Neutrophils of Blood, %	0,499
E. coli attenuated faeces, %	0,496
$CD56^+$ Natural Killer Lymphocytes, %	-0,542
Killing Index vs E. coli, %	-0,476
Killing Index vs Staph. aureus, %	-0,446
Pan-Lymphocytes of Blood, %	-0,436
Entropy of Immunocytogram	-0,425
Urea Excretion, mM/24 h	-0,475
Creatinine Plasma, μM/L	-0,464
$(Cau•UAu/Mgu•Cru)^{0,25}$ as Urolithogenicity, uns	-0,408
Calcium Plasma, mM/L	-0,259
Chloride Excretion, mM/24 h	-0,252
Sodium Excretion, mM/24 h	-0,252
Glucose Plasma, mM/L	0,275

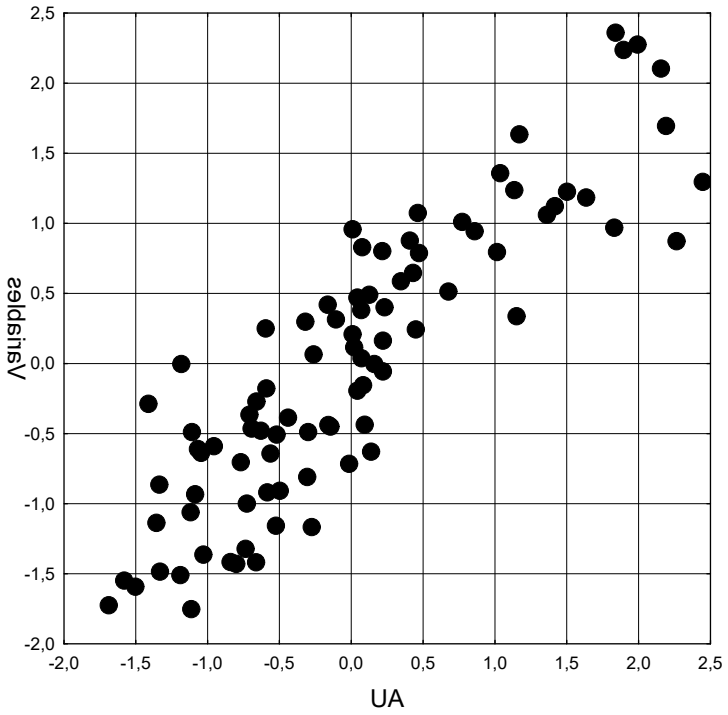

$R=0,878$; $R^2=0,771$; $\chi^2_{(76)}=152$; $p<10^{-6}$; Lambda Prime=0,098

Fig. 3.61. Scatterplot of the canonical correlation between parameters of uric acid exchange (line X) and neuroendocrine, immune and metabolic parameters (line Y). The second pair of roots

The influence of uric acid on the registered parameters is even more noticeable when analyzing the relationships between **individual changes** in parameters as a result of adaptogenic balneotherapy.

A canonical correlation analysis conducted using a similar algorithm also revealed two pairs of canonical roots. The first pair demonstrates that the dynamics of uricosuria and uricemia positively determine the dynamics of, first, the PSD of theta-rhythm in the T3 locus and beta-rhythm in the O2 locus, PTH level as well as HRV-markers of vagal tone and sympatho-vagal balance; secondly, of diuresis and excretion of urea, magnesium, sodium, phosphates, calcium,

potassium and chloride, as well as calcemia and magnesiumemia; thirdly, of serum IgG and CIC. Instead, changes in cortisolemia and testosteroneemia as well as TNF-alpha and the intensity of Staph. aureus phagocytosis are subject to negative determination (Table 3.86).

The dynamics of such a constellation of parameters is determined by the dynamics of uric acid by 96% (Fig. 3.62).

Table 3.86. Factor structure of the first pair of canonical roots of changes in parameters of uric acid (left set) and neuro-endocrine, metabolic and immune parameters (right set)

Left set	Root 1
Uricosuria, mM/24 h	-0,835
Uricemia, mM/L	-0,539
Right set	Root 1
PSD T3-θ, %	-0,332
PSD O2-β, %	-0,289
LF/HF as Sympatho/Vagal balance	-0,218
RMSSD HRV, msec	-0,213
Parathyroid hormone, pM/L	-0,200
Cortisol, nM/L	0,270
Testosterone, nM/L	0,139
Diurese, L/24 h	-0,664
Urea Excretion, mM/24 h	-0,630
Magnesium Excretion, mM/24 h	-0,307
Sodium Excretion, mM/24 h	-0,247
Phosphates Excretion, mM/24 h	-0,213
Calcium Excretion, mM/24 h	-0,194
Potassium Excretion, mM/24 h	-0,189
Chloride Excretion, mM/24 h	-0,143
Calcium Plasma, mM/L	-0,211
Magnesium Plasma, mM/L	-0,122
IgG Serum, g/L	-0,266
Circulating Immune Complicis, units	-0,201
Microbian Count vs Staph. aur., Bact/Phagocyte	0,263
TNF-alpha, ng/L	0,106

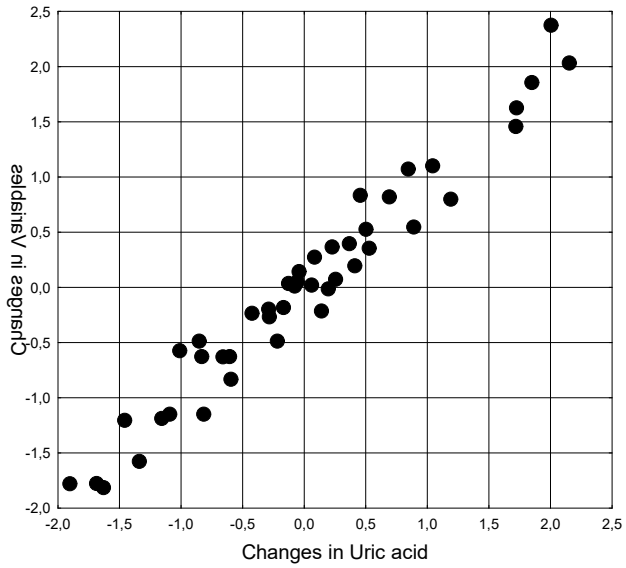

R=0,978; R^2=0,956; $\chi^2_{(76)}$=135; $p<10^{-4}$; Lambda Prime=0,003

Fig. 3.62. Scatterplot of the canonical correlation between changes in uricosuria and uricemia (line X) and neuro-endocrine, metabolic, and immune parameters (line Y). The first pair of roots

The factor structure of the second pair of roots is heterogeneous, therefore more difficult to interpret (Table 3.87). The dynamics of uricemia - the major element of the uric acid root - negatively determines the PSD dynamics of the beta-rhythm in 5 loci and the alpha-rhythm in the T5 locus, as well as calcitonin and T-helpers. Instead, the PSD of the delta-rhythm in the T5 locus, the alpha-rhythm in the P4 and P3 loci, electrolyte markers of sympatho-vagal balance, levels in the blood of chloride, sodium, calcium and magnesium, as well as monocytes and CIC are subject to upregulation. The dynamics of uricosuria - a minor element of the uric acid root - negatively determines the dynamics of the alpha-rhythm index and testosteroneemia, but positively – HRV-markers of vagal tone and sympatho-vagal balance, PTH level as well as diuresis and excretion of urea, magnesium, phosphates, calcium, and potassium. In general, uric acid determination of the dynamics of the listed parameters is 94% (Fig. 3.63).

Table 3.87. Factor structure of the second pair of roots of changes in parameters of Uric acid exchange (left set) and neuro-endocrine, metabolic and immune parameters (right set)

Left set	Root 2
Uricemia, mM/L	-0,842
Uricosuria, mM/24 h	0,550
Right set	Root 2
PSD P4-β, %	0,588
PSD P3-β, %	0,553
PSD T6-β, %	0,473
PSD C4-β, %	0,402
PSD C3-β, %	0,363
PSD T5-α, %	0,268
Calcitonin, ng/L	0,251
$CD4^+CD3^+$ T-helper Lymphocytes, %	0,612
PSD T5-δ, %	-0,308
PSD P4-α, $\mu V^2/Hz$	-0,305
PSD P3-α, $\mu V^2/Hz$	-0,252
$(Ca/K)^{0,5}$ Plasma as Sympatho/Vagal balance	-0,308
Chloride Plasma, mM/L	-0,276
Sodium Plasma, mM/L	-0,276
Calcium Plasma, mM/L	-0,201
Magnesium Plasma, mM/L	-0,136
Monocytes of Blood, %	-0,309
Circulating Immune Complicis, units	-0,238
Index α, %	-0,325
Testosterone, nM/L	-0,159
LF/HF as Sympatho/Vagal balance	0,170
RMSSD HRV, msec	0,163
Parathyroid hormone, pM/L	0,200
Urea Excretion, mM/24 h	0,474
Diurese, L/24 h	0,462
Calcium Excretion, mM/24 h	0,372
Phosphates Excretion, mM/24 h	0,319
Magnesium Excretion, mM/24 h	0,245
Potassium Plasma, mM/L	0,175

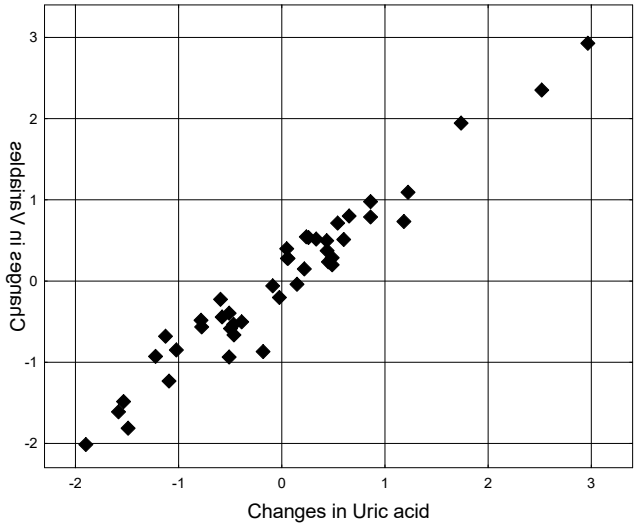

R=0,971; R^2=0,943; $\chi^2_{(37)}$=65; p=0,0033; Lambda Prime=0,057

Fig. 3.63. Scatterplot of the canonical correlation between changes in UA (line X) and neuro-endocrine, metabolic, and immune parameters (line Y). The second pair of roots

In conclusion, we will analyze neuroendocrine-metabolic and neuroendocrine-immune interrelationships. It was found that the dynamics of neuroendocrine parameters determines the dynamics of metabolic parameters by 85% (Tables 3.88 and 3.89, Fig. 3.64).

Table 3.88. Factor structure of canonical roots of changes in neuroendocrine (left set) and metabolic (right set) parameters

Left set	R
PSD O2-β, %	0,655
PSD T6-β, %	0,633
PSD P4-β, %	0,614
PSD C4-β, %	0,472
PSD C3-β, %	0,409
PSD T3-θ, %	0,357
PSD P3-β, %	0,312
PSD T5-α, %	0,518
Parathyroid hormone, pM/L	0,750
Calcitonin, ng/L	0,249
LF/HF as Sympatho/Vagal balance	0,204
PSD P4-α, μV^2/Hz	-0,602
PSD P3-α, μV^2/Hz	-0,520
Index α, %	-0,599
PSD T5-δ, %	-0,536
Cortisol, nM/L	-0,391
Testosterone, nM/L	-0,175
Right set	**R**
Calcium Excretion, mM/24 h	0,774
Diurese, L/24 h	0,461
Phosphates Excretion, mM/24 h	0,441
Magnesium Excretion, mM/24 h	0,387
Urea Excretion, mM/24 h	0,187
Potassium Plasma, mM/L	0,578
Magnesium Plasma, mM/L	-0,540
Chloride Excretion, mM/24 h	-0,295
Sodium Excretion, mM/24 h	-0,334

Table 3.89. Correlation matrix for changes in neuroendocrine and metabolic parameters

variable	Correlations, left set with right set								
	Urea E	Mg	K	Diur	Ca Ex	P Ex	Mg Ex	Cl Ex	Na Ex
Cortisol	-0,12	0,21	-0,37	-0,12	-0,29	-0,08	-0,11	0,18	0,17
Calcitonin	-0,13	-0,06	0,32	-0,06	0,03	0,08	-0,11	-0,42	-0,39
PTH	0,33	-0,16	0,36	0,44	0,89	0,83	0,63	0,04	0,05
Testosterone	-0,06	0,22	0,06	-0,11	-0,19	-0,44	-0,05	0,14	0,13
LF/HF	0,34	-0,25	0,11	0,24	0,17	0,01	0,30	0,04	0,05
Index Alpha	-0,07	0,53	-0,19	-0,19	-0,51	-0,36	-0,27	0,20	0,21
T3T%	0,25	-0,00	0,10	0,42	0,26	0,04	0,20	0,19	0,19
T5A%	0,01	-0,49	0,36	-0,05	0,44	0,02	0,05	-0,15	-0,30
T5D%	-0,08	0,43	-0,36	-0,06	-0,41	0,01	-0,07	0,11	0,23
C3B%	0,08	-0,32	0,21	0,17	0,20	0,01	0,15	-0,06	-0,08
C4B%	0,17	-0,28	0,20	0,28	0,25	0,03	0,30	-0,09	-0,11
T6B%	0,11	-0,47	0,28	0,24	0,42	0,15	0,32	-0,10	-0,15
P3B%	0,13	-0,21	0,15	0,15	0,29	0,09	0,22	0,04	0,01
P3A	-0,06	0,43	-0,20	-0,11	-0,46	-0,28	-0,21	0,22	0,27
P4B%	0,19	-0,29	0,38	0,33	0,33	0,21	0,25	-0,17	-0,19
P4A	-0,04	0,41	-0,28	-0,12	-0,53	-0,35	-0,37	0,23	0,28
O2B%	0,01	-0,36	0,27	0,31	0,35	0,09	0,13	-0,08	-0,09

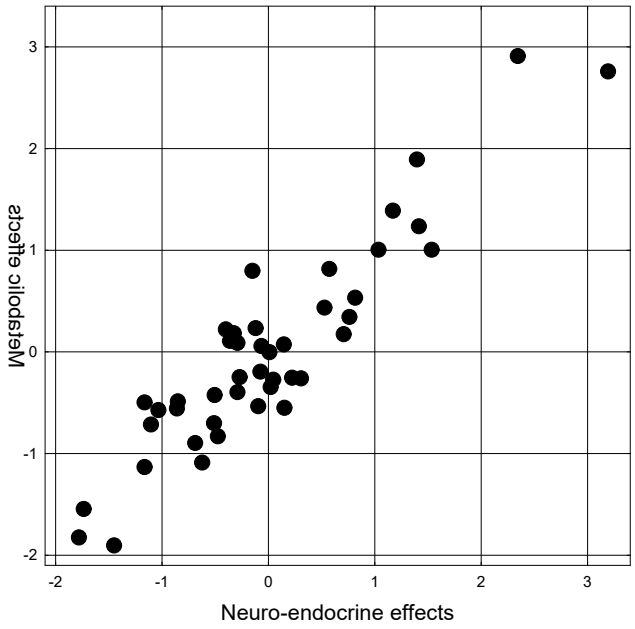

R=0,921; R^2=0,848; $\chi^2_{(153)}$=183; p=0,047; Lambda Prime=0,002

Fig. 3.64. Scatterplot of canonical correlation between changes in neuroendocrine (line X) and metabolic (line Y) parameters

Neuroendocrine determination of immune parameters is 54% (Tables 3.90 and 3.9, Fig. 3.65).

Table 3.90. Factor structure of canonical roots of changes in neuroendocrine (left set) and immune (right set) parameters

Left set	R
Calcitonin, ng/L	0,785
RMSSD HRV, msec	0,327
PSD P4-β, %	0,542
PSD P3-β, %	0,393

PSD T6-β, %	0,333
PSD C4-β, %	0,272
PSD C3-β, %	0,256
PSD P4-α, $\mu V^2/Hz$	-0,402
Right set	**R**
Circulating Immune Complicis, units	-0,507
Microbian Count vs Staph. aur., Bact/Phag	-0,213
$CD4^+CD3^+$ T-helper Lymphocytes, %	0,677
TNF-alpha, ng/L	0,393
Monocytes of Blood, %	0,124

Table 3.91. Correlation matrix for changes in neuroendocrine and immune parameters

Root Removed	Correlations, left set with right set				
	TNFa	MC Sa	Mon	TH	CIC
Calcitonin	0,33	-0,02	0,08	0,25	-0,44
RMSSD	0,11	-0,35	0,23	0,20	0,12
C3B%	0,10	0,08	0,08	0,14	-0,14
C4B%	0,18	-0,00	0,04	0,24	0,04
T6B%	0,27	0,03	-0,01	0,13	-0,12
P3B%	0,02	-0,02	-0,11	0,26	-0,17
P4B%	0,21	0,01	0,07	0,32	-0,17
P4A	-0,14	-0,00	-0,07	-0,32	0,04

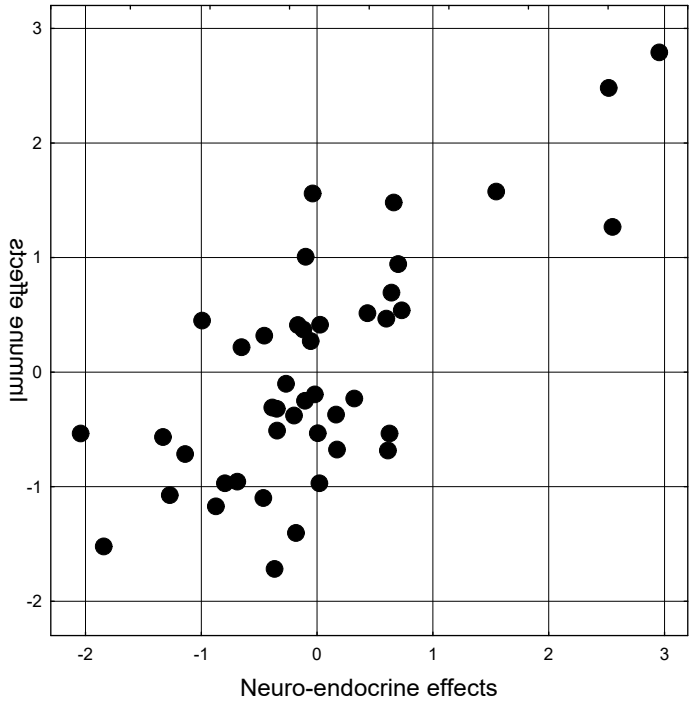

R=0,735; R^2=0,540; $\chi^2_{(40)}$=57; p=0,040; Lambda Prime=0,205

Fig. 3.65. Scatterplot of canonical correlation between changes in neuro-endocrine (line X) and immune (line Y) parameters

CHAPTER 4

SEXUAL DIMORPHISM IN RELATIONSHIPS BETWEEN SERUM URIC ACID AND SOME PSYCHO-NEURO-ENDOCRINE PARAMETERS

Earlier we found that relationships between plasma nitrogenous metabolites such as urea, creatinine, bilirubin and neuro-endocrine parameters, as well as anxiety, are significantly different in men and women of different ages [Bombushkar IS, Gozhenko AI et al, 2022; Bombushkar IS, Korda MM et al, 2022; Bombushkar IS, Anchev AS et al, 2022; Popovych IL et al, 2022]. The purpose of this chapter is to analyze the relationships between the serum uric acid level and some psycho-neuro-endocrine parameters in the same cohort.

The object of observation were employees of the clinical sanatorium "Moldova" and PrJSC “Truskavets’ Spa”: 31 males (24÷69 y) and 30 females, from among them 18 postmenopausal (45÷76 y) and 12 of reproductive age (30÷42 y). The volunteers were considered practically healthy (without a clinical diagnosis), but the initial testing revealed deviations from the norm in a number of parameters of the neuro-endocrine-immune complex as a manifestation of maladaptation. Testing was performed twice with an interval of 4 (in 11 men and 10 women; "Moldova") or 7 (in 10 men and 10 women; “Truskavets’ Spa”) days.

We determined the serum levels of the Uric acid as well as main adaptation hormones Cortisol, Aldosterone, Testosterone, Triiodothyronine and Calcitonin; registered HRV and EEG. In addition, we estimated the levels of the trait and reactive anxiety by STAI of Spielberger ChD [1983] in modification of Khanin YL [1998].

Screening of correlations of uricemia with psycho-neuro-endocrine parameters in men revealed the strongest positive relationship with testosteroneemia (Fig. 4.1).

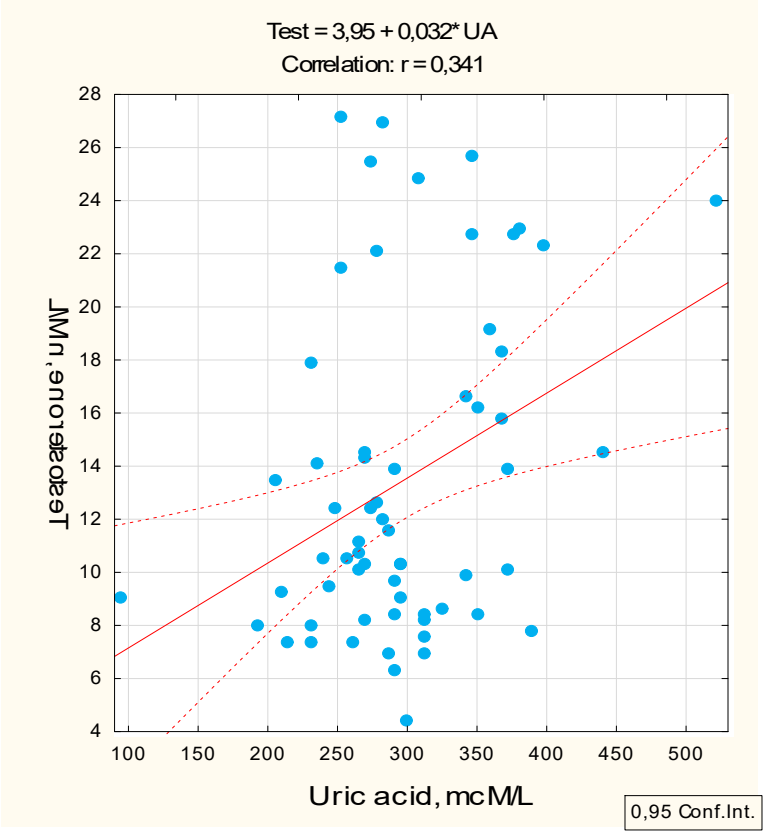

Fig. 4.1. Scatterplot of correlation between Uricemia (X-line) and Testosterone level (Y-line) in Men

The strongest negative relationship was found with PSD of δ-rhythm in O1 locus (Fig. 4.2). By chance, we would like to draw attention to the fact that an abnormally low level of uricemia

accompanies a drastically large PSD. This is about the problem of so-called outliers and the need to remove them from the analysis. In favor of their non-removal, Fig. 4.3.

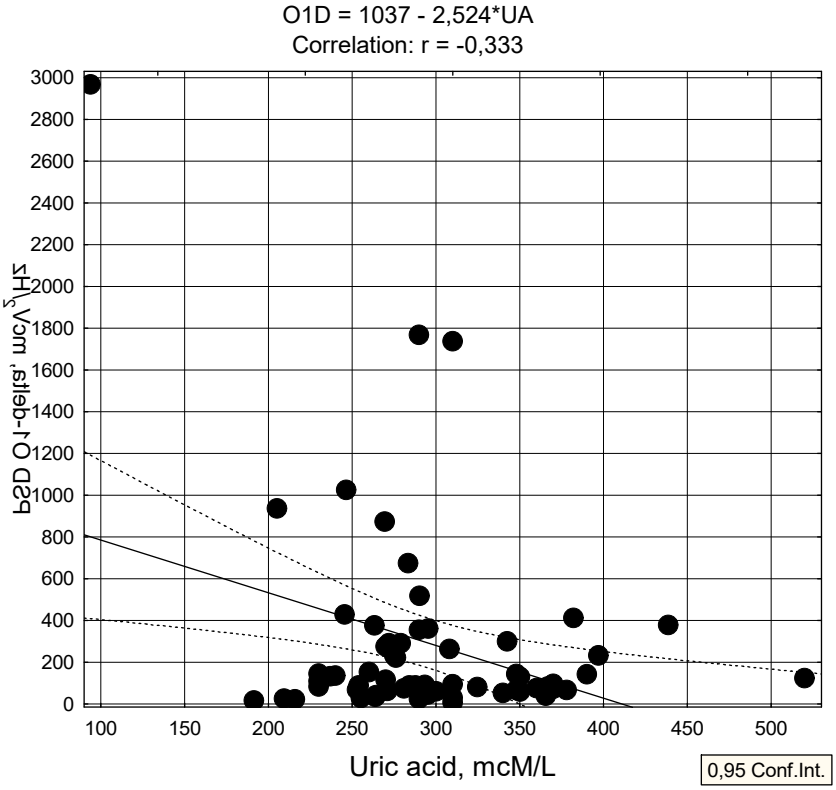

Fig. 4.2. Scatterplot of correlation between Uricemia (X-line) and absolute PSD of delta-rhythm in O1 locus (Y-line) in Men

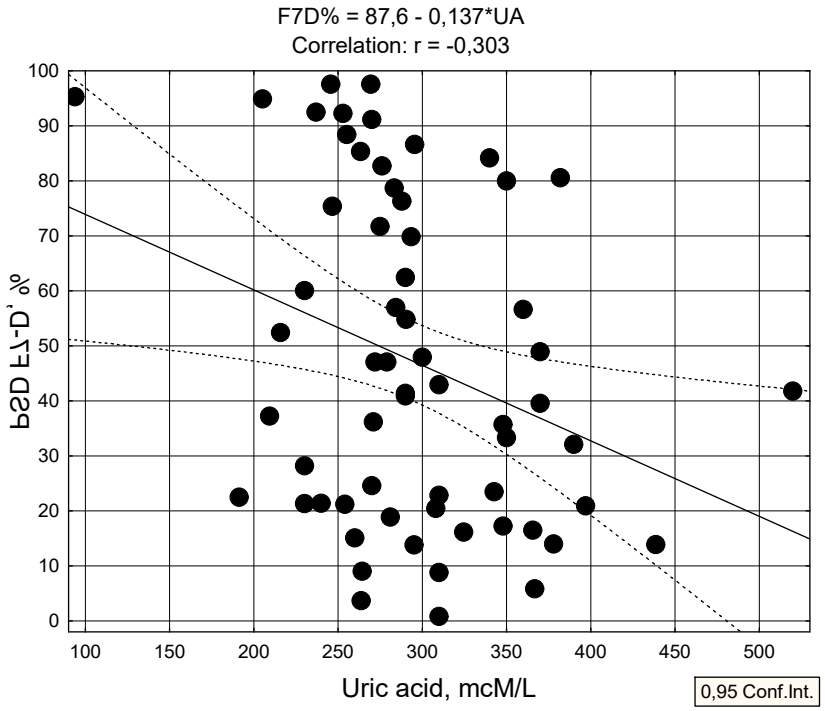

Fig. 4.3. Scatterplot of correlation between Uricemia (X-line) and relative PSD of delta-rhythm in F7 locus (Y-line) in Men

No significant correlations between uricemia and other hormones, as well as anxiety and HRV parameters, were found.

By uric acid regression models with stepwise exclusion, it was found that in men uricemia downregulates the PSD of β-rhythm in P4 and δ-rhythm in others 4 loci, but upregulates the asymmetry of δ-rhythm, variability of α-rhythm, PSD of θ-rhythm in P3 and O1 loci, Entropy of EEG in T4 as well as Testosterone level. The measure of determination is 54,5% (Table 4.1 and Fig. 4.4).

Table 4.1. Regression Summary for Uricemia in Men

R=0,738; R^2=0,545; Adjusted R^2=0,433; $F_{(12,5)}$=4,9; $p<10^{-4}$

N=62		Beta	St. Err. of Beta	B	SE of B	$t_{(49)}$	p-level
Variables	r		Intercpt	182,2	51,5	3,54	0,001
P4-β PSD, %	**-0,30**	-0,228	0,114	-1,328	0,664	-2,00	0,051
O1-δ PSD, μV^2/Hz	**-0,33**	-0,431	0,132	-0,057	0,017	-3,28	0,002
F7-δ PSD, %	**-0,30**	-0,386	0,154	-0,851	0,339	-2,51	0,015
Fp1-δ PSD, μV^2/Hz	**-0,30**	-0,407	0,166	-0,030	0,012	-2,45	0,018
Fp1-δ PSD, %	**-0,22**	0,446	0,194	1,087	0,473	2,30	0,026
O2-δ PSD, μV^2/Hz	**-0,22**	0,324	0,165	0,030	0,015	1,97	0,055
Asymmetry-δ, %	**0,23**	0,415	0,111	0,998	0,268	3,72	0,001
Testosterone, mM/L	**0,34**	0,138	0,108	1,466	1,147	1,28	0,207
Deviation-α, Hz	**0,23**	0,339	0,112	45,31	15,02	3,02	0,004
Entropy PSD T4	**0,23**	0,197	0,149	56,83	42,85	1,33	0,191
P3-θ PSD, μV^2/Hz	**0,21**	0,198	0,126	0,357	0,227	1,57	0,122
O1-θ PSD, %	**0,21**	-0,176	0,127	-2,217	1,599	-1,39	0,172

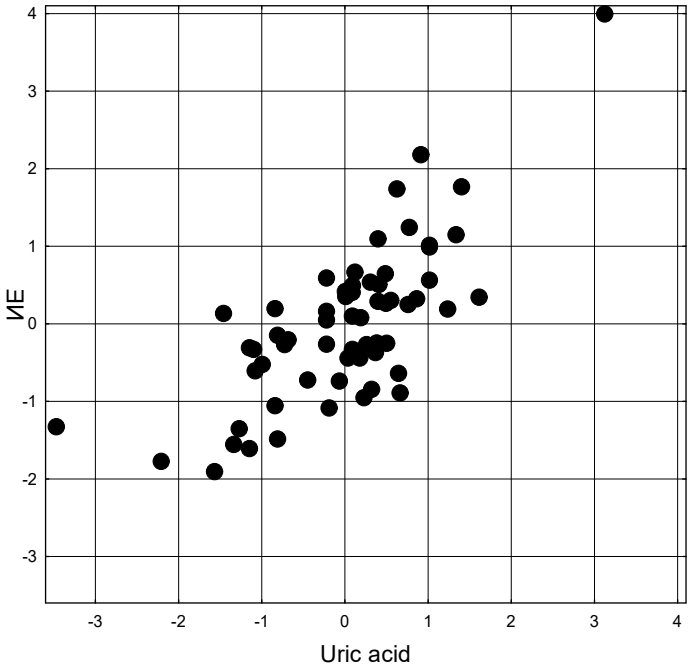

R=0,738; R^2=0,545; $\chi^2_{(12)}$=42; $p<10^{-4}$; Λ Prime=0,455

Fig. 4.4. Scatterplot of canonical correlation between Uricemia (X-line) and Neuro-Endocrine parameters (Y-line) in Men

In postmenopausal women, uricemia downregulates the Amplitude of β-rhythm (Fig. 4.5) and its PSD in 8 loci (Fig. 4.6 and Table 4.2) as well as sympathetic tone (Fig. 4.7 and Table 4.2), but upregulates the PSD of HF and VLF bands HRV (Table 4.2), Testosterone level (Fig. 4.8), PSD of θ-rhythm in F3 (Fig. 4.9) and O2 loci as well as the Laterality of δ-rhythm (Table 4.2).

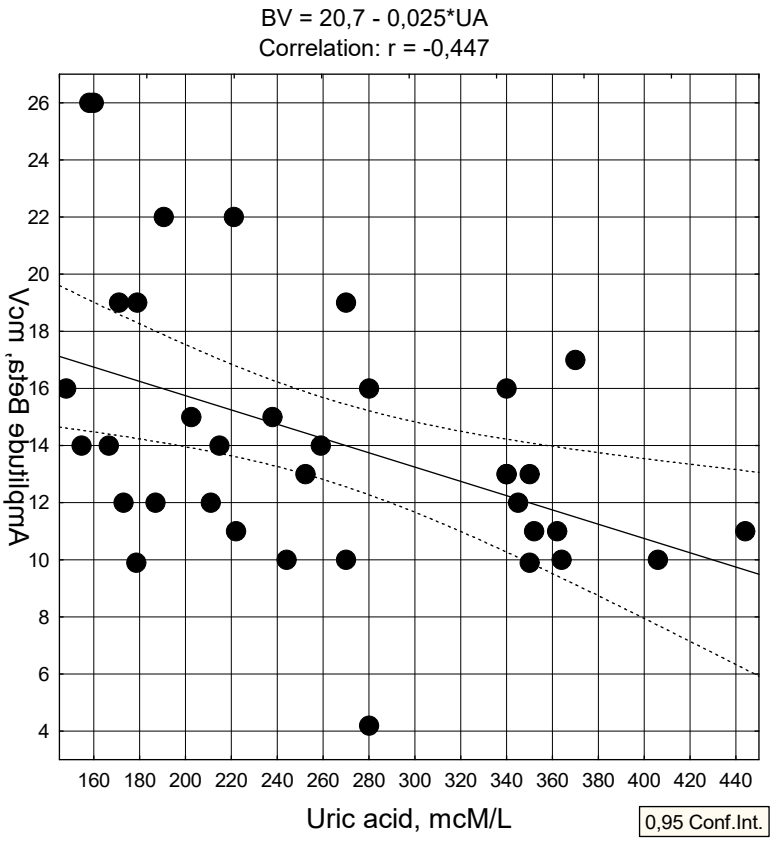

Fig. 4.5. Scatterplot of correlation between Uricemia (X-line) and Amplitude of beta-rhythm (Y-line) in postmenopausal Women

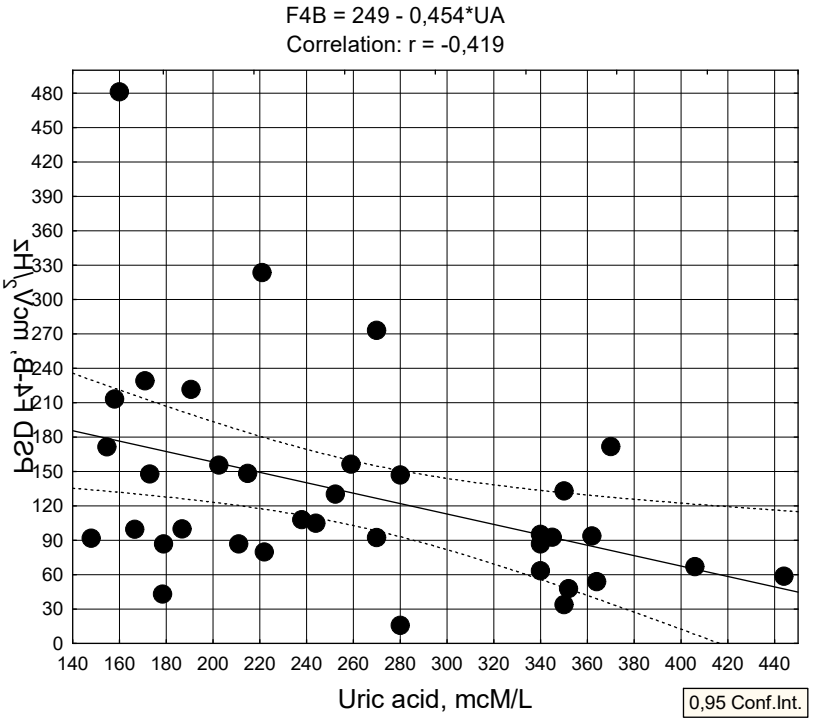

Fig. 4.6. Scatterplot of correlation between Uricemia (X-line) and absolute PSD of beta-rhythm in F4 locus (Y-line) in postmenopausal Women

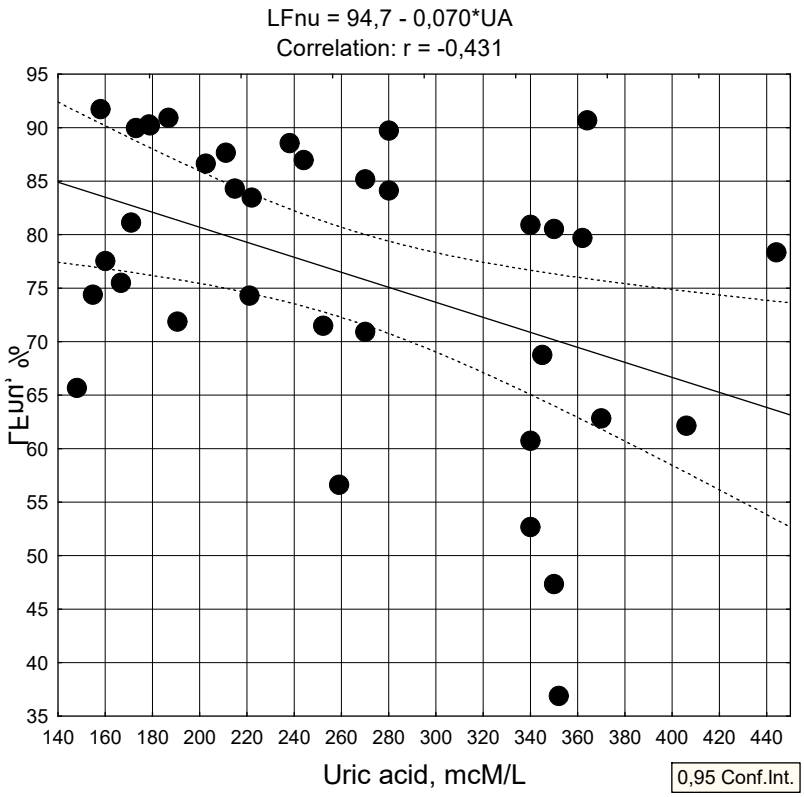

Fig. 4.7. Scatterplot of correlation between Uricemia (X-line) and LFnu HRV (Y-line) in postmenopausal Women

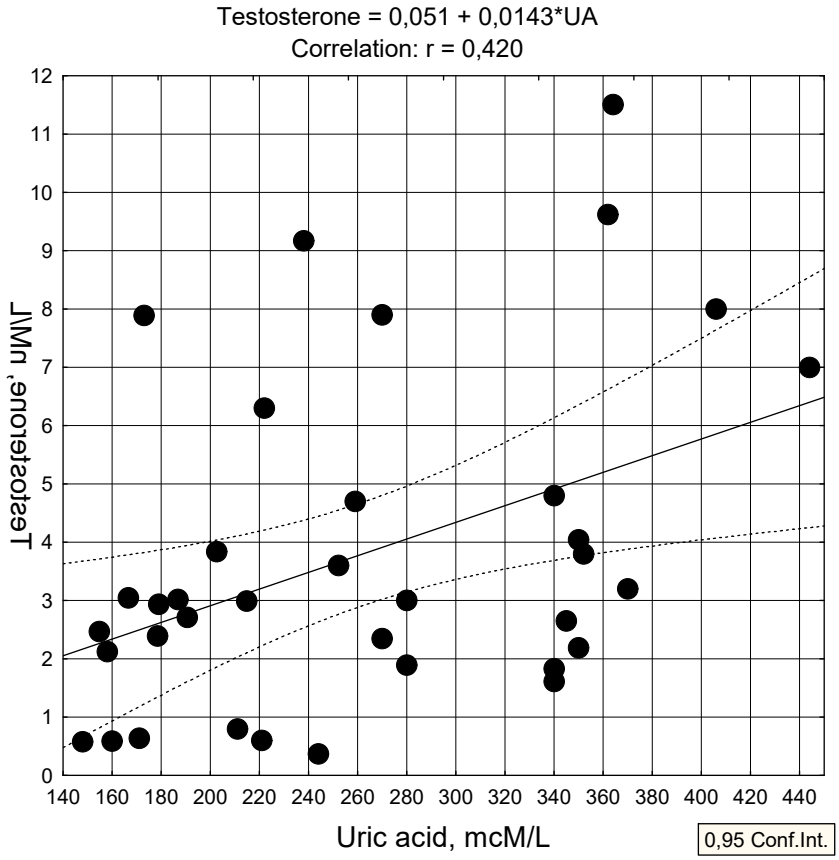

Fig. 4.8. Scatterplot of correlation between Uricemia (X-line) and Testosterone level (Y-line) in postmenopausal Women

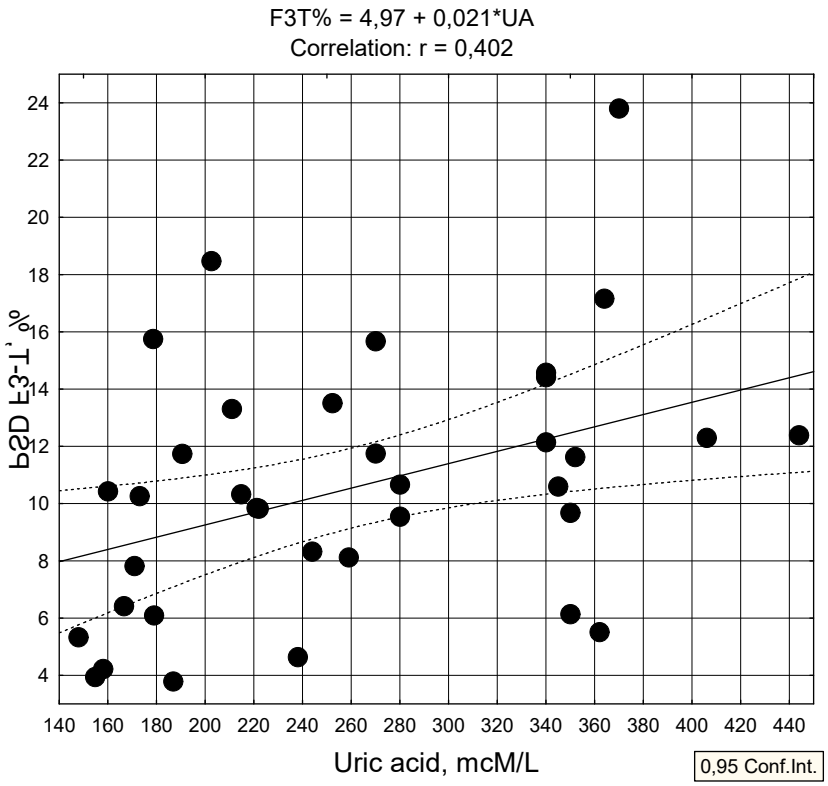

Fig. 4.9. Scatterplot of correlation between Uricemia (X-line) and relative PSD of theta-rhythm in F3 locus (Y-line) in postmenopausal Women

In addition, significant relationships with Mode HRV (Fig. 4.10) and Reactive Anxiety (Fig. 4.11) were found.

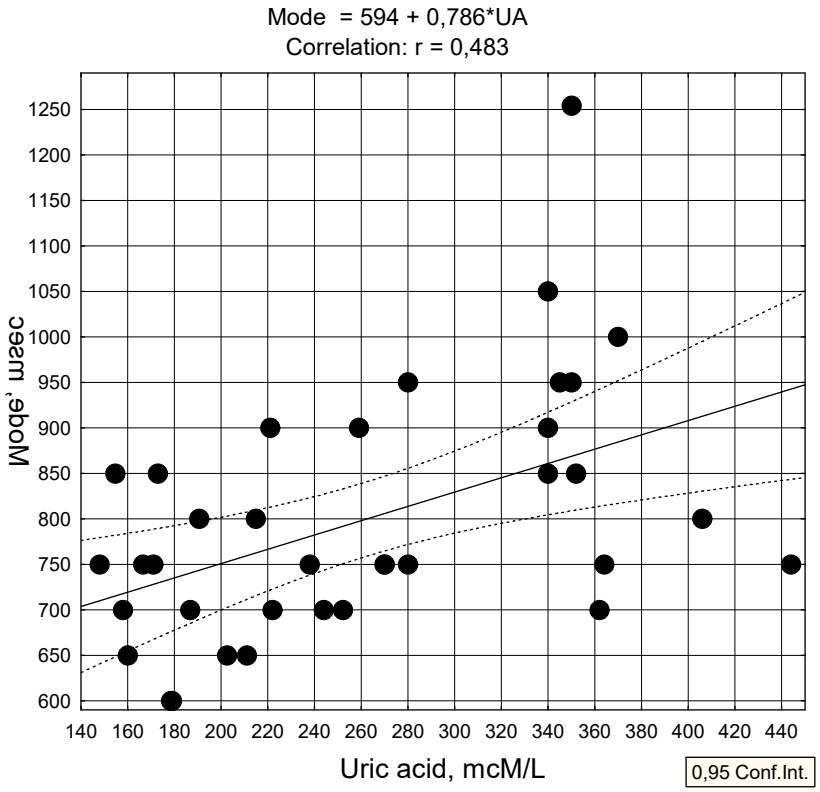

Fig. 4.10. Scatterplot of correlation between Uricemia (X-line) and Mode HRV (Y-line) in postmenopausal Women

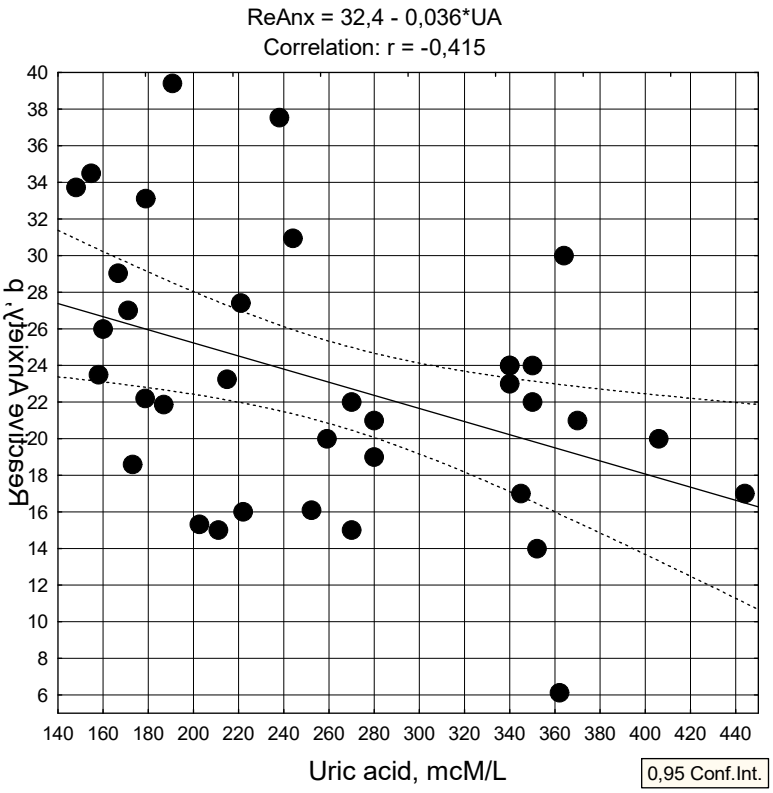

Fig. 4.11. Scatterplot of correlation between Uricemia (X-line) and Reactive Anxiety (Y-line) in postmenopausal Women

However, the last two parameters were not included by the program in the regression model. But even without them degree of determination of neuro-endocrine parameters is 94,4% (Table 4.2 and Fig. 4.13).

Table 2. Regression Summary for Uricemia in postmenopausal Women
R=0,972; R^2=0,944; Adjusted R^2=0,850; $F_{(22,1)}$=10,0; $p<10^{-4}$

N=36		Beta	St. Err. of Beta	B	SE of B	$t_{(13)}$	p-level
Variables	r		Intercpt	-236,8	121,4	-1,95	0,073
Amplitude β, μV	**-0,45**	0,818	0,301	14,62	5,38	2,72	0,018
F4-β PSD, μV²/Hz	**-0,42**	0,773	0,360	0,713	0,333	2,14	0,052
LFnu, %	**-0,43**	0,770	0,227	4,726	1,392	3,40	0,005
LF HRV PSD, %	**-0,43**	-0,361	0,226	-1,805	1,131	-1,60	0,135
LF/HF Ratio	**-0,39**	-1,044	0,214	-28,75	5,91	-4,87	10^{-3}
Kerdö's Veget Ind, un	**-0,32**	-0,265	0,097	-0,825	0,303	-2,72	0,018
C4-β PSD, %	**-0,39**	1,046	0,247	7,431	1,755	4,24	0,001
C4-β PSD, μV²/Hz	**-0,28**	2,297	0,568	1,877	0,464	4,04	0,001
T4-β PSD, μV²/Hz	**-0,38**	-1,341	0,397	-1,017	0,301	-3,37	0,005
T4-β PSD, %	**-0,31**	-0,954	0,209	-5,768	1,266	-4,56	0,001
Fp1-β PSD, μV²/Hz	**-0,38**	-0,687	0,212	-0,816	0,251	-3,25	0,006
P3-β PSD, μV²/Hz	**-0,35**	2,060	0,359	1,580	0,276	5,73	10^{-4}
O1-β PSD, μV²/Hz	**-0,33**	-0,735	0,233	-0,685	0,217	-3,16	0,008
P4-β PSD, μV²/Hz	**-0,30**	-0,686	0,366	-0,673	0,359	-1,88	0,083
C3-β PSD, μV²/Hz	**-0,26**	-4,212	0,827	-3,357	0,660	-5,09	10^{-3}
F3-θ PSD, %	**0,40**	0,647	0,123	12,16	2,32	5,24	10^{-3}
O2-θ PSD, %	**0,35**	0,583	0,148	11,35	2,88	3,94	0,002
Laterality δ, %	**0,36**	-0,814	0,169	-1,860	0,386	-4,82	10^{-3}
Testosterone, nM/L	**0,42**	0,330	0,098	9,687	2,872	3,37	0,005
VLF HRV PSD, msec²	**0,39**	-0,457	0,147	-0,066	0,021	-3,11	0,008
VLF HRV PSD, %	**0,31**	0,623	0,230	2,864	1,056	2,71	0,018
HF HRV PSD, msec²	**0,29**	0,538	0,135	0,149	0,038	3,98	0,002

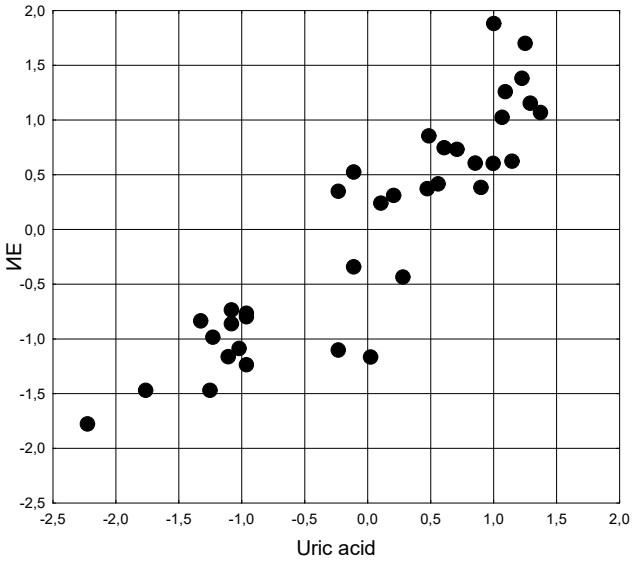

R=0,972; R^2=0,944; $\chi^2_{(21)}$=41; $p<10^{-4}$; Λ Prime=0,173

Fig. 4.12. Scatterplot of canonical correlation between Uricemia (X-line) and EEG parameters (Y-line) in premenopausal Women

Let's remember that HF band is an undeniable marker of vagal tone and VLF band directly reflects both vagal and sympathetic tone or vagal tone only [Akselrod S et al, 1981; Berntson CG et al, 1997; Taylor JA et al, 1998; Schaffer F & Ginsberg JP, 2017] as well as saliva testosterone level [Theorell T et al, 2007]. In addition to the fact that Mode HRV is an inverse marker of circulating catecholamines, there is a clear impression that in this cohort of women, uricemia exerts vagotonic and sympathoinhibitory effects.

In women of reproductive age uricemia upregulates the Asymmetry and Amplitude of β-rhythm and its PSD in F8 (Fig. 4.13) and other 5 loci (Table 3), the Amplitude and Laterality of θ-rhythm and its PSD in F8 locus, as well as the PSD of α-rhythm in F8 locus (Table 4.3).

Upregulation of testosterone level (Fig. 4.14) while downregulation of sympathetic tone (Fig. 4.15) and reactive anxiety (r=-0,34) were also found for this cohort, but these parameters were outside the regression model. Nevertheless, degree of positive determination of EEGs parameters is 95,5% (Table 4.3 and Fig. 4.16).

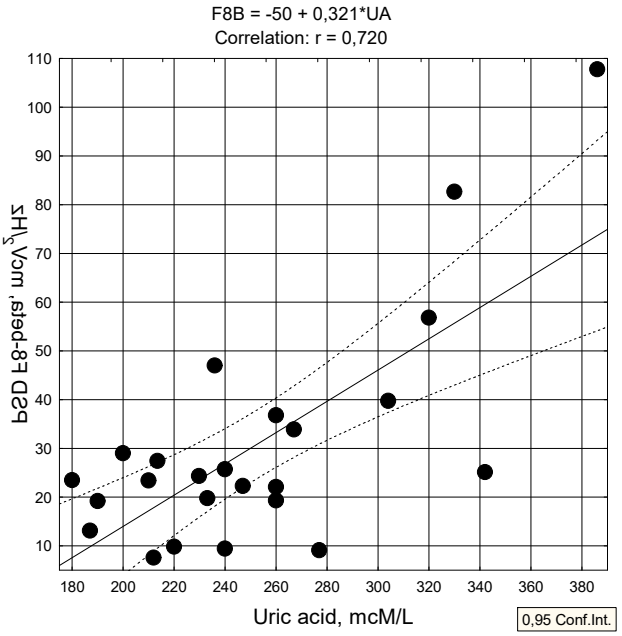

Fig. 4.13. Scatterplot of correlation between Uricemia (X-line) and absolute PSD of beta-rhythm in F8 locus (Y-line) in premenopausal Women

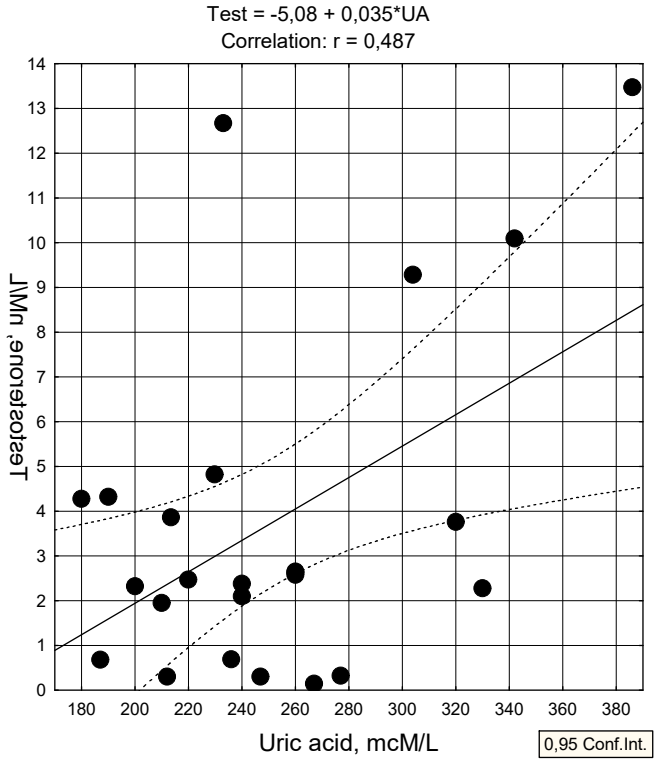

Fig. 4.14. Scatterplot of correlation between Uricemia (X-line) and Testosterone level (Y-line) in premenopausal Women

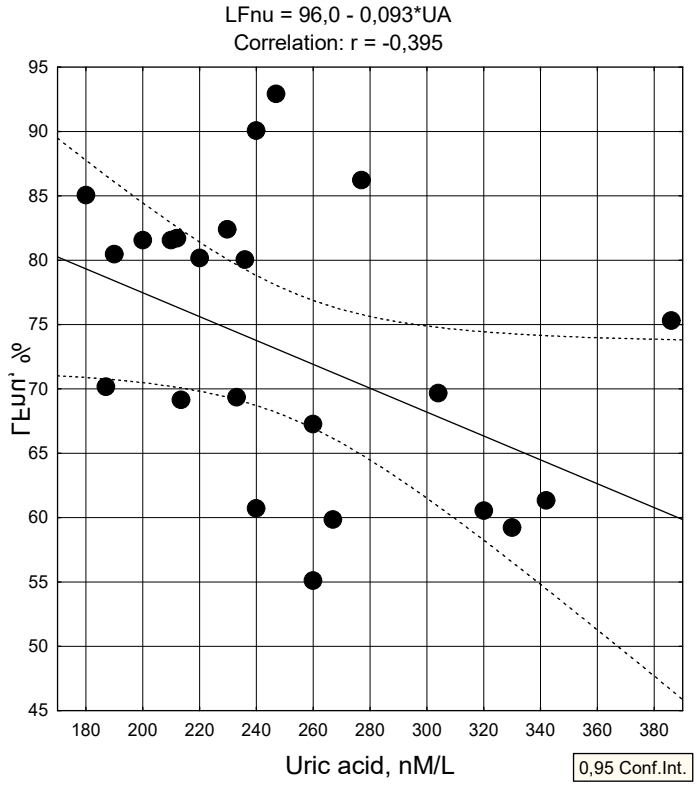

Fig. 4.15. Scatterplot of correlation between Uricemia (X-line) and LFnu HRV (Y-line) in premenopausal Women

Table 4.3. Regression Summary for Uricemia in premenopausal Women
R=0,977; R^2=0,955; Adjusted R^2=0,885; $F_{(14,9)}$=13,7; p=0,0002

N=24		Beta	St. Err. of Beta	B	SE of B	$t_{(9)}$	p-level
Variables	r		Intercpt	148,9	47,0	3,17	0,011
Amplitude β, μV	**0,69**	-1,421	0,407	-23,85	6,83	-3,49	0,007
F8-β PSD, $μV^2$/Hz	**0,72**	1,237	0,463	2,776	1,040	2,67	0,026
Fp2-β PSD, %	**0,66**	1,672	0,240	5,471	0,786	6,96	10^{-4}
F4-β PSD, $μV^2$/Hz	**0,65**	-0,278	0,256	-0,680	0,625	-1,09	0,305
T6-β PSD, $μV^2$/Hz	**0,56**	0,900	0,170	1,019	0,192	5,30	10^{-3}
O1-β PSD, $μV^2$/Hz	**0,52**	0,385	0,254	0,401	0,265	1,52	0,164
T3-β PSD, $μV^2$/Hz	**0,45**	-0,516	0,279	-0,540	0,292	-1,85	0,097
Asymmetry β, %	**0,53**	-0,708	0,284	-2,201	0,883	-2,49	0,034
Amplitude θ, μV	**0,44**	1,364	0,198	24,76	3,60	6,88	10^{-4}
F8-θ PSD, $μV^2$/Hz	**0,56**	0,620	0,296	1,031	0,492	2,09	0,066
F8-θ PSD, %	**0,44**	-0,399	0,172	-3,594	1,544	-2,33	0,045
Laterality θ, %	**0,44**	0,212	0,120	0,429	0,244	1,76	0,112
F8-α PSD, $μV^2$/Hz	**0,49**	-0,549	0,239	-1,321	0,575	-2,30	0,047

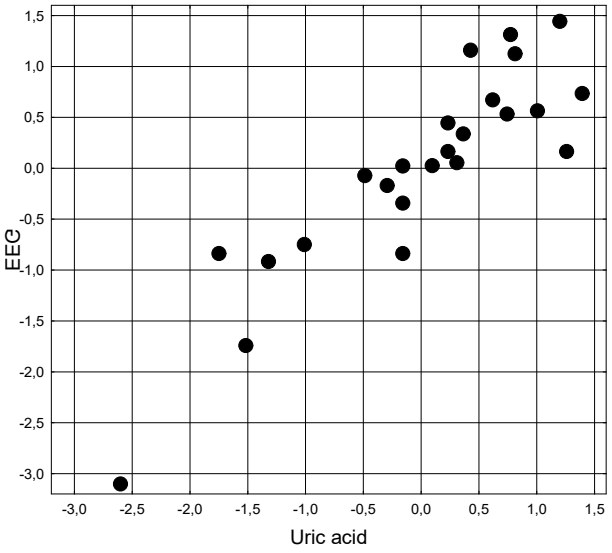

R=0,977; R^2=0,955; $\chi^2_{(12)}$=42; p=0,0002; Λ Prime=0,455

Fig. 4.16. Scatterplot of canonical correlation between Uricemia (X-line) and EEG parameters (Y-line) in premenopausal Women

In order to visualize the strength and directionality of the relationships between plasma uric acid levels and psycho-neuro-endocrine parameters at premenopausal and postmenopausal women as well as men, three profiles were created (Fig. 4.17).

Next, the parameters were grouped into clusters (Fig. 4.18).

The first cluster of correlation coefficients, the largest in terms of the number of variables, reflects the enhancing effect of uricemia on neurons that generate β-rhythm specifically in women of reproductive age, while an inhibitory neurotropic effect in postmenopausal women with full areactivity of these nervous structures in men. The next cluster differs from the previous one by a marginally pronounced inhibitory effect on β-rhythm generating neurons.

The third cluster reflects, first of all, the ability of uric acid to cause a rightward shift of β- and θ-rhythms as well as enhance PSD of α- and θ-rhythms in F8 locus, but only in women of reproductive age. The fourth cluster reflects downregulation by uric acid of sympathetic tone and reactive anxiety in all women, but not in men. The fifth cluster unites the other two markers of sympathetic tone and three β-rhythm parameters, which are subject to downregulation only in postmenopausal women. Instead, three markers of vagal tone and PSD of θ-rhythms in F3 and O2 loci are subject to upregulation by uric acid exclusively in these same women. The following

clusters contain only 1-2 parameters. Of greatest interest is the last cluster, which reflects approximately the same upregulation by uric acid testosterone levels in all three cohorts.

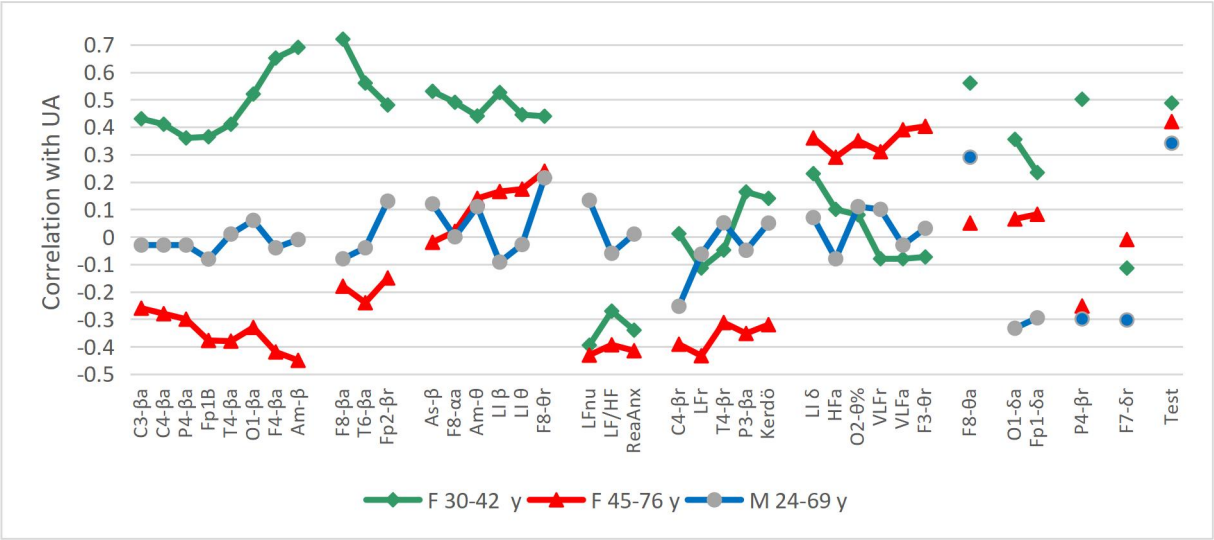

Fig. 4.17. Profiles of relationships between Uricemia and and Psycho-Neuro-Endocrine parameters at premenopausal and postmenopausal Females as well as Males

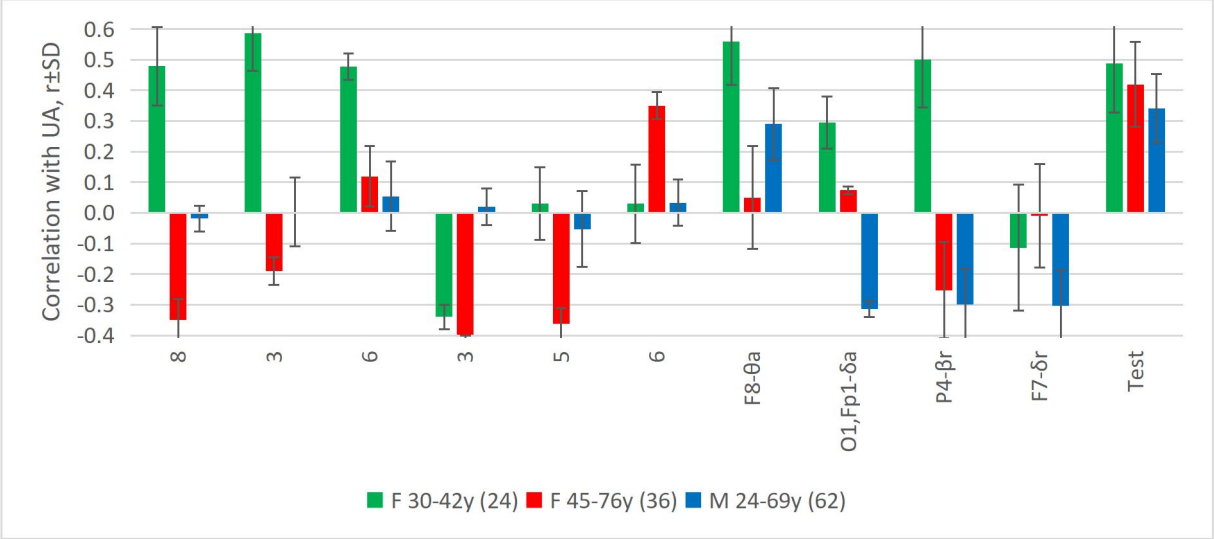

Fig. 4.18. Clusters of relationships between Uricemia and Psycho-Neuro-Endocrine parameters at premenopausal and postmenopausal Females as well as Males. The number of variables in the cluster is given

We know that in neurons, A_{2A} adenosine receptors have been identified both pre- and post-synaptically, where they control neurotransmitter release and neuronal stimulation, respectively [Schiffmann SN et al, 1991; Rosin DL et al, 1998; Svenningsson et al, 1999; Rebola N et al, 2005]. Moreover, cells involved in the neuroinflammatory response such as astroglia, microglia and bone marrow-derived cells all express the A_{2A} receptor [Fiebich BL et al, 1996; Saura J et al, 2005].

The similarity of the molecule of uric acid (**2,6,8**-tri**oxipurine**) to the molecules of methylxanthines: caffeine (**2,6**-di**oxi**-1,3,7-trimethyl**purine**) and theophylline (**2,6**-di**oxi**-1,3-dimethyl**purine** or 1,3-dimethyl**xantine**), which in turn are a structural homolog of adenosine [(2R,3R,4R,5R)-2-(6-amino**purine**-il)-5-(hydroximethyl) oxolan-3,4-diol)] and capable of 0,2 mM/L at blocking adenosine A_1- and A_{2A} receptors [Pousti A et al, 2004] back in 2004 led our laboratory [Ivassivka SV et al, 2004] to hypothesize that uric acid, the level of which in plasma of the same order (normal range: 0,12÷0,58 mM/L), is also an endogenous non-selective adenosine receptor antagonist.

In the excellent review of Morelli M et al [2010] hypothesized that urate and caffeine as adenosine A_{2A} antagonists are a novel target for neuroprotection. Initially, analysis of women in the NHS study revealed no clear relationship between Parkinson's disease (PD) and caffeine or coffee intake. However, later it became clear that amongst women who did not use postmenopausal estrogens, caffeine was in fact associated with a reduction in the risk of subsequent PD (just as in men). Conversely, for women who had used estrogen replacement caffeine use did not carry a lower risk of PD, suggesting a hormonal basis for the sex difference in caffeine's association with PD [Ascherio A et al, 2003; 2004; 2009].

Based on the above, the differences in serum uric acid relationships with psycho-neuro-endocrine parameters of men and post- and premenopausal women found in this study are somehow due to the effect of estradiol on the expression of A_{2A} adenosine receptors of neurons and/or their sensitivity to uric acid.

CHAPTER 5

CONCLUSION

More than a century has passed since Garrod demonstrated that uric acid is the cause of gout. Clinically, the incidence of gout is increasing due to various lifestyle and demographic factors [Terkeltaub R, 2010]. Relatively recently, it has been shown that the pathogenic culprit of gout - the deposition of uric acid crystals in the tissues - is a strong stimulator of inflammation. In recent years, the mechanisms by which uric acid crystals contribute to inflammation have attracted increasing interest among rheumatologists and immunologists. Uric acid has been identified as an endogenous adjuvant that drives immune responses in the absence of microbial stimulation. Because uric acid is a ubiquitous metabolite that is produced in large quantities when cells are damaged, the consequences of its exposure can be significant in health and disease. Uric acid crystals have also been shown to induce interleukin-1β-mediated inflammation by activating the NOD-like receptor protein (NLRP)3 inflammasome, a multimolecular complex whose activation appears to be central to many pathological inflammatory conditions [Schett G et al, 2016].

Uric acid in the form of sodium urate (MSU) crystals precipitates in synovial cavities and other anatomical sites, causing severe inflammation and debilitating pain. The main parameters of gout pathogenesis and treatment are well established. Nevertheless, gout remains a clinical problem affecting about 1% of the population, and interest in uric acid as a regulator of inflammation and immune responses has steadily increased in recent years. Renewed interest in uric acid and gout is driven by observations showing that uric acid is an endogenous danger signal and induces NLPR3 protein-dependent inflammation. Both effects are important for systemic inflammatory reactions [Martinon F et al, 2006]. Thus, the relationship between uric acid and the biology of the body touches on issues of evolution, biophysics, and immune regulation itself.

Hyperuricemia is a longstanding topic in the field of metabolic disorders and a common underlying disease not only in gout, but also renal dysfunction, diabetes, hypertension, and cardiovascular disease [Kutzing MK & Firestein BL, 2008; Cleophas MC et al, 2017]. The disease is attracting more and more attention from biologists and medical scientists due to its high morbidity and economic burden. Hyperuricemia has a male predominance and can be diagnosed for men by a serum uric acid level above 386 μM/L [Kutzing MK & Firestein BL, 2008] or 420 μM/L [Yu KH, 2018] and for women by concentration above 360 μM/L [Kutzing MK & Firestein BL, 2008].

The main cause of hyperuricemia is the accumulation of uric acid in the body. Uric acid is the end product of purine nucleoside metabolism, synthesized by xanthine dehydrogenase (Xdh) in humans, although it can be further transformed into allantoin by uricase (Uox) in other animals, except some birds and reptiles [Keebaugh AC, Thomas JW, 2010]. Uric acid can be found in cells, tissues and organs, and the level of uric acid varies from organ to organ. It was assumed that the liver is the most important organ for the formation of uric acid [Basseville A, Bates S, 2011; Maiuolo J et al, 2016], but surprisingly, it is not the organ with the highest level of uric acid [Yun Y et al, 2017]. The dominant source of uric acid (about 2/3 or more) is its generation from endogenous purines, and the rest from exogenous ones [Basseville A, Bates S, 2011]. It is certain that two-thirds or more of uric acid is excreted through the kidneys, and the rest through feces [Basseville A, Bates S, 2011]. Although there were systematic data on the distribution of uric acid in rats [Yun Y et al, 2017], the significance of uric acid in different organs was poorly understood.

Uric acid was thought to be a metabolic waste product of nucleosides in the same way that urea is for proteins, since there was almost no functional impairment when serum uric acid levels were profoundly reduced by uricase/rasburicase [Gutman AB, 1965; Cammalleri L, Malaguarnera M, 2007; Hyndman D et al, 2016]. However, it is noted that uric acid plays a role in some physiological functions and should not be eliminated thoroughly [Góth L, 2008; Hosomi

A et al, 2012]. Due to its antioxidant activity, uric acid was believed to protect neuronal cells, which contributes to the evolution and development of the brain [Hosomi A et al, 2012; Alvarez-Lario B et al, 2010; Johnson RJ et al, 2005], and also play a role in maintaining blood pressure [Hosomi A et al, 2012; Watanabe S et al, 2002]. However, the antioxidant activity of uric acid is not more powerful than that of hydrophilic vitamin C or hydrophobic vitamin E based on its chemical structure. The effects of antioxidant activity can be easily replaced by taking two vitamins [Tian H et al, 2016; Zakharova I et al, 2017] and other food products containing restorative chemicals [Carito V et al, 2016]. Therefore, its antioxidant activity is not as important as previously assumed.

Despite these remarks, it is believed that a reduced uric acid concentration has been linked to multiple sclerosis, Parkinson's disease, Alzhemer's disease, and optic neuritis. Hipouricemia is generally definedas a uric acid level of less than 120 μM/L [Kutzing MK & Firestein BL, 2008].

So, although the function of uric acid in the body has been a hot topic, it is still unclear. The foregoing prompted us to focus our research on the immunotropic effects of uric acid. However, due attention was paid to neurotropic and endocrine effects.

Therefore, within the framework of the "Physiological activity of uric acid" project, we demonstrated that despite the wide variability of uricemia and uricosuria both in healthy rats and in patients of the Truskavets spa with chronic pyelonephritis against the background of maladaptation, both parameters of uric acid exchange are significantly correlated with EEG, HRV, hormones of adaptation, immunity, as well as exchange of electrolytes, creatinine, urea and glucose parameters. Moreover, we found a correlation of uricemia with the level of reactive anxiety in postmenopausal women.

Li S. et al. [2022] found that prevalence of hyperuricemia and increased serum uric acid levels were higher in the manic group (62,1%) than in the depressive (34,3%) or euthymia group (17,0%) ($p<0,001$); additionally, the severity of mania was positively correlated with the uric acid level ($r=0,410$, $p<0,001$). Young IK et al [2016] found that the bipolar disorder group showed higher scores on the Young Mania Rating Scale (YMRS). Patients in their manic episodes showed higher plasma uric acid levels (4,9±1,3 mg/dL) than healthy control subjects (4,2±0,9 mg/dL; $p<0,05$). Uric acid levels showed correlation with severity of manic symptoms as assessed using the YMRS in all participants ($\rho=0,28$, $p<0,05$).

In Ortiz's R et al [2015] excellent review, conflicting data are collected. Elevated uric acid levels have been observed in acute mania. In addition, these levels were positively correlated with symptom severity and with the improvement of manic symptoms in diverse studies. Plasma uric acid levels were found to be higher in bipolar disorders (BD) patients than controls. As a result of these findings, testing for uric acid levels has been proposed as a screening test in acute mania. Uric acid levels have also been correlated with specific character traits including drive and disinhibition, both of which are common in mania. However, at least one study found no differences in uric acid levels between BD subjects and healthy controls. Uric acid, as one of a cluster of urinary metabolites, was correlated with first depressive episode in drug-naïve mood disorders disease (MDD) subjects. Another study compared healthy controls and MDD patients and found that lower levels of uric acid were associated with MDD; indeed, the authors noted a strong inverse relation between Hamilton Depression Rating Scale (HDRS) scores and uric acid levels after 12 weeks of antidepressant treatment. Interestingly, in another study, subjects with MDD showed lower plasma uric acid levels than healthy controls and BD patients. A smaller study also found that lower levels of uric acid were associated with MDD compared to other psychiatric conditions; these normalized after five weeks of antidepressant treatment, though no significant differences were observed between those with depressive and anxiety disorders.

Fully aware that correlational relationships do not necessarily reflect functional relationships, we nevertheless take responsibility for asserting that (psycho)neurotropic, immunotropic, hormonal, and metabolic activity of the uric acid molecule has been established in our study. Additional evidence in favor of such a statement is the fact that correlations between balneotherapy-induced parameter **changes** were more numerous and generally stronger than in

the **entire sample**. But the main argument should be considered the structural similarity of the molecules of uric acid (**2,6,8**-tri**oxipurine**) and adenosine [(2R,3R,4R,5R)-2-(6-amino**purine**-il)-5-(hydroximethyl) oxolan-3,4-diol)], and especially its antagonists such as theophylline (**2,6**-di**oxi**-1,3-dimethyl**purine** or 1,3-dimethyl**xantine**), caffeine (**2,6**-di**oxi**-1,3,7-trimethyl**purine** or 1,3,7-trimethyl**xantine**) and other methylxanthines.

The ubiquitous signaling nucleoside molecule, adenosine is found in different cells of the human body to provide its numerous physio/pharmacological role. The associated actions of endogenous adenosine are largely dependent on conformational change of the widely expressed heterodimeric G-protein-coupled A_1, A_{2A}, A_{2B}, and A_3 adenosine receptors. These receptors are well conserved on the surface of specific cells, where potent neuromodulatory properties of this bioactive molecule reflected by its easy passage through the rigid blood-brainbarrier, to simultaneously act on the central nervous system. The minimal concentration of adenosine in body fluids (30-300 nM) is adequate to exert its neuromodulatory action in the CNS [Morelli M et al, 2010; Choudhury K et al, 2013; Jamwal S et al, 2019; Effendi WI et al, 2020]. Its physiological importance depends on the affinity of these receptors and the extracellular concentrations reached. Adenosine has been traditionally considered an **inhibitor of neuronal activity** and a regulator of cerebral blood flow [Jamwal S et al, 2019]. In the only one found by us on the PubMed resource article, that is similar to our work [Young IK et al, 2016], the bipolar disorder group showed **decreased** relative delta and alpha activity in the fronto-temporo-occipital region compared to the control group ($p<0,05$). However relative beta in Fp1 (frontopolar), Cz (central mid-line), and Pz (parietal mid-line) and relative gamma in Fp1 were **increased** in the bipolar disorder group, relative to the control group ($p<0,05$). The relative beta ($\rho=0,47$, $p<0,05$) and gamma ($\rho=0,41$, $p<0,05$) in Fp1 electrodes showed positive correlation with the YMRS scores. Authors concluded that adenosinergic transmission dysfunction may lead to occurrence of manic symptoms, considering that a key role of central nervous system adenosinergic receptors is to inhibit the release of various neurotransmitters and limit neuronal excitability. In addition, QEEG appeared to indicate excitatory neuro-modulation in manic patients. In contrast to bipolar disorder patients with an elevated level of uricemia, the vast majority of the cohort we observed was characterized by hypouricemia, a minority had a normal level of uric acid, and only 5 had an elevated level. And precisely in the members of the cluster with normouricemia, significantly increased delta activity in the T4 and C3 loci and theta activity in the F7 locus were found. When analyzing the individual effects of balneotherapy, we agree with Jamwal S et al [2019] stated a diffuse **inhibitory** effect of uric acid on beta- and alpha-rhythm-generating neurons of the CNS, but at the same time uric acid exerted an **activating** effect on neurons that generate delta- and theta-rhythms.

The figures presented by Winkelmann T et al [2017] give us reason to assume that the loci C3/C4 projected precentral gyrus, T3/T4 – inferior temporal gyrus, T5/T6 – transverse temporal cortex, P3/P4 – supramarginal gyrus. The **thickness** of these cortical structures is positively correlated with the HF HRV as marker of vagal tone. We found an inhibitory effect of uric acid on beta-rhythm generating neurons that project to loci P3 ($r=-0,58$), P4 ($r=-0,51$), T4 ($r=-0,53$), T3 ($r=-0,43$), T6 ($r=-0,42$), C4 ($r=-0,32$), and C3 ($r=-0,31$). Montenegro RA et al [2011] assessed the effects of anodal direct current stimulation over the T3 scalp position (aims to reach the insular cortex) on measures of cardiac autonomic control. The authors found that the parasympathetic activity (HF(log)) increased and the sympathetic activity (LF(log)) and sympatho-vagal balance (LF/HF(log)) decreased in athletes but not in untrained individuals. No significant changes in HRV indexes were provoked by sham stimulation in both groups. The authors attributed the specific results to neuroanatomical and functional changes in the brain induced by long-term exercise training. Furthermore, Piccirillo G et al [2016] demonstrated that anodal tDCS over T3 scalp position reduced sinus sympathetic activity and increased vagal sinus activity and baroreflex sensitivity in older, but not younger individuals.

This is in excellent agreement with our data on negative relationships of uric acid with HRV-markers of vagal tone (MxDMn: -0,37; TNN: -0,35; SDNN: -0,31; TP HRV: -0,30; LF: -

0,37) and positive with HRV-markers of sympathetic tone (AMo: 0,32; Stress Index: 0,34), which indicates the ability of uric acid to influence the brainstem and subcortical autonomous nuclei (NA, DMV, RVLM, locus coeruleus). Such influence is more likely to be exerted precisely through the cortical nuclei [Vanneste S & De Ridder D, 2013; Popovych IL et al, 2013; Popovych IL et al, 2014], although the possibility of direct influence of uric acid on autonomous nuclei should not be excluded.

According to the excellent concept of "central autonomic network (CAN)" [Palma JA & Benarroch EE, 2014] it include following cortical, subcortical, and medullary structures (Fig. 5.1): the anterior cingulate, insular, orbitofrontal, and ventromedial cortices; the central nucleus of the amygdala (CeA); the paraventricular and related nuclei of the hypothalamus; the periaqueductal gray matter; the nucleus of the solitary tract; the nucleus ambiguous; the ventrolateral medulla; the ventromedial medulla and the medullary tegmental field. The primary output of the CAN is mediated through the preganglionic sympathetic and parasympathetic neurons, which exert control over the heart via the stellate ganglia and the vagus nerve, respectively.

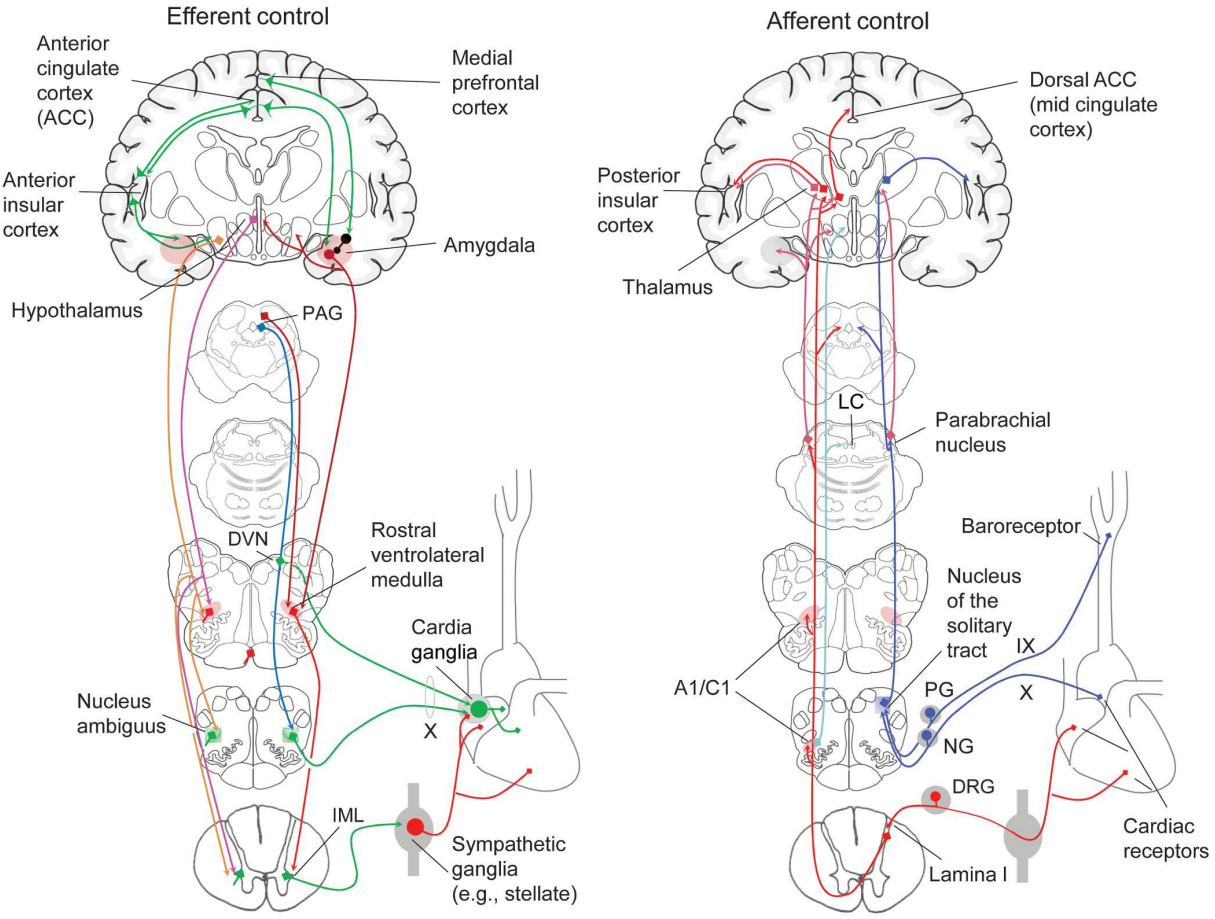

Fig. 5.1. Central autonomic network and control of cardiac function [Palma JE & Benarroch EE, 2014]

The interplay of sympathetic and parasympathetic influences on sinoatrial node pacemaker activity generates the complex variability that characterizes the healthy heart rate rhythm, which is called HRV. A fundamental principle of the neural control of the heart is its hierarchical organization, with cortical structures providing inhibitory control over limbic and brainstem sympathoexcitatory, cardioacceleratory circuits. The prefrontal, cingulate, and insula cortices form an interconnected network with bi-directional communication with the amygdala. The amygdala is under tonic inhibitory control via prefrontal vagal pathways to intercalated cells in the amygdala. The activation of the CeA inhibits the nucleus of the solitary tract (NTS) which in

turn inhibits inhibitory caudal ventrolateral medullary (CVLM) inputs to the rostral ventrolateral medullary (RVLM) sympathoexcitatory neurons, and simultaneously inhibits vagal motor neurons in the nucleus ambiguus (NA) and the dorsal vagal motor nucleus (DVN). In addition, the CeA can directly activate the sympathoexcitatory neurons in the RVLM.

Mo J et al [2019] presented their CAN visualization (Figs 5.2 and 5.3).

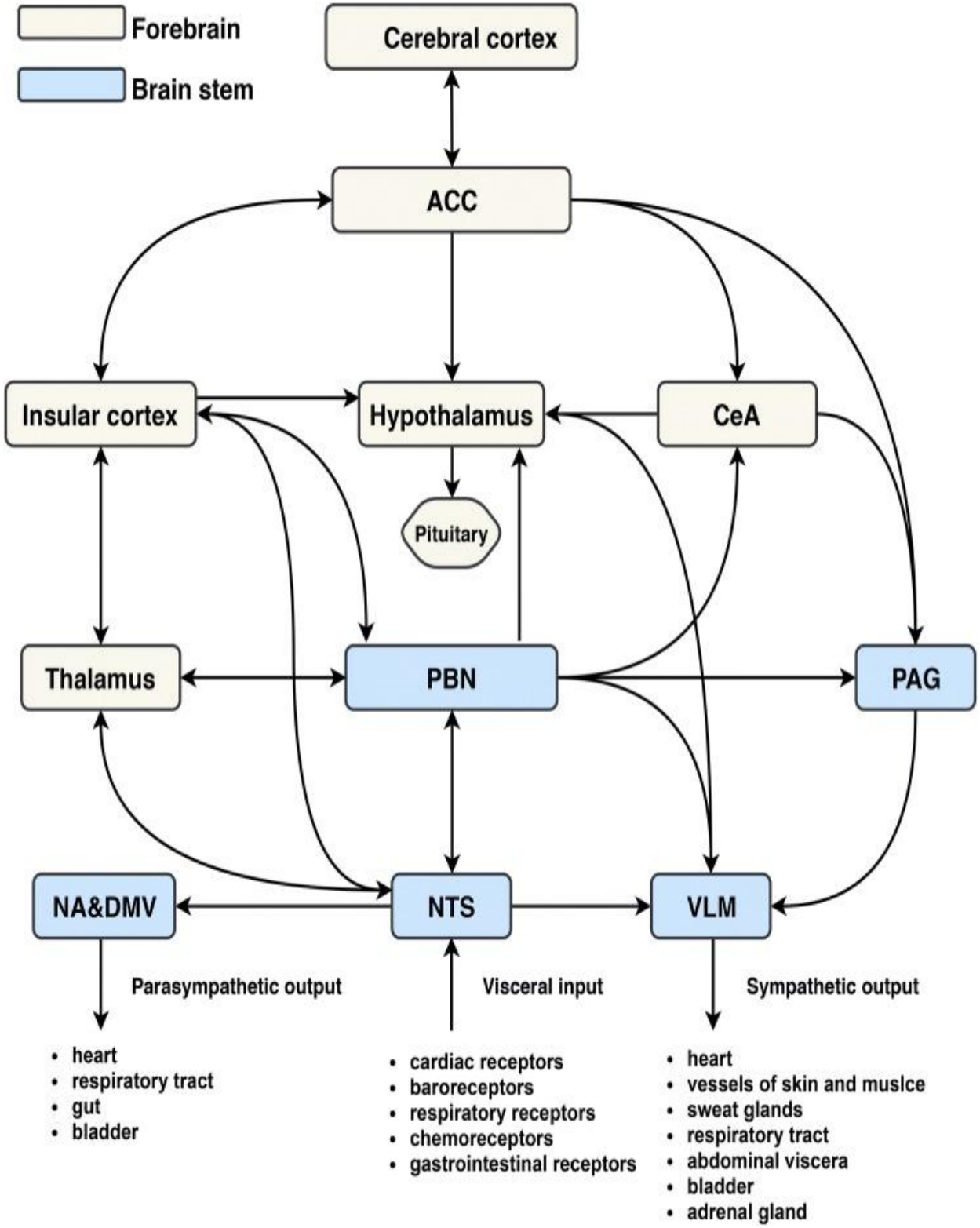

Fig. 5.2. Diagram of the central autonomic network

Visceral information is relayed through the NTS and PBN to forebrain areas such as the hypothalamus, amygdala, thalamus, and insular cortex. The insular cortex has dense reciprocal connections with the ACC, lateral hypothalamic area, NTS, and PBN. These regions are also reciprocally connected. ACC, anterior cingulate cortex; CeA, central amygdala; PBN, parabrachial nucleus; PAG, periaqueductal gray; NA, nucleus ambiguus; DMV,

dorsal motor nucleus of the vagus; NTS, nucleus of the solitary tract; VLM, ventrolateral medulla [Mo J, Huang L, Peng J, Ocak U, Zhang J, Zhang JH, 2019].

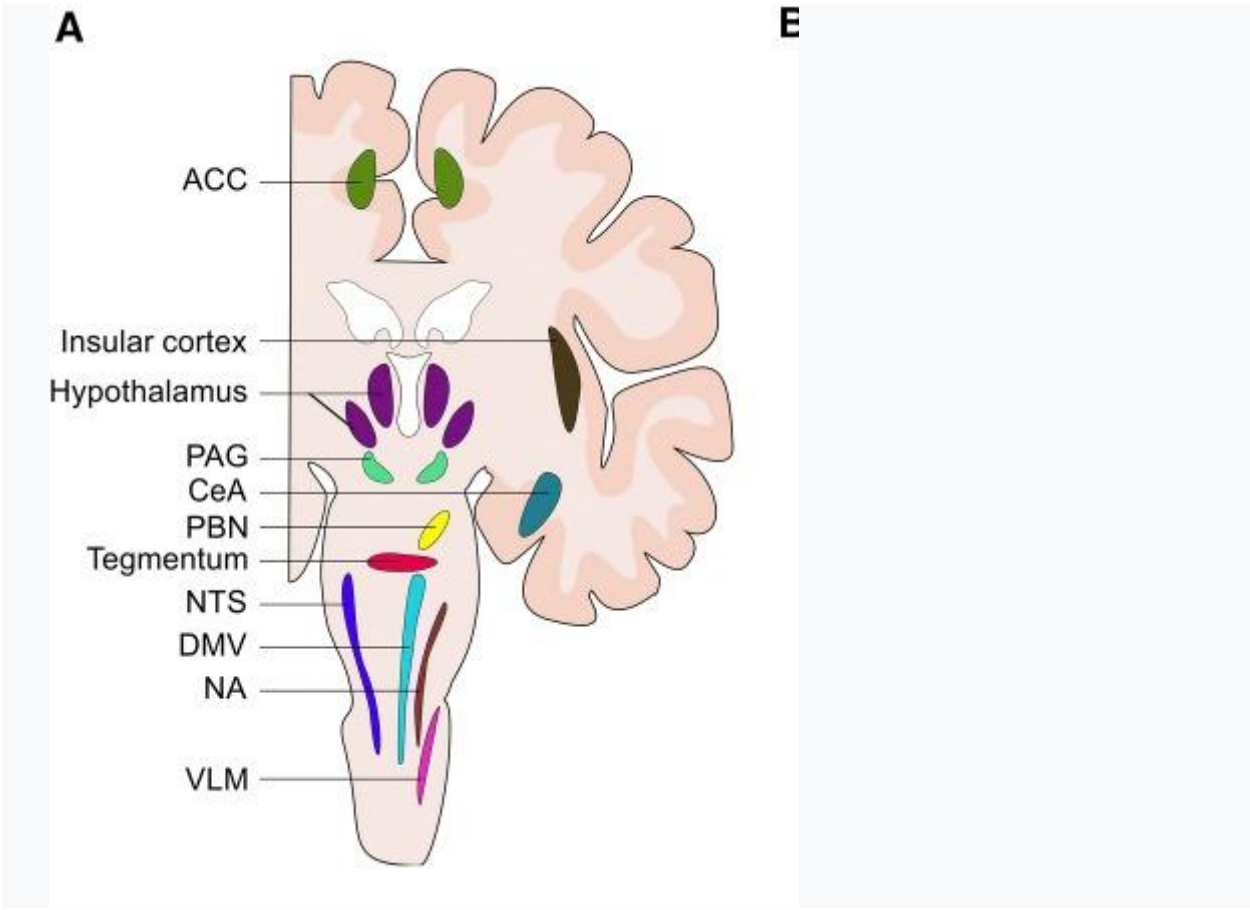

Fig. 5.3. Brain structures of the central autonomic network
ACC, anterior cingulate cortex; PAG, periaqueductal gray; CeA, central amygdala; PBN, parabrachial nucleus; NTS, nucleus of the solitary tract; DMV, dorsal motor nucleus of the vagus; NA, nucleus ambiguus; VLM, ventrolateral medulla [Mo J, Huang L, Peng J , Ocak U, Zhang J, Zhang JH, 2019].

Indeed, disruption of prefrontal activity leads to disinhibition of sympathoexcitatory circuits, with a resultant increase in heart rate and decrease in vagally-mediated HRV. Such **neurotropic** effects of uric acid - upregulation of sympathetic nuclei while downregulation of vagal nuclei and some cortical nuclei - were detected in the observed cohort of patients.

Adenosine receptors express also virtually all populations of immunocytes such as T, NK, B lymphocytes, macrophages, neutrophils, dendritic and endothelial cells [Huang S et al, 1997; Apasov S et al, 2000; Hoskin DW et al, 2008; Navalta JW et al, 2016; Vigano S et al, 2019]. Therefore, the possibility of a direct effect of uric acid on these immunocytes seems quite obvious.

Significantly, 34 of the 41 immune parameters reported in this study were somehow associated with parameters of uric acid exchange, mainly uricemia.

In rats, we found that the level of uric acid was positively correlated with both the activity and the intensity of phagocytosis of *Staphylococcus aureus*, while uric acid negatively affects the level of natural killers in the blood.

In this direction, we found only one work [Carvalho LAC et al, 2018], which shows that incubation with uric acid inhibits the killing activity of neutrophil-like cells (HL-60) against *Pseudomonas aeruginosa*, simultaneously increasing the production of superoxide anions. Another study [Gao L et al, 2018] reported that men with hyperuricemia had lower NK cells before and after a low-purine diet.

It is known that the level of immunocytes in the blood is the result of the interaction of three processes. As for $CD4^+$ T-lymphocytes and polymorphonuclear neutrophils, it is, first, a decrease

in the influx of cells into the blood from the thymus and bone marrow, respectively; secondly, an increase in the migration of cells from the blood to the spleen, lymph nodes, etc.; third, intensification of cell death by apoptosis, efferocytosis, lysis, etc.

In an experiment on rats, we found that the level of uric acid was positively correlated with the content of lymphocytes and macrophages in the thymus, but negatively correlated with the content of epitheliocytes, reticulocytes and Hassall's bodies. If these data are extrapolated to humans, it could be hypothesized that uric acid stimulates the differentiation of thymocytes into $CD8^+$ T cells, while instead reducing the generation of $CD4^+$ T cells. According to the concept that uric acid is a structural homologue of caffeine, which in turn is a structural homologue of adenosine [Morelli M et al, 2010; Sofaer JA, Emery AF, 1981], of particular interest are data showing that peripheral T-cell depletion is a consequence of inhibition of T-lymphocyte expansion by means of extracellular adenosine signaling through A_{2A} receptors [Huang S et al, 1997].

Regarding the negative correlation between uric acid levels and polymorphonuclear neutrophils, we have no reason to speculate. They can migrate to the spleen and/or become blocked in the bone marrow.

In general, we consider the effect of uric acid on immune parameters to be favorable, except for the reduction of T-helpers in blood and IgG in saliva. However, it is known that a low level of uric acid in blood plasma is associated with autoimmune inflammatory diseases [El Ridi R & Tallima H, 2017]. So these suppressor effects are probably also physiologically beneficial.

Given the maximum correlation, the relationship between changes in parameters of uric acid metabolism and $CD4^+$ T-helper levels is the main priority of the discussion. Here it is appropriate to mention the classics.

In a landmark study by Limatibul S, Shore A, Dosch HM and Gelfand EW [1978], three subpopulations of rosette-forming T-lymphocytes were delineated: theophylline-sensitive T-cells (TS), which lose their ability to form an E-rosette after treatment; theophylline-resistant T-cells (TR), which are not affected by the drug; and theophylline-dependent cells, which acquire the ability to form E-rosettes after incubation with theophylline. It was shown that the effect of theophylline is dose-dependent (in the range 10^{-5}÷10 мМ/л). Concentrations in the range of 1÷5 mM/l are usually used for immunoassays. TR-lymphocytes possess RFcμ receptors, but lack RFcγ receptors and function as inducers of B-lymphocyte differentiation. In contrast, TS-lymphocytes express RFcγ receptors, but are devoid of RFcμ receptors and suppress the differentiation of B-lymphocytes.

Birch RE, Rosenthall AK and Polmer SH [1982] first showed that treatment with adenosine (0,01 mM/l) resulted in changes in OKT4 and OKT8 reactivity within the TR subgroup. OKT4 expression was reduced from 71,8% to 58,3% after adenosine treatment, while the percentage of OKT8 reactive cells increased from 16,5% to 33,0%. The twofold increase in OKT8 expression is approximately equal in magnitude to the change observed in RFcγ expression under the same conditions. After treatment with adenosine, only a slight change in reactivity to OKT4 was observed in the Ttotal fraction, but a significantly increased percentage of $OKT8^+$ cells was observed. According to the authors, TR cells expressing OKT8 after treatment with adenosine most likely derive, at least in part, from TR cells that were OKT4. This is evidenced by the fact that the sum of $OKT4^+$ and $OKT8^+$ TR cells remains constant before and after adenosine treatment. The authors brilliantly suggested that the expression of Fcγ receptors of T-lymphocytes is regulated by agents acting on adenosine receptors.

It is now known that the immunotropic effect of adenosine is realized through its receptors (A_1, A_{2A}, A_{2B}, A_3), which are expressed by almost all populations of immunocytes: T-, NK-, B-lymphocytes, macrophages, neutrophils, dendritic and endothelial cells. Theophylline is a structural homologue of adenosine and at a dose of 30 mg/l (0,2 mM/l) is able to block adenosine receptors A_1 and A_{2A} [Pousti A et al, 2004]. Caffeine and other methylxanthines, which are introduced into the human body almost daily with coffee, tea, cocoa, etc, are non-selective antagonists of adenosine receptors, mainly A_{2A} [Morelli M et al, 2010; Navalta JW et al, 2016].

At the same time, the realization of the immunotropic effects of uric acid through the central and autonomic nervous systems is no less likely.

According to the Tracey KJ [2007] (Fig. 4.4), there is a structured, somatotopically organized neural network that controls specific components of the immune response through input and output communication. Such a theoretical organization is similar to the classical homunculus, which demonstrates that certain areas of the brain control certain parts of the body, and in the future it will be possible to build an "immunological homunculus". For example, one area of the brain may control cytokine responses in the liver, while another may control the activation of T cells in the spleen or lymph nodes. Some centers may integrate information on antigen presentation, while others may integrate information on the maturation process of dendritic cells. Individual neurological domains in the central nervous system can regulate the state of general readiness of the innate immune system to respond to pathogens or damage.

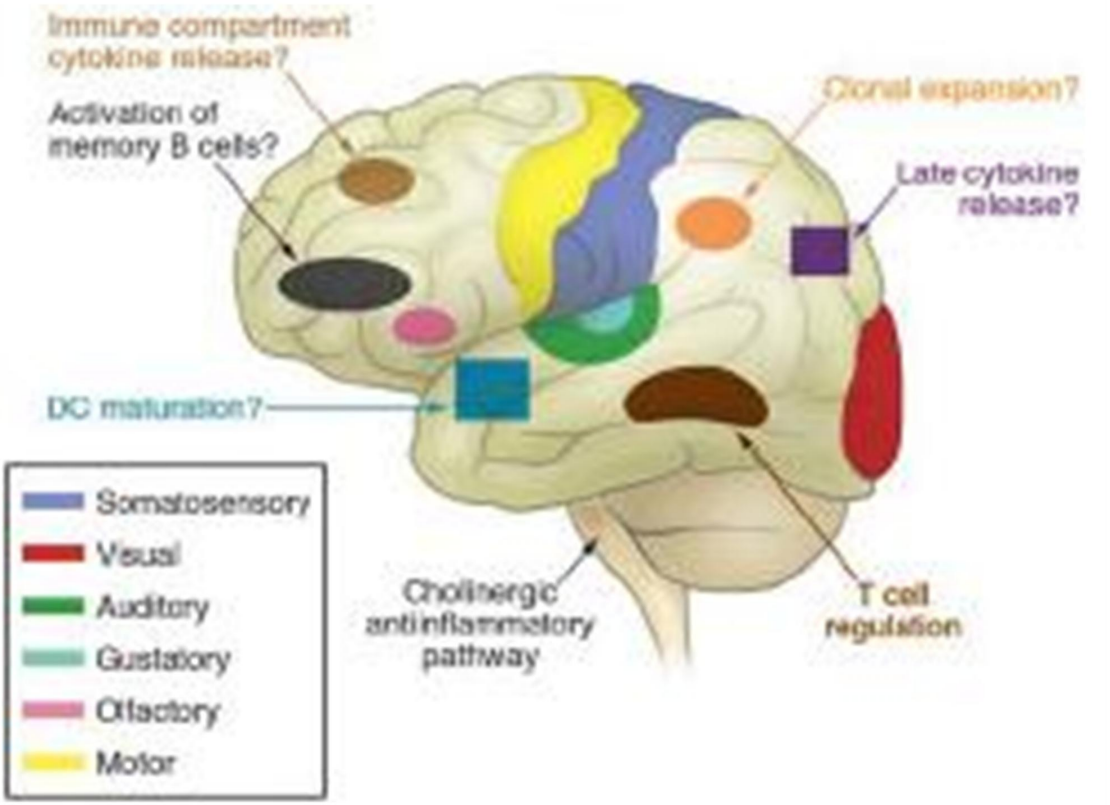

Fig. 5.4. Scheme of the immunological homunculus [Tracey KJ, 2007]

The existence of neuroanatomical maps of the cholinergic anti-inflammatory reflex is a significant step toward identifying other domains in the immunological homunculus that are critical for maximizing the body's protection and health maintenance during immune responses. However, in subsequent publications of this laboratory [Pavlov VA & Tracey KJ, 2012; Chavan SS & Tracey KJ, 2017; Chavan SS et al, 2017], this hypothesis was not advanced. And only in 2018 was there a mention of it in the authors' review [Pavlov VA et al, 2018], but, unfortunately, without clarification.

We draw attention to the fact that the author's scheme has a question mark (?) at the end of each signature, that is, it is not a statement, but a hypothesis. Under the influence of this hypothesis, our laboratory conducted research to verify it [Kul'chyns'kyi AB, Popovych IL et al, 2016; 2017; 2017a; 2017b; Popovych IL et al, 2017; 2018; Mel'nyk OI, Popovych IL et al, 2019].

How do the results of our laboratory fit into the immunological homunculus concept/hypothesis?

As can be seen from the comparative Table 5.1, in the presumed cortical *Center of B-cell of memory activation*, inhibition of the activity of generating θ-rhythm neurons is accompanied by a

decrease in the content of immunoglobulins M and A in the blood. *Center for Late Cytokine Release*, by Tracey KJ [2007], is projected between the parietal and occipital loci. This is consistent with our data on the association of decreased IL-1 and C-reactive protein levels with inhibition of β-rhythm generating neurons in the O2 and P4 loci, simultaneously with activation of δ-rhythm generating neurons localized there. If we assume that the cortical *Center of T-lymphocyte regulation* is projected onto the T6 locus, it turns out that it has an inhibitory effect on the level of T-regulatory and T-cytolytic lymphocytes in the blood. At the same time, the data obtained by us provide grounds for putting forward an alternative hypothesis regarding the upregulation of T-lymphocytes by neurons generating δ- and α-rhythms, which are projected onto prefrontal loci. Finally, our laboratory modest contribution to the concept of the immunological homunculus is a hypothesis about localization in the right occipital part of the cerebral cortex of δ-rhythm generating neurons responsible for the *regulation of phagocytosis*.

Table 5.1. Agreed and divergent propositions of the immunological homunculus

EEG and Immune Variables	EEG and Immune response	EEG and Immune Variables	EEG and Immune response
Tracey's hypothesis		Tracey's hypothesis	
Activation of memory B cells		Late cytokine release	
Fp2-θ PSDr	-0,26±0,12	P4-δ PSDr	+0,34±0,17
IgM	-0,39±0,22	P4-β PSDr	-0,34±0,12
IgA	-0,24±0,14	O2-β PSDr	-0,33±0,13
		Interleukin-1	-0,42±0,27
		C-reactive Protein	-0,26±0,06
Tracey's hypothesis		Popovych's hypothesis	
T cells regulation		T cells regulation?	
T6-β PSDr	-0,25±0,12	Fp2-δ PSDa	+3,13±1,56
$CD3^+CD25^+$ T-regulatory Lym	+0,51±0,19	Fp1-δ PSDa	+3,14±1,59
$CD3^+CD8^+$ T-cytolytic Lymph	+0,60±0,26	F3-δ PSDa	+2,53±1,34
Popovych's hypothesis		F8-δ PSDa	+7,62±3,11
Activation of Phagocytosis?		F7-α PSDr	+0,29±0,12
O2-δ PSDr	+0,42±0,17	F8 PSD Entropy	-0,46±0,21
Microbial Count vs E. coli	+0,40±0,17	$CD3^+CD25^+$T-regulatory	+0,51±0,19
Microbial Count vs St. aureus	+0,39±0,13	$CD3^+CD8^+$T-cytolytic	+0,60±0,26
Killing Index vs Staph. aureus	+0,79±0,20		
Killing Index vs E. coli	+0,65±0,12		
Bactericidity vs E. coli	+1,64±0,39		
Bactericidity vs Staph. aureus	+1,54±0,42		
CIC	+0,43±0,13		

Now recall that changes in the state of uric acid metabolism determine EEG changes by 87% (Table 3.58 and Fig. 3.47). In turn, changes in EEG as well as vagal tone and calcitonin levels determine changes in the immune constellation by 54% (Table 3.90 and Fig. 3.65). On the other hand, the rate of uric acid determination of the immune constellation is 60% (Table 3.24 and Fig. 3.16). This gives grounds for the assumption of a neuro-endocrine mechanism of the immunotropic effects of uric acid.

The central autonomic network also includes the hypothalamus and pituitary gland in its structure (Figs 5.2 and 5.3). This is the basis for the assumption of a neurogenic mechanism of the endocrine effects of uric acid revealed in this study: downregulation of testosterone, cortisol, circulating catecholamines while upregulation of triiodothyronine. Since the lion's share of circulating catecholamines is adrenaline of the medullary zone of the adrenal glands, and the source of testosterone in women is the reticular zone of the cortex, we can talk about the downregulating effect of uric acid on adrenals in general, with the exception of the glomerular zone.

At the same time, both upregulation of PTH and downregulation of calcitonin are carried out by uric acid by as yet unknown mechanisms.

The effect of uric acid on the levels of adaptation hormones is carried out, presumably, through mediators of both neurons (ACh, NA, GABA, ACTH, LH, etc.) and immunocytes (cytokines, ACTH, etc.) within the framework of a triune neuro-endocrine-immune network/complex [Besedovsky H & Sorkin E, 1977; Besedovsky H & del Rey A, 1996; Nance DM & Sanders VM, 2007; Thayer JF & Sternberg EM, 2010; Popovych IL, 2009; 2011], as well as through adenosine receptors of endocrinocytes.

It is difficult for us to imagine a direct regulatory effect on the metabolites registered in this study. Instead, there is reason to speculate that the metabolic effects of uric acid are mediated by its neurohormonal effects. We have shown that changes in the metabolic constellation are determined by changes in the constellation of EEG parameters as well as LF/HF, PTH, calcitonin, cortisol and testosterone by 85% (Table 3.88 and Fig. 3.64). At least with regard to electrolytes, such speculations are quite realistic.

One of the cornerstones of information medicine is entropy. The concept of entropy is multifaceted. In information theory, entropy is a measure of the uncertainty of a situation, a measure of disorder, the degree of chaos present in a system. Shannon SE [1948] connected the concepts of information and entropy, which characterizes the degree of orderliness of the system, by mathematical dependence. This assessment of the amount of information coincides with the assessment of the quantitative degree of uncertainty elimination, the degree of organization of the system. According to Biloshytskyi PV [2007], the mathematical formula directly indicates the possibility of changing the orderliness of the system by quantitative change of information, which in relation to biosystems can mean a change in quality (stability, work capacity, health, etc.) and thus indicate the way of purposeful use of bioinformation in medical practice. By chance, the author suggests using the term reliability of the organism's functioning instead of the term entropy.

Calculation of entropy is acceptable, in particular, in relation to the leukocytogram of peripheral blood, which is a closed system of various form elements. Informational analysis of the cytogram allows to assess the state of morpho-functional adaptive and protective systems, information about which is contained in the cytogram [Avtandylov GG, 1990; Yushkovska OG, 2001]. Popovych IL [2007] first used this approach to evaluate the immunocytogram of peripheral blood, as well as the splenocytogram and thymocytogram of smears-imprints in rats. The experimental and clinical-physiological studies of our laboratory conducted in this direction showed that, on the one hand, an increase in entropy is not an unambiguously physiologically unfavorable process, and on the other hand, a decrease in entropy is not unambiguously physiologically favorable for the human body and animals [Popadynets OO et al, 2020; Korda MM et al, 2021].

In our experiments and clinical observations, the influence of uric acid on the entropy of immunocytes was revealed for the first time. In particular, the proentropic effect on the immunocytogram of blood was established both in humans and in rats, and on the leukocytogram - only in humans. In rats, uric acid also has a negentropic effect on thymocytogram and splenocytogram. It is also a priority to identify the connections of uric acid with EEG entropy in C3, F7, F8 loci.

Ivassivka SV, Popovych IL, Aksentiychuk BI and Flyunt IS [2004] suggested that uric acid is an endogenous non-selective antagonist of adenosine receptors. In this study, new data were obtained in favor of this assumption. In particular, the level of uric acid in the serum through the corresponding nuclei of the cortex, amygdala, brainstem and medulla upregulate sympathetic tone and downregulate vagal tone, that is, it acts similarly to caffeine.

However, the fact we obtained about a weak, but still **positive** ($r=0.22$) relationship between changes in uricemia (the level of which is comparable to the concentrations of adenosine and theophylline in in vitro immune tests) and relative content of $CD8^+$ T cells in the blood, that is, theophylline-sensitive, at first glance, contradicts the classical position. However, other authors found that caffeine increases the death and migration of $CD8^+$ T-lymphocytes (but not $CD4^+$ T-

lymphocytes, as well as B-lymphocytes) in caffeine-accustomed, but not naïve, individuals after moderate-intensity exercise [Navalta JW et al, 2016]. That is, the situation is ambiguous.

These data led us to divide the sample into three clusters (Fig. 5.5). In 14 patients, a close inverse correlation (r=-0,85) was found between the dynamics of uricemia and the percentage of theophylline-sensitive T-lymphocytes, that is, uric acid acted similarly to caffeine, blocking adenosine receptors, therefore the cluster is designated AR-. Instead, in 19 patients of the second cluster, a direct correlation was established (r=0,66), i.e., uric acid acted as an adenosine receptor agonist (AR+ cluster). In the remaining 11 people, no connection was found between changes in the levels of uricemia and theophylline-sensitive T-lymphocytes (R0).

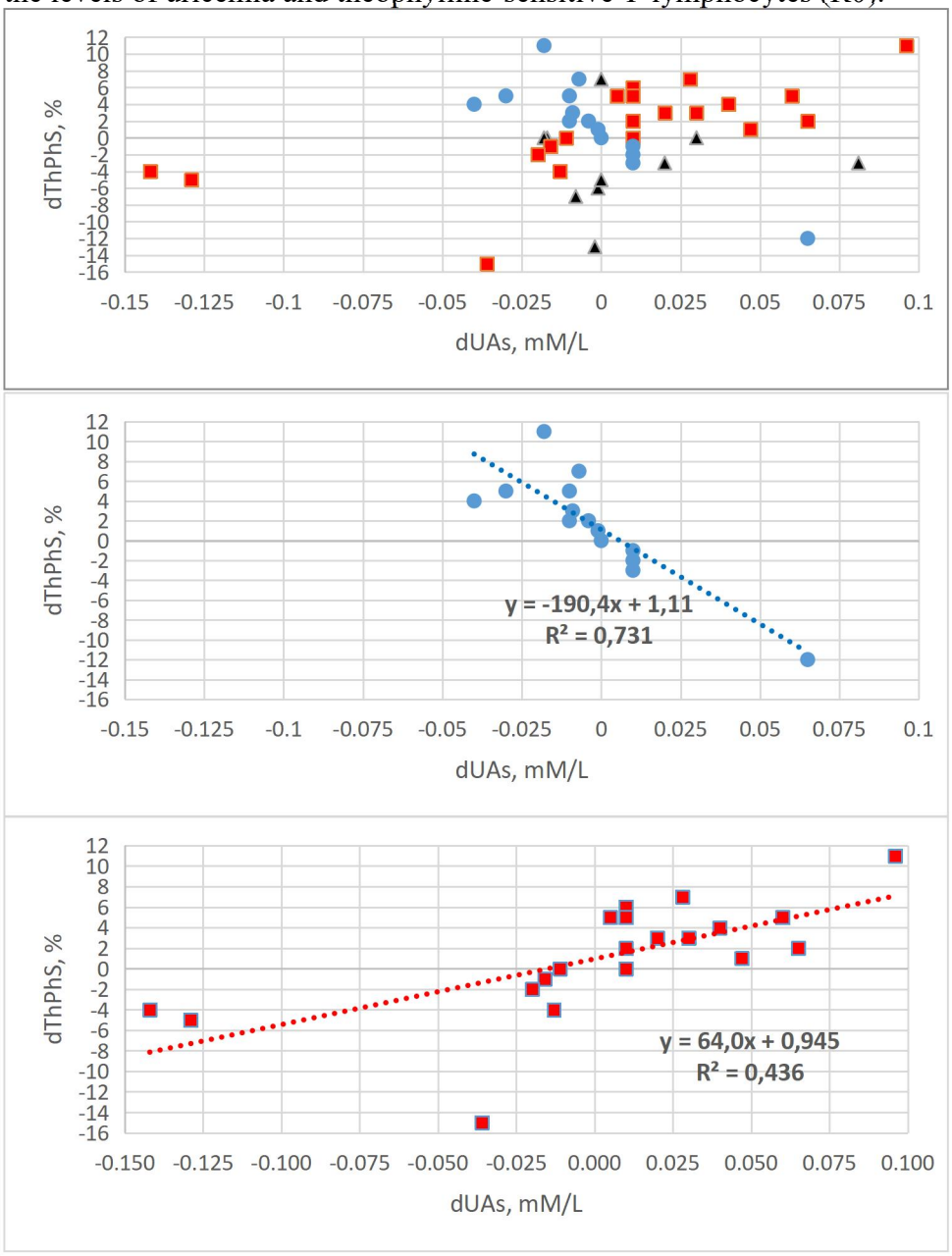

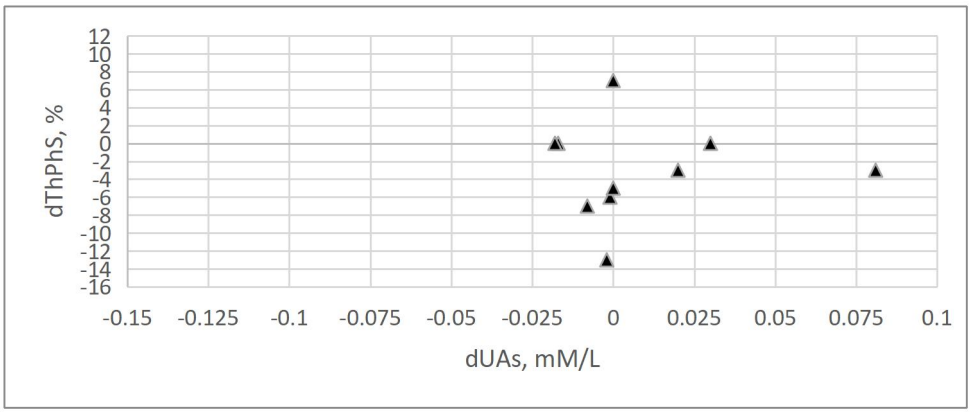

Fig. 5.5. Variants of relationships between changes in Uricemia (X-line) and $CD8^+$ theophylline-sensitive T-lymphocyte (Y-line)

Following the previously accepted algorithm, the registered baseline parameters of the patients were normalized. A subsequent screening revealed those by which the three clusters differ from each other. Then the 9 patterns were formed (Fig. 5.6).

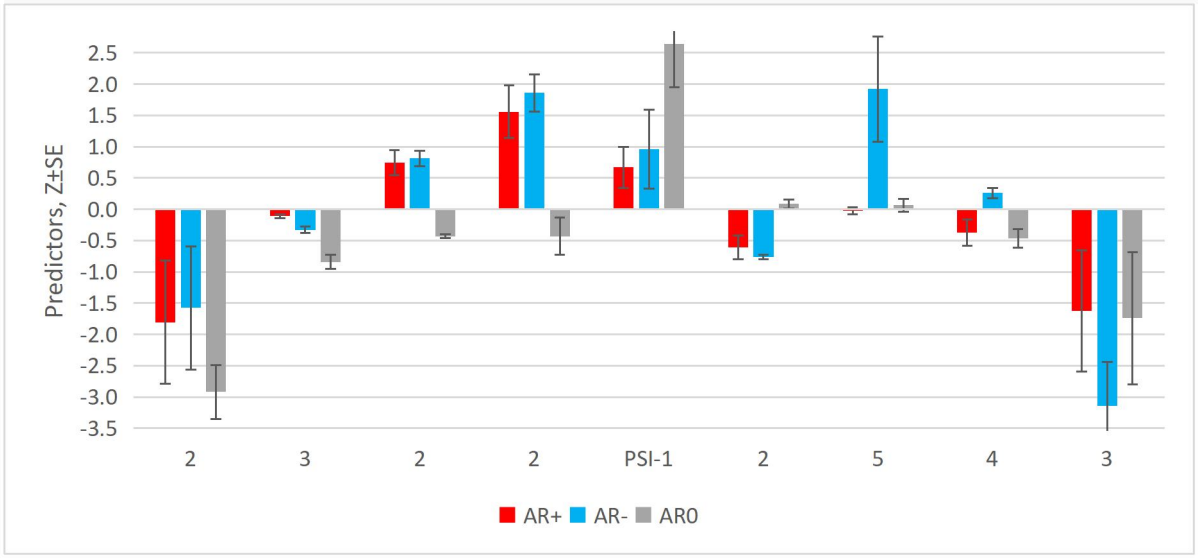

Fig. 5.6. Patterns of predictors of three variants of relationships between changes in uricemia and blood level of theophylline-sensitive T-lymphocytes. ***The number of parameters in the pattern is indicated; see Table 5.3 for details***

As a result of discriminant analysis (forward stepwise method) [], 23 predictors were included in the model, and one was left out of the model due to duplication/excess of discriminating information (Table 5.2). Among the predictors, 10 reflect the PSD of all 4 **EEG rhythms**, 2 – **EEG entropy**, **Autonomous reactivity**, 2 – **hormones**, 4 – **immunity**, 2 – **metabolism,** and another 2 – **leukocytary indices** of Strain and Adaptation.

Table 5.2. Summary of discriminant function analysis for predictors

Step 23, N of vars in model: 23; Grouping: 3 grps; Wilks' Λ: 0,0187; appro. $F_{(46)}=5,21$; $p<10^{-6}$

Variables currently in the model	Clusters of UA/$CD8^+$ relationship (n)			Parameters of Wilks' Statistics					
	AR+ (19)	AR- (14)	AR0 (11)	Wilks Λ	Par-tial Λ	F-re-move (2,19)	p-level	Tole-rancy	Refe-rence Cv
Triglycerides, mM/L	1,20 0,13	1,50 0,18	0,81 0,13	0,026	0,709	3,898	0,038	0,384	1,16 0,606
IgG Serum, g/L	15,3 0,7	15,2 1,1	11,7 1,0	0,042	0,447	11,77	10^{-3}	0,193	12,75 0,206
Popovych's Adaptation	0,84	0,60	0,76	0,024	0,776	2,736	0,090	0,377	1,71

Index-2, points	0,09	0,07	0,07						0,245
PSD F8-δ, $\mu V^2/Hz$	64 20	349 134	139 64	0,025	0,750	3,172	0,065	0,088	92 1,642
PSD F7-θ, %	7,2 0,7	11,3 1,6	6,3 1,4	0,067	0,278	24,71	10^{-5}	0,040	10,0 0,458
PSD F7 Entropy	0,77 0,03	0,80 0,07	0,58 0,08	0,053	0,352	17,50	10^{-4}	0,085	0,821 0,187
Popovych's Strain Index-1, points	0,13 0,02	0,15 0,03	0,24 0,04	0,035	0,533	8,337	0,003	0,207	0,10 0,559
PSD T5-θ, $\mu V^2/Hz$	26 6	51 11	32 9	0,026	0,707	3,937	0,037	0,190	29 0,906
Aldosterone, pM/L	231 5	227 6	209 9	0,030	0,627	5,648	0,012	0,217	238 0,187
PSD Fp1-β, $\mu V^2/Hz$	69 12	85 16	50 6	0,026	0,719	3,707	0,044	0,361	63 0,721
PSD T4-θ, %	9,8 1,8	12,7 1,5	8,2 1,3	0,022	0,859	1,558	0,236	0,223	9,7 0,482
PSD F8-α, $\mu V^2/Hz$	31 4	51 9	34 8	0,037	0,505	9,310	0,002	0,226	42 1,202
PSD F7-α, %	27 4	23 4	13 2	0,025	0,746	3,227	0,062	0,119	27,6 0,522
Autonomous reactivity, units	1,98 0,71	2,16 0,63	-1,15 1,36	0,045	0,412	13,57	10^{-3}	0,057	3,10
PSD F3 Entropy	0,77 0,04	0,87 0,03	0,79 0,05	0,035	0,532	8,359	0,002	0,240	0,862 0,130
IgM Serum, g/L	1,46 0,08	1,57 0,06	1,23 0,06	0,023	0,813	2,187	0,140	0,348	1,15 0,239
Potassium Plasma, mM/L	4,17 0,16	4,21 0,15	4,62 0,16	0,024	0,783	2,629	0,098	0,288	4,55 0,104
Bactericidity vs *Staph. aureus*, 10^9 Bacteria/L	96 5	77 4	98 6	0,027	0,705	3,973	0,036	0,284	106 0,100
PSD C3-θ, $\mu V^2/Hz$	47 10	88 19	44 13	0,024	0,782	2,641	0,097	0,145	44 0,851
PSD Fp1-δ, $\mu V^2/Hz$	64 16	398 172	67 20	0,025	0,750	3,166	0,065	0,105	58 1,132
PSD T5-α, %	20 4	33 4	27 5	0,023	0,803	2,326	0,125	0,099	35 0,516
PTH, pM/L	3,39 0,17	3,06 0,18	3,75 0,22	0,023	0,803	2,333	0,124	0,394	3,75 0,130
$CD4^+$ T-helper Lymphocytes, %	30,5 2,1	31,2 1,6	28,6 2,8	0,022	0,857	1,580	0,232	0,300	39,5 0,082
Variables currently not in the model	**AR+ (19)**	**AR- (14)**	**AR0 (11)**	Wilks Λ	Partial Λ	F to enter	p-level	Tolerancy	Reference Cv
Bactericidity vs *Escherichia coli*, 10^9 B/L	95 8	77 5	92 7	0,018	0,950	0,450	0,640	0,250	99 0,100

At the next stage of the analysis, normalized parameters were grouped into three discriminant roots based on the structural coefficients (Table 5.3). In addition to discriminant variables, the table also presents the variable that are not included in the model, but are still informal carriers of identifying information.

Table 5.3. Correlations of variables with canonical roots, root mean values and Z-values of predictors

Variables	Correlations Variables-Roots		AR+ (19)	AR- (14)	AR0 (11)
Root 1 (78,5%)	R 1	R 2	-3,22	0,41	5,05
PSD F7 Entropy	**-0,085**	-0,115	-0,82	-0,59	**-2,49**
$CD4^+$ T-helper Lymphocytes	**-0,025**	-0,050	-2,79	-2,56	**-3,35**
Aldosterone	**-0,105**	-0,059	-0,15	-0,25	**-0,65**
PSD T5-α	**-0,074**	0,010	-0,13	-0,43	**-0,83**

PSD F7-α	**-0,092**	-0,027	-0,05	-0,30	**-1,04**
Triglycerides	**-0,109**	-0,236	0,55	0,69	**-0,46**
IgG Serum	**-0,118**	-0,117	0,95	0,94	**-0,40**
Autonomous reactivity	**-0,090**	-0,088	1,98	2,16	**-1,15**
IgM Serum	**-0,092**	-0,206	1,14	1,54	**0,29**
Popovych's Strain Index-1	**0,116**	0,078	0,67	0,96	**2,64**
Potassium	**0,109**	0,138	-0,80	-0,73	**0,16**
PTH	**0,053**	0,178	-0,42	-0,80	**0,01**
Root 2 (21,5%)	**R 1**	**R 2**	1,04	**-2,52**	1,41
PSD Fp1-δ	0,019	**-0,224**	0,10	**5,21**	0,15
PSD F8-δ	0,043	**-0,208**	-0,19	**1,70**	0,31
PSD C3-θ	0,011	**-0,193**	0,09	**1,19**	0,02
PSD T5-θ	0,037	**-0,178**	-0,12	**0,87**	0,15
PSD T4-θ	-0,013	**-0,132**	0,01	**0,64**	-0,31
PSD F7-θ	0,001	**-0,245**	-0,62	**0,29**	-0,80
PSD F8-α	0,030	**-0,215**	-0,21	**0,20**	-0,16
PSD Fp1-β	-0,031	**-0,110**	0,13	**0,47**	-0,29
PSD F3 Entropy	0,027	**-0,154**	-0,79	**0,08**	-0,61
Bactericidity vs *Staph. aureus*	0,003	**0,279**	-0,96	**-2,75**	-0,73
Bactericidity vs E. *coli*	currently not in model		-0,37	**-2,17**	-0,64
Popovych's Adaptation Index-2, points	-0,053	**0,155**	-3,53	**-4,50**	-3,85

The result of the analysis is the visualization of each patient in the information space of discriminant roots (Fig. 5.7, see also Fig 5.6).

The localization of members of the R0 cluster in the extreme right zone of the axis of the first root reflects, first, drastically reduced levels of EEG entropy in the F7 locus, autonomous reactivity, and theophylline-resistant $CD4^+$ T-lymphocytes; secondly, moderately reduced levels of PSD of alpha-rhythm in F7 and T5 loci as well as serum aldosterone, thirdly, normal, but minimal for the sample levels of triglycerides and Igg G&M, which are negatively correlated with the root.

On the other hand, predictors of insensitivity of adenosine receptors of $CD8^+$ T-lymphocytes to uric acid are drastically high Popovych's Strain Index-1, as well as normal, but maximum for the sample, potassium and PTH levels. At the opposite pole of the axis of the first root, there are patients whose levels of the listed parameters differ significantly from those in the previous cluster, but are approximately the same.

Instead, there are significant differences between the parameters, the information about which is condensed in the second root. Patients in whom uric acid exerts a caffeine-like effect on theophylline-sensitive T-lymphocytes, i.e. downregulates adenosine receptors, are characterized by significantly increased levels of PSD of delta-rhythm in Fp1 and F8 loci as well as theta-rhythm in C3, T4 and T5 loci in combination with significantly reduced levels of Popovych's Adaptation Index-2 and Bactericidity of neutrophils against both gram-positive and gram-negative bacteria.

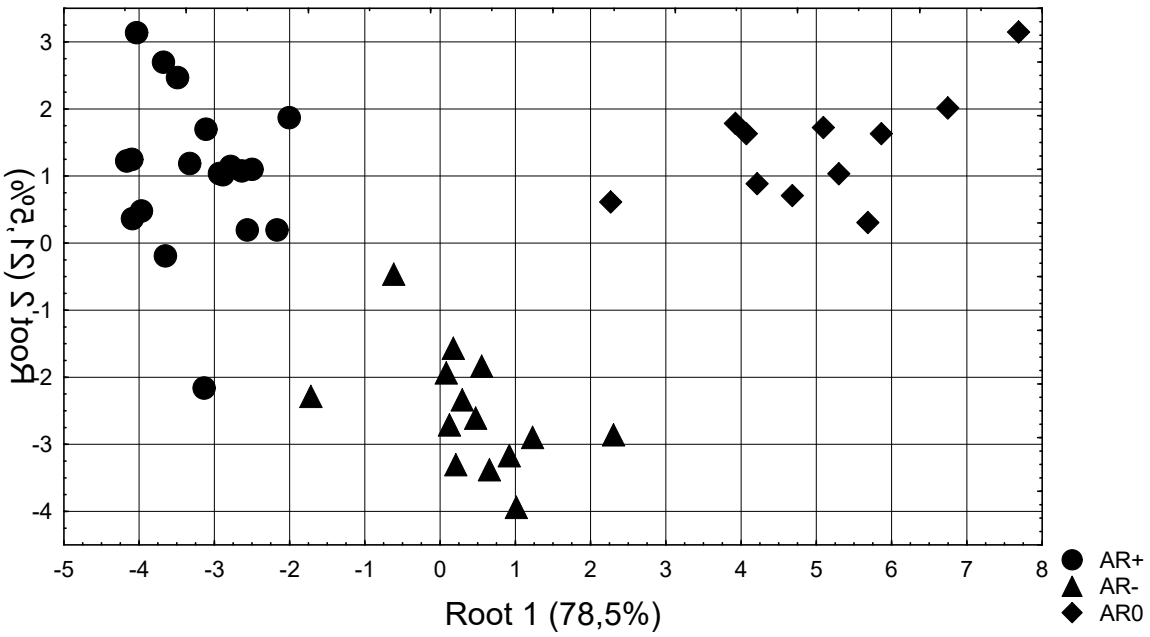

Fig. 3. Scattering of individual values of the discriminant roots of patients with different relationships between changes in Uricemia and blood level of theophylline-sensitive T-lymphocytes

The apparent clear demarcation of all four clusters is documented by the calculation of Mahalanobis distances (Table 5.4).

Table 5.4. Squares of Mahalanobis distances between clusters, F-criterions (df=23,2) and p-levels

Clusters	AR+ (19)	AR- (14)	AR0 (11)
AR+ (19)	0	25,9	68,5
AR- (14)	4,2 10^{-3}	0	37,0
AR0 (11)	9,6 10^{-6}	4,6 10^{-3}	0

The main goal of discriminant analysis - predicting each of the three variants of the relationship between changes in uricemia and the blood level of theophylline-sensitive T-lymphocytes - is achieved by calculating individual classification functions by summing the products of predictors by coefficients with the addition of constants (Table. 5.5). The accuracy of the forecast is 100%.

Table 5.5. Coefficients and constants for classification functions

Clusters	AR+	AR-	AR0
Variables	p=,43	p=,32	p=,25
Triglycerides, mM/L	137,4	132,1	120,7
IgG Serum, g/L	32,05	30,04	27,90
Popovych's Adaptation Index-2, points	-103,2	-100,6	-85,06
PSD F8-δ, $\mu V^2/Hz$	0,486	0,455	0,441
PSD F7-θ, %	-41,98	-37,15	-33,71
PSD F7 Entropy	601,1	543,1	477,3
Popovych's Strain Index-1, points	-354,8	-310,8	-236,8
PSD T5-θ, $\mu V^2/Hz$	1,065	0,924	0,707
Aldosterone, pM/L	4,488	4,269	4,034

PSD Fp1-β, μV^2/Hz	0,793	0,772	0,650
PSD T4-θ, %	3,244	2,754	2,112
PSD F8-α, μV^2/Hz	-3,432	-3,082	-2,859
PSD F7-α, %	5,220	4,686	4,537
Autonomous reactivity, units	1547	1422	1334
PSD F3 Entropy	-426,4	-377,9	-340,4
IgM Serum, g/L	-128,0	-113,8	-109,6
Potassium Plasma, mM/L	172,2	163,9	159,7
Bactericidity vs *Staph. aur.*, 10^9 B/L	2,649	2,383	2,537
PSD C3-θ, μV^2/Hz	0,398	0,295	0,403
PSD Fp1-δ, μV^2/Hz	0,094	0,093	0,064
PSD T5-α, %	3,366	3,176	2,668
PTH, pM/L	-0,922	3,629	7,035
$CD4^+$ T-helper Lymphocytes, %	-3,253	-2,835	-2,593
Constants	-1875	-1691	-1550

It seems that the nature of the interaction of uric acid and adenosine receptors is determined by a certain biochemical and physiological situation. A somewhat similar situation, such as A_{2A} receptor dependent and A_{2A} receptor independent effects of extracellular adenosine, was discovered by Apasov S et al [2000].

Allow us to conclude the monograph by expressing the hope that the results we have obtained confirms and develops both old [Sofaer JA & Emery AF, 1981; Ivassivka SV, Popovych IL, Aksentiychuk BI & Flyunt IS, 2004] and modern [Morelli M, Carta AR, Kachroo A & Schwarzschild Al, 2010; Ghaemi-Oskouie F & Shi Y, 2011; El Ridi R & Tallima H, 2017] hypotheses about the physiological activity of uric acid.

Uric acid is the end product of nucleic acid metabolism. About 500-800 mg is formed per day, and clearance is about 10% of creatinine. Consequently, most of it is retained in the body. This suggests that retention of most of the uric acid is necessary to perform some function. Considering that uric acid is not used in metabolism and its role in the regulation of water exchange is rather not of great importance, it can be assumed that it plays a regulatory role. The antioxidant role has been proven, but our data on the effect of uric acid on the neuro-endocrine-immune complex indicate its direct regulatory role.

ACKNOWLEDGMENT

We express sincere gratitude to colleagues from sanatorium “Moldova” for help in conducting this investigation.

REFERENCES

1. Автандилов Г.Г. Медицинская морфометрия. М: Медицина; 1990: 384.
2. Баевский Р.М., Кириллов О.И., Клецкин С.З. Математический анализ изменений ритма сердца при стрессе. Москва: Наука; 1984: 221.
3. Баевский Р.М., Иванов Г.Г. Вариабельность ритма сердца: теоретические аспекты и возможности клинического применения. Ультразвуковая и функциональная диагностика. 2001; 3: 106-127.
4. Базарнова М.А. Цитологическое исследование пунктатов селезёнки. Руководство к практическим занятиям по клинической лабораторной диагностике. К: Вища школа; 1988: 263-264.
5. Балановський В.П., Попович І.Л., Карпинець СВ. Про амбівалентно-еквілібраторний характер впливу лікувальної води Нафтуся на організм людини. Доповіді АНУ. Мат., прир., техн. науки. 1993; 3: 154-158.
6. Белоусова ОИ, Федотова МИ. Сравнительные данные об изменении количества лимфоцитов селезенки, зобной железы и костного мозга в ранние сроки после облучения в широком диапазоне доз. Радиобиология-радиотерапия. 1968; 9(3): 309-313.
7. Білас В.Р., Попович І.Л. Роль мікрофлори та органічних речовин води Нафтуся у її модулювальному впливі на нейроендокринно-імунний комплекс та метаболізм. Медична гідрологія та реабілітація. 2009; 7(1): 68-102.
8. Білошицький П.В. Температура, інформація, вода, анабіоз, безсмертя. Здоров'я та довголіття. Київ; 2007: 46-47.
9. Бомбушкар ІС, Гоженко АІ, Бадюк НС, Смаглій ВС, Корда ММ, Попович ІЛ, Блавацька ОМ. Зв'язки між параметрами обміну сечової кислоти і нейро-ендокринними факторами адаптації. Вісник морської медицини. 2022; 2(95): 59-74.
10. Гаркави Л.Х., Квакина Е.Б., Кузьменко Т.С. Антистрессорные реакции и активирующая терапия. Москва. Имедис; 1998: 654.
11. Гаркави Л.Х., Квакина Е.Б., Уколова М.А. Адаптационные реакции и резистентность организма. Ростов-на-Дону. Издательство Ростовского Университета, 3-е изд; 1990: 224.
12. Гаркави Л.Х., Ромасюк С.И., Баранцев Ф.Г., Кузьменко Т.С., Откидач С.А., Татков О.В., Баранцева Л.П. Активационная терапия в комплексе санаторно-курортного этапа реабилитации больных с заболеваниями внутренних органов. Сочи; 2000: 94.
13. Гоженко А.И. Теория болезни. Одеса. Фенікс; 2018: 236.
14. Гоженко А.І. Дисрегуляція як основа патофізіології гомеостазу. Клінічна та експериментальна патологія. 2004; 3 (2): 191-193.
15. Гоженко А.И. Функционально-метаболический континуум. Ж НАМН України. 2016; 22(1): 3-8.
16. Гоженко А.І., Корда М.М., Смаглій В.С., Бадюк Н.С., Жуков В.А., Кліщ І.М., Корда І.В., Бомбушкар І.С., Попович І.Л. Сечова кислота, метаболізм, нейро-ендокринно-імунний комплекс. Одеса. Фенікс; 2023: 229.
17. Гончаренко М.С. (редактор). Valeological toolkit hardware-software diagnostics and monitoring of health. Харків. В-во ХНУ ім.В.Н. Каразіна; 2011: 135.
18. Гончаренко М.С., Єрещенко Я.А. Тест система для оцінки фізіологічного стану організму за електрофоретичними властивостями клітин буккального епітелію: Методичні рекомендації. Харків; 1992.
19. Горячковский А.М. Клиническая биохимия. Одеса: Астропринт; 1998: 608.
20. Дацько О.Р., Бубняк А.Б., Івасівка С.В. Органічна складова мінеральної води Нафтуся. Розвиток уявлення про її склад та походження. Медична гідрологія та реабілітація. 2008; 6(1): 168-174.
21. Івасівка С.В., Попович І.Л., Аксентійчук Б.І., Флюнт І.С. Фізіологічна активність сечової кислоти та її роль в механізмі дії води Нафтуся. К. Комп'ютерпрес; 2004: 163.
22. Лаповець Л.Й., Луцик Б.Д. Лабораторна імунологія. Київ. 2004. 173.
23. Передерий В.Г, Земсков А.М, Бычкова Н.Г, Земсков В.М. Иммунный статус, принципы его оценки и коррекции иммунных нарушений. К. Здоров'я; 1995: 211.
24. Попович І.Л. Інформаційні ефекти біоактивної води Нафтуся у щурів: модуляція ентропійної, відвернення десинхронізувальної та обмеження дизгармонізувальної дії водно-імерсійного стресу на інформаційні складові нейро-ендокринно-імунної системи і метаболізму, що корелює з гастропротективим ефектом. Медична гідрологія та реабілітація. 2007; 5(3): 50-70.
25. Поповыч И.Л. Концепция нейро-эндокринно-иммунного комплекса. Медична гідрологія та реабілітація. 2009; 7(2): 9-18.
26. Попович І.Л. Стреслімітуючий адаптогенний механізм біологічної та лікувальної активності води Нафтуся. Київ. Комп'ютерпрес; 2011: 300.
27. Попович І.Л., Флюнт І.С., Алєксєєв О.І. та ін. Саногенетичні засади реабілітації на курорті Трускавець урологічних хворих чорнобильського контингенту. Київ. Комп'ютерпрес; 2003: 192.
28. Попович І.Л., Флюнт І.С., Ніщета І.В., Лобода М.В., Аксентійчук Б.І., Прийма Б.Г., Церковнюк Р.Г. Загальні адаптаційні реакції і резистентність організму ліквідаторів аварії на ЧАЕС. Київ. Комп'ютерпрес; 2000: 117.

29. Портниченко А.Г. Українська бальнеологія: наукові тенденції останнього десятиліття (наукометричний аналіз). Медична гідрологія та реабілітація. 2015; 13(4): 41-52.
30. Смаглий В.С., Гоженко А.И., Бадюк Н.С., Поповыч И.Л. Варианты метаболизма мочевой кислоты и их иммунные и микробиотные аккомпанименты у пациентов с нейро-эндокринно-иммунной комплексной дисфункцией. В: VIII Національний конгрес патофізіологів України "Патологічна фізіологія - охороні здоров'я України" (Одеса, 13-15 травня 2020 р). Одеса; 2020: 314-315.
31. Хаитов Р.М., Пинегин Б.В., Истамов Х.И. Экологическая иммунология. Москва. ВНИРО; 1995: 219.
32. Хмелевский Ю.В., Усатенко О.К. Основные биохимические константы человека в норме и при патологии. Київ. Здоров'я; 1987: 160.
33. Шахбазов В.Г., Колупаева Т.В., Набоков А.Л.Новый метод для оценки биологического возраста людей. Лабораторное дело. 1986; 7: 404-407.
34. Эфроимсон В.П. Некоторые биологические факторы умственной активности. ВИЕТ. 1987; 4: 74-84.
35. Юшковська О.Г. Використання теорії інформації для вивчення адаптивних реакцій організму спортсменів. Медична реабілітація Курортологія Фізіотерапія. 2001; 1 (25): 40-43.
36. Abdel Aziz N., Tallima H., Hafez E.A., El Ridi R. Papain-based vaccination modulates *Schistosoma mansoni* infection-induced cytokine signals. Scand J Immunol. 2016;83(2):128–138.
37. Ahbap E., Sakaci T., Kara E., Sahutoglu T., Koc Y., Basturk T. Serum uric acid levels and inflammatory markers with respect to dipping status: a retrospective analysis of hypertensive patients with or without chronic kidney disease. Clin Exp Hypertens. 2016;38(6):555–563.
38. Akbar S.R., Long D.M., Hussain K., Alhajhusain A., Ahmed U.S., Iqbal H.I. Hyperuricemia: an early marker for severity of illness in sepsis. Int J Nephrol. 2015;301021.
39. Akselrod S, Gordon D, Ubel FA, Shannon DC, Barger AC, Cohen RJ. Power spectrum analysis rate fluctuation: a quantitative probe of beat-to-beat cardiovascular control. Science (NY). 1981; 213(4504): 220-222.
40. Alberti K.G., Eckel R.H., Grundy S.M., Zimmet P.Z., Cleeman J.I., Donato K.A. Harmonizing the metabolic syndrome: a joint interim statement of the international diabetes federation task force on epidemiology and prevention; national heart, lung, and blood institute; american heart association; world heart federation; international atherosclerosis society; and international association for the study of obesity. Circulation. 2009;120(16):1640–1645.
41. Aldenderfer M.S., Blashfield R.K. Cluster analysis (Second printing, 1985) [transl. from English in Russian]. In: Factor, Discriminant and Cluster Analysis. Moskva. Finansy i Statistika; 1989: 139-214.
42. Alvarez-Lario B., Macarrón-Vicente J. Is there anything good in uric acid? QJM. 2011;104(12):1015–1024.]
43. Alvarez-Lario B., Macarron-Vicente J. Uric acid and evolution. Rheumatology. 2010;49(11):2010–2015.
44. Amaral F.A., Costa V.V., Tavares L.D., Sachs D., Coelho F.M., Fagundes C.T. NLRP3 inflammasome-mediated neutrophil recruitment and hypernociception depend on leukotriene B(4) in a murine model of gout. Arthritis Rheum. 2012;64(2):474–484.
45. Amaral K.B., Silva T.P., Malta K.K., Carmo L.A.S., Dias F.F., Almeida M.R. Natural Schistosoma mansoni infection in the wild reservoir Nectomys squamipes leads to excessive lipid droplet accumulation in hepatocytes in the absence of liver functional impairment. Plos One. 2016;11(11):e0166979.
46. Amaral L.M., Cunningham M.W., Jr, Cornelius D.C., LaMarca B. Preeclampsia: long-term consequences for vascular health. Vasc Health Risk Manage. 2015;11:403–415.
47. Ames B.N., Cathcart R., Schwiers E., Hochstein P. Uric acid provides an antioxidant defense in humans against oxidant- and radical-caused aging and cancer: a hypothesis. Proc Natl Acad Sci U S A. 1981;78(11):6858–6862.
48. Amsellem V., Abid S., Poupel L., Parpaleix A., Rodero M., Gary-Bobo G., Latiri M., Dubois-Rande J.L., Lipskaia L., Combadiere C., et al. Roles for the CX3CL1/CX3CR1 and CCL2/CCR2 Chemokine Systems in Hypoxic Pulmonary Hypertension. Am. J. Respir. Cell. Mol. Biol. 2017;56:597–608.
49. Ando K., Takahashi H., Watanabe T., Daidoji H., Otaki Y., Nishiyama S. Impact of serum uric acid levels on coronary plaque stability evaluated using integrated backscatter intravascular ultrasound in patients with coronary artery disease. J Atheroscler Thromb. 2016;23(8):932–939.
50. Andreadou E., Nikolaou C., Gournaras F., Rentzos M., Boufidou F., Tsoutsou A. Serum uric acid levels in patients with Parkinson's disease: their relationship to treatment and disease duration. Clin Neurol Neurosurg. 2009;111(9):724–728.
51. Annanmaki T., Muuronen A., Murros K. Low plasma uric acid level in Parkinson's disease. Mov Disord. 2007;22(8):1133–1137.
52. Anthony R.M., Rutitzky L.I., Urban J.F., Jr., Stadecker M.J., Gause W.C. Protective immune mechanisms in helminth infecton. Nat Rev Immunol. 2007;7(12):975–987. Review.
53. Anzai N., Ichida K., Jutabha P., Kimura T., Babu E., Jin C.J. Plasma urate level is directly regulated by a voltage-driven urate efflux transporter URATv1 (SLC2A9) in humans. J Biol Chem. 2008;283(40):26834–26838.
54. Apasov S, Chen JF, Smith P, Sitkovsky M. A_{2A} receptor dependent and A_{2A} receptor independent effects of extracellular adenosine on murine thymocytes in condicion of adenosine deaminase deficiency. Blood. 2000; 95(12): 3859-3867.

55. Araya J., Rodrigo R., Videla L.A., Thielemann L., Orellana M., Pettinelli P. Increase in long-chain polyunsaturated fatty acid n - 6/n - 3 ratio in relation to hepatic steatosis in patients with non-alcoholic fatty liver disease. Clin Sci (Lond) 2004;106(6):635–643.
56. Aribas A., Kayrak M., Ulucan S., Keser A., Demir K., Alibasic H. The relationship between uric acid and erectile dysfunction in hypertensive subjects. Blood Press. 2014;23:370–376.
57. Arvola L, Bertelsen G, Hassaf D, Ytrehus K. Positive inotropic and sustained anti-beta-adrenergic effect of diadenosine pentaphosphate in human and guinea pig hearts. Role of dinucleotide receptors and adenosine receptors. Acta Physiol Scand. 2004;182(3):277-285.
58. Arnold I.C., Mathisen S., Schulthess J., Danne C., Hegazy A.N., Powrie F. CD11c(+) monocyte/macrophages promote chronic Helicobacter hepaticus-induced intestinal inflammation through the production of IL-23. Mucosal Immunol. 2016;9:352–363.
59. Ascherio A, Chen H, Schwarschild MA, Zhang SM, Colditz GA, Speizer FE. Caffeine, postmenopausal estrogen, and risk of Parkinson's disease. Neurology. 2003; 60: 790–795.]
60. Ascherio A, LeWitt PA, Xu K, Eberly S, Watts A, Matson WR, et al. Urate as a predictor of the rate of clinical decline in Parkinson disease. Arch Neurol. 2009; 66: 1460–1468.
61. Ascherio A, Weisskopf MG, O'Reilly EJ, McCullough ML, Calle EE, Rodriguez C, Thun MJ. Coffee consumption, gender, and Parkinson's disease mortality in the cancer prevention study II cohort: the modifying effects of estrogen. Am J Epidemiol. 2004; 160(1): 977–984.
62. Auerbach A. Dose-Response Analysis When There Is a Correlation between Affinity and Efficacy. Mol. Pharmacol. 2016;89:297–302.
63. Babio N., Martínez-González M.A., Estruch R., Wärnberg J., Recondo J., Ortega-Calvo M. Associations between serum uric acid concentrations and metabolic syndrome and its components in the PREDIMED study. Nutr Metab Cardiovasc Dis. 2015;25(2):173–180.
64. Baevsky RM, Berseneva AP. Use KARDIVAR system for determination of the stress level and estimation of the body adaptability. Standards of measurements and physiological interpretation. Moscow-Prague; 2008: 41.
65. Bakhtiari S., Toosi P., Samadi S., Bakhshi M. Assessment of uric acid level in the saliva of patients with oral lichen planus. Med Princ Pract. 2017;26(1):57–60.
66. Barabé F, Gilbert C, Liao N, Bourgoin SG, Naccache PH. Crystal-induced neutrophil activationVI. Involvement of FcgammaRIIIB (CD16) and CD11b in response to inflammatory microcrystals. FASEB J. 1998;12(2):209-220. doi:10.1096/fasebj.12.2.209
67. Barakat R., Abou El-Ela N.E., Sharaf S., El Sagheer O., Selim S., Tallima H. Efficacy and safety of arachidonic acid for treatment of school-age children in Schistosoma mansoni high-endemicity regions. Am J Trop Med Hyg. 2015;92(4):797–804.
68. Bardin T., Richette P. Definition of hyperuricemia and gouty conditions. Curr. Opin. Rheumatol. 2014;26:186–191.
69. Barikbin B., Yousefi M., Rahimi H., Hedayati M., Razavi S.M., Lotfi S. Antioxidant status in patients with lichen planus. Clin Exp Dermatol. 2011;36(8):851–854.
70. Bartáková V., Kuricová K., Pácal L., Nová Z., Dvořáková V., Švrčková M. Hyperuricemia contributes to the faster progression of diabetic kidney disease in type 2 diabetes mellitus. J Diabetes Complications. 2016;30(7):1300–1307.
71. Barylyak L.G., Malyuchkova R.V., Tolstanov O.B., Tymochko O.B., Hryvnak R.F., Uhryn M.R. Comparative estimation of informativeness of leucocytary index of adaptation by Garkavi and by Popovych. Medical Hydrology and Rehabilitation. 2013; 11(1): 5-20.
72. Basseville A., Bates S. Gout, genetics and ABC transporters. F1000 Biology Reports. 2011;3: 23.
73. Beck L.H. Requiem for gouty nephropathy. Kidney Int. 1986;30(2):280–287.
74. Becker B.F. Towards the physiological function of uric acid. Free Radic Biol Med. 1993;14(6):615–631.
75. Bellomo G., Venanzi S., Verdura C., Saronio P., Esposito A., Timio M. Association of uric acid with change in kidney function in healthy normotensive individuals. Am J Kidney Dis. 2010;56(2):264–272.
76. Berntson GG, Bigger JT jr, Eckberg DL, Grossman P, Kaufman PG, Malik M, Nagaraja HN, Porges SW, Saul JP, Stone PH, Van der Molen MW. Heart Rate Variability: Origines, methods, and interpretive caveats. Psychophysiology. 1997; 34: 623-648.
77. Besedovsky H & Sorkin E. Network of immune-neuroendocrine interaction. Clin Exp Immunol. 1977; 27(1): 1-12.
78. Besedovsky H & del Rey A. Immune-neuro-endocrine interactions: facts and hypotheses. Endocrine reviews. 1996; 17(1): 64–102.
79. Bianco C. Population of lymphocytes bearing a membrane receptor for antigen-antibody complex. J Exp Med. 1970; 134(4): 702-720.
80. Bjorkander S., Heidari-Hamedani G., Bremme K., Gunnarsson I., Holmlund U. Peripheral monocyte expression of the chemokine receptors CCR2, CCR5 and CXCR3 is altered at parturition in healthy women and in women with systemic lupus erythematosus. Scand. J. Immunol. 2013;77:200–212.
81. Birch RE, Rosenthal AK, Polmer SH. Pharmacological modification of immunoregulatory T lymphocytes. II. Modulation of T lymphocyte cell surface characteristics. Clin Exp Immunol. 1982; 48(1): 231-238.

82. Bjornstad P., Lanaspa M.A., Ishimoto T., Kosugi T., Kume S., Jalal D. Fructose and uric acid in diabetic nephropathy. Diabetologia. 2015;58(9):1993–2002.
83. Bjornstad P., Maahs D.M., Johnson R.J., Rewers M., Snell-Bergeon J.K. Estimated insulin sensitivity predicts regression of albuminuria in Type 1 diabetes. Diabet Med. 2015;32(2):257–261.
84. Bjornstad P., Roncal C., Milagres T., Pyle L., Lanaspa M.A., Bishop F.K. Hyperfiltration and uricosuria in adolescents with type 1 diabetes. Pediatr Nephrol. 2016;(5):787–793.
85. Bjornstad P., Snell-Bergeon J.K., McFann K., Wadwa R.P., Rewers M., Rivard C.J. Serum uric acid and insulin sensitivity in adolescents and adults with and without type 1 diabetes. J Diabetes Complications. 2014;28(3):298–304.
86. Bombushkar IS, Gozhenko AI, Korda IV, Badiuk NS, Zukow W, Popovych IL. Features of the exchange of electrolytes and nitrogenous metabolites under different options of uric acid exchange in healthy female rats. Journal of Education, Health and Sport. 2020; 10(4): 405-415.
87. Bombushkar IS. Features of the state of the neuroendocrine-immune complex and electrolyte-nitrogenous exchange under different variations of uric acid metabolism in female rats. Journal of Education, Health and Sport. 2020; 10(5): 410-421.
88. Bombushkar IS, Gozhenko AI, Korda MM, Żukow X, Popovych IL. Relationships between plasma levels of nitrogenous metabolites and some psycho-neuro-endocrine parameters. Journal of Education, Health and Sport. 2022; 12(6): 365-383.
89. Bombushkar IS, Korda MM, Gozhenko AI, Żukow X, Popovych IL. Psycho-neuro-endocrine accompaniments of individual variants of nitrogenous metabolites exchange. Journal of Education, Health and Sport. 2022; 12(7): 994-1008.
90. Bombushkar IS, Anchev AS, Żukow X, Popovych IL. Sexual dimorphism in relationships between of plasma urea and some psycho-neuro-endocrine parameters Journal of Education, Health and Sport. 2022; 12(8): 1198-1205.
91. Bombushkar IS, Anchev AS, Żukow X, Popovych IL. Sexual dimorphism in relationships between of plasma creatinine and some neuro-endocrine parameters. Journal of Education, Health and Sport. 2022; 12(9): 985-997.
92. Bombushkar IS, Gozhenko AI, Korda MM, Żukow X, Popovych IL. Peculiarities of relationships between plasma levels of nitrogenous metabolites and EEG&HRV parameters in patients with postradiation encephalopaty. Journal of Education, Health and Sport. 2022; 12(10): 335-355.
93. Bombushkar IS, Anchev AS, Żukow X, Popovych IL. Sexual dimorphism in relationships between of plasma bilirubin and some neuro-endocrine parameters. Journal of Education, Health and Sport. 2022; 12(11): 381-389.
94. Bombushkar IS, Gozhenko AI, Korda MM, Popovych IL. Plasma levels of nitrogenous metabolites are closely correlated with some psycho-neuro-endocrine parameters. В: Матер. XIII Всеукраїнської наук.-практ. конф. "Актуальні питання патології за умов дії надзвичайних факторів на організм" (Тернопіль, 26-28 жовтня 2022 р). Тернопіль; 2022: 80-81.
95. Bombushkar IS. Metabolic accompaniments of variants of uric acid exchange. Journal of Education, Health and Sport. 2022; 12(12): 373-390.
96. Bombushkar IS, Popovych IL, Zukow W. Relationships between the parameters of uric acid exchange and electroencephalograms in humans. Journal of Education, Health and Sport. 2023; 13(3): 458-485.
97. Bobulescu I.A., Moe O.W. Renal transport of uric acid: evolving concepts and uncertainties. Adv Chronic Kidney Dis. 2012;19(6):358–371.
98. Bocarsly M.E., Powell E.S., Avena N.M., Hoebel B.G. High-fructose corn syrup causes characteristics of obesity in rats: increased body weight, body fat and triglyceride levels. Pharmacol Biochem Behav. 2010;97:101–106.
99. Broz P., Dixit V.M. Inflammasomes: mechanism of assembly, regulation and signalling. Nat Rev Immunol. 2016;16(7):407–420.
100. Bruno C.M., Pricoco G., Cantone D., Elisa Marino E., Bruno F. Tubular handling of uric acid and factors influencing its renal excretion: a short review. EMJ Nephrol. 2016;4(1):92–97.
101. Busso N., Ea H.K. The mechanisms of inflammation in gout and pseudogout (CPP-induced arthritis) Reumatismo. 2012;63(4):230–237.
102. Busso N., So A. Mechanisms of inflammation in gout. Arthritis Res Ther. 2010;12(2):206.
103. Busso N., So A. Microcrystals as DAMPs and their role in joint inflammation. Rheumatology (Oxford) 2012;51(7):1154–1160.
104. Cammalleri L., Malaguarnera M. Rasburicase represents a new tool for hyperuricemia in tumor lysis syndrome and in gout. International Journal of Medical Sciences. 2007;4(2):83–93. doi: 10.7150/ijms.4.83.
105. Campion E.W., Glynn R.J., DeLabry L.O. Asymptomatic hyperuricemia. Risks and consequences in the Normative Aging Study. Am J Med. 1987;82:421.
106. Carito V., Ceccanti M., Tarani L., Ferraguti G., Chaldakov G. N., Fiore M. Neurotrophins' modulation by olive polyphenols. Current Medicinal Chemistry. 2016;23(28):3189–3197.

107. Carvalho LAC, Lopes JPPB, Kaihami GH, Silva RP, Bruni-Cordoso A, Baldini RL, Meotti FC. Uric acid disrupts hypochlorous acid production and bactericidal activity of HL-60 cells. Redox Biology. 2018; 16: 179-188.
108. Chakraborti G., Biswas R., Chakraborti S., Sen P.K. Altered serum uric acid level in lichen planus patients. Indian J Dermatol. 2014;59(6):558–561.
109. Chang B.S. Ancient insights into uric acid metabolism in primates. Proc Natl Acad Sci USA. 2014;111(10):3657–3658.
110. Chaudhary K., Malhotra K., Sowers J., Aroor A. Uric Acid - key ingredient in the recipe for cardiorenal metabolic syndrome. Cardiorenal Med. 2013;3(3):208–220.
111. Chavan SS, Pavlov VA, Tracey KJ. Mechanism and therapeutic relevance of neuro-imune communication. Immunity. 2017; 46(6): 927-942.
112. Chavan SS, Tracey KJ. Essencial neuroscience in immunology. J Immunol. 2017; 198: 3389-3397.
113. Chen CJ, Shi Y, Hearn A, et al. MyD88-dependent IL-1 receptor signaling is essential for gouty inflammation stimulated by monosodium urate crystals. J Clin Invest. 2006;116(8):2262-2271.
114. Chen H., Cao G., Chen D. Q., et al. Metabolomics insights into activated redox signaling and lipid metabolism dysfunction in chronic kidney disease progression. Redox Biology. 2016;10:168–178.
115. Chen Y., Xu B., Sun W., Sun J., Wang T., Xu Y. Impact of the serum uric acid level on subclinical atherosclerosis in middle-aged and elderly chinese. J Atheroscler Thromb. 2015;22(8):823–832.
116. Chen-Xu M., Yokose C., Rai S.K., Pillinger M.H., Choi H.K. Contemporary Prevalence of Gout and Hyperuricemia in the United States and Decadal Trends: The National Health and Nutrition Examination Survey, 2007–2016. Arthritis Rheumatol. 2019;71:991–999.
117. Cheung K.J., Tzameli I., Pissios P., Rovira I., Gavrilova O., Ohtsubo T. Xanthine oxidoreductase is a regulator of adipogenesis and PPARγ activity. Cell Metab. 2007;5:115–128.
118. Cheungpasitporn W., Thongprayoon C., Harrison A.M., Erickson S.B. Admission hyperuricemia increases the risk of acute kidney injury in hospitalized patients. Clin Kidney J. 2016;9(1):51–56.
119. Chiquete E., Ruiz-Sandoval J.L., Murillo-Bonilla L.M., Arauz A., Orozco-Valera D.R., Ochoa-Guzmán A. Serum uric acid and outcome after acute ischemic stroke: PREMIER study. Cerebrovasc Dis. 2013;35(2):168–174.
120. Cho J., Kim C., Kang D.R., Park J. Hyperuricemia and uncontrolled hypertension in treated hypertensive patients: K-MetS study. Medicine (Baltimore) 2016;95(28):e4177.
121. Choi H.K., Curhan G. Independent impact of gout on mortality and risk for coronary heart disease. Circulation. 2007;116(8):894–900.
122. Choi H.K., Ford E.S. Prevalence of the metabolic syndrome in individuals with hyperuricemia. Am J Med. 2007;120(5):442–447.
123. Choi Y.J., Shin H.S., Choi H.S., Park J.W., Jo I., Oh E.S. Uric acid induces fat accumulation via generation of endoplasmic reticulum stress and SREBP-1c activation in hepatocytes. Lab Invest. 2014;94(10):1114–1125.
124. Chou Y.C., Kuan J.C., Yang T., Chou W.Y., Hsieh P.C., Bai C.H. Elevated uric acid level as a significant predictor of chronic kidney disease: a cohort study with repeated measurements. J Nephrol. 2015;28(4):457–462.
125. Cicerchi C., Li N., Kratzer J., Garcia G., Roncal-Jimenez C.A., Tanabe K. Uric acid-dependent inhibition of AMP kinase induces hepatic glucose production in diabetes and starvation: evolutionary implications of the uricase loss in hominids. FASEB J. 2014;(8):3339–3350.
126. Cicero A., Rosticci M., Tartagni E., Parini A., Grandi E., D'Addato S. Serum uric acid level, but not renal function or arterial stiffness, is associated to worse blood pressure control in general practice: data from the brisighella heart study. J Hypertens. 2015;33(Suppl 1):e22.
127. Cicero A.F., Rosticci M., Fogacci F., Grandi E., D'Addato S., Borghi C. High serum uric acid is associated to poorly controlled blood pressure and higher arterial stiffness in hypertensive subjects. Eur J Intern Med. 2017;37:38–42.
128. Cinel I, Gür S. Direct inotropic effects of propofol and adenosine on rat atrial muscle: possible mechanisms. Pharmacol Res. 2000;42(2):123-128.
129. Clarson L.E., Chandratre P., Hider S.L., Belcher J., Heneghan C., Roddy E. Increased cardiovascular mortality associated with gout: a systematic review and meta-analysis. Eur J Prev Cardiol. 2015;22(3):335–343.
130. Clémençon B., Lüscher B.P., Fine M., Baumann M.U., Surbek D.V., Bonny O. Expression, purification, and structural insights for the human uric acid transporter, GLUT9, using the Xenopus laevis oocytes system. PLoS ONE. 2014;9(10):e108852.
131. Cleophas M. C., Joosten L. A., Stamp L. K., Dalbeth N., Woodward O. M., Merriman T. R. ABCG2 polymorphisms in gout: insights into disease susceptibility and treatment approaches. Pharmacogenomics and Personalized Medicine. 2017;10:129–142.
132. Conen D, Wietlisbach V, Bovet P, Shamlaye C, Riesen W, Paccaud F, et al. Prevalence of hyperuricemia and relation of serum uric acid with cardiovascular risk factors in a developing country. BMC public health. 2004;4:9.

133. Convento M.S., Pessoa E., Dalboni M.A., Borges F.T., Schor N. Pro-inflammatory and oxidative effects of noncrystalline uric acid in human mesangial cells: contribution to hyperuricemic glomerular damage. Urol Res. 2011;39(1):21–27.
134. Cristóbal-García M., García-Arroyo F.E., Tapia E., Osorio H., Arellano-Buendía A.S., Madero M. Renal oxidative stress induced by long-term hyperuricemia alters mitochondrial function and maintains systemic hypertension. Oxid Med Cell Longev. 2015;535686.
135. Culleton B.F., Larson M.G., Kannel W.B., Levy D. Serum uric acid and risk for cardiovascular disease and death: the Framingham Heart Study. Ann Intern Med. 1999;131(1):7–13.
136. Dalbeth N., Merriman T. Crystal ball gazing: new therapeutic targets for hyperuricaemia and gout. Rheumatology (Oxford). 2009;48(3):222–226.
137. De Cosmo S., Viazzi F., Pacilli A., Giorda C., Ceriello A., Gentile S. Serum uric acid and risk of CKD in Type 2 diabetes. Clin J Am Soc Nephrol. 2015;10(11):1921–1929.
138. De Duve C, Wattiaux R. Functions of lysosomes. Annu Rev Physiol. 1966;28:435–492.
139. De Vera M., Rahman M.M., Rankin J., Kopec J., Gao X., Choi H. Gout and the risk of Parkinson's disease: a cohort study. Arthritis Rheum. 2008 Nov 15;59(11):1549–1554.
140. Deci M.B., Ferguson S.W., Scatigno S.L., Nguyen J. Modulating Macrophage Polarization through CCR2 Inhibition and Multivalent Engagement. Mol. Pharm. 2018;15:2721–2731.
141. Dehghan A., van Hoek M., Sijbrands E.J., Hofman A., Witteman J.C. High serum uric acid as a novel risk factor for type 2 diabetes. Diabetes Care. 2008;31(2):361–362.]
142. Denoble A.E., Huffman K.M., Stabler T.V., Kelly S.J., Hershfield M.S., McDaniel G.E. Uric acid is a danger signal of increasing risk for osteoarthritis through inflammasome activation. Proc Natl Acad Sci USA. 2011;108(5):2088–2093.
143. Desaulniers P, Fernandes M, Gilbert C, Bourgoin SG, Naccache PH. Crystal-induced neutrophil activation. VII. Involvement of Syk in the responses to monosodium urate crystals. J Leukoc Biol. 2001;70(4):659-668.
144. Desaulniers P., Marois S., Paré G., Popa-Nita O., Gilbert C., Naccache P.H. Characterization of an activation factor released from human neutrophils after stimulation by triclinic monosodium urate crystals. J Rheumatol. 2006;33(5):928–938.
145. DiBianco J.M., Jarrett T.W., Mufarrij P. Metabolic syndrome and nephrolithiasis risk: should the medical management of nephrolithiasis include the treatment of metabolic syndrome? Rev Urol. 2015;17(3):117–128.
146. Doehner W., Jankowska E.A., Springer J., Lainscak M., Anker S.D. Uric acid and xanthine oxidase in heart failure – emerging data and therapeutic implications. Int J Cardiol. 2016;15(213):15–19.
147. Dogan M., Uz O., Aparci M., Atalay M. Confounders of uric acid level for assessing cardiovascular outcomes. J Geriatr Cardiol. 2016;13(2):197–198.
148. Döring A., Gieger C., Mehta D., Gohlke H., Prokisch H., Coassin S. SLC2A9 influences uric acid concentrations with pronounced sex-specific effects. Nat Genet. 2008;40(4):430–436.
149. Douglas SD, Quie PG. Investigation of Phagocytes in Disease. Churchil; 1981: 110 p.
150. Drulović J., Dujmović I., Stojsavljević N., Mesaros S., Andjelković S., Miljković D. Uric acid levels in sera from patients with multiple sclerosis. J Neurol. 2001;248(2):121–126.
151. Duckworth D. A treatise on gout. London. C Griffin & Co; 1889: 476 p.
152. Dunn JP, Brooks GW, Mausner J, Rodnan GP, Cobb S. Social class gradient of serum uric acid levels in males. JAMA. 1963;185:431–436.
153. Effendi WI, Nagano T, Kobayashi K, Nishimura Y. Focusing on Adenosine Receptors as a Potential Targeted Therapy in Human Diseases. Cells. 2020;9(3):785.
154. Eisen A., Benderly M., Goldbourt U., Haim M. Is serum uric acid level an independent predictor of heart failure among patients with coronary artery disease? Clin Cardiol. 2013;36(2):110–116.
155. Eisenbarth SC, Colegio OR, O'Connor W, Sutterwala FS, Flavell RA. Crucial role for the Nalp3 inflammasome in the immunostimulatory properties of aluminium adjuvants. Nature. 2008;453(7198):1122-1126. doi:10.1038/nature06939
156. Ejaz A.A., Alquadan K.F., Dass B., Shimada M., Kanbay M., Johnson R.J. Effects of serum uric acid on estimated GFR in cardiac surgery patients: a pilot study. Am J Nephrol. 2015;42(6):402–409.
157. Ejaz A.A., Mu W., Kang D.H., Roncal C., Sautin Y.Y., Henderson G. Could uric acid have a role in acute renal failure? Clin J Am Soc Nephrol. 2007;2(1):16–21.
158. Ekici B., Kütük U., Alhan A., Töre H.F. The relationship between serum uric acid levels and angiographic severity of coronary heart disease. Kardiol Pol. 2015;73(7):533–538.
159. El Ridi R, Tallima H. Physiological functions and pathogenic potential of uric acid: A review. J Adv Res. 2017;8(5):487-493.
160. El Ridi R., Aboueldahab M., Tallima H., Salah M., Mahana N., Fawzi S. In vitro and in vivo activities of arachidonic acid against Schistosoma mansoni and Schistosoma haematobium. Antimicrob Agents Chemother. 2010;54(8):3383–3389.
161. El Ridi R., Tallima H. Vaccine-induced protection against murine schistosomiasis mansoni with larval excretory-secretory antigens and papain or type-2 cytokines. J Parasitol. 2013;99(2):194–202.

162. El Ridi R., Tallima H., Dalton J.P., Donnelly S. Induction of protective immune responses against schistosomiasis using functionally active cysteine peptidases. Front Genet. 2014;5:119.
163. El Ridi R., Tallima H., Migliardo F. Biochemical and biophysical methodologies open the road for effective schistosomiasis therapy and vaccination. Biochim Biophys Acta. 2016;1861(1 Pt B):3613–3620.
164. El Ridi R., Tallima H., Salah M., Aboueldahab M., Fahmy O.M., Al-Halbosiy M.F. Efficacy and mechanism of action of arachidonic acid in the treatment of hamsters infected with Schistosoma mansoni or Schistosoma haematobium. Int J Antimicrob Agents. 2012;39(3):232–239.
165. El Ridi R., Tallima H., Selim S., Donnelly S., Cotton S., Gonzales Santana B. Cysteine peptidases as schistosomiasis vaccines with inbuilt adjuvanticity. PLoS One. 2014;9(1):e85401.
166. Elmas O., Elmas O., Aliciguzel Y., Simsek T. The relationship between hypertension and plasma allantoin, uric acid, xanthine oxidase activity and nitrite, and their predictive capacity in severe preeclampsia. J Obstet Gynaecol. 2016;36(1):34–38.
167. Enomoto A., Kimura H., Chairoungdua A., Shigeta Y., Jutabha P., Cha S.H. Molecular identification of a renal urate anion exchanger that regulates blood urate levels. Nature. 2002;417(6887):447–452.
168. Erdogan D., Gullu H., Caliskan M., Yildirim E., Bilgi M., Ulus T. Relationship of serum uric acid to measures of endothelial function and atherosclerosis in healthy adults. Int J Clin Pract. 2005;59(11):1276–1282.
169. Erdogan D., Tayyar S., Ali Uysal B.A., Icli A., Karabacak M., Ozaydin M. Effects of allopurinol on coronary microvascular and left ventricular function in patients with idiopathic dilated cardiomyopathy. Can J Cardiol. 2012;28:721–727.
170. Erkmen Uyar M., Sezer S., Bal Z., Guliyev O., Tutal E., Kulah E. Post-transplant Hyperuricemıa as a Cardıovascular Risk Factor. Transplant Proc. 2015;47(4):1146–1151.
171. Facchini F.1., Chen Y.D., Hollenbeck C.B., Reaven G.M. Relationship between resistance to insulin-mediated glucose uptake, urinary uric acid clearance, and plasma uric acid concentration. JAMA. 1992;266(21):3008–3011.
172. Fajda OI, Hrinchenko BV, Snihur OV, Barylyak LG, Zukow W. What Kerdoe's Vegetative Index really reflects? Journal of Education, Health and Sport. 2015; 5(12): 279-288.
173. Fajda OI, Drach OV, Barylyak LG, Zukow W. Relationships between Ca/K plasma ratio and parameters of Heart Rate Variability at patients with diathesis urica. Journal of Education, Health and Sport. 2016; 6(1): 295-301.
174. Fang P., Li X., Luo J.J., Wang H., Yang X.F. A double-edged sword: uric acid and neurological disorders. Brain Disord Ther. 2013;2(2):109.
175. Feig D.I., Johnson R.J. Hyperuricemia in childhood primary hypertension. Hypertension. 2003;42:247–252.
176. Fessel W.J. Renal outcomes of gout and hyperuricemia. Am J Med. 1979;67:74.
177. Ficociello L.H., Rosolowsky E.T., Niewczas M.A., Maselli N.J., Weinberg J.M., Aschengrau A. High-normal serum uric acid increases risk of early progressive renal function loss in type 1 diabetes: results of a 6-year follow-up. Diabetes Care. 2010;33(6):1337–1343.
178. Fiddis RW, Vlachos N, Calvert PD. Studies of urate crystallisation in relation to gout. Ann Rheum Dis. 1983;42 Suppl 1(Suppl 1):12-15.
179. Fiebich BL, Biber K, Lieb K, van Calker D, Berger M, Bauer J, Gebicke-Haerter PJ. Cyclooxygenase-2 expression in rat microglia is induced by adenosine A2a receptors. Glia. 1996; 18: 152–60.
180. Fields TR, Abramson SB, Weissmann G, Kaplan AP, Ghebrehiwet B. Activation of the alternative pathway of complement by monosodium urate crystals. Clin Immunol Immunopathol. 1983;26(2):249-257.
181. Flyunt VR, Flyunt I-SS, Fil' VM, Kovbasnyuk MM, Hryvnak RF, Popel SL, Zukow W. Relationships between caused by drinking of bioactive water Naftussya changes in urine lithogenicity and neuro-humoral-immune factors in humans with theirs abnormalities. Journal of Education, Health and Sport. 2017; 7(3): 11-30.
182. Franchi L., Eigenbrod T., Muñoz-Planillo R., Nuñez G. The inflammasome: a caspase-1-activation platform that regulates immune responses and disease pathogenesis. Nat Immunol. 2009;10(3):241–247.
183. Freitas H.S., Anhê G.F., Melo K.F., Okamoto M.M., Oliveira-Souza M., Bordin S. $Na^{(+)}$-glucose transporter-2 messenger ribonucleic acid expression in kidney of diabetic rats correlates with glycemic levels: involvement of hepatocyte nuclear factor-1alpha expression and activity. Endocrinology. 2008;149(2):717–724.
184. Gaipov A., Solak Y., Turkmen K., Toker A., Baysal A.N., Cicekler H. Serum uric acid may predict development of progressive acute kidney injury after open heart surgery. Ren Fail. 2015;37(1):96–102.
185. Galluzzi L., Vitale I., Aaronson S. A., et al. Molecular mechanisms of cell death: recommendations of the Nomenclature Committee on Cell Death 2018. Cell Death & Differentiation. 2018;25(3):486–541.
186. Gao L, Jiang Y, Wang Y, Qu X, Li L, Lou X, Wang Y, GuoW, Liu Y. Male asymptomatic hyperuticemia patients display a lower number of $NKG2D^{+}$ NK cells before and after a low-purine diet. Medicine (Baltimore). 2018; 97(50): e13668.
187. Geraci G., Mulè G., Mogavero M., Geraci C., Nardi E., Cottone S. Association between uric acid and renal hemodynamics: pathophysiological implications for renal damage in hypertensive patients. J Clin Hypertens (Greenwich) 2016;18(10):1007–1014.

188. Gerring Z., Pearson J. F., Morrin H. R., Robinson B. A., Harris G. C., Walker L. C. Phosphohistone H3 outperforms Ki67 as a marker of outcome for breast cancer patients. Histopathology. 2015;67(4):538–547.
189. Gertler M.M., Garn S.M., Levine S.A. Serum uric acid in relation to age and physique in health and in coronary heart disease. Ann Intern Med. 1951;34(6):1421–1431.
190. Ghaemi-Oskouie F, Shi Y. The role of uric acid as an endogenous danger signal in immunity and inflammation. Curr Rheumatol Rep. 2011;13(2):160-166.
191. Giallauria F., Predotti P., Casciello A., Grieco A., Russo A., Viggiano A. Serum uric acid is associated with non-dipping circadian pattern in young patients (30–40 years old) with newly diagnosed essential hypertension. Clin Exp Hypertens. 2016;38(2):233–237.
192. Gille C., Spring B., Tewes L., Poets C.F., Orlikowsky T. A new method to quantify phagocytosis and intracellular degradation using green fluorescent protein-labeled Escherichia coli: Comparison of cord blood macrophages and peripheral blood macrophages of healthy adults. Cytom. A. 2006;69:152–154.
193. Givertz M.M., Anstrom K.J., Redfield M.M., Deswal A., Haddad H., Butler J. Effects of xanthine oxidase inhibition in hyperuricemic heart failure patients: the xanthine oxidase inhibition for hyperuricemic heart failure patients (EXACT-HF) study. Circulation. 2015;131(20):1763–1771.
194. Glantzounis G.K., Tsimoyiannis E.C., Kappas A.M., Galaris D.A. Uric acid and oxidative stress. Curr Pharm Des. 2005;11(32):4145–4151.
195. Gold M.J., Hiebert P.R., Park H.Y., Stefanowicz D., Le A., Starkey M.R. Mucosal production of uric acid by airway epithelial cells contributes to particulate matter-induced allergic sensitization. Mucosal Immunol. 2016;9(3):809–820.
196. Góth L. The rasburicase therapy may cause hydrogen peroxide shock. Orvosi Hetilap. 2008;149(34):1587–1590. doi: 10.1556/OH.2008.28422.
197. Gozhenko AI, Smagliy SS, Korda IV, Badiuk NS, Zukow W, Popovych IL. Functional relationships between parameters of uric acid exchange and immunity in female rats. Actual problems of transport medicine. 2019; 4 (54): 123–131.
198. Gozhenko AI, Smagliy SS, Korda IV, Badiuk NS, Zukow W, Popovych IL. Features of immune status in different states of uric acid metabolism in female rats. Journal of Education, Health and Sport. 2019; 9(12): 167-180.
199. Gozhenko AI, Smagliy SS, Korda IV, Zukow W, Popovych IL. Cluster analysis of uric acid exchange parameters in female rats. Journal of Education, Health and Sport. 2019; 9(11): 277-286.
200. Gozhenko AI, Smagliy VS, Korda IV, Badiuk NS, Zukow W, Kovbasnyuk MM, Popovych IL. relationships between parameters of uric acid exchange and immunity as well as microbiota in patients with neuroendocrine-immune complex dysfunction. Journal of Education, Health and Sport. 2020; 10(1): 165-175.
201. Gozhenko AI, Smagliy VS, Korda IV, Badiuk NS, Zukow W, Popovych IL. Functional relationships between parameters of uric acid exchange and immunity in female rats. In: Rehabilitation Medicine and Health-Resort Institutions Development. Proceedings of the 19th International Applied Research Conference (Kyïv, 11-12 December 2019). Edited by O. Gozhenko, W. Zukow. Toruń, Kyiv. 2019: 23-24.
202. Gozhenko AI, Sydoruk NO, Babelyuk VYe, Dubkowa GI, Flyunt VR, Hubyts'kyi VYo, Zukow W, Barylyak LG, Popovych IL. Modulating effects of bioactive water Naftussya from layers Truskavets' and Pomyarky on some metabolic and biophysic parameters at humans with dysfunction of neuro-endocrine-immune complex. Journal of Education, Health and Sport. 2016; 6(12): 826-842.
203. Gozhenko AI, Zukow W, Polovynko IS, Zajats LM, Yanchij RI, Portnichenko VI, Popovych IL. Individual Immune Responses to Chronic Stress and their Neuro-Endocrine Accompaniment. RSW. UMK. Radom. Torun; 2019: 200 p.
204. Grebe A., Hoss F., Latz E. NLRP3 Inflammasome and the IL-1 Pathway in Atherosclerosis. Circ. Res. 2018;122:1722–1740.
205. Greenberg K., McAdams-DeMarco M.A., Köttgen A., Appel L.J., Coresh J., Grams M.E. Plasma urate and risk of a hospital stay with AKI: the atherosclerosis risk in communitis study. Clin J Am Soc Nephrol. 2015;10(5):776–783.
206. Gutman A. B. Significance of uric acid as a nitrogenous waste in vertebrate evolution. Arthritis & Rheumatism. 1965;8(4):614–626. doi: 10.1002/art.1780080422.
207. Gwang H.B., Yang J.H., Park T.K., Song Y.B., Hahn J.Y., Choi J.H., Lee J.H., Lee S.H., Gwon H.C., Choi S.H. Uric acid level has a U-shaped assotioation with clinical outcomes in patients with vasospastic angina. J Korean Med Sci. 2017; 32(8): 1275-1280/
208. Haig A. J, Churchill A. Uric acid as a factor in the causation of disease. London. 1897.
209. Hall A.P., Barry P.E., Dawber T.R., McNamara P.M. Epidemiology of gout and hyperuricemia. A long-term population study. Am J Med. 1967;42:27.
210. Hammad H., Lambrecht B.N. Barrier epithelial cells and the control of type 2 immunity. Immunity. 2015;43(1):29–40.
211. Hara K., Iijima K., Elias M.K., Seno S., Tojima I., Kobayashi T. Airway uric acid is a sensor of inhaled protease allergens and initiates type 2 immune responses in respiratory mucosa. J Immunol. 2014;192(9):4032–4042.

212. Harada K., Ohira S., Isse K., Ozaki S., Zen Y., Sato Y., Nakanuma Y. Lipopolysaccharide activates nuclear factor-kappaB through toll-like receptors and related molecules in cultured biliary epithelial cells. Lab. Investig. 2003;83:1657–1667.
213. Harambat J., Dubourg L., Ranchin B., Hadj-Aïssa A., Fargue S., Rivet C. Hyperuricemia after liver transplantation in children. Pediatr Transplant. 2008;12(8):847–853.
214. Haryono A., Nugrahaningsih D.A.A., Sari D.C.R., Romi M.M., Arfian N. Reduction of Serum Uric Acid Associated with Attenuation of Renal Injury, Inflammation and Macrophages M1/M2 Ratio in Hyperuricemic Mice Model. Kobe. J. Med. Sci. 2018;64:E107–E114.
215. He Y., Franchi L., Nunez G. TLR agonists stimulate Nlrp3-dependent IL-1beta production independently of the purinergic P2X7 receptor in dendritic cells and in vivo. J. Immunol. 2013;190:334–339.
216. Hediger M.A., Johnson R.J., Miyazaki H., Endou H. Molecular physiology of urate transport. Physiology. 2005;20:125–133.
217. Heesen M., Renckens R., de Vos A.F., Kunz D., van der Poll T. Human endotoxemia induces down-regulation of monocyte CC chemokine receptor 2. Clin. Vaccine. Immunol. 2006;13:156–159.
218. Henaut L, Candellier A, Boudot S, Grissi M, Mentaverri R, Choukroun G, Brazier M, Kamel S, Massy ZA. New insights into the roles of monocytes/macrophages in cardiovascular calcification associated with chronic kidney disease. Toxins (Basel). 2019; 11(9): 529.
219. Hjortnaes J., Algra A., Olijhoek J., Huisman M., Jacobs J., van der Graaf Y. Serum uric acid levels and risk for vascular diseases in patients with metabolic syndrome. J Rheumatol. 2007;34(9):1882–1887.
220. Hoffman HM, Scott P, Mueller JL, et al. Role of the leucine-rich repeat domain of cryopyrin/NALP3 in monosodium urate crystal-induced inflammation in mice. Arthritis Rheum. 2010;62(7):2170-2179.
221. Holme I., Aastveit A.H., Hammar N., Jungner I., Walldius G. Uric acid and risk of myocardial infarction, stroke and congestive heart failure in 417,734 men and women in the Apolipoprotein MOrtality RISk study (AMORIS) J Intern Med. 2009;266(6):558–570.
222. Hooper D.C., Spitsin S., Kean R.B., Champion J.M., Dickson G.M., Chaudhry I. Uric acid, a natural scavenger of peroxynitrite, in experimental allergic encephalomyelitis and multiple sclerosis. Proc Natl Acad Sci USA. 1998;95(2):675–680.
223. Hornung V, Bauernfeind F, Halle A, et al. Silica crystals and aluminum salts activate the NALP3 inflammasome through phagosomal destabilization. Nat Immunol. 2008;9(8):847-856.
224. Hoskin D.W., Mader J.S., Furlong S.J., Conrad D.M., Blay J. Inhibition of T cell and NK cell function by adenosine and its contribution to immune evasion by tumor cells (Review). Int J Oncol. 2008; 32(3): 527-535.
225. Hosomi A., Nakanishi T., Fujita T., Tamai I. Extra-renal elimination of uric acid via intestinal efflux transporter BCRP/ABCG2. PLoS One. 2012;7(2):e30456.
226. Hovind P., Rossing P., Tarnow L., Johnson R.J., Parving H.H. Serum uric acid as a predictor for development of diabetic nephropathy in type 1 diabetes: an inception cohort study. Diabetes. 2009;58(7):1668–1671.
227. Heart Rate Variability. Standards of Measurement, Physiological Interpretation, and Clinical Use. Task Force of ESC and NASPE. Circulation. 1996; 93(5): 1043-1065.
228. Huang H., Huang B., Li Y., Huang Y., Li J., Yao H. Uric acid and risk of heart failure: a systematic review and meta-analysis. Eur J Heart Fail. 2014;16(1):15–24.
229. Huang S, Apasov S, Koshiba M, SitkovskiM. Role of A_{2A} extracellular adenosine receptor mediated signaling in adenosine mediated inhibition of of T-cell activation and expansion. Blood. 1997; 90(4): 1600-1610.
230. Huang W.M., Hsu P.F., Cheng H.M., Lu D.Y., Cheng Y.L., Guo C.Y. Determinants and prognostic impact of hyperuricemia in hospitalization for acute heart failure. Circ J. 2016;80(2):404–410.
231. Huls M., Brown C.D., Windass A.S., Sayer R., van den Heuvel J.J., Heemskerk S. The breast cancer resistance protein transporter ABCG2 is expressed in the human kidney proximal tubule apical membrane. Kidney Int. 2008;73(2):220–225.
232. Hyndman D., Liu S., Miner J. N. Urate handling in the human body. Current Rheumatology Reports. 2016;18(6):34.
233. Iso T., Kurabayashi M. Extremely low levels of serum uric acid are associated with endothelial dysfunction in humans. Circ J. 2015;79(5):978–980.
234. Iwata H, Nishio S, Yokoyama M, Matsumoto A, Takeuchi M. Solubility of uric acid and supersaturation of monosodium urate: why is uric acid so highly soluble in urine? J Urol. 1989 Oct;142(4):1095-8.
235. Jalal D.I. Hyperuricemia, the kidneys, and the spectrum of associated diseases: a narrative review. Curr Med Res Opin. 2016;26:1–7.
236. Jalal D.I., Rivard C.J., Johnson R.J., Maahs D.M., McFann K., Rewers M. Serum uric acid levels predict the development of albuminuria over 6 years in patients with type 1 diabetes: findings from the Coronary Artery Calcification in Type 1 Diabetes study. Nephrol Dial Transplant. 2010;25(6):1865–1869.
237. Jamwal S, Mittal A, Kumar P, Alhayani DM, Al-Aboudi A. Therapeutic Potential of Agonists and Antagonists of A1, A2a, A2b and A3 Adenosine Receptors. Curr Pharm Des. 2019;25(26):2892-2905.

238. Jayashankar C.A., Andrews H.P., Vijayasarathi Pinnelli V.B., Shashidharan B., Nithin Kumar H.N., Vemulapalli S. Serum uric acid and low-density lipoprotein cholesterol levels are independent predictors of coronary artery disease in Asian Indian patients with type 2 diabetes mellitus. J Nat Sci Biol Med. 2016;7(2):161–165.
239. Jeong J.H., Jung J.H., Lee J.S., Oh J.S., Kim Y.G., Lee C.K., Yoo B., Hong S. Prominent Inflammatory Features of Monocytes/Macrophages in Acute Calcium Pyrophosphate Crystal Arthritis: A Comparison with Acute Gouty Arthritis. Immune Netw. 2019;19:e21.
240. Jia L., Xing J., Ding Y., Shen Y., Shi X., Ren W., Wan M., Guo J., Zheng S., Liu Y., et al. Hyperuricemia causes pancreatic beta-cell death and dysfunction through NF-kappaB signaling pathway. PLoS ONE. 2013;8:e78284.
241. Johnson R. J., Titte S., Cade J. R., Rideout B. A., Oliver W. J. Uric acid, evolution and primitive cultures. Seminars in Nephrology. 2005;25(1):3–8.
242. Johnson R.J., Merriman T., Lanaspa M.A. Causal or noncausal relationship of uric acid with diabetes. Diabetes. 2015;64(8):2720–2722.
243. Johnson R.J., Nakagawa T., Jalal D., Sánchez-Lozada L.G., Kang D.H., Ritz E. Uric acid and chronic kidney disease: which is chasing which? Nephrol Dial Transplant. 2013;28(9):2221–2228.
244. Johnson R.J., Nakagawa T., Sanchez-Lozada L.G., Shafiu M., Sundaram S., Le M. Sugar, uric acid, and the etiology of diabetes and obesity. Diabetes. 2013;62(10):3307–3315.
245. Johnson R.J., Segal M.S., Srinivas T., Ejaz A., Mu W., Roncal C. Essential hypertension, progressive renal disease, and uric acid: a pathogenetic link? J Am Soc Nephrol. 2005;16(7):1909–1919.
246. Johnson R.J., Stenvinkel P., Martin S.L., Jani A., Sánchez-Lozada L.G., Hill J.O. Redefining metabolic syndrome as a fat storage condition based on studies of comparative physiology. Obesity (Silver Spring) 2013;21(4):659–664.
247. Jondal M, Holm G, Wigzell H. Surface markers on human T and B lymphocytes. I. A large population of lymphocytes forming nonimmune rosettes with sheep red blood cells. J Exp Med. 1972; 136(2): 207-215.
248. Joosten L.A., Ea H.K., Netea M.G., Busso N. Interleukin-1β activation during acute joint inflammation: a limited role for the NLRP3 inflammasome in vivo. Joint Bone Spine. 2011;78(2):107–110.
249. Joosten L.A., Netea M.G., Mylona E., Koenders M.I., Malireddi R.K., Oosting M. Engagement of fatty acids with Toll-like receptor 2 drives interleukin-1β production via the ASC/caspase 1 pathway in monosodium urate monohydrate crystal-induced gouty arthritis. Arthritis Rheum. 2010;62(11):3237–3248.
250. Joung K.W., Choi S.S., Kong Y.G., Yu J., Lim J., Hwang J.H. Incidence and risk factors of acute kidney injury after radical cystectomy: importance of preoperative serum uric acid level. Int J Med Sci. 2015;12(7):599–604.
251. Kam M, Perl-Treves D, Caspi D, Addadi L. Antibodies against crystals. FASEB J. 1992;6(8):2608-2613.
252. Kam M, Perl-Treves D, Sfez R, Addadi L. Specificity in the recognition of crystals by antibodies. J Mol Recognit. 1994;7(4):257-264.
253. Kanbay M., Jensen T., Solak Y., Le M., Roncal-Jimenez C., Rivard C. Uric acid in metabolic syndrome: from an innocent bystander to a central player. Eur J Intern Med. 2016;29:3–8.
254. Kanbay M., Segal M., Afsar B., Kang D.H., Rodriguez-Iturbe B., Johnson R.J. The role of uric acid in the pathogenesis of human cardiovascular disease. Heart. 2013;99(11):759–766.
255. Kanbay M., Solak Y., Afsar B., Nistor I., Aslan G., Çağlayan O.H. Serum uric acid and risk for acute kidney injury following contrast: an evaluation of epidemiology, clinical trials, and potential mechanisms. Angiology. 2017;68(2):132–144.
256. Kanbay M., Yilmaz M.I., Sonmez A., Turgut F., Saglam M., Cakir E. Serum uric acid level and endothelial dysfunction in patients with nondiabetic chronic kidney disease. Am J Nephrol. 2011;33:298–304.
257. Kanellis J., Watanabe S., Li J.H., Kang D.H., Li P., Nakagawa T. Uric acid stimulates monocyte chemoattractant protein-1 production in vascular smooth muscle cells via mitogen-activated protein kinase and cyclooxygenase-2. Hypertension. 2003;41(6):1287–1293.
258. Kanevets U, Sharma K, Dresser K, Shi Y. A role of IgM antibodies in monosodium urate crystal formation and associated adjuvanticity. J Immunol. 2009;182(4):1912-1918.
259. Kang D.H., Chen W. Uric acid and chronic kidney disease: new understanding of an old problem. Semin Nephrol. 2011;31(5):447–452.
260. Kang D.H., Park S.K., Lee I.K., Johnson R.J. Uric acid-induced C-reactive protein expression: implication on cell proliferation and nitric oxide production of human vascular cells. J Am Soc Nephrol. 2005;16(12):3553–3562.
261. Kaplanov I., Carmi Y., Kornetsky R., Shemesh A., Shurin G.V., Shurin M.R., Dinarello C.A., Voronov E., Apte R.N. Blocking IL-1beta reverses the immunosuppression in mouse breast cancer and synergizes with anti-PD-1 for tumor abrogation. Proc. Natl. Acad. Sci. USA. 2019;116:1361–1369.
262. Kato M., Hisatome I., Tomikura Y., Kotani K., Kinugawa T., Ogino K. Status of endothelial dependent vasodilation in patients with hyperuricemia. Am J Cardiol. 2005;96(11):1576–1578.
263. Kawabe M., Sato A., Hoshi T., Sakai S., Hiraya D., Watabe H. Gender differences in the association between serum uric acid and prognosis in patients with acute coronary syndrome. J Cardiol. 2016;67(2):170–176.

264. Keebaugh A. C., Thomas J. W. The evolutionary fate of the genes encoding the purine catabolic enzymes in hominoids, birds, and reptiles. Molecular Biology and Evolution. 2010;27(6):1359–1369.
265. Keenan T., Zhao W., Rasheed A., Ho W.K., Malik R., Felix J.F. Causal assessment of serum urate levels in cardiometabolic diseases through a mendelian randomization study. J Am Coll Cardiol. 2016;67(4):407–416.
266. Kelkar A., Kuo A., Frishman W.H. Allopurinol as a cardiovascular drug. Cardiol Rev. 2011;19(6):265–271.
267. Kim S.M., Lee S.H., Kim Y.G., Kim S.Y., Seo J.W., Choi Y.W. Hyperuricemia-induced NLRP3 activation of macrophages contributes to the progression of diabetic nephropathy. Am J Physiol Renal Physiol. 2015;308(9):F993–F1003.
268. Kim Y.G., Huang X.R., Suga S., Mazzali M., Tang D., Metz C. Involvement of macrophage migration inhibitory factor (MIF) in experimental uric acid nephropathy. Mol Med. 2000;6(10):837–848.
269. Kippen I, Klinenberg JR, Weinberger A, Wilcox WR. Factors affecting urate solubility in vitro. Ann Rheum Dis. 1974;33(4):313-317.
270. Kırça M., Oğuz N., Çetin A., Uzuner F., Yeşilkaya A. Uric acid stimulates proliferative pathways in vascular smooth muscle cells through the activation of p38 MAPK, p44/42 MAPK and PDGFRβ J Recept Signal Transduct Res. 2016;12:1–7.
271. Kleber M.E., Delgado G., Grammer T.B., Silbernagel G., Huang J., Krämer B.K. Uric acid and cardiovascular events: a mendelian randomization study. J Am Soc Nephrol. 2015;26(11):2831–2838.
272. Klecka W.R. Discriminant Analysis [trans. from English in Russian] (Seventh Printing, 1986). In: Factor, Discriminant and Cluster Analysis. Moskwa. Finansy i Statistika; 1989: 78-138.
273. Kohagura K., Tana T., Higa A., Yamazato M., Ishida A., Nagahama K. Effects of xanthine oxidase inhibitors on renal function and blood pressure in hypertensive patients with hyperuricemia. Hypertens Res. 2016 Aug;39(8):593–597.
274. Kono H., Chen C.J., Ontiveros F., Rock K.L. Uric acid promotes an acute inflammatory response to sterile cell death in mice. J Clin Invest. 2010;120(6):1939–1949.
275. Kool M, Pétrilli V, De Smedt T, et al. Cutting edge: alum adjuvant stimulates inflammatory dendritic cells through activation of the NALP3 inflammasome. J Immunol. 2008;181(6):3755-3759.
276. Kool M, Soullié T, van Nimwegen M, et al. Alum adjuvant boosts adaptive immunity by inducing uric acid and activating inflammatory dendritic cells. J Exp Med. 2008;205(4):869-882.
277. Kool M., Willart M.A., van Nimwegen M., Bergen I., Pouliot P., Virchow J.C. An unexpected role for uric acid as an inducer of T helper 2 cell immunity to inhaled antigens and inflammatory mediator of allergic asthma. Immunity. 2011;34(4):527–540.
278. Koratala A. Tumor lysis syndrome with massive hyperphosphatemia and hyperuricemia. Clinical Case Reports. 2017;5(12):2158–2159. doi: 10.1002/ccr3.1268.
279. Köttgen A., Albrecht E., Teumer A., Vitart V., Krumsiek J., Hundertmark C. Genome-wide association analyses identify 18 new loci associated with serum urate concentrations. Nat Genet. 2013;45:145–154.
280. Kozin F, McCarty DJ. Molecular orientation of immunoglobulin G adsorbed to microcrystalline monosodium urate monohydrate. J Lab Clin Med. 1980;95(1):49-58.
281. Kozyavkina NV, Popovych IL, Popovych DV, Zukow W, Bombushkar IS. Sexual dimorphism in some psycho-neuro-endocrine parameters at human. Journal of Education, Health and Sport. 2021; 11(5): 370-391.
282. Kratzer J.T., Lanaspa M.A., Murphy M.N., Cicerchi C., Graves C.L., Tipton P.A. Evolutionary history and metabolic insights of ancient mammalian uricases. Proc Natl Acad Sci USA. 2014;111(10):3763–3768.
283. Krishnan E., Pandya B.J., Chung L., Hariri A., Dabbous O. Hyperuricemia in young adults and risk of insulin resistance, prediabetes, and diabetes: a 15-year follow-up study. Am J Epidemiol. 2012;176(2):108–116.
284. Kul'chyns'kyi AB, Gozhenko AI, Zukow W, Popovych IL. Neuro-immune relationships at patients with chronic pyelonephrite and cholecystite. Communication 3. Correlations between parameters EEG, HRV and Immunogram. Journal of Education, Health and Sport. 2017; 7(3): 53-71.
285. Kul'chyns'kyi AB, Kovbasnyuk MM, Kyjenko VM., Zukow W, Popovych IL. Neuro-immune relationships at patients with chronic pyelonephrite and cholecystite. Communication 2. Correlations between parameters EEG, HRV and Phagocytosis. Journal of Education, Health and Sport. 2016; 6(10): 377-401.
286. Kul'chyns'kyi AB, Kyjenko VM, Zukow W, Popovych IL. Causal neuro-immune relationships at patients with chronic pyelonephritis and cholecystitis. Correlations between parameters EEG, HRV and white blood cell count. Open Medicine. 2017; 12(1): 201-213.
287. Kul'chyns'kyi AB, Zukow W, Korolyshyn TA, Popovych IL. Interrelations between changes in parameters of HRV, EEG and humoral immunity at patients with chronic pyelonephritis and cholecystitis. Journal of Education, Health and Sport. 2017; 7(9): 439-459.
288. Kumagai T., Ota T., Tamura Y., Chang W.X., Shibata S., Uchida S. Time to target uric acid to retard CKD progression. Clin Exp Nephrol. 2017;21(2):182–192.
289. Kunikullaya K.U., Purushottam N., Prakash V., Mohan S., Chinnaswamy R. Correlation of serum uric acid with heart rate variability in hypertension. Hipertens Riesgo Vasc. 2015;32(4):133–141.

290. Kushiyama A., Okubo H., Sakoda H., Kikuchi T., Fujishiro M., Sato H., Kushiyama S., Iwashita M., Nishimura F., Fukushima T., et al. Xanthine oxidoreductase is involved in macrophage foam cell formation and atherosclerosis development. Arterioscler. Thromb. Vasc. Biol. 2012;32:291–298.
291. Lam R.S., O'Brien-Simpson N.M., Holden J.A., Lenzo J.C., Fong S.B., Reynolds E.C. Unprimed, M1 and M2 Macrophages Differentially Interact with Porphyromonas gingivalis. PLoS ONE. 2016;11:e0158629.
292. Lambrecht B.N., Hammad H. Allergens and the airway epithelium response: gateway to allergic sensitization. J Allergy Clin Immunol. 2014;134(3):499–507.
293. Lanaspa M.A., Cicerchi C., Garcia G., Li N., Roncal-Jimenez C.A., Rivard C.J. Counteracting roles of AMP deaminase and AMP kinase in the development of fatty liver. PLoS ONE. 2012;7(11):e48801.
294. Lanaspa M.A., Epperson L.E., Li N., Cicerchi C., Garcia G.E., Roncal-Jimenez C.A. Opposing activity changes in AMP deaminase and AMP-activated protein kinase in the hibernating ground squirrel. PLoS ONE. 2015;10(4):e0123509.
295. Lanaspa M.A., Sanchez-Lozada L.G., Choi Y.J., Cicerchi C., Kanbay M., Roncal-Jimenez C.A. Uric acid induces hepatic steatosis by generation of mitochondrial oxidative stress: potential role in fructose-dependent and -independent fatty liver. J Biol Chem. 2012;287(48):40732–40744.
296. Lanaspa M.A., Sanchez-Lozada L.G., Cicerchi C., Li N., Roncal-Jimenez C.A., Ishimoto T. Uric acid stimulates fructokinase and accelerates fructose metabolism in the development of fatty liver. PLoS ONE. 2012;7(10):e47948.
297. Landis RC, Haskard DO. Pathogenesis of crystal-induced inflammation. Curr Rheumatol Rep. 2001;3(1):36-41.
298. Langford H.G., Blaufox M.D., Borhani N.O., Curb J.D., Molteni A., Schneider K.A. Is thiazide-produced uric acid elevation harmful? Analysis of data from the hypertension detection and follow-up program. Arch Intern Med. 1987;147:645.
299. Lazzeri C., Valente S., Chiostri M., Gensini G.F. Long-term prognostic role of uric acid in patients with ST-elevation myocardial infarction and renal dysfunction. J Cardiovasc Med (Hagerstown) 2015;16(11):790–794.
300. Lee E.H., Choi J.H., Joung K.W., Kim J.Y., Baek S.H., Ji S.M. Relationship between serum uric acid concentration and acute kidney injury after coronary artery bypass surgery. J Korean Med Sci. 2015;30(10):1509–1516.
301. Lee J.J., Ahn J., Hwang J., Han S.W., Lee K.N., Kim J.B. Relationship between uric acid and blood pressure in different age groups. Clin Hypertens. 2015 Jul;15(21):14.
302. Lee M., Lee Y., Song J., Lee J., Chang S.Y. Tissue-specific Role of CX3CR1 Expressing Immune Cells and Their Relationships with Human Disease. Immune Netw. 2018;18:e5.
303. Leiba A., Vinker S., Dinour D., Holtzman E.J., Shani M. Uric acid levels within the normal range predict increased risk of hypertension: a cohort study. J Am Soc Hypertens. 2015;9(8):600–609.
304. Li G., Qiao W., Zhang W., Li F., Shi J., Dong N. The shift of macrophages toward M1 phenotype promotes aortic valvular calcification. J. Thorac. Cardiovasc. Surg. 2017;153:1318–1327.
305. Li L., Yang C., Zhao Y., Zeng X., Liu F., Fu P. Is hyperuricemia an independent risk factor for new-onset chronic kidney disease? A systematic review and meta-analysis based on observational cohort studies. BMC Nephrol. 2014;27(15):122.
306. Li P., Zhang L., Zhang M., Zhou C., Lin N. Uric acid enhances PKC-dependent eNOS phosphorylation and mediates cellular ER stress: a mechanism for uric acid-induced endothelial dysfunction. Int J Mol Med. 2016;37(4):989–997.
307. Li S, Lu X, Chen X, Huang Z, Zhou H, Li Z, Ning Y. The prevalence and associated clinical correlates of hyperuricemia in patients with bipolar disorder. Front Neurosci. 2022;16:998747.
308. Liang C.C., Lin P.C., Lee M.Y., Chen S.C., Shin S.J., Hsiao P.J. Association of serum uric acid concentration with diabetic retinopathy and albuminuria in Taiwanese patients with type 2 diabetes mellitus. Int J Mol Sci. 2016;17(8)
309. Liang J., Pei Y., Gong Y., Liu X.K., Dou L.J., Zou C.Y. Serum uric acid and non-alcoholic fatty liver disease in non-hypertensive Chinese adults: Cardiometabolic Risk in Chinese (CRC) study. Eur Rev Med Pharmacol Sci. 2015;19(2):305–311.
310. Liang J., Zhang P., Hu X., Zhi L. Elevated serum uric acid after injury correlates with the early acute kidney in severe burns. Burns. 2015 Dec;41(8):1724–1731.
311. Liang M.H., Fries J.F. Asymptomatic hyperuricemia: the case for conservative management. Ann Intern Med. 1978;88:666.
312. Lieske J.C., de la Vega L.S., Gettman M.T., Slezak J.M., Bergstralh E.J., Melton L.J., 3rd Diabetes mellitus and the risk of urinary tract stones: a population-based case-control study. Am J Kidney Dis. 2006;48(6):897–904.
313. Limatibul S, Shore A, Dosch H.M., Gelfand E.W. Theophylline modulation of E-rosette formation: an indicator of T-cell maturation. Clin Exp Immunol. 1978; 33(3): 503-513.
314. Lin X., Kong J., Wu Q., Yang Y., Ji P. Effect of TLR4/MyD88 signaling pathway on expression of IL-1beta and TNF-alpha in synovial fibroblasts from temporomandibular joint exposed to lipopolysaccharide. Mediat. Inflamm. 2015;329405.

315. Lin Y., Zhu J., Wang Y., Li Q., Lin S. Identification of differentially expressed genes through RNA sequencing in goats (Capra hircus) at different postnatal stages. PLoS One. 2017;12(8):e0182602.
316. Linnane J.W., Burry A.F., Emmerson B.T. Urate deposits in the renal medulla. Prevalence and associations. Nephron. 1981;29(5–6):216–222.
317. List J.F., Whaley J.M. Glucose dynamics and mechanistic implications of SGLT2 inhibitors in animals and humans. Kidney Int Suppl. 2011;120 S20-7.
318. Liu D, Yun Y, Yang D, et al. What Is the Biological Function of Uric Acid? An Antioxidant for Neural Protection or a Biomarker for Cell Death. Dis Markers. 2019;4081962.
319. Liu P., Wang H., Zhang F., Chen Y., Wang D., Wang Y. The effects of allopurinol on the carotid intima-media thickness in patients with Type 2 diabetes and asymptomatic hyperuricemia: a three-year randomized parallel-controlled study. Intern Med. 2015;54(17):2129–2137.
320. Liu Z., Que S., Zhou L., Zheng S. Dose-response Relationship of Serum Uric Acid with Metabolic Syndrome and Non-alcoholic Fatty Liver Disease Incidence: A Meta-analysis of Prospective Studies. Sci. Rep. 2015;5:14325.
321. Liu-Bryan R, Pritzker K, Firestein GS, Terkeltaub R. TLR2 signaling in chondrocytes drives calcium pyrophosphate dihydrate and monosodium urate crystal-induced nitric oxide generation. J Immunol. 2005;174(8):5016-5023.
322. Liu-Bryan R, Scott P, Sydlaske A, Rose DM, Terkeltaub R. Innate immunity conferred by Toll-like receptors 2 and 4 and myeloid differentiation factor 88 expression is pivotal to monosodium urate monohydrate crystal-induced inflammation. Arthritis Rheum. 2005;52(9):2936-2946.
323. Liu-Bryan R., Lioté F. Monosodium urate and calcium pyrophosphate dihydrate (CPPD) crystals, inflammation, and cellular signaling. Jt. Bone Spine. 2005;72:295–302.
324. Lu N., Dubreuil M., Zhang Y., Neogi T., Rai S.K., Ascherio A. Gout and the risk of Alzheimer's disease: a population-based, BMI-matched cohort study. Ann Rheum Dis. 2016;75(3):547–551.
325. Lu W., Xu Y., Shao X., Gao F., Li Y., Hu J., Zuo Z., Shao X., Zhou L., Zhao Y., et al. Uric Acid Produces an Inflammatory Response through Activation of NF-kappaB in the Hypothalamus: Implications for the Pathogenesis of Metabolic Disorders. Sci. Rep. 2015;5:12144.
326. Lv Q., Meng X.F., He F.F., Chen S., Su H., Xiong J. High serum uric acid and increased risk of type 2 diabetes: a systemic review and meta-analysis of prospective cohort studies. PLoS One. 2013;8(2):e56864.
327. Lyngdoh T., Marques-Vidal P., Paccaud F., Preisig M., Waeber G., Bochud M., Vollenweider P. Elevated serum uric acid is associated with high circulating inflammatory cytokines in the population-based Colaus study. PLoS ONE. 2011;6:e19901.
328. Ma D.W., Arendt B.M., Hillyer L.M., Fung S.K., McGilvray I., Guindi M. Plasma phospholipids and fatty acid composition differ between liver biopsy-proven nonalcoholic fatty liver disease and healthy subjects. Nutr Diabetes. 2016;6(7):e220.
329. Madero M., Rodríguez Castellanos F.E., Jalal D., Villalobos-Martín M., Salazar J., Vazquez-Rangel A. A pilot study on the impact of a low fructose diet and allopurinol on clinic blood pressure among overweight and prehypertensive subjects: a randomized placebo controlled trial. J Am Soc Hypertens. 2015;9(11):837–844.
330. Maesaka J.K., Fishbane S. Regulation of renal urate excretion: a critical review. Am J Kidney Dis. 1998;32:917–933.
331. Maesaka J.K., Wolf-Klein G., Piccione J.M., Ma C.M. Hypouricemia, abnormal renal tubular urate transport, and plasma natriuretic factor(s) in patients with Alzheimer's disease. J Am Geriatr Soc. 1993;41(5):501–506.
332. Mahomed F.A. On chronic Bright's disease, and its essential symptoms. Lancet. 1879;1:399–401.
333. Maiuolo J., Oppedisano F., Gratteri S., Muscoli C., Mollace V. Regulation of uric acid metabolism and excretion. Int J Cardiol. 2016;213:8–14.
334. Mallamaci F., Testa A., Leonardis D., Tripepi R., Pisano A., Spoto B. A polymorphism in the major gene regulating serum uric acid associates with clinic SBP and the white-coat effect in a family-based study. J Hypertens. 2014;32(8):1621–1628.
335. Mandel NS. The structural basis of crystal-induced membranolysis. Arthritis Rheum. 1976;19 Suppl 3:439-445.
336. Mantovani A., Rigolon R., Pichiri I., Pernigo M., Bergamini C., Zoppini G. Hyperuricemia is associated with an increased prevalence of atrial fibrillation in hospitalized patients with type 2 diabetes. J Endocrinol Invest. 2016;39(2):159–167.
337. Marchesini G., Bugianesi E., Forlani G., Cerrelli F., Lenzi M., Manini R. Nonalcoholic fatty liver, steatohepatitis, and the metabolic syndrome. Hepatology. 2003;37(4):917–923.
338. Marotta T., Liccardo M., Schettini F., Verde F., Ferrara A.L. Association of hyperuricemia with conventional cardiovascular risk factors in elderly patients. J Clin Hypertens (Greenwich) 2015;17(1):27–32.
339. Martinez F.O., Gordon S., Locati M., Mantovani A. Transcriptional profiling of the human monocyte-to-macrophage differentiation and polarization: New molecules and patterns of gene expression. J. Immunol. 2006;177:7303–7311.

340. Martínez-Reyes CP, Manjarrez-Reyna AN, Méndez-García LA, et al. Uric Acid Has Direct Proinflammatory Effects on Human Macrophages by Increasing Proinflammatory Mediators and Bacterial Phagocytosis Probably via URAT1. Biomolecules. 2020;10(4):576.
341. Martinon F. Mechanisms of uric acid crystal-mediated autoinflammation. Immunol Rev. 2010;33(1):218–232.
342. Martinon F. Update on biology: uric acid and the activation of immune and inflammatory cells. Curr Rheumatol Rep. 2010;12(2):135–141.
343. Martinon F., Pétrilli V., Mayor A., Tardivel A., Tschopp J. Gout-associated uric acid crystals activate the NALP3 inflammasome. Nature. 2006;440(7081):237–241.
344. Masuo K., Kawaguchi H., Mikami H., Ogihara T., Tuck M.L. Serum uric acid and plasma norepinephrine concentrations predict subsequent weight gain and blood pressure elevation. Hypertension. 2003;42:474–480.
345. Mazzali M., Hughes J., Kim Y.G., Jefferson J.A., Kang D.H., Gordon K.L. Elevated uric acid increases blood pressure in the rat by a novel crystal-independent mechanism. Hypertension. 2001;38:1101–1106.
346. Mazzali M., Kanbay M., Segal M.S., Shafiu M., Jalal D., Feig D.I. Uric acid and hypertension: cause or effect? Curr Rheumatol Rep. 2010;12(2):108–117.
347. McCarty D.J., Hollander J.L. Identification of urate crystals in gouty synovial fluid. Ann Intern Med. 1961;54:452–460.
348. McGeough M.D., Wree A., Inzaugarat M.E., Haimovich A., Johnson C.D., Pena C.A., Goldbach-Mansky R., Broderick L., Feldstein A.E., Hoffman H.M. TNF regulates transcription of NLRP3 inflammasome components and inflammatory molecules in cryopyrinopathies. J. Clin. Investig. 2017;127:4488–4497.
349. Mehta T., Nuccio E., McFann K., Madero M., Sarnak M.J., Jalal D. Association of uric acid with vascular stiffness in the Framingham heart study. Am J Hypertens. 2015;28(7):877–883.
350. Mel'nyk OI, Lukyanchenko OI, Gozhenko OA, Popovych IL. Features of the parameters of EEG in persons whose immune status is susceptible or resistant to chronic stress. Experimental and Clinical Physiology and Biochemistry. 2019; 2(86): 11-23.
351. Mendi M.A., Afsar B., Oksuz F., Turak O., Yayla C., Ozcan F. Uric acid is a useful tool to predict contrast-induced nephropathy. Angiology. 2017;68(7):627–632.
352. Mitroulis I., Kambas K., Chrysanthopoulou A., Skendros P., Apostolidou E., Kourtzelis I. Neutrophil extracellular trap formation is associated with IL-1β and autophagy-related signaling in gout. PLoS One. 2011;6(12):e29318.
353. Mitroulis I., Kambas K., Ritis K. Neutrophils, IL-1β, and gout: is there a link? Semin Immunopathol. 2013;35(4):501–512.
354. Mo J, Huang L, Peng J, Ocak U, Zhang J, Zhang JH. Autonomic Disturbances in Acute Cerebrovascular Disease. Neurosci Bull. 2019; 35(1): 133-144.
355. Mohamedali K. A., Guicherit O. M., Kellems R. E., Rudolph F. B. The highest levels of purine catabolic enzymes in mice are present in the proximal small intestine. Journal of Biological Chemistry. 1993;268(31):23728–23733.
356. Monahan TS, Sawmiller DR, Fenton RA, Dobson JG Jr. Adenosine A(2a)-receptor activation increases contractility in isolated perfused hearts. Am J Physiol Heart Circ Physiol. 2000;279(4):H1472-H1481.
357. Montenegro RA, Farinatti P de TV, Fontes EB, Soares PP da S, Cunha da FA, Gurgel JL et al. Transcranial direct current stimulation influences the cardiac autonomic nervous control. Neurosci Lett. 2011;497(1):32-36.
358. Morelli M., Carta A.R., Kachroo A., Schwarzschild A. Pathophysiological roles for purines: adenosine, caffeine and urate. Prog Brain Res. 2010; 183: 183-208.
359. Mortada I. Hyperuricemia, type 2 diabetes mellitus, and hypertension: an emerging association. Current Hypertension Reports. 2017;19(9):69.
360. Murray P.J. Macrophage Polarization. Annu. Rev. Physiol. 2017;79:541–566.
361. Naff GB, Byers PH. Complement as a mediator of inflammation in acute gouty arthritis. I. Studies on the reaction between human serum complement and sodium urate crystals. J Lab Clin Med. 1973;81(5):747-760.
362. Nagase M, Baker DG, Schumacher HR Jr. Immunoglobulin G coating on crystals and ceramics enhances polymorphonuclear cell superoxide production: correlation with immunoglobulin G adsorbed. J Rheumatol. 1989;16(7):971-976.
363. Nagayama D., Yamaguchi T., Saiki A., Imamura H., Sato Y., Ban N. High serum uric acid is associated with increased cardio-ankle vascular index (CAVI) in healthy Japanese subjects: a cross-sectional study. Atherosclerosis. 2015;239(1):163–168.
364. Nakagawa T., Hu H., Zharikov S., Tuttle K.R., Short R.A., Glushakova O. A causal role for uric acid in fructose-induced metabolic syndrome. Am J Physiol Renal Physiol. 2006;290(3) F625-31.
365. Nakagawa T., Kang D.H., Feig D., Sanchez-Lozada L.G., Srinivas T.R., Sautin Y. Unearthing uric acid: an ancient factor with recently found significance in renal and cardiovascular disease. Kidney Int. 2006;69(10):1722–1725.

366. Nakagawa T., Mazzali M., Kang D.H., Kanellis J., Watanabe S., Sanchez-Lozada L.G. Hyperuricemia causes glomerular hypertrophy in the rat. Am J Nephrol. 2003;23:2–7.
367. Nakagawa T., Mazzali M., Kang D.H., Sánchez-Lozada L.G., Herrera-Acosta J., Johnson R.J. Uric acid – a uremic toxin? Blood Purif. 2006;24(1):67–70.
368. Nance DM, Sanders VM. Autonomic innervation and regulation of immune system (1987-2007). Brain Behav Immun. 2007; 21(6): 736-745.
369. Navalta J.W., Fedor E.A., Schafer M.A., Lyons T.S., Tibana R.A., Pereira G.B., Prestes J. Caffeine affects $CD8^+$ lymphocyte differently in naïve and familiar individuals following moderate intensity exercise. Int J Immunopathol Pharmacol. 2016; 29(2): 288-294.
370. Nawaz A., Aminuddin A., Kado T., Takikawa A., Yamamoto S., Tsuneyama K., Igarashi Y., Ikutani M., Nishida Y., Nagai Y., et al. CD206(+) M2-like macrophages regulate systemic glucose metabolism by inhibiting proliferation of adipocyte progenitors. Nat. Commun. 2017;8:286.
371. Nery R.A., Kahlow B.S., Skare T.L., Tabushi F.I., do Amaral e Castro A. Uric acid and tissue repair. Arq Bras Cir Dig. 2015;28(4):290–292.
372. Ng G, Sharma K, Ward SM, et al. Receptor-independent, direct membrane binding leads to cell-surface lipid sorting and Syk kinase activation in dendritic cells. Immunity. 2008;29(5):807-818.
373. Nogi S., Fujita S., Okamoto Y., Kizawa S., Morita H., Ito T. Serum uric acid is associated with cardiac diastolic dysfunction among women with preserved ejection fraction. Am J Physiol Heart Circ Physiol. 2015;309(5) H986-94.
374. Oberbach A., Neuhaus J., Jehmlich N., Schlichting N., Heinrich M., Kullnick Y. A global proteome approach in uric acid stimulated human aortic endothelial cells revealed regulation of multiple major cellular pathways. Int J Cardiol. 2014;176(3):746–752.
375. Obermayr R.P., Temml C., Gutjahr G., Knechtelsdorfer M., Oberbauer R., Klauser-Braun R. Elevated uric acid increases the risk for kidney disease. J Am Soc Nephrol. 2008;19(12):2407–2413.
376. Ogino K., Kato M., Furuse Y., Kinugasa Y., Ishida K., Osaki S. Uric acid-lowering treatment with benzbromarone in patients with heart failure: a double-blind placebo-controlled crossover preliminary study. Circ Heart Fail. 2010;3:73–81.
377. Okazaki H., Shirakabe A., Kobayashi N., Hata N., Shinada T., Matsushita M. The prognostic impact of uric acid in patients with severely decompensated acute heart failure. J Cardiol. 2016;68(5):384–391.
378. Ortiz R, Ulrich H, Zarate CA Jr, Machado-Vieira R. Purinergic system dysfunction in mood disorders: a key target for developing improved therapeutics. Prog Neuropsychopharmacol Biol Psychiatry. 2015;57:117-31.
379. Ortiz-Bravo E, Sieck MS, Schumacher HR Jr. Changes in the proteins coating monosodium urate crystals during active and subsiding inflammation. Immunogold studies of synovial fluid from patients with gout and of fluid obtained using the rat subcutaneous air pouch model. Arthritis Rheum. 1993;36(9):1274-1285.
380. Otomo K., Horino T., Miki T., Kataoka H., Hatakeyama Y., Matsumoto T. Serum uric acid level as a risk factor for acute kidney injury in hospitalized patients: a retrospective database analysis using the integrated medical information system at Kochi Medical School hospital. Clin Exp Nephrol. 2016;20(2):235–243.
381. Pachot A., Cazalis M.A., Venet F., Turrel F., Faudot C., Voirin N., Diasparra J., Bourgoin N., Poitevin F., Mougin B., et al. Decreased expression of the fractalkine receptor CX3CR1 on circulating monocytes as new feature of sepsis-induced immunosuppression. J. Immunol. 2008;180:6421–6429.
382. Palazzuoli A., Ruocco G., Pellegrini M., Beltrami M., Giordano N., Nuti R. Prognostic significance of hyperuricemia in patients with acute heart failure. Am J Cardiol. 2016;117(10):1616–1621.
383. Palma JA, Benarroch EE. Neural control of the heart: recent concepts and clinical correlations. Neurology. 2014; 83(3): 261-271.
384. Pan M., Gao H., Long L., Xu Y., Liu M., Zou J. Serum uric acid in patients with Parkinson's disease and vascular parkinsonism: a cross-sectional study. Neuroimmunomodulation. 2013;20(1):19–28.
385. Park B.S., Lee J.O. Recognition of lipopolysaccharide pattern by TLR4 complexes. Exp. Mol. Med. 2013;45:e66.
386. Park J.H., Jin Y.M., Hwang S., Cho D.H., Kang D.H., Jo I. Uric acid attenuates nitric oxide production by decreasing the interaction between endothelial nitric oxide synthase and calmodulin in human umbilical vein endothelial cells: a mechanism for uric acid-induced cardiovascular disease development. Nitric oxide. 2013;32:36–42.
387. Parsa A., Brown E., Weir M.R., Fink J.C., Shuldiner A.R., Mitchell B.D. Genotype-based changes in serum uric acid affect blood pressure. Kidney Int. 2012;81(5):502–507.
388. Patel H.J., Patel B.M. TNF-alpha and cancer cachexia: Molecular insights and clinical implications. Life Sci. 2017;170:56–63.
389. Pavlov VA, Tracey KJ. The vagus nerve and the inflammatory reflex-linking immunity and metabolism. Nat Rev Endocrinol. 2012; 8(12): 743-754.
390. Pavlov VA, Chavan SS, Tracey KJ. Molecular and functional neuroscience in immunity. Annu Rev Immunol. 2018; 36: 783-812.
391. Peden D.B., Hohman R., Brown M.E., Mason R.T., Berkebile C., Fales H.M. Uric acid is a major antioxidant in human nasal airway secretions. Proc Natl Acad Sci USA. 1990;87(19):7638–7642.

392. Peden D.B., Swiersz M., Ohkubo K., Hahn B., Emery B., Kaliner M.A. Nasal secretion of the ozone scavenger uric acid. Am Rev Respir Dis. 1993;148(2):455–461.
393. Peracoli M.T., Bannwart C.F., Cristofalo R., Borges V.T., Costa R.A., Witkin S.S., Peracoli J.C. Increased reactive oxygen species and tumor necrosis factor-alpha production by monocytes are associated with elevated levels of uric acid in pre-eclamptic women. Am. J. Reprod. Immunol. 2011;66:460–467.
394. Perheentupa J., Raivio K. Fructose-induced hyperuricaemia. Lancet. 1967;2(7515):528–531.
395. Petsyukh S.V., Petsyukh M.S., Kovbasnyuk M.M., Barylyak L.G., Zukow W. Relationships between Popovych's Adaptation Index and parameters of ongoiging HRV and EEG in patients with chronic pyelonephrite and cholecystite in remission. Journal of Education, Health and Sport. 2016; 6(2): 99-110.
396. Pfister R., Barnes D., Luben R., Forouhi N.G., Bochud M., Khaw K.T. No evidence for a causal link between uric acid and type 2 diabetes: Mendelian randomisation approach. Diabetologia. 2011;54(10):2561–2569.
397. Piccirillo G, Ottaviani C, Fiorucci C, Petrocci N, Moscucci F, Di Iorio C et al. Transcranial direct current stimulation improves the QT variability index and autonomic cardiac control in healthy subjects older than 60 years. Clin Interv Aging. 2016;11:1687-1695.
398. Popadynets' OO, Gozhenko AI, Zukow W, Popovych IL. Relationships between the entropies of EEG, HRV, immunocytogram and leukocytogram. Journal of Education, Health and Sport. 2019; 9(5): 651-666.
399. Popa-Nita O., Naccache P.H. Crystal-induced neutrophil activation. Immunol Cell Biol. 2010;88(1):32–40.
400. Popovych AI. Features of the immunotropic effects of partial components of the balneotherapeutic complex of spa Truskavets'. Journal of Education, Health and Sport. 2018; 8(12): 919-935.
401. Popovych AI. Features of the neurotropic effects of partial components of the balneotherapeutic complex of spa Truskavets'. Journal of Education, Health and Sport. 2019; 9(1): 396-409.
402. Popovych IL, Lukovych YuS, Korolyshyn TA, Barylyak LG, Kovalska LB, Zukow W. Relationship between the parameters heart rate variability and background EEG activity in healthy men. Journal of Health Sciences. 2013; 3(4): 217-240.
403. Popovych IL, Kozyavkina OV, Kozyavkina NV, Korolyshyn TA, Lukovych YuS, Barylyak LG. Correlation between Indices of the Heart Rate Variability and Parameters of Ongoing EEG in Patients Suffering from Chronic Renal Pathology. Neurophysiology. 2014; 46(2): 139-148.
404. Popovych IL, Gozhenko AI, Zukow W, Polovynko IS. Variety of Immune Responses to Chronic Stress and their Neuro-Endocrine Accompaniment. Riga: Scholars' Press; 2020: 172.
405. Popovych IL, Kul'chyns'kyi AB, Korolyshyn TA, Zukow W. Interrelations between changes in parameters of HRV, EEG and cellular immunity at patients with chronic pyelonephritis and cholecystitis. Journal of Education, Health and Sport. 2017; 7(10): 11-23.
406. Popovych IL, Kul'chyns'kyi AB, Gozhenko AI, Zukow W, Kovbasnyuk MM, Korolyshyn TA. Interrelations between changes in parameters of HRV, EEG and phagocytosis at patients with chronic pyelonephritis and cholecystitis. Journal of Education, Health and Sport. 2018; 8(2): 135-156.
407. Popovych IL, Gozhenko AI, Bombushkar IS, Korda MM, Zukow W. Sexual dimorphism in relationships between of uricemia and some psycho-neuro-endocrine parameters. Journal of Education, Health and Sport. 2015; 5(5): 556-581.
408. Popovych IL, Bombushkar IS, Badiuk NS, Korda IV, Zukow W, Gozhenko AI. Features of the state of neuro-endocrine factors of adaptation under different options of uric acid metabolism in healthy female rats. Journal of Education, Health and Sport. 2020; 10(3): 352-362.
409. Popovych IL, Gozhenko AI, Bombushkar IS, Anchev AS, Zukow W. Sexual dimophism in plasma nitrogenous metabolites levels and some psycho-neuro-endocrine parameters. Quality in Sport. 2022; 8(4): 46-57.
410. Popovych IL, Gozhenko AI, Korda MM, Klishch IM, Popovych DV, Zukow W (editors). Mineral Waters, Metabolism, Neuro-Endocrine-Immune Complex. Odesa. Feniks; 2022: 252.
411. Popovych IL, Bombushkar IS, Żukow X, Kovalchuk HY. Uric acid, neuroendocrine-immune complex and metabolism: relationships. Journal of Education, Health and Sport. 2023; 36(1): 135-159.
412. Popovych IL, Kul'chyns'kyi AB, Gozhenko AI, Zukow W, Kovbasnyuk MM, Korolyshyn TA. Interrelations between changes in parameters of HRV, EEG and phagocytosis at patients with chronic pyelonephritis and cholecystitis. Journal of Education, Health and Sport. 2018; 8(2): 135-156.
413. Popovych IL, Kul'chyns'kyi AB, Korolyshyn TA, Zukow W. Interrelations between changes in parameters of HRV, EEG and cellular immunity at patients with chronic pyelonephritis and cholecystitis. Journal of Education, Health and Sport. 2017; 7(10): 11-23.
414. Popovych IL, Lukovych YuS, Korolyshyn TA, Barylyak LG, Kovalska LB, Zukow W. Relationship between the parameters heart rate variability and background EEG activity in healthy men. Journal of Health Sciences. 2013; 3(4): 217-240.
415. Pousti A, Deemyad T, Malihi G. Mechanism of inhibitory effect of citalopram on isolated guinea-pig atria in relation to adenosine receptor. Hum Psychopharmacol. 2004;19(5):347-350. doi:10.1002/hup.593
416. Practical psychodiagnostics. Techniques and tests [in Russian]. Samara. Bakhrakh; 1998: 59-64.
417. Price KL, Sautin YY, Long DA, et al. Human vascular smooth muscle cells express a urate transporter. J Am Soc Nephrol. 2006;17(7):1791-1795. doi:10.1681/ASN.2006030264

418. Raijmakers M.T., Dechend R., Poston L. Oxidative stress and pre-eclampsia: rationale for antioxidant clinical trials. Hypertension. 2004;44(4):374–380.
419. Rasheed H., McKinney C., Stamp L.K., Dalbeth N., Topless R.K., Day R., Kannangara D., Williams K., Smith M., Janssen M., et al. The Toll-Like Receptor 4 (TLR4) Variant rs2149356 and Risk of Gout in European and Polynesian Sample Sets. PLoS ONE. 2016;11:e0147939.
420. Rebola N, Canas PM, Oliveira CR, Cunha RA. Different synaptic and subsynaptic localization of adenosine A2A receptors in the hippocampus and striatum of the rat. Neuroscience. 2005; 132: 893–903.
421. Rentzos M., Nikolaou C., Anagnostouli M., Rombos A., Tsakanikas K., Economou M. Serum uric acid and multiple sclerosis. Clin Neurol Neurosurg. 2006;108(6):527–531.
422. Reschke L.D., Miller E.R., 3rd, Fadrowski J.J., Loeffler L.F., Holmes K.W., Appel L.J. Elevated uric acid and obesity-related cardiovascular disease risk factors among hypertensive youth. Pediatr Nephrol. 2015;30(12):2169–2176.
423. Rocha D.M., Caldas A.P., Oliveira L.L., Bressan J., Hermsdorff H.H. Saturated fatty acids trigger TLR4-mediated inflammatory response. Atherosclerosis. 2016;244:211–215. doi: 10.1016/j.atherosclerosis.2015.11.015.
424. Roch-Ramel F., Werner D., Guisan B. Urate transport in brushborder membrane of human kidney. Am J Physiol Renal Physiol. 1994;266:F797–F805.
425. Roncal-Jimenez C.A., Ishimoto T., Lanaspa M.A., Milagres T., Andres-Hernando A., Jensen T. Aging-associated renal disease in mice is fructokinase dependent. Am J Physiol Renal Physiol. 2016;311(4):F722–F730.
426. Roncal-Jimenez C.A., Lanaspa M.A., Rivard C.J., Nakagawa T., Sanchez-Lozada L.G., Jalal D. Sucrose induces fatty liver and pancreatic inflammation in male breeder rats independent of excess energy intake. Metabolism. 2011;60:1259–1270.
427. Rosin DL, Robeva A, Woodard RL, Guyenet PG, Linden J. Immunohistochemical localization of adenosine A2A receptors in the rat central nervous system. J Comp Neurol. 1998; 401: 163–186.
428. Roy D., Perreault M., Marette A. Insulin stimulation of glucose uptake in skeletal muscles and adipose tissues in vivo is NO dependent. Am J Physiol. 1998;274(4 Pt 1) E692-9.
429. Ryu E.-S., Kim M.J., Shin H.-S., Jang Y.H., Choi H.S., Jo I. Uric acid-induced phenotypic transition of renal tubular cells as a novel mechanism of chronic kidney disease. Am J Physiol Renal Physiol. 2013;304 F471-80.
430. Salahudeen M.S., Nishtala P.S. An overview of pharmacodynamic modelling, ligand-binding approach and its application in clinical practice. Saudi. Pharm. J. 2017;25:165–175.
431. Sánchez-Lozada L.G., Lanaspa M.A., Cristóbal-García M., García-Arroyo F., Soto V., Cruz-Robles D. Uric acid-induced endothelial dysfunction is associated with mitochondrial alterations and decreased intracellular ATP concentrations. Nephron Exp Nephrol. 2012;121(3–4) e71-8.
432. Sánchez-Lozada L.G., Nakagawa T., Kang D.H., Feig D.I., Franco M., Johnson R.J. Hormonal and cytokine effects of uric acid. Curr Opin Nephrol Hypertens. 2006;15(1):30–33.
433. Sanchez-Lozada L.G., Tapia E., Santamaria J., Avila-Casado C., Soto V., Nepomuceno T. Mild hyperuricemia induces vasoconstriction and maintains glomerular hypertension in normal and remnant kidney rats. Kidney Int. 2005;67:237–247.
434. Saura J, Angulo E, Ejarque A, Casadó V, Tusell JM, Moratalla R, Chen JF, Schwarzschild MA, Lluis C, Franco R, Serratosa J. Adenosine A2A receptor stimulation potentiates nitric oxide release by activated microglia. J Neurochem. 2005; 95: 919–929.
435. Sautin Y.Y., Johnson R.J. Uric acid: the oxidant-antioxidant paradox. Nucleosides Nucleotides Nucl Acids. 2008;27(6):608–619.
436. Sautin Y.Y., Nakagawa T., Zharikov S., Johnson R.J. Adverse effects of the classic antioxidant uric acid in adipocytes: NADPH oxidase-mediated oxidative/nitrosative stress. Am. J. Physiol. Cell Physiol. 2007;293:C584–C596.
437. Shaffer F, Ginsberg JP. An Overview of Heart Rate Variability Metrics and Norms. Front Public Health. 2017; 5: 258.
438. Schett G., Dayer J.M., Manger B. Interleukin-1 function and role in rheumatic disease. Nat Rev Rheumatol. 2016;12(1):14–24.
439. Schiffmann SN, Jacobs O, Vanderhaeghen JJ. Striatal restricted adenosine A2 receptor (RDC8) is expressed by enkephalin but not by substance P neurons: an in situ hybridization histochemistry study. J Neurochem. 1991; 57: 1062–1067.
440. Schlesinger I., Schlesinger N. Uric acid in Parkinson's disease. Mov Disord. 2008;23(12):1653–1657.
441. Schlesinger N, Norquist JM, Watson DJ. Serum urate during acute gout [published correction appears in J Rheumatol. 2009 Aug;36(8):1851]. J Rheumatol. 2009;36(6):1287-1289. doi:10.3899/jrheum.080938
442. Schorn C., Frey B., Lauber K., Janko C., Strysio M., Keppeler H. Sodium overload and water influx activate the NALP3 inflammasome. J Biol Chem. 2011;286(1):35–41.
443. Schroder K., Zhou R., Tschopp J. The NLRP3 inflammasome: a sensor for metabolic danger? Science. 2010;327(5963):296–300.

444. Schwarzmeier J.D., Marktl W., Moser K., Lujf A. Fructose induced hyperuricemia. Effects of fructose on the de novo synthesis of adenine nucleotides in the liver and skeletal muscles of rats. Res Exp Med (Berl) 1974;162(4):341–346.
445. Scott P, Ma H, Viriyakosol S, Terkeltaub R, Liu-Bryan R. Engagement of CD14 mediates the inflammatory potential of monosodium urate crystals. J Immunol. 2006;177(9):6370-6378.
446. Seet RC, Kasiman K, Gruber J, et al. Is uric acid protective or deleterious in acute ischemic stroke? A prospective cohort study. Atherosclerosis. 2010;209(1):215-219.
447. Selim S., El Sagheer O., El Amir A., Barakat R., Hadley K., Bruins M.J. Efficacy and safety of arachidonic acid for treatment of Schistosoma mansoni-infected children in Menoufiya, Egypt. Am J Trop Med Hyg. 2014;91(5):973–981.
448. Shafiu M., Johnson R.J., Turner S.T., Langaee T., Gong Y., Chapman A.B. Urate transporter gene SLC22A12 polymorphisms associated with obesity and metabolic syndrome in Caucasians with hypertension. Kidney Blood Press Res. 2012;35(6):477–482.
449. Shani M., Vinker S., Dinour D., Leiba M., Twig G., Holtzman E.J. High normal uric acid levels are associated with an increased risk of diabetes in lean, normoglycemic healthy women. J Clin Endocrinol Metab. 2016;101(10):3772–3778.
450. Shannon CE. A mathematical theory of information. Bell Syst Tech J. 1948; 27: 379-423.
451. Shannon C.E. Works on the theory of informatics and cybernetics [transl. from English to Russian]. Moskwa: Inostrannaya literatura; 1963: 329.
452. Sharaf El Din UAA, Salem MM, Abdulazim DO. Uric acid in the pathogenesis of metabolic, renal, and cardiovascular diseases: A review. J Adv Res. 2017;8(5):537-548.
453. Shi Y., Chen W., Jalal D., Li Z., Chen W., Mao H. Clinical outcome of hyperuricemia in IgA nephropathy: a retrospective cohort study and randomized controlled trial. Kidney Blood Press Res. 2012;35(3):153–160.
454. Shi Y., Evans J.E., Rock K.L. Molecular identification of a danger signal that alerts the immune system to dying cells. Nature. 2003;425(6957):516–521.
455. Shih M.H., Lazo M., Liu S.H., Bonekamp S., Hernaez R., Clark J.M. Association between serum uric acid and nonalcoholic fatty liver disease in the US population. J Formos Med Assoc. 2015;114(4):314–320.
456. Shimizu T., Yoshihisa A., Kanno Y., Takiguchi M., Sato A., Miura S. Relationship of hyperuricemia with mortality in heart failure patients with preserved ejection fraction. Am J Physiol Heart Circ Physiol. 2015;309:H1123–H1129.
457. Sluijs I., Holmes M.V., van der Schouw Y.T., Beulens J.W., Asselbergs F.W., Huerta J.M. A Mendelian randomizationstudy of circulating uric acid and type 2 diabetes. Diabetes. 2015;64(8):3028–3036.
458. Smárason A.K., Allman K.G., Young D., Redman C.W. Elevated levels of serum nitrate, a stable end product of nitric oxide, in women with pre-eclampsia. Br J Obstet Gynaecol. 1997;104(5):538–543.
459. Smyth CJ, Holers VM. Gout, Hyperuricemia, and Other Crystal-Associated Arthropathies. New York: Marcel Dekker; 1998.
460. Snigdha S., Smith E. D., Prieto G. A., Cotman C. W. Caspase-3 activation as a bifurcation point between plasticity and cell death. Neuroscience Bulletin. 2012;28(1):14–24.
461. Sofaer JA, Emery AE. Genes for super-intelligence? J Med Genet. 1981;18(6):410-413.
462. Soletsky B., Feig D.I. Uric acid reduction rectifies prehypertension in obese adolescents. Hypertension. 2012;60(5):1148–1156.
463. Sotgiu S., Pugliatti M., Sanna A., Sotgiu A., Fois M.L., Arru G. Serum uric acid and multiple sclerosis. Neurol Sci. 2002;23(4):183–188.
464. Spahis S., Alvarez F., Dubois J., Ahmed N., Peretti N., Levy E. Plasma fatty acid composition in French-Canadian children with non-alcoholic fatty liver disease: effect of n-3 PUFA supplementation. Prostaglandins Leukot Essent Fatty Acids. 2015;99:25–34.
465. Spilberg I. Current concepts of the mechanism of acute inflammation in gouty arthritis. Arthritis Rheum. 1975;18(2):129–134.
466. Spielberger CD. Manual for the State-Trait Anxiety Inventory (Form Y) Consulting Psychologists Press; Palo Alto (CA): 1983.
467. Stack A.G., Hanley A., Casserly L.F., Cronin C.J., Abdalla A.A., Kiernan T.J. Independent and conjoint associations of gout and hyperuricaemia with total and cardiovascular mortality. QJM. 2013;106(7):647–658.
468. Steele TH. Hyperuricemic nephropathies. Nephron. 1999;81 Suppl 1:45-49.
469. Struk ZD, Mel'nyk OI, Zukow W, Popovych IL. The diversity of immune reactions to balneotherapy and their accompaniments. Journal of Education, Health and Sport. 2019; 9(11): 349-373.
470. Sugihara S., Hisatome I., Kuwabara M., Niwa K., Maharani N., Kato M. Depletion of uric acid due to SLC22A12 (URAT1) loss-of-function mutation causes endothelial dysfunction in hypouricemia. Circ J. 2015;79(5):1125–1132.
471. Sun H.L., Pei D., Lue K.H., Chen Y.L. Uric acid levels can predict metabolic syndrome and hypertension in adolescents: a 10-year longitudinal study. PLoS ONE. 2015;10(11):e0143786.

472. Svenningsson P, Fourreau L, Bloch B, Fredholm BB, Gonon F, Le Moine C. Opposite tonic modulation of dopamine and adenosine on c-fos gene expression in striatopallidal neurons. Neuroscience. 1999; 89: 827–837.
473. Sydoruk NO, Zukow W. Differences between the effects of water Naftussya from fields of Truskavets' and Pomyarky on the parameters of the EEG, HRV, immunity and metabolism. Journal of Education, Health and Sport. 2019; 9(1): 287-293.
474. Szabo G., Csak T. Inflammasomes in liver diseases. J Hepatol. 2012;57(3):642–654.
475. Tak HK, Cooper SM, Wilcox WR. Studies on the nucleation of monosodium urate at 37 degrees c. Arthritis Rheum. 1980;23(5):574-580.
476. Takae K., Nagata M., Hata J., Mukai N., Hirakawa Y., Yoshida D. Serum uric acid as a risk factor for chronic kidney disease in a Japanese community – the Hisayama study. Circ J. 2016;80(8):1857–1862.
477. Takir M., Kostek O., Ozkok A., Elcioglu O.C., Bakan A., Erek A. Lowering uric acid with allopurinol improves insulin resistance and systemic inflammation in asymptomatic hyperuricemia. J Investig Med. 2015;63(8):924–929.
478. Talbott J.H., Terplan K.L. The kidney in gout. Medicine. 1960;39:405–467.
479. Tallima H, Dvořák J, Kareem S, et al. Protective immune responses against Schistosoma mansoni infection by immunization with functionally active gut-derived cysteine peptidases alone and in combination with glyceraldehyde 3-phosphate dehydrogenase. PLoS Negl Trop Dis. 2017;11(3):e0005443.
480. Tallima H., Dalton J.P., El Ridi R. Induction of protective immune responses against Schistosomiasis haematobium in hamsters and mice using cysteine peptidase-based vaccine. Front Immunol. 2015;6:130.
481. Tan P.K., Ostertag T.M., Miner J.N. Mechanism of high affinity inhibition of the human urate transporter URAT1. Sci. Rep. 2016;6:34995.
482. Tang L., Xu Y., Wei Y., He X. Uric acid induces the expression of TNFalpha via the ROSMAPKNFkappaB signaling pathway in rat vascular smooth muscle cells. Mol. Med. Rep. 2017;16:6928–6933.
483. Tani S., Nagao K., Hirayama A. Effect of febuxostat, a xanthine oxidase inhibitor, on cardiovascular risk in hyperuricemic patients with hypertension: a prospective, open-label, Pilot Study. Clin Drug Investig. 2015;35(12):823–831.
484. Taniguchi K., Tamura Y., Kumagai T., Shibata S., Uchida S. Stimulation of V1a receptor increases renal uric acid clearance via urate transporters: insight into pathogenesis of hypouricemia in SIADH. Clin Exp Nephrol. 2016;20(6):845–852.
485. Taylor JA, Carr DL, Myers CW, Eckberg DL. Mechanisms underlying very-low-frequency RR-interval oscillations in humans. Circulation. 1998; 98(6): 547-555.
486. Terkeltaub R, Tenner AJ, Kozin F, Ginsberg MH. Plasma protein binding by monosodium urate crystals. Analysis by two-dimensional gel electrophoresis. Arthritis Rheum. 1983;26(6):775-783.
487. Terkeltaub R. Update on gout: new therapeutic strategies and options. Nat Rev Rheumatol. 2010;6(1):30-38.
488. Testa A., Mallamaci F., Spoto B., Pisano A., Sanguedolce M.C., Tripepi G. Association of a polymorphism in a gene encoding a urate transporter with CKD progression. Clin J Am Soc Nephrol. 2014;9(6):1059–1065.
489. Thayer JF, Sternberg EM. Neural aspects of immunomodulation: Focus on the vagus nerve. Brain Behav Immun. 2010; 24(8): 1223-1228.
490. Theorell T, Liljeholm-Johansson Y, Björk H, Ericson M. Saliva testosterone and heart rate variability in the professional symphony orchestra after "public faintings" of an orchestra member. Psychoneuroendocrinology. 2007; 32(6): 660-668.
491. Tian H., Ye X., Hou X., Yang X., Yang J., Wu C. SVCT2, a potential therapeutic target, protects against oxidative stress during ethanol-induced neurotoxicity via JNK/p38 MAPKs, NF-κB and miRNA125a-5p. Free Radical Biology and Medicine. 2016;96:362–373.
492. Tiselius HS. A biochemical basis for grouping of patients with urolithiasis. Europ Urol. 1978; 4: 241-249.
493. Torres-Castro I., Arroyo-Camarena U.D., Martinez-Reyes C.P., Gomez-Arauz A.Y., Duenas-Andrade Y., Hernandez-Ruiz J., Bejar Y.L., Zaga-Clavellina V., Morales-Montor J., Terrazas L.I., et al. Human monocytes and macrophages undergo M1-type inflammatory polarization in response to high levels of glucose. Immunol. Lett. 2016;176:81–89.
494. Tracey KJ. Physiology and immunology of the cholinergic antiinflammatory pathway. J Clin Invest. 2007; 117(2): 289-296.
495. Tracey K.J. Understanding immunity requires more than immunology. Nature Immunology. 2010; 11(7): 561-564.
496. Tramontini N, Huber C, Liu-Bryan R, Terkeltaub RA, Kilgore KS. Central role of complement membrane attack complex in monosodium urate crystal-induced neutrophilic rabbit knee synovitis. Arthritis Rheum. 2004;50(8):2633-2639.
497. Trapnell C., Williams B. A., Pertea G., et al. Transcript assembly and quantification by RNA-Seq reveals unannotated transcripts and isoform switching during cell differentiation. Nature Biotechnology. 2010;28(5):511–515.

498. Tschopp J., Schroder K. NLRP3 inflammasome activation: The convergence of multiple signalling pathways on ROS production? Nat Rev Immunol. 2010;10(3):210–215.
499. Uchida S., Chang W.X., Ota T., Tamura Y., Shiraishi T., Kumagai T. Targeting uric acid and the inhibition of progression to end-stage renal disease – a propensity score analysis. PLoS ONE. 2015;10(12):e0145506.
500. Vanneste S, De Ridder D. Brain Areas Controlling Heart Rate Variability in Tinnitus and Tinnitus-Related Distress. PloS ONE. 2013; 8(3): e59728.
501. Viazzi F., Rebora P., Giussani M., Orlando A., Stella A., Antolini L. Increased serum uric acid levels blunt the antihypertensive efficacy of lifestyle modifications in children at cardiovascular risk. Hypertension. 2016;67(5):934–940.
502. Vigano S, Alatzoglou D, Irving M, Menetrier-Caux Ch, Caux Ch, Romero P, Coukos G. Targeting adenosine in cancer immunotherapy to enhance T-cell function. Front Immunol. 2019; 10: 925.
503. Vitart V, Rudan I, Hayward C, et al. SLC2A9 is a newly identified urate transporter influencing serum urate concentration, urate excretion and gout. Nat Genet. 2008;40(4):437-442.
504. Von Lueder T.G., Girerd N., Atar D., Agewall S., Lamiral Z., Kanbay M. Serum uric acid is associated with mortality and heart failure hospitalizations in patients with complicated myocardial infarction: findings from the High-Risk Myocardial Infarction Database Initiative. Eur J Heart Fail. 2015;17(11):1144–1151.
505. Wang J., Qin T., Chen J., Li Y., Wang L., Huang H. Hyperuricemia and risk of incident hypertension: a systematic review and meta-analysis of observational studies. PLoS ONE. 2014;9(12):e114259.
506. Wang L., Hu W., Wang J., Qian W., Xiao H. Low serum uric acid levels in patients with multiple sclerosis and neuromyelitis optica: an updated meta-analysis. Mult Scler Relat Disord. 2016;9:17–22.
507. Wang W., Wang C., Ding X.Q., Pan Y., Gu T.T., Wang M.X. Quercetin and allopurinol reduce liver thioredoxin-interacting protein to alleviate inflammation and lipid accumulation in diabetic rats. Br J Pharmacol. 2013;169(6):1352–1371.
508. Wang Y, Ma X, Su Ch, Peng B, Du J, Jia H, Luo M, Fang Ch, Wei Y. Uric acid enhanced the antitumor immunity of dendritic cell-based vaccine. Sci Rep. 2015; 5: 16427.
509. Wang Z., Lin Y., Liu Y., Chen Y., Wang B., Li C. Serum uric acid levels and outcomes after acute ischemic stroke. Mol Neurobiol. 2016;53(3):1753–1759.
510. Watanabe S, Kang DH, Feng L, et al. Uric acid, hominoid evolution, and the pathogenesis of salt-sensitivity. Hypertension. 2002;40(3):355-360.
511. Wei F., Sun N., Cai C., Feng S., Tian J., Shi W. Associations between serum uric acid and the incidence of hypertension: a Chinese senior dynamic cohort study. J Transl Med. 2016;14(1):110.
512. Willart M.A., Poulliot P., Lambrecht B.N., Kool M. PAMPs and DAMPs in allergy exacerbation models. Meth Mol Biol. 2013;1032:185–204.
513. Winkelmann T, Thayer JF, Pohlak ST, Nees F, Grimm O, Flor H. Structural brain correlates of heart rate variability in healthy young adult population. Brain Structure and Function. 2017; 222(2): 1061-1068.
514. Wu A.H., Gladden J.D., Ahmed M., Ahmed A., Filippatos G. Relation of serum uric acid to cardiovascular disease. Int J Cardiol. 2016;15(213):4–7.
515. Wu C.Y., Hu H.Y., Chou Y.J., Huang N., Chou Y.C., Lee M.S. High serum uric acid levels are associated with all-cause and cardiovascular, but not cancer, mortality in elderly adults. J Am Geriatr Soc. 2015;63(9):1829–1836.
516. Wu H., Jia Q., Liu G., Liu L., Pu Y., Zhao X. Decreased uric acid levels correlate with poor outcomes in acute ischemic stroke patients, but not in cerebral hemorrhage patients. J Stroke Cerebrovasc Dis. 2014;23(3):469–475.
517. Wu J., Qiu L., Cheng X.Q., Xu T., Wu W., Zeng X.J., Ye Y.C., Guo X.Z., Cheng Q., Liu Q., et al. Hyperuricemia and clustering of cardiovascular risk factors in the Chinese adult population. Sci. Rep. 2017;7:5456.
518. Wynn T.A., Chawla A., Pollard J.W. Macrophage biology in development, homeostasis and disease. Nature. 2013;496:445–455.
519. Xia X., Luo Q., Li B., Lin Z., Yu X., Huang F. Serum uric acid and mortality in chronic kidney disease: a systematic review and meta-analysis. Metabolism. 2016;65(9):1326–1341.
520. Xiao J., Fu C., Zhang X., Zhu D., Chen W., Lu Y. Soluble monosodium urate, but not its crystal, induces toll like receptor 4-dependent immune activation in renal mesangial cells. Mol Immunol. 2015;66(2):310–318.
521. Xiao J., Zhang X.L., Fu C., Han R., Chen W., Lu Y. Soluble uric acid increases NALP3 inflammasome and interleukin-1β expression in human primary renal proximal tubule epithelial cells through the Toll-like receptor 4-mediated pathway. Int J Mol Med. 2015;35(5):1347–1354.
522. Xu W., Huang Y., Li L., Sun Z., Shen Y., Xing J. Hyperuricemia induces hypertension through activation of renal epithelial sodium channel (ENaC) Metabolism. 2016;65(3):73–83.
523. Xu X., Hu J., Song N., Chen R., Zhang T., Ding X. Hyperuricemia increases the risk of acute kidney injury: a systematic review and meta-analysis. BMC Nephrol. 2017;18(1):27.
524. Yakoob M.Y. Vitamin D deficiency during pregnancy and the risk of preeclampsia. J Pak Med Assoc. 2011;61(8):827–828.

525. Yan D., Tu Y., Jiang F., Wang J., Zhang R., Sun X. Uric acid is independently associated with diabetic kidney disease: a cross-sectional study in a Chinese population. PLoS ONE. 2015;10(6):e0129797.
526. Yano H., Tamura Y., Kobayashi K., Tanemoto M., Uchida S. Uric acid transporter ABCG2 is increased in the intestine of the 5/6 nephrectomy rat model of chronic kidney disease. Clin Exp Nephrol. 2014;18(1):50–55.
527. Yin H., Hou X., Tao T., Lv X., Zhang L., Duan W. Neurite outgrowth resistance to rho kinase inhibitors in PC12 Adh cell. Cell Biology International. 2015;39(5):563–576.
528. Yokoi Y., Kondo T., Okumura N., Shimokata K., Osugi S., Maeda K. Serum uric acid as a predictor of future hypertension: stratified analysis based on body mass index and age. Prev Med. 2016;9(90):201–206.
529. Yokokawa H., Fukuda H., Suzuki A., Fujibayashi K., Naito T., Uehara Y. Association between serum uric acid levels/hyperuricemia and hypertension among 85,286 japanese workers. J Clin Hypertens (Greenwich) 2016 Jan;18(1):53–59.
530. Yoshitomi R., Fukui A., Nakayama M., Ura Y., Ikeda H., Oniki H. Sex differences in the association between serum uric acid levels and cardiac hypertrophy in patients with chronic kidney disease. Hypertens Res. 2014;37(3):246–252.
531. Young In Kim, Sun Mi Kim, Ji Sun Hong, Jinuk Song, Doug Hyun Han, Kyung Joon Min, Young Sik Lee. The Correlation between Clinical Symptoms, Serum Uric Acid Level and EEG in Patient with Bipolar I Disorder [transl from Korean to English]. Journal of Korean Neuropsychiatric Association 2016; 55(1): 25-32.
532. Yousefi M., Rahimi H., Barikbin B., Toossi P., Lotfi S., Hedayati M. Uric acid: a new antioxidant in patients with pemphigus vulgaris. Indian J Dermatol. 2011;56(3):278–281.
533. Yu K. H., Chen D. Y., Chen J. H., et al. Management of gout and hyperuricemia: multidisciplinary consensus in Taiwan. International Journal of Rheumatic Diseases. 2018;21(4):772–787. doi: 10.1111/1756-185X.13266.
534. Yu M., Ling K., Teng Y., Li Q., Mei F., Li Y. Serum uric acid is associated with increased risk of idiopathic venous thromboembolism in high HDL-C population: a case-control study. Exp Ther Med. 2016;11(6):2314–2320.
535. Yu M.A., Sánchez-Lozada L.G., Johnson R.J., Kang D.H. Oxidative stress with an activation of the renin-angiotensin system in human vascular endothelial cells as a novel mechanism of uric acid-induced endothelial dysfunction. J Hypertens. 2010;28(6):1234–1242.
536. Yu S., Yang H., Guo X., Zheng L., Sun Y. Hyperuricemia is independently associated with left ventricular hypertrophy in post-menopausal women but not in pre-menopausal women in rural Northeast China. Gynecol Endocrinol. 2015;31(9):736–741.
537. Yu T.Y., Jee J.H., Bae J.C., Jin S.M., Baek J.H., Lee M.K., Kim J.H. Serum uric acid: A strong and independent predictor of metabolic syndrome after adjusting for body composition. Metabolism. 2016;65:432–440.
538. Yu X., Shi J., Jiang C., Xu J., You S., Cao Y. Association study of serum uric acid levels with clinical outcome and hemorrhagic transformation in stroke patients with rt-PA intravenous thrombolysis. Zhonghua Yi Xue Za Zhi. 2015;95(29):2351–2354.
539. Yuan H., Yu C., Li X., Sun L., Zhu X., Zhao C. Serum uric acid levels and risk of metabolic syndrome: a dose-response meta-analysis of prospective studies. J Clin Endocrinol Metab. 2015;100(11):4198–4207.
540. Yun Y., Yin H., Gao Z., et al. Intestinal tract is an important organ for lowering serum uric acid in rats. PLoS One. 2017;12(12):e0190194.
541. Zakharova I., Sokolova T., Vlasova Y., Bayunova L., Rychkova M., Avrova N. α-Tocopherol at nanomolar concentration protects cortical neurons against oxidative stress. International Journal of Molecular Sciences. 2017;18(1):216.
542. Zhang B., Duan M., Long B., Zhang B., Wang D., Zhang Y., Chen J., Huang X., Jiao Y., Zhu L., et al. Urate transport capacity of glucose transporter 9 and urate transporter 1 in cartilage chondrocytes. Mol. Med. Rep. 2019;20:1645–1654.
543. Zhang J., Diao B., Lin X., Xu J., Tang F. TLR2 and TLR4 mediate an activation of adipose tissue renin-angiotensin system induced by uric acid. Biochimie. 2019;162:125–133.
544. Zhang M., Hutter G., Kahn S.A., Azad T.D., Gholamin S., Xu C.Y., Liu J., Achrol A.S., Richard C., Sommerkamp P., et al. Anti-CD47 Treatment Stimulates Phagocytosis of Glioblastoma by M1 and M2 Polarized Macrophages and Promotes M1 Polarized Macrophages In Vivo. PLoS ONE. 2016;11:e0153550.
545. Zhang W., Iso H., Murakami Y., Miura K., Nagai M., Sugiyama D. Serum uric acid and mortality form cardiovascular disease: EPOCH-JAPAN study. J Atheroscler Thromb. 2016;23(6):692–703.
546. Zhang X., Zhang J.H., Chen X.Y., Hu Q.H., Wang M.X., Jin R. Reactive oxygen species-induced TXNIP drives fructose-mediated hepatic inflammation and lipid accumulation through NLRP3 inflammasome activation. Antioxid Redox Signal. 2015;22(10):848–870.
547. Zhao J., Zheng D.Y., Yang J.M., Wang M., Zhang X.T., Sun L. Maternal serum uric acid concentration is associated with the expression of tumour necrosis factor-α and intercellular adhesion molecule-1 in patients with preeclampsia. J Hum Hypertens. 2016;30(7):456–462.

548. Zhou Y., Hu W., Chen P., et al. Ki67 is a biological marker of malignant risk of gastrointestinal stromal tumors: a systematic review and meta-analysis. Medicine. 2017;96(34):e7911.
549. Zhou Y., Yang Y., Warr G., Bravo R. LPS down-regulates the expression of chemokine receptor CCR2 in mice and abolishes macrophage infiltration in acute inflammation. J. Leukoc. Biol. 1999;65:265–269.
550. Zhu L., Wang J., Wang Y., Jia L., Sun K., Wang H. Plasma uric acid as a prognostic marker in patients with hypertrophic cardiomyopathy. Can J Cardiol. 2015;31(10):1252–1258.
551. Zoccali C., Maio R., Mallamaci F., Sesti G., Perticone F. Uric acid and endothelial dysfunction in essential hypertension. J Am Soc Nephrol. 2006;17:1466–1471.
552. Zurlo A., Veronese N., Giantin V., Maselli M., Zambon S., Maggi S. High serum uric acid levels increase the risk of metabolic syndrome in elderly women: the PRO.V.A study. Nutr Metab Cardiovasc Dis. 2016;26(1):27–35.

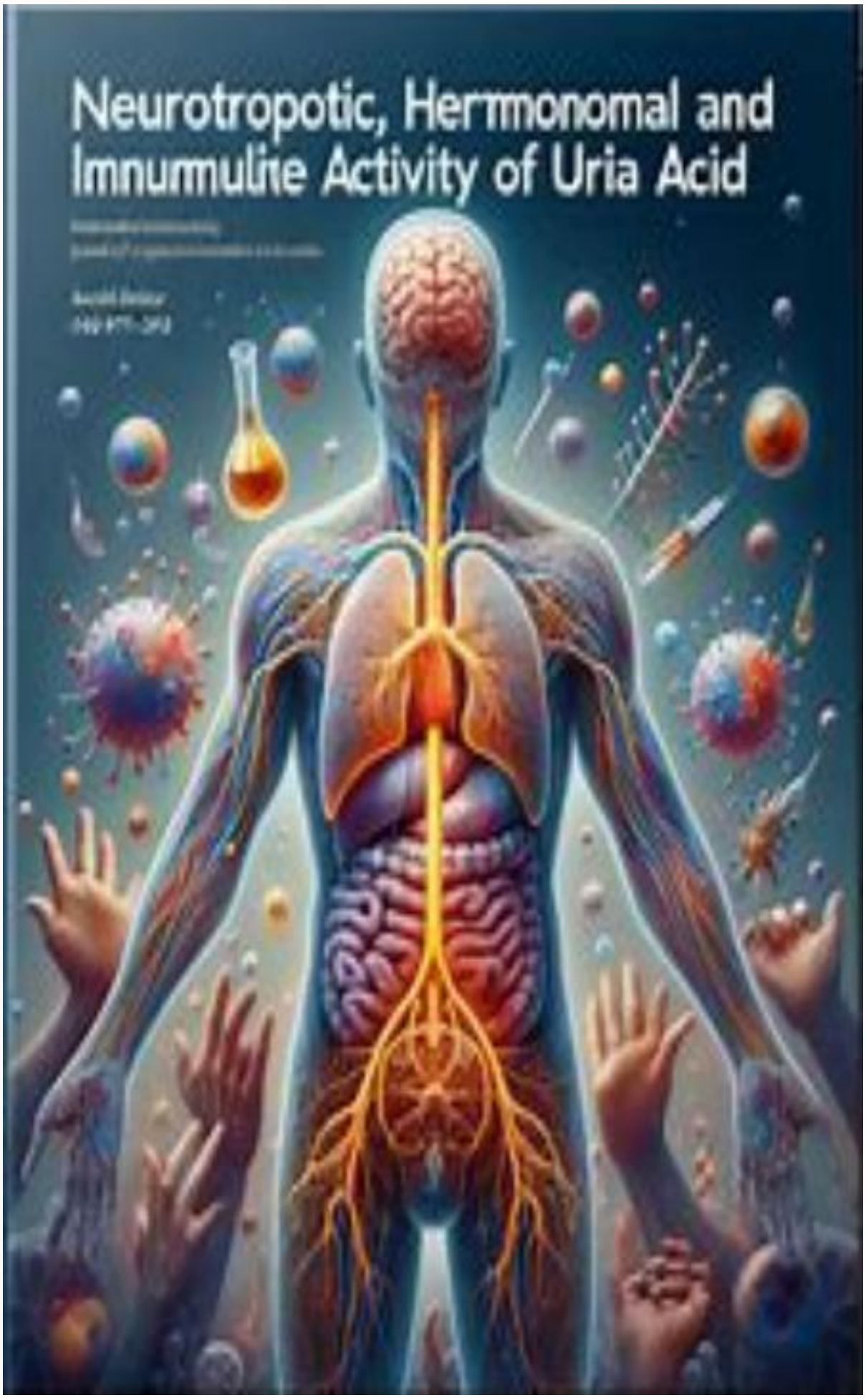
Neurotropotic, Hermonomal and
Immumulite Activity of Uria Acid

Horbachevskyi National Medical University, Ternopil', Ukraine
Ukrainian Scientific Research Institute of Medicine of Transport, Odesa, Ukraine
Bohomolets' Institute of Physiology of NAS, Kyïv, Ukraine
Nicolaus Copernicus University, Torun, Poland

Editors

Mykhaylo M. Korda
Anatoliy I. Gozhenko
Igor L. Popovych
Ivan M. Klishch

NEUROTROPIC, HORMONAL AND IMMUNOTROPIC ACTIVITY OF URIC ACID

MONOGRAPH

TERNOPIL'
Ukrmedknyha
2024

Recommended for publication by the Academic Council State Institution
"Horbachevskyi National Medical University"
(Protocol No. 3 of March 27, 2024)

Reviewers:
Roman Ivanovych Yanchiy, Doctor of Biological Sciences, Professor, laureate of the O.O. Bogomolets Prize, Head of the Immunophysiology Department at the O.O. Bogomolets Institute of Physiology of the National Academy of Sciences of Ukraine.
Ruslan Serhiyovych Vastiyanov, Doctor of Medical Sciences, Professor, Honored Scientist and Technologist of Ukraine, Head of the Department of General and Clinical Physiology named after V.V. Pidvysotsky of Odesa National Medical University.

DEDICATED TO IVAN YAKOVYCH HORBACHEVSKYI

Korda MM, Gozhenko AI, Popovych IL, Klishch IM, Bombushkar IS, Korda IV, Badiuk NS, Zukow WA, Smagliy VS. Neurotropic, hormonal and immunotropic activity of uric acid. Monograph. Ternopil': Ukrmedknyha; 2024: 206 p. ISBN 978-966-673-487-0 DOI https://doi.org/10.5281/zenodo.10990426

This monograph presents the results of priority experimental and clinical-physiological research on the relationship between uricemia and uricosuria with parameters of urea, creatinine, electrolyte exchange, as well as the nervous, endocrine and immune systems. In line with the concepts of the neuroendocrine-immune complex and the functional-metabolic continuum, using discriminant and canonical correlation analysis methods, it is demonstrated that the uric acid molecule exhibits significant physiological activity and can be considered the fourth endogenous signaling molecule alongside NO, CO, and H_2S.

For biochemists, pathophysiologists, neurologist, endocrinologists, and immunologists.

ISBN 978-966-673-487-0 DOI https://doi.org/10.5281/zenodo.10990426

9 789666 734870